

# THE DISTRIBUTION OF BACTERIOHOPANEPOLYOLS IN TERRESTRIAL GEOTHERMAL ECOSYSTEMS

BY

ROBERT A. GIBSON

SEPTEMBER, 2009

A thesis submitted to the Newcastle University in partial fulfilment of the requirements for the degree of Doctor of Philosophy in the Faculty of Science, Agriculture and Engineering

School of Civil Engineering and Geosciences  
Newcastle University,  
Newcastle-upon-Tyne,  
NE1 7RU,  
U.K.

## DECLARATION

I hereby certify that the work presented in this thesis is my own, except where otherwise acknowledged, and has not been submitted previously for a degree at this, or any other University.

Robert A. Gibson

## ACKNOWLEDGEMENTS

...And so it comes to expressing my gratitude to all those who have contributed towards the completion of this work. Undeniably this process would not have been possible without the input, scientific or otherwise, from a great number of people. First and foremost, thanks to my PhD supervisor, Dr. Helen Talbot. Your supervision has taken a student with an interest and turned him into a scientist with a passion. Thank You. At Newcastle I have been fortunate enough to have scientific input from many people including Ian Head, Paul Donohoe and Berni Bowler. Simon Poulton has been the distributor of many pearls of wisdom and pints of beer. I have made many friends during my time as a PhD student – (in no particular order) Ali Mcanena, Jamie Hinks, Lynsay Blake, Joe Harwood, Ulf Boeker, Martin Cooke, Rob Hunter, Ian Harrison, Luke Handley, Taz and Ernest and special thanks to my close friend Sharon Mason. To my fellow students, we probably don't realise it now, but the time and experiences we share during the completion of our PhDs will one day be looked back upon with great fondness. I wish you all the best of luck in your future careers and the rest of your lives. To everyone at CEGs, thank you for making the past four years so enjoyable.

Outside of Newcastle, I wish to thank Richard Pancost, Bruce Mountain, Vernon Phoenix, Roger Summons and Chuanlun Zhang for providing samples and their respective inputs. Marcel van der Meer is thanked for input regarding microbial mats. My new employers at the NIOZ are thanked for allowing me to finish writing aspects of this thesis whilst working as a scientist in the department of Marine Organic Biogeochemistry. Extra special thanks to Preeti Kaur without whom this project would have been very different.

Good friends Dave Harrop, Kenny Sanger and Oxford Mike have helped keep me grounded throughout this whole process. I wish to thank Helen Lister, my brother Sean, Jen, my grandparents, family members and many others who have provided friendship and

encouragement. Finally I wish to thank to my parents, Ruth and Alan, who have provided an immeasurable amount of support throughout my studies.

## ABSTRACT

Organic geochemical investigations of terrestrial geothermal vents have provided a veritable treasure chest of unusual results. In particular, recent investigations of microbial lipids preserved in mineral and organo-sedimentary depositions have been shown to be useful in reconstructing vent populations, recording changes in physico-chemical conditions over time and inferring the presence of uncharacterised microbiota. Studies centred on geothermal environments provide a rich source of information that is directly applicable to a range of scientific disciplines including those concerned with the early evolution of life on Earth and other planetary bodies. The organic geochemistry of a particular group of bacterial lipid biomarkers, bacteriohopanepolyols, and their degraded counterparts, geohopanoids, contained within sinters from silica-depositing geothermal vents from New Zealand and Chile provides the basis for this study. This has been complimented with an investigation of BHP distributions that derive from mat-forming microbial consortia that colonise the outflow channels of geothermal vents from California, Nevada and New Zealand.

Examination of BHP and hopanoid distributions preserved in siliceous sinters using Atmospheric Pressure Chemical Ionisation-High Performance Liquid Chromatography-Multistage Mass Spectrometry (APCI-HPLC-MS<sup>n</sup>) and Gas Chromatography-Mass Spectrometry (GC-MS) shows that polyfunctionalised composite BHPs deposited in sinters are well preserved. BHPs and geohopanoids have been analysed from five geothermal locations within the Taupo Volcanic Zone (TVZ). Composite-BHPs, such as bacteriohopanetetrol cyclitol ether and bacteriohopanepentol cyclitol ether, are commonly observed as the most abundant compounds in sinters from Champagne Pool (CP), Loop Road (LR) and Rotokawa (RK). A diverse array of additional BHPs is detected in sinter samples collected from these sites, including a number of novel BHPs. A suite of BHPs have been tentatively-assigned as 'oxo-BHPs', i.e. with a ketone group, most likely at C-32 or C-31 of the side chain. Guanidine-

substituted bacteriohopanepentol cyclitol ether was also identified and may indicate the presence of methylotrophic bacteria at the sites. Sinters collected from Opaheke Pool (OP) contain BHPs that indicate the presence of methanotrophic bacteria and cyanobacteria. Likewise, 2-methyl BHPs indicative of cyanobacteria were identified in sinters collected from Orakei Korako (OK), including a vent of 97.8°C, potentially indicating another source of 2-methyl BHPs at this site. Sinters from the El-Tatio Geyser Field (ETGF) show a predominance of cyanobacterial signatures that likely derive from endolithic cyanobacterial colonies. Concentrations and the structural diversity of BHPs are greater in sinters from the TVZ when compared to those from ETGF. A survey of the BHP distributions of mat-forming microbial consortia from geothermal locations in Nevada, California and New Zealand highlighted the presence of six currently uncharacterised composite BHP structures with the same novel terminal group at C-35 that appear to comprise a diagnostic BHP signature for mat-forming microbial consortia.

Hopanoic acids are the most abundant geohopanoids identified in older sinters and C<sub>32</sub> ββ hopanoic acid is the predominant diagenetic product. Geohopanols are more abundant in sinters deposited under acidic conditions, such as those collected from CP, LR and RK and C<sub>31</sub> ββ homohopanol is the most abundant geohopanol identified in sinters from these sites. The observed difference is thought to derive from reduction of hopanoic acids to hopanols. The diagenetic end products from each location appear to be different to any previously studied environmental setting indicating an unusual degradation pathway affecting BHP preservation in silica sinters. This indicates that depositional setting not biological input is the key factor determining geohopanoic acid distributions in these environmental samples.

The results of this study complement previous investigations concerning the influence of environmental conditions upon BHP and hopanoic acid distributions and further elaborate upon the ecology of known BHP-producing bacteria contributing to the sedimentary record.

# PREFACE

## INTRODUCTION TO THE THESIS

In this thesis, BHP and geohopanoid (See Section 1.4) distributions have been analysed from a number of depositional regimes from geothermal ecosystems from around the globe. The main focus for this study has been silica-depositing systems. Previous work (Pancost *et al.*, 2005, 2006; Talbot *et al.*, 2005) has shown the potential of organic material to be preserved during incorporation into silica-based geothermal mineral deposits. Presented here are the results of a study centred upon BHP and hopanoid distributions from silica sinters, organo-sedimentary accumulations and mat-forming microbial consortia from terrestrial geothermal environments from around the world, including:

- 1) The Taupo Volcanic Zone, North Island, New Zealand
- 2) The El-Tatio Geyser Field, Chile
- 3) Geothermal areas in California and Nevada, USA.

The study of the distribution of BHPs and hopanoids from various depositional regimes within a sample site and comparisons from different geothermal areas from around the world has provided insight into the effect of elevated temperature, variations in pH, high-UV radiation and exposure to harmful chemical species on the hopanoid biomarker record and demonstrates the utility of BHPs and hopanoids in profiling vent geochemistry, past and present.

**Chapter 1** (introduction) offers a review of BHP-producing bacteria and previous work concerning the distribution of this class of compound in a range of environmental settings. The work in this thesis requires an understanding of the microbiology and geochemistry of the environments in question. A discussion of the biogenic nature and mechanisms of formation of silica sinters provides a basis for the interpretation of microbiological records that become

preserved in mineral depositions associated with geothermal ecosystems. The methods of analysis that enable the complexities and detail contained within preserved BHP and hopanoid distributions to be deduced are provided in **Chapter 2**. **Chapter 3** presents the results of an investigation centred upon actively precipitating facies and microbial mats from the Taupo Volcanic Zone (New Zealand), El-Tatio Geysir Field (Chile) and geothermal areas of Nevada and California (USA). The purpose of this is to understand and determine the BHP distributions from depositional settings that reflect the living portions of the vents in question. This study highlighted significant structural diversity within BHP distributions and also showed that common signatures were present in geographically distinct locations. As a means to investigate the long-term preservation potential of BHPs in sinter material, **Chapter 4** investigates the BHP distributions that are preserved in older, non-active sinters. These investigations showed that lipid distributions are based upon a complex relationship of changing bacterial communities and physiological response to changing environmental conditions. A number of novel structures were tentatively identified throughout the investigations carried out in Chapters 3 and 4, the presentation of which provides the basis for **Chapter 5**. One of the central themes of BHP research is the development of this class of compounds as ‘true’ chemotaxonomic biomarkers and to recognise the extent of bacteria capable of BHP-biosynthesis. As more structures become known this extends our knowledge of BHP-biosynthesis; possible novel BHPs detected throughout this study are reported and the implication of such findings are also discussed. **Chapter 6** concentrates upon the distributions of geohopanoids in silica sinters with a view to understanding the intermediate diagenetic processes affecting BHP preservation. Discussions of subjects that arise, directly and indirectly, as a consequence of this study can be found in the Conclusions (**Chapter 7**). Spectra of possible novel BHPs that did not merit inclusion or further discussion within the thesis are provided in **Appendix I**.

## AIMS AND HYPOTHESIS

*'BHPs have an unrealised potential to investigate bacterial populations and biogeochemical processes occurring in terrestrial geothermal vents'*

Investigation of the composition, abundance and variation of hopanoids, i.e. BHPs, biohopanoids and geohopanoids that become preserved in geothermal sinters and other lithological facies from a range of terrestrial geothermal locations will provide insight into the utility of hopanoid biomarkers for bacterial populations and biogeochemical processes occurring *in-situ*. Hopanoids have been shown to be useful in reconstructing bacterial populations in modern and ancient ecosystems (Summons *et al.*, 1999; Farrimond *et al.*, 2000; Talbot *et al.*, 2003c; Eigenbrode *et al.*, 2008); the major aim of this study is to determine the distribution of structures, investigate the origin and fate of hopanoid compounds in the depositional environments studied and to determine the potential of this class of compound as biomarkers in terrestrial geothermal settings.

*'Uncharacterised microbial populations are an untapped source of geochemical information that can be used in refining paleobiological and paleoclimatological investigations'*

Previous reports upon the distribution of microbial lipids that are preserved within sinter material have highlighted the presence of uncharacterised microbial species (Pancost *et al.*, 2005, 2006). The lipids identified derive from microbiota that are adapted to the conditions of the vent which can may include elevated temperature, low pH, anoxia, euxinia and can be located in hyper-arid locations that are exposed to high levels of UV radiation such as those situated in the El-Tatio Geyser Field. The examination of BHPs and hopanoids from high-temperature, acidic and hyper-arid locations will provide insight into the physiological response of BHP-producing bacteria to such environmental conditions. By comparing BHP distributions

as functions of environmental physico-chemical parameters and assessing intermediate diagenetic processes, it is hoped that this will provide an understanding of hopanoid distributions of ancient systems with respect to high temperature, anoxia or euxinia.

*'Diagenetic processes affecting the preservation of BHPs in sinters and associated depositions are reflective of environmental situation and are recorded in distributions of geohopanoids'*

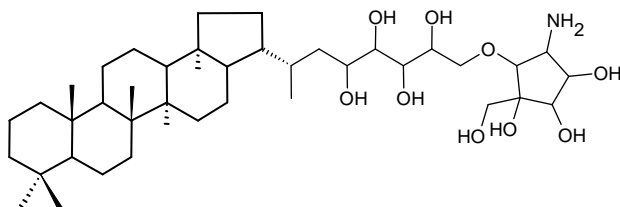
Distributions of geohopanoids that become preserved in silica sinters will allow investigation of the products of the intermediate stages of diagenesis. This should allow determination of the major diagenetic pathways affecting BHP preservation in silica sinters. The distributions of geohopanoids observed in this study will be compared to investigations of geohopanoids in other depositional settings, i.e. lacustrine and marine, to determine whether any common pathways are observable.

## NOMENCLATURE USED THROUGHOUT THE THESIS

The work in this thesis is based upon the detection and interpretation of naturally occurring compounds that contain a number of chemical functionalities. It is rather unusual that in this particular case there is no commonly accepted shorthand notation for describing BHP compounds. Therefore, a shorthand scheme for naming BHPs to be used throughout this thesis will be introduced.

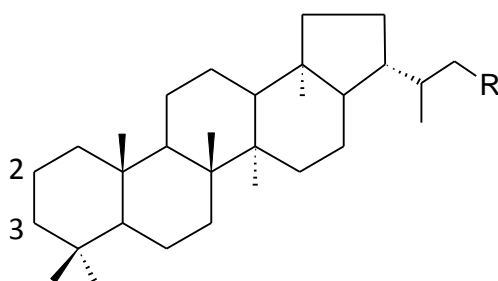
BH is used as a prefix to shorten *BacterioHopane*, a suffix then presented in italics will denote the degree of functionality contained within the side chain, i.e. tetrol, pentol or hexol. For example, *BHtetrol* is used as a shortened version of bacteriohopanetetrol, or BHT. For the purpose of this study, BHT will be referred to as *BHtetrol*. Likewise bacteriohopanepentol will be shortened to *BHpentol*. This will alleviate any confusion that would arise between the terms ‘BHPs’ and shortening bacteriohopanepentol to BHP. It follows that bacteriohopanehexol will be written as *BHhexol*. Naming of bacteriohopanepolyols containing an amino group at C-35 will follow that used by Talbot *et al.* (2001). For example, aminobacteriohopanetriol will be shortened to ‘aminotriol’. ‘Aminotetrol’ and ‘aminopentol’ will be used to refer to aminobacteriohopanetetrol and aminobacteriohopanepentol respectively. BHPs have also been reported which contain extra functional groups that are linked, via an ether or amino group, to C-35 of the carbon skeleton (e.g. Talbot *et al.*, 2007a). BHPs containing additional functionality at C-35 are referred to as ‘composite BHPs’ in this thesis. Composite BHP compounds which contain cyclitol ethers (e.g. example of nomenclature 1) will take the suffix ‘-cyc’, likewise BHP-compounds containing a  $\beta$ -linked glucosamine moiety will be referred to as ‘-gly’. In this case ‘gly’ will be used to avoid confusion with already standard nomenclature for naming amino acids, where ‘glu’ relates to glutamine. It follows that tetra-functionalised, composite cyclitol ether will be shortened to *BHTcyc*, where ‘T’ indicates the general nature of complexity contained with the side-chain. Shorthand versions of structures are given throughout the thesis

followed by a number in brackets which refers to the numbered structures shown in this section on pages xiv – xvi, which are shown in the order of appearance in the thesis. A list of compounds with abbreviations and corresponding structure numbers is given in the table presented on pages xvii – xx.

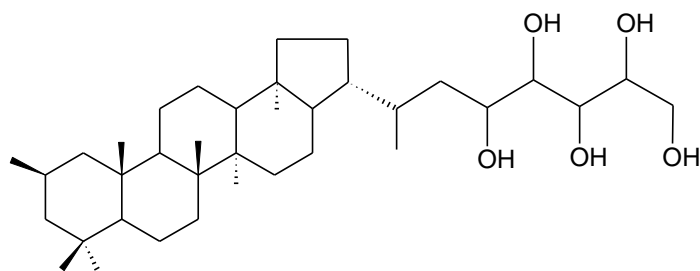


*Example of nomenclature 1: 35-O-β-cyclitol Bacteriohopane-31,32,33,34,35-ol. To be referred to as ‘BHPcyc’ throughout this study.*

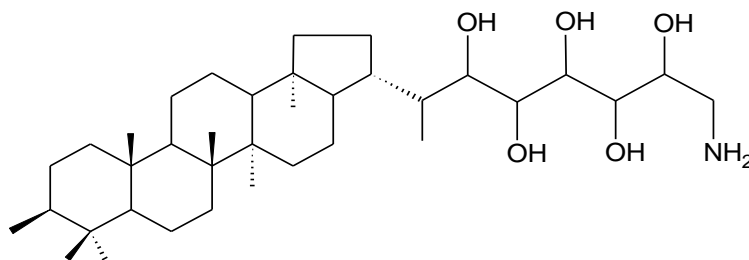
Structural modifications to the pentacyclic hydrocarbon system in the form of additional methyl groups or unsaturations are known. Additional methylations at C-2 and C-3 will be represented by a prefix of 2-me or 3-me respectively (example 2). A roman numeral II or III is used to refer to additional methyl groups at C-2 and C-3 respectively and will be added to the number given in brackets. For example, C-2 methylated bacteriohopanepentol will be shortened to 2-me BH*pentol* (**II-13**; See example 3) and C-3 methylated aminobacteriohopanepentol will be shortened to 3-me aminopentol (**III-15**; See example 4). Unsaturation is commonly noted with ‘Δ’ (e.g. Talbot *et al.*, 2007b) with the position of the unsaturations noted as a superscript numeral, e.g. Δ<sup>6</sup> indicating an unsaturation between C-6 and C-7 (see example 5 and 6).



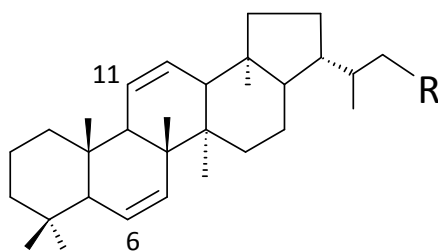
*Example of nomenclature 2: Hopane hydrocarbon showing C-2 and C-3 position.*



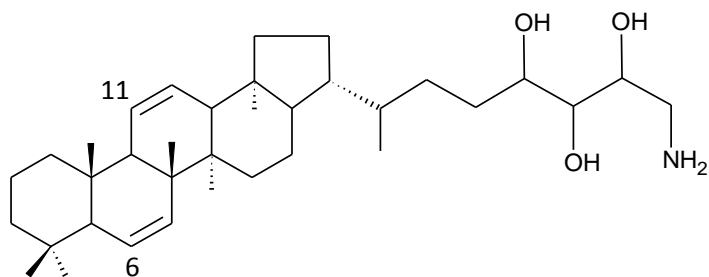
Example of nomenclature 3: C-2 methylated bacteriohopanepentol, in the thesis will be written as 2-me BHpentol (II-13).



Example of nomenclature 4: C-3 methylated aminobacteriohopanepentol, in the thesis will be written as 3-me aminopentol (III-15).



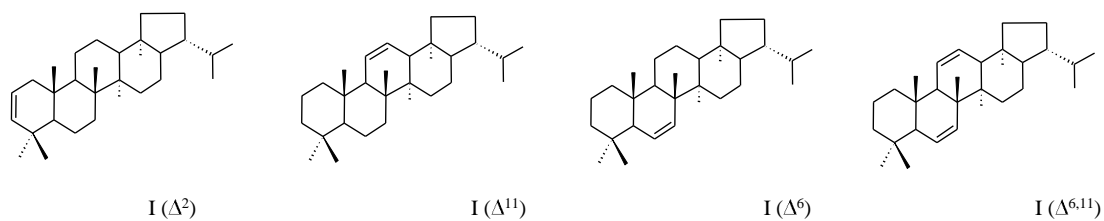
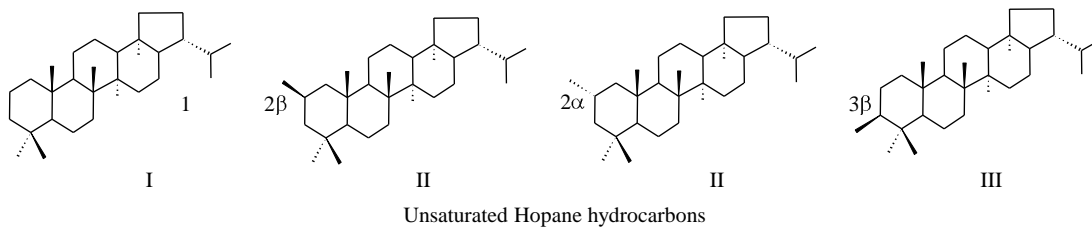
Example of nomenclature 5: Hopane hydrocarbon showing unsaturations at C-6 and C-11.



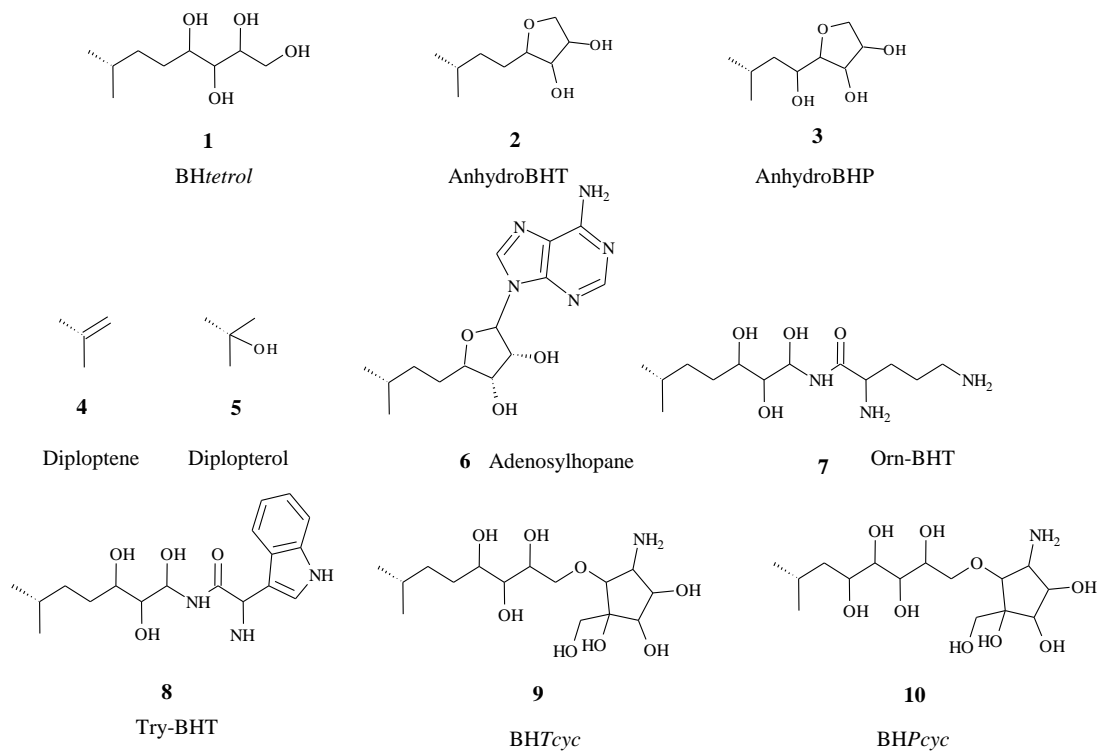
Example of nomenclature 6: Di unsaturated aminobacteriohopanetriol, in the thesis will be written as  $\Delta^{6,11}$  aminotriol ( $\Delta^{6,11}$ -22).

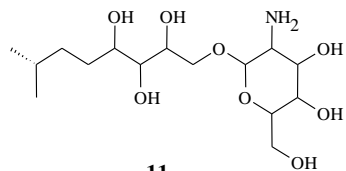
## STRUCTURES USED THROUGHOUT THE THESIS

### C<sub>30</sub> Hopane hydrocarbons plus methylated derivatives

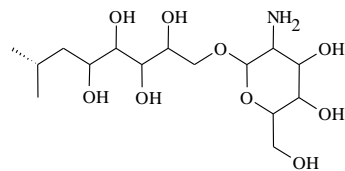


### Polyfunctionalised side-chain derivatives

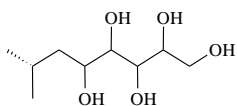




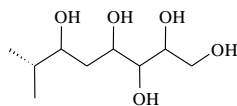
**11**  
BHTgly



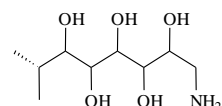
**12**  
BHPgly



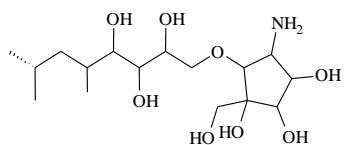
**13**  
BHpentol



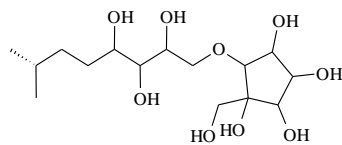
**14**  
Iso-BHpentol



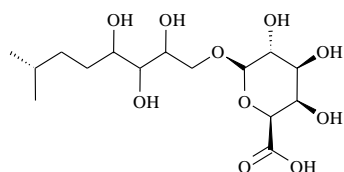
**15**  
Aminopentol



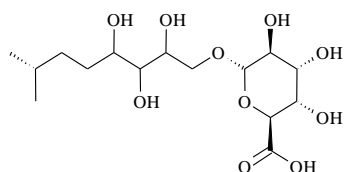
**16**  
31-me BHTcyc



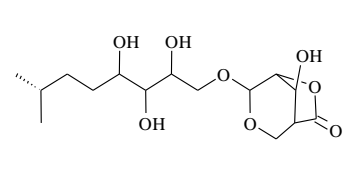
**17**  
PE BHT



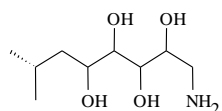
**18**  
GP BHT



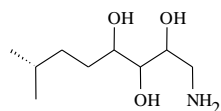
**19**  
AGP BHT



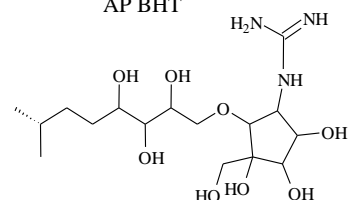
**20**  
AP BHT



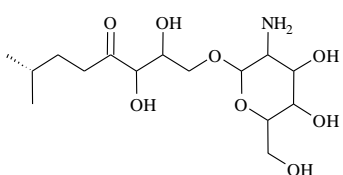
**21**  
Aminotetrol



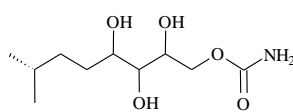
**22**  
Aminotriol



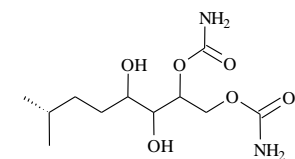
**23**  
Guanidine BHTcyc



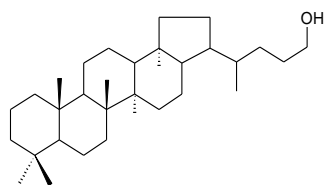
**24**  
Oxo-BHTcyc



**25**  
Carba-BHT

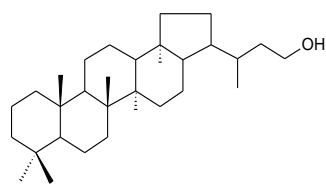


**26**  
Dicarba-BHT



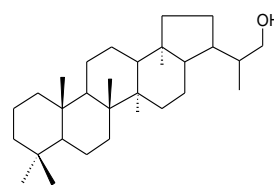
**46**

C<sub>32</sub> 17β(H), 21β(H) bishomohopanol



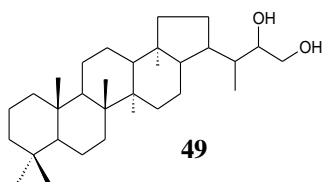
**47**

C<sub>31</sub> 17β(H), 21β(H) homohopanol



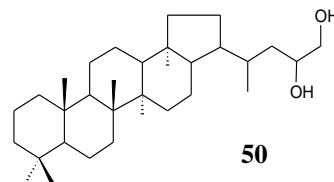
**48**

C<sub>30</sub> 17β(H), 21β(H) hopanol



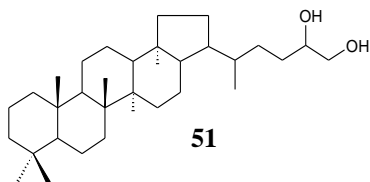
**49**

C<sub>31</sub> 17β(H), 21β(H) homohopanediol



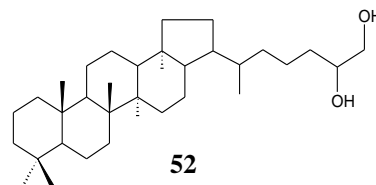
**50**

C<sub>32</sub> 17β(H), 21β(H) bishomopanediol



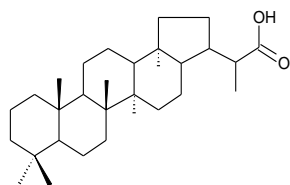
**51**

C<sub>33</sub> 17β(H), 21β(H) trishomopanediol



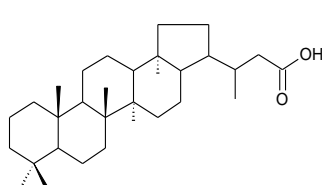
**52**

C<sub>34</sub> 17β(H), 21β(H) tetrakishopanediol



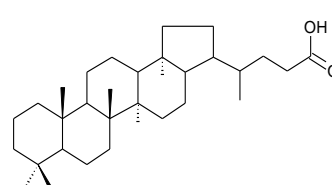
**53**

C<sub>30</sub> 17β(H), 21β(H) hopanoic acid



**54**

C<sub>31</sub> 17β(H), 21β(H) homohopanoic acid



**55**

C<sub>32</sub> 17β(H), 21β(H) bishomohopanoic acid

*Structures are not known for novel BHPs represented by numbers 27 – 36*

*The orientation of the stereochemical centres on compounds 1 -17 and 20 – 26 are not shown, although in many cases the stereochemistry has previously been determined (e.g. Talbot et al., 2001 and Talbot et al., 2008a and references therein), it was not possible to determine the stereochemistry using the methods employed in this thesis. Structures 18 and 19 are shown with stereochemistry within the sugar moiety as this determines the name of the compound and has been previously elucidated by NMR (Llopiz et al., 1992; Simonin et al., 1992).*

COMPOUND ABBREVIATIONS USED THROUGHOUT THE THESIS

No.	Compound	Abbreviation	Reference
1	32,33,34,35 bacteriohopanetetrol	BH <i>tetrol</i>	Langworthy <i>et al.</i> , 1976
2	32,35 anhydrobacteriohopanetetrol	AnhydroBHT	Bednarzyk <i>et al.</i> , 2004
3	31 hydroxyl-32,35-anhydrobacteriohopanetetrol	AnhydroBHP	Talbot <i>et al.</i> , 2005
4	Diploptene	-	
5	Diplopterol	-	
6	30- (5'-adenosyl) hopane	Adenosylhopane	Neunlist and Rohmer, 1985b
7	<i>N</i> -Ornithinyl-35-aminobacteriohopane-32,33,34-triol	orn-BHT	Neunlist <i>et al.</i> , 1985
8	<i>N</i> -Tryptophanyl-35-aminobacteriohopane 32,33,34-triol	Try-BHT	Neunlist <i>et al.</i> , 1985
9	Bacteriohopanetetrol cyclitol ether	BHT <i>cyc</i>	Renoux and Rohmer, 1985
10	Bacteriohopanepentol cyclitol ether	BHP <i>cyc</i>	Renoux and Rohmer, 1985
11	$\beta$ glycoside bacteriohopanetetrol	BHT <i>gly</i>	Rohmer, 1993
12	$\beta$ glycoside bacteriohopanepentol	BHP <i>gly</i>	Coolen <i>et al.</i> , 2008
13	31,32,33,34,35 pentahydroxybacteriohopane	BH <i>pentol</i>	Bisseret <i>et al.</i> , 1985
14	30,32,33,34,35 pentahydroxybacteriohopane	Iso-BH <i>pentol</i>	Bisseret <i>et al.</i> , 1985
15	(2 <i>S</i> )-35-aminobacteriohopane-30,31,32,33,34-pentol	Aminopentol	Neunlist and Rohmer, 1985c
16	31-methyl bacteriohopanetetrol cyclitol ether	31-methylBHT <i>cyc</i>	Simonin <i>et al.</i> , 1994
17	Bacteriohopanetetrol carbaspuedopentose ether	PE BHT	Talbot <i>et al.</i> , 2008a
18	O- $\alpha$ -D-glucuronopyranosylbacteriohopanetetrol	GP-BHT	Llopiz <i>et al.</i> , 1992
19	35-alturogalacturopyranosylbacteriohopanetetrol	AGP-BHT	Simonin <i>et al.</i> , 1992
20	3,5-Anhydrogalacturonopyranosylbacteriohopanetetrol	AP-BHT	Simonin <i>et al.</i> , 1992
21	35-amino-bacteriohopane-31,32,33,34-tetrol	Aminotetrol	Neunlist and Rohmer, 1985a
22	35-amino-bacteriohopane-32,33,34-triol	Aminotriol	Neunlist and Rohmer, 1985a
23	Guanidine-substituted bacteriohopanetetrol cyclitol ether	Guanidine-BHT <i>cyc</i>	Renoux and Rohmer, 1985
24	32-oxobacteriohopane-33,34,35-triol $\beta$ -glycoside	Oxo-BHT <i>cyc</i>	Flesch and Rohmer, 1989
25	35-carbamoylbacteriohopane-32,33,34-triol	Carba-BHT	Neunlist <i>et al.</i> , 1988

26	34,35-dicarbamoylbacteriohopane-32,33-diol	<i>Dicarba-BHT</i>	Neunlist <i>et al.</i> , 1988
27	35-O-β cyclitol ether 32-oxo-acteriohopane-33,34,35-ol*	<i>Oxo-BHTcyc</i>	
28	[M+H] <sup>+</sup> = m/z 1256	-	
29	[M+H] <sup>+</sup> = m/z 1018	-	
30	35-O-β guanidine-substituted cyclitol ether bacteriohopane-31,32,33,34,35-pentol*	<i>Guanidine BHPcyc</i>	
31	[M+H] <sup>+</sup> = m/z 1032	-	
32	[M+H] <sup>+</sup> = m/z 1046	-	
33	[M+H] <sup>+</sup> = m/z 974	-	
34	[M+H] <sup>+</sup> = m/z 988	-	
35	[M+H] <sup>+</sup> = m/z 1198	-	
36	35-O-β cyclitol ether 31-oxo bacteriohopane-32,33,34,35-tetrol*	<i>Oxo-BHPcyc</i>	
37	31-oxo-bacteriohopane-32,33,34,35-tetrol*	<i>Oxo-BHPentol</i>	
38	32-oxo-bacteriohopane-33,34,35-triol*	<i>Oxo-BHtetrol</i>	
39	Bacteriohopanehexol cyclitol ether	<i>BHHcyc</i>	
40	[M+H] <sup>+</sup> = m/z 1204	-	
41	[M+H] <sup>+</sup> = m/z 1146	-	
42	[M+H] <sup>+</sup> = m/z 984	-	
43	[M+H] <sup>+</sup> = m/z 960	-	
44	[M+H] <sup>+</sup> = m/z 1100	-	
45	[M+H] <sup>+</sup> = m/z 1114	-	
46	C <sub>30</sub> hopanol	C <sub>30</sub> hopanol	
47	C <sub>31</sub> homohopanol	C <sub>31</sub> hopanol	
48	C <sub>32</sub> bishomohomohopanol	C <sub>32</sub> hopanol	
49	C <sub>31</sub> homohopane-30,31-diol	C <sub>31</sub> hopanediol	
50	C <sub>32</sub> bishomohopane-31,32-diol	C <sub>32</sub> hopanediol	
51	C <sub>33</sub> trishomohopane-32,33-diol	C <sub>33</sub> hopanediol	
52	C <sub>34</sub> tetrakishomohopane-33,34-diol	C <sub>34</sub> hopanediol	

53	C <sub>33</sub> trishomohopane-31,32,33-triol	C <sub>33</sub> hopanetriol
54	C <sub>31</sub> homohopanoic acid	C <sub>31</sub> hopanoic acid
55	C <sub>32</sub> bishomohopanoic acid	C <sub>32</sub> hopanoic acid
56	C <sub>33</sub> trishomohopanoic acid	C <sub>33</sub> hopanoic acid
57	C <sub>33</sub> trishomohopanol	C <sub>33</sub> hopanol
58	C <sub>33</sub> trishomohopene-31,32,33-triol	C <sub>33</sub> hopenetriol
59	C <sub>32</sub> bishomohopanone	C <sub>32</sub> hopanone
60	C <sub>33</sub> trishomohopanone	C <sub>33</sub> hopanone
61	C <sub>32</sub> bishomohopane-30,32-diol	C <sub>32</sub> hopane-30,32-diol

\* Indicates tentatively assigned structures. Where it has not been possible to structurally characterise a BHP the peracetylated parent ion (i.e. [M+H]<sup>+</sup> or [M+H – AcOH]<sup>+</sup>) of the MS<sup>2</sup> spectra is used for reporting the presence in sinters or mats. Chemical nomenclature is that used by Rohmer and co-workers.

## TABLE OF CONTENTS

DECLARATION	II
ACKNOWLEDGEMENTS	III
ABSTRACT	V
PREFACE	VII
AIMS AND HYPOTHESIS	IX
NOMENCLATURE USED THROUGHOUT THE THESIS	XI
STRUCTURES USED THROUGHOUT THE THESIS	XIV
COMPOUND ABBREVIATIONS USED THROUGHOUT THE THESIS	XVII
TABLE OF CONTENTS	XX
LIST OF FIGURES	XXIX
LIST OF TABLES	XXXV
1 INTRODUCTION .....	1
1.1 Geothermal ecosystems.....	1
1.2 Biomineralisation and the preservation of biological records.....	3
1.2.1 Silica sinters.....	4
1.3 Lipids preserved in silica sinters.....	6
1.4 Bacteriohopanepolyols.....	7
1.4.1 Biohopanoid.....	9
1.4.2 Geohopanoid.....	9
1.5 BHPs: Origin and distribution in bacteria.....	10
1.5.1 The discovery of extended bacterial hopanoids.....	10
1.5.2 Biochemistry of bacteriohopanepolyols.....	12
1.5.3 The origin of the side chain.....	14
1.5.4 Structural variations.....	15
1.5.5 Distribution of BHPs in bacteria.....	17
1.5.5.1 Cyanobacteria.....	18
1.5.5.2 Methane oxidising bacteria.....	21
1.5.5.3 Acetic acid bacteria.....	22
1.5.5.4 Obligate anaerobic bacteria - The O <sub>2</sub> paradox.....	23
1.5.5.5 Purple non-sulphur bacteria.....	24

1.6	Distribution and significance of BHPs and hopanoids in environmental settings.....	25
1.6.1	Sedimentary biohopanoids.....	25
1.6.2	BHPs and geohopanoids as source indicators.....	26
2	SAMPLES, LOCATIONS AND METHODOLOGY.....	31
2.1	Samples.....	31
2.1.1	Sinters.....	31
2.1.2	Microbial mats.....	31
2.2	Sample suite and locations.....	31
2.2.1	Taupo Volcanic Zone, North Island, New Zealand.....	32
2.2.1.1	Champagne Pool.....	33
2.2.1.2	Orakei Korako.....	33
2.2.1.3	Loop Road.....	36
2.2.1.4	Opaheke Pool.....	36
2.2.1.5	Rotokawa.....	37
2.2.2	El-Tatio Geyser Field, Chile.....	40
2.2.2.1	Terrace springs.....	40
2.2.3	Geothermal areas of California and Nevada.....	42
2.3	Chemical methods.....	44
2.3.1	Extraction procedures.....	44
2.3.1.1	Bligh and Dyer extraction.....	44
2.3.1.2	Soxtherm extraction.....	45
2.3.1.3	Accelerated solvent extraction.....	45
2.3.1.4	Comparison of extraction techniques.....	45
2.3.2	Derivatisation.....	47
2.3.2.1	Acetylation.....	47
2.3.2.2	Methylation of hopanoic acids.....	48
2.3.2.3	PA/NaBH <sub>4</sub> cleavage of polyfunctionalised BHPs....	48
2.3.2.4	Silylation.....	49
2.3.3	Purification of lipid extracts from sinter samples.....	50

2.4	Analytical methods.....	51
2.4.1	High Performance Liquid Chromatography Atmospheric Pressure Chemical Ionization Multistage Mass Spectrometry (HPLC-APCI-MS <sup>n</sup> ).....	51
2.4.2	Gas Chromatography-Mass Spectrometry (GC-MS).....	52
3	DISTRIBUTIONS OF INTACT BACTERIOHOPANEPOLYOLS IN ACTIVE BIOFACIES OF TERRESTRIAL GEOTHERMAL SYSTEMS.....	56
3.1	Introduction.....	56
3.1.1	Aims and scope of this study.....	60
3.2	Results.....	61
3.2.1	Results: Analysis of BHP distributions from active facies of Champagne Pool.....	61
3.2.1.1	Floc material.....	61
3.2.1.2	Active sinter.....	62
3.2.2	BHP distributions of active sinters from Orakei Korako....	63
3.2.2.1	Fred and Maggie's Pool: Vent.....	63
3.2.2.2	Fred and Maggie's Pool: Outflow channel.....	66
3.2.2.3	Active sinter facies from Loop Road.....	67
3.2.2.4	Active sinter facies of Opaheke Pool.....	70
3.2.3	El-Tatio Geysers Field, Chile.....	71
3.3	Results: APCI HPLC MS <sup>n</sup> analysis of microbial mats.....	74
3.3.1	Nevada hot springs.....	75
3.3.1.1	Great Boiling Spring.....	75
3.3.1.2	Rick's Hot Creek.....	75
3.3.1.3	Paradise Valley.....	76
3.3.2	California hot springs.....	77
3.3.2.1	Surprise Valley.....	77
3.3.2.2	Eagleville.....	78
3.3.3	New Zealand hot springs.....	78
3.4	Discussion.....	81
3.4.1	Composition of BHP distributions of active sinters.....	81

3.4.1.1	Champagne Pool.....	81
3.4.1.2	Orakei Korako geothermal field.....	82
3.4.1.3	Loop Road hot springs.....	84
3.4.1.4	Opaheke Pool.....	85
3.4.1.5	El-Tatio Geyser Field.....	85
3.4.2	Composition of BHP distributions of microbial mats.....	87
3.4.3	Sources of BHPs in silica sinters.....	88
3.4.3.1	Anaerobic bacteria.....	88
3.4.3.2	Oxic-anoxic transition zone.....	89
3.4.4	Sources of BHPs in microbial mats.....	91
3.4.4.1	Cyanobacteria.....	91
3.4.4.2	Methanotrophic bacteria.....	94
3.4.5	Similarities and general trends.....	94
3.4.6	The natural laboratory.....	96
3.4.6.1	Temperature.....	96
3.4.6.2	pH.....	98
3.4.6.3	UV Intensity.....	99
3.5	Conclusions.....	99

4	INTACT BHPs OF NON-ACTIVE SINTER FORMATIONS IN TERRESTRIAL GEOTHERMAL ECOSYSTEMS.....	102
4.1	Introduction.....	102
4.1.1	Aims.....	103
4.2	Locations and sample suite.....	103
4.3	Results.....	103
4.3.1	BHP distributions of non-active sinters from Champagne Pool.....	103
4.3.1.1	CP3N.....	104
4.3.1.2	CP6N.....	104
4.3.1.3	CP7N.....	105
4.3.1.4	CP8N.....	105
4.3.1.5	CP11N.....	106
4.3.1.6	CP5N.....	106

4.3.2	BHP distributions of non-active sinters from Orakei Korako	110
	.....	110
4.3.2.1	OK4N.....	110
4.3.2.2	OK5N.....	110
4.3.2.3	OK6N.....	111
4.3.3	BHP distributions of non-active sinters from Loop Road....	113
4.3.3.1	LR3N.....	113
4.3.3.2	LR4N.....	113
4.3.3.3	LR5R.....	114
4.3.3.4	LR6R.....	114
4.3.4	BHP distributions of non-active sinters from Opaheke Pool	117
4.3.4.1	OP4N.....	117
4.3.4.2	OP5N.....	118
4.3.4.3	OP6N.....	118
4.3.5	BHP distributions of non-active sinters from Rotokawa.....	120
4.3.5.1	RK2N.....	120
4.3.5.2	RK3N.....	121
4.4	Discussion.....	125
4.4.1	Origins of BHPs detected in non-active sinters.....	125
4.4.1.1	Champagne Pool.....	125
4.4.1.2	Orakei Korako geothermal field.....	129
4.4.1.3	Loop Road hot springs.....	131
4.4.1.4	Opaheke Pool .....	132
4.4.1.5	Rotokawa .....	133
4.4.2	General trends and similarities.....	134
4.4.2.1	BHP signatures of cyanobacteria.....	138
4.4.2.2	BHPs distributions over spatial and temporal scales.	138
4.4.2.3	BHPs distributions in active vs. non-active sinters...	140
4.4.2.4	Novel bacteriohopanepolyols.....	142
4.5	Conclusions.....	142

5	NOVEL BHPs: NEW BIOMARKERS FOR BIOGEOCHEMISTRY AND INSIGHTS INTO THE EXTENT OF BHP-PRODUCING BACTERIA.....	145
5.1	Introduction.....	145
5.2	Aims.....	147
5.3	Structural assignment of novel BHPs based upon interpretation of APCI MS <sup>2</sup> spectra.....	147
5.3.1	Guanidine-substituted cyclitol ether BHPs.....	147
5.3.2	‘Oxo’-BHPs.....	151
5.3.2.1	Oxo-BHT <sub>cyc</sub> .....	151
5.3.2.2	Oxo-BHP <sub>cyc</sub> .....	152
5.3.2.3	Oxo-BHT <sub>triol</sub> .....	153
5.3.2.4	Oxo-BHT <sub>tetrol</sub> .....	153
5.3.3	Novel composite BHPs.....	157
5.3.3.1	Novel BHPs with a terminal group of mass 305 Da..	158
5.3.3.2	Novel BHPs with a terminal group of mass 433 Da..	161
5.3.3.3	Novel BHPs with a terminal group of mass 543 Da..	162
5.4	Structural assignment of novel BHPs based upon interpretation of APCI MS <sup>2</sup> and MS <sup>3</sup> spectra.....	165
5.4.1	Novel BHPs with a terminal group of mass 319 Da.....	165
5.4.2	Novel BHPs with a terminal group of mass 329 Da.....	169
5.4.3	Other novel BHPs.....	171
5.5	Discussion.....	177
5.5.1	Identification of novel BHPs in environmental matrices and bacterial cultures.....	179
5.5.2	Novel bacteriohopanepolyols.....	180
5.5.2.1	Guanidine-substituted bacteriohopanepentol cyclitol ether...	181
5.5.2.2	Oxo bacteriohopanepolyols.....	182
5.5.2.3	Novel composite BHPs.....	183
5.6	Conclusions.....	184

6	INVESTIGATING BHP DIAGENESIS IN SILICA SINTERS	186
6.1	Introduction.....	186
6.2	Aims.....	189
6.3	Results.....	190
6.3.1	GC-MS analysis of hopanoid distributions from active facies of Champagne Pool.....	195
6.3.1.1	CPf.....	195
6.3.1.2	CP1A.....	195
6.3.2	GC-MS analysis of hopanoid distributions from non-active facies of Champagne Pool.....	196
6.3.2.1	CP3N.....	196
6.3.2.2	CP6N.....	196
6.3.2.3	CP7N.....	197
6.3.2.4	CP8N.....	197
6.3.2.5	CP11N.....	198
6.3.2.6	CP5N.....	198
6.3.3	GC-MS analysis of active sinters from Orakei Korako.....	199
6.3.3.1	Fred and Maggie's Pool: Vent.....	199
6.3.3.2	Fred and Maggie's Pool: Outflow channel.....	202
6.3.4	GC-MS analysis of non-active sinters of Orakei Korako....	202
6.3.4.1	OK4N.....	202
6.3.4.2	OK5N.....	203
6.3.4.3	OK6N.....	203
6.3.5	GC-MS analysis of active sinters from Loop Road.....	204
6.3.5.1	LR2AS.....	204
6.3.5.2	LR2A.....	205
6.3.5.3	LR3A.....	205
6.3.6	GC-MS analysis of non-active sinter facies of Loop Road..	206
6.3.6.1	LR3N.....	206
6.3.6.2	LR4N.....	206
6.3.6.3	LR5R.....	207
6.3.6.4	LR6R.....	207
6.3.7	GC-MS analysis of active sinter facies of Opaheke Pool.....	208
6.3.7.1	OP2A.....	208

6.3.7.2	OP7A.....	208
6.3.8	GC-MS analysis of non-active sinters from Opaheke Pool.	209
6.3.8.1	OP4N.....	209
6.3.8.2	OP5N.....	210
6.3.8.3	OP6N.....	211
6.3.9	GC-MS analysis of non-active sinters from Rotokawa.....	212
6.3.9.1	RK2N.....	212
6.3.9.2	RK3N.....	212
6.3.10	El-Tatio Geysler Field, Chile.....	215
6.3.10.1	ET1A.....	215
6.3.10.2	ET25A.....	216
6.3.10.3	ET26A.....	216
6.4	Discussion.....	217
6.4.1	Geohopanoide composition of silica sinters.....	217
6.4.1.1	Hopanols.....	217
6.4.1.2	Hopanediols and hopanetriols.....	221
6.4.1.3	Hopanoic acids.....	222
6.4.2	Distribution of intermediate diagenetic product groups in sinters.....	226
6.4.2.1	Champagne Pool.....	226
6.4.2.2	Orakei Korako.....	227
6.4.2.3	Loop Road.....	228
6.4.2.4	Rotokawa.....	229
6.4.2.5	Opaheke Pool.....	229
6.4.2.6	El-Tatio Geysler Field.....	230
6.4.3	General trends and similarities.....	234
6.4.3.1	Active versus non-active sinters.....	235
6.4.4	C <sub>31</sub> hopanol anomaly: Origin and significance.....	236
6.5	Conclusions.....	238

7	CONCLUSIONS AND FUTURE WORK .....	239
7.1	Conclusions.....	239
7.1.1	Distribution of BHPs in active biofacies.....	240
7.1.1.1	Actively precipitating silica sinters.....	240
7.1.1.2	Sub-aqueous floc material.....	243
7.1.1.3	Microbial mats.....	244
7.1.2	BHP distributions of non-active sinters.....	245
7.1.3	Distributions of geohopanoids in silica sinters.....	248
7.1.3.1	Hopanoids as biomarkers for ancient geothermal systems.....	250
7.1.4	The identification of novel BHPs.....	251
7.1.5	Summary.....	253
7.2	Future work and recommendations.....	255
7.2.1	Parallel microbiological investigations.....	255
7.2.2	BHP signatures from mat-forming cyanobacteria.....	257
7.2.3	Diagenesis of BHPs.....	258
7.2.4	Other extreme environmental settings.....	259
	REFERENCES .....	262
	APPENDIX – MS <sup>2</sup> AND MS <sup>3</sup> SPECTRA OF POSSIBLE NOVEL BHPs.....	297

## LIST OF FIGURES

### PREFACE

Example of nomenclature 1: Bacteriohopanepentol cyclitol ether.....	xii
Example of nomenclature 2: Hopane hydrocarbon.....	xii
Example of nomenclature 3: 2-methyl bacteriohopanepentol.....	xiii
Example of nomenclature 4: 3-methyl aminobacteriohopanepentol.....	xiii
Example of nomenclature 5: Hopane hydrocarbon showing unsaturations.....	xiii
Example of nomenclature 6: Di unsaturated aminobacteriohopanetriol.....	xiii

### CHAPTER 1 - INTRODUCTION

Figure 1.1 Silica-depositing terrestrial geothermal vents of the Taupo Volcanic Zone.....	5
Figure 1.2 Generic BHP structure.....	8
Figure 1.3 Isomeric forms observed in bacteriohopanetetrol.....	9
Figure 1.4 Formation of hopane hydrocarbon.....	13
Figure 1.5 Formation of sterane hydrocarbon.....	13
Figure 1.6 Formation of isoprene units via mevalonate pathway.....	14
Figure 1.7 Formation of isoprene units via methylerythritol pathway.....	14
Figure 1.8 Hypothetical formation of 2-methylbacteriohopanepolyols.....	17
Figure 1.9 Phyla tested for BHP biosynthesis.....	19
Figure 1.10 Pathways of post-depositional alteration of BHPs.....	28

### CHAPTER 2 – SAMPLES, LOCATIONS AND METHODOLOGY

Figure 2.1 Taupo Volcanic Zone.....	32
Figure 2.2 Geothermal areas of the Taupo Volcanic Zone.....	32
Figure 2.3 Photographs of Champagne Pool.....	33
Figure 2.4 Photographs of Fred and Maggie's Pool, Orakei Korako.....	35
Figure 2.5 Photographs of Fred and Maggies Pool, Orakei Korako.....	35
Figure 2.6 Photograph of Golden Fleece Terrace, Orakei Korako.....	35
Figure 2.8 Panoramic photograph of Orakei Korako Geothermal Field.....	36
Figure 2.9 Sample locations.....	38
Figure 2.10 Geographical location of the El-Tatio Geyser Field .....	40
Figure 2.11 Comparison of extraction procedures 1.....	46

Figure 2.12 Comparison of extraction techniques 2.....	47
Figure 2.13 Comparison of abundances during runs of acetylated fractions.....	53
Figure 2.14 Comparison of abundances during runs of PA/NaBH <sub>4</sub> fractions.....	54
Figure 2.15 Schematic of analytical methodology.....	55

### CHAPTER 3 – ACTIVE BIOFACIES

Figure 3.1 Sinter formations at Champagne Pool.....	58
Figure 3.2 Partial mass chromatogram showing BHP distribution observed in floc material from Champagne Pool.....	62
Figure 3.3 Partial mass chromatograms showing distribution of BHPs in sinter from air-water interface from Champagne Pool.....	63
Figure 3.4 BHP distributions of active sinter collected from the vent of Fred and Maggie’s Pool.....	65
Figure 3.5 Partial mass chromatogram showing BHPs detected in active sinter taken from outflow channel of Fred and Maggie’s Pool.....	67
Figure 3.6 Partial mass chromatogram showing BHPs detected in active sinters of Loop Road.....	69
Figure 3.7 Partial mass chromatogram showing BHPs detected in active sinter from Opaheke Pool.....	70
Figure 3.8 Partial mass chromatograms showing BHPs detected in active sinter from El-Tatio Geyser Field.....	72
Figure 3.9 Partial mass chromatograms showing BHPs detected in active sinter from El-Tatio Geyser Field.....	72
Figure 3.10 Typical distribution of novel BHPs from mat-forming microbial consortia.....	74
Figure 3.11 Distribution of known BHPs detected in a microbial mat from Surprise Valley.....	78
Figure 3.12 Graph showing BHP abundance of active sinters from Taupo Volcanic Zone plotted as a function of temperature.....	97
Figure 3.13 BHP abundance as function of sample environment pH.....	98

## CHAPTER 4 – BHPs IN NON-ACTIVE SINTERS

Figure 4.1 Partial mass chromatograms showing BHP distribution observed in sample CP3N.....	107
Figure 4.2 Partial mass chromatograms showing BHP distribution observed in sample CP6N.....	107
Figure 4.3 Partial mass chromatograms showing BHP distribution observed in sample CP7N.....	108
Figure 4.4 Partial mass chromatograms showing BHP distribution observed in sample CP8N.....	108
Figure 4.5 Partial mass chromatograms showing BHP distribution observed in sample CP11N.....	109
Figure 4.6 Partial mass chromatograms showing BHP distribution observed in sample CP5N.....	109
Figure 4.7 Partial mass chromatograms showing BHP distribution observed in sample OK4N.....	111
Figure 4.8 Partial mass chromatograms showing BHP distribution observed in sample OK5N.....	112
Figure 4.9 Partial mass chromatograms showing BHP distribution observed in sample OK6N.....	112
Figure 4.10 Partial mass chromatograms showing BHP distribution observed in sample LR3N .....	116
Figure 4.11 Partial mass chromatograms showing BHP distribution observed in sample LR4N .....	116
Figure 4.12 Partial mass chromatograms showing BHP distribution observed in sample LR5R .....	117
Figure 4.13 Partial mass chromatograms showing BHP distribution observed in sample LR6R.....	117
Figure 4.14 Partial mass chromatograms showing BHP distribution observed in sample OP4N.....	119
Figure 4.15 Partial mass chromatograms showing BHP distribution observed in sample OP5.....	120
Figure 4.16 Partial mass chromatograms showing BHP distribution observed in sample OP6.....	120
Figure 4.17 Partial mass chromatograms showing BHP distribution observed in	

sample RK2N.....	122
Figure 4.18 Partial mass chromatograms showing BHP structures observed in sample RK3N.....	123
Figure 4.19 Percentage of BHP assemblage as BHPs containing a C-35 ether linked composite functionality of total BHPs detected in Champagne Pool study....	126
Figure 4.20 Composition of BHP assemblage detected in Champagne Pool sinters.	129
Figure 4.21 Sinter terrace at Orakei Korako.....	130
Figure 4.22 Relative distribution of tetra-, penta-, and hexafunctionalised BHPs from certain environmental conditions.....	137
Figure 4.23 Total abundance of BHPs in silica sinters of Champagne Pool.....	140

## CHAPTER 5 – NOVEL BHPs

Figure 5.1 MS <sup>2</sup> spectrum of [M+H] <sup>+</sup> = m/z 1086 and m/z 1144.....	149
Figure 5.2 Peracetylated structures of guanidine-BHT and guanidine-BHP.....	149
Figure 5.3 Partial mass chromatograms showing retention time of guanidine-substituted BHT <sub>cyc</sub> and guanidine-substituted BHP <sub>cyc</sub> relative to retention times of BHT <sub>cyc</sub> and BHP <sub>cyc</sub> .....	149
Figure 5.4 Figure showing MS <sup>2</sup> spectra of proposed novel ‘oxo-BHPs’ detected in silica sinters.....	154
Figure 5.5 Tentatively-assigned structures of novel ‘oxo-BHPs’ detected throughout silica sinters of the Taupo Volcanic Zone.....	155
Figure 5.6 Partial mass chromatogram showing relative retention times of tentatively-assigned novel composite oxo-BHPs compounds to BHP <sub>cyc</sub> and BHT <sub>cyc</sub> .....	158
Figure 5.7 Characteristic fragmentation pathways expected in composite BHPs.....	158
Figure 5.8 Characteristic fragmentation pathways expected in composite BHPs containing an A-ring methylation.....	159
Figure 5.9 MS <sup>2</sup> spectra of novel composite BHPs with terminal group of mass 305 Da.....	159
Figure 5.10 Characteristic fragmentations of novel BHPs with terminal group of mass 305 Da.....	159
Figure 5.11 Possible structures of tentatively-assigned novel BHPs containing terminal group of mass 305 Da.....	160
Figure 5.12 Partial mass chromatogram showing retention times of tentatively-assigned novel composite BHPs compounds relative to BHP <sub>cyc</sub> and	

BHT <sub>cyc</sub> .....	160
Figure 5.13 MS <sup>2</sup> spectra of [M+H] <sup>+</sup> = m/z 1204 and m/z 1146.....	162
Figure 5.14 MS <sup>2</sup> spectrum [M+H] <sup>+</sup> = m/z 1256 and m/z 1198.....	163
Figure 5.15 Partial mass chromatogram showing distribution of novel BHPs from mat- forming cyanobacteria.....	166
Figure 5.16 Products released via PA/NaBH <sub>4</sub> cleavage of BHPs extracted from microbial mats.....	166
Figure 5.17 Schematic of cleavage of side-chain component of novel BHPs and resulting GC-MS amenable products.....	167
Figure 5.18 MS <sup>2</sup> and MS <sup>3</sup> spectra of novel BHPs identified in mat-forming cyanobacteria.....	167
Figure 5.19 Structures of novel compounds identified in microbial mats from geothermal vents.....	168
Figure 5.20 MS <sup>2</sup> and MS <sup>3</sup> Spectra of [M+H] <sup>+</sup> = m/z 984.....	170
Figure 5.21 Possible structures and fragmentations that enable tentative structural assignment of novel BHP relating to m/z 984.....	171
Figure 5.22 MS <sup>2</sup> and MS <sup>3</sup> spectra of novel BHPs with [M+H] <sup>+</sup> = m/z 1100 and m/z 1114.....	173
Figure 5.23 Putative structure showing main fragmentations observed during APCI-MS <sup>n</sup> analysis of [M+H] <sup>+</sup> = m/z 1100 and 1114.....	173
Figure 5.24 Tentative structural assignment of guanidine-substituted BHP <sub>cyc</sub> .....	181
Figure 5.25 Oxo-BHPs. Tentative structural characterisation of structures detected in Champagne Pool sinters.....	182
Figure 5.26 Structure of oxo bacteriohopanetetrol glucosamine.....	183

## CHAPTER 6 – BHP DIAGENESIS

Figure 6.1 Formation of C <sub>32</sub> ββ hopanol from BH <sub>tetrol</sub> via sequential degradation of side-chain component.....	187
Figure 6.2 Formation of C <sub>32</sub> ββ hopanol from BH <sub>tetrol</sub> via oxidation and decarboxylation of terminal alcohol group.....	187
Figure 6.3 Formation of anhydroBHT via intramolecular cyclisation of BH <sub>tetrol</sub> ..	188
Figure 6.4 Hypothetical formation of anhydroBHT from adenosylhopane.....	188
Figure 6.5 Partial m/z 191 chromatogram of acetylated fraction showing typical distribution of hopanoids.....	191

Figure 6.6 Partial m/z 191 chromatogram showing distribution of hopanoic acids.	191
Figure 6.7 Partial m/z 191 mass chromatogram showing distribution of geohopanoids identified in acetylated fraction of sample OK1-TA.....	200
Figure 6.8 GC-MS spectra of early eluting isomer of acetylated C <sub>33</sub> ββ hopanol...	200
Figure 6.9 Partial m/z 191 mass chromatogram showing geohopanoids identified in sample OP4N.....	209
Figure 6.10 Partial m/z 191 mass chromatogram showing geohopanoids identified in sample RK2N.....	212
Figure 6.11 GC-MS spectra of C <sub>32</sub> ββ hopanone.....	212
Figure 6.12 GC-MS spectra of C <sub>33</sub> ββ hopanone.....	212
Figure 6.13 GC-MS spectra of C <sub>32</sub> ββ hopane-30,32-diol.....	213
Figure 6.14 Partial m/z 191 mass chromatogram showing geohopanoids identified in sample ET1A.....	214
Figure 6.15 Ratios of geohopanoids and BHPs in active sinters.....	216
Figure 6.16 Ratios of geohopanoids and BHPs in non-active sinters.....	216
Figure 6.17 Relative distributions of terminal hopanols surveyed during this study	220
Figure 6.19 Composition of geohopanoid distributions observed in silica sinters from Orakei Korako.....	231
Figure 6.20 Composition of geohopanoid distributions observed in silica sinters from Loop Road.....	231
Figure 6.21 Composition of geohopanoid distributions observed in silica sinters from Opaheke Pool.....	232
Figure 6.22 Composition of geohopanoid distributions observed in silica sinters from Rotokawa.....	232
Figure 6.23 Composition of geohopanoid distributions observed in silica sinters from El-Tatio Geyser Field.....	232
Figure 6.24 Reduction of hopanoic acids to terminal hopanols.....	234

## APPENDIX

Figure A1 Spectra of possible novel BHP compounds with $[M+H]^+ = m/z$ 731.....	300
Figure A2 Spectra of possible novel BHP compounds with $[M+H]^+ = m/z$ 847.....	301
Figure A3 Spectra of possible novel BHP compounds with $[M+H]^+ = m/z$ 916.....	302
Figure A4 Spectra of possible novel BHP compounds with $[M+H]^+ = m/z$ 918.....	303
Figure A5 Spectra of possible novel BHP compounds with $[M+H]^+ = m/z$ 1040....	304
Figure A6 Spectra of possible novel BHP compounds with $[M+H]^+ = m/z$ 1100....	305

## LIST OF TABLES

### CHAPTER 1 – INTRODUCTION

Table 1.1 BHPs and polyfunctionalised hopanoids as source indicators in bacteria and observations from environmental settings.....	29
Table 1.2 Geohopanoids as source indicators.....	30

### CHAPTER 2 – SAMPLES, LOCATIONS AND METHODOLOGY

Table 2.1 Chemical composition of vent fluid of Fred and Maggie’s Pool.....	34
Table 2.2 Composition of vent fluid from Rotokawa vent.....	39
Table 2.3 Lithographical setting and notes of sinter samples used in this study.....	41
Table 2.4 Location and environmental conditions of microbial mats.....	43

### CHAPTER 3 – BHP DISTRIBUTIONS OF ACTIVE BIOFACIES

Table 3.1 Abundances of BHPs detected in active sinters from Taupo Volcanic Zone and El-Tatio Geysir Field.....	72
Table 3.2 Abundances of BHPs detected in microbial mats.....	80
Table 3.3 Occurrences of novel BHPs during analyses of microbial mats.....	93

### CHAPTER 4 – NON-ACTIVE SINTERS

Table 4.1 Abundances of BHPs identified in non-active sinters of the Taupo Volcanic Zone.....	124
---	-----

## CHAPTER 5 – NOVEL BHPs

Table 5.1 Assignment of ions for guanidine-substituted BHPs.....	150
Table 5.2 Assignment of ions observed in APCI-MS <sup>2</sup> spectra of oxo-BHPs.....	156
Table 5.3 Characteristic ions observed during APCI fragmentations of novel BHPs .....	164
Table 5.4 Assignment of ions observed in APCI-MS <sup>n</sup> spectra of novel BHPs from mat-forming microbial consortia.....	168
Table 5.5 Characteristic ions observed during APCI fragmentations of tentatively assigned novel BHPs.....	174
Table 5.6 Abundance of tentatively-assigned BHPs observed in the study of floc, active and non-active sinters from Taupo Volcanic Zone and El-Tatio Geysir Field.....	175
Table 5.7 Abundance of tentatively-assigned BHPs observed in the study of microbial mats from geothermal regions in Taupo Volcanic Zone, Nevada and California.....	176
Table 5.8 Diagnostic ions of tetra-, penta- and hexafunctionalised BHPs.....	180
Table 5.9 Tentatively-assigned novel BHPs as identified during APCI MS <sup>n</sup> analysis.....	184

## CHAPTER 6 - GEOHOPANOIDS

Table 6.1 Structures, abbreviations and peak numbers of geohopanoids.....	192
Table 6.2 Abundances of geohopanoids identified in active sinters of Taupo Volcanic Zone and El-Tatio Geysir Field.....	193
Table 6.3 Abundances of geohopanoids identified in non-active sinters of Taupo Volcanic Zone.....	194
Table 6.4 Composition of distributions of geohopanoids and BHPs of active sinters.....	223
Table 6.5 Composition of distributions of geohopanoids and BHPs of non-active sinters.....	224

# 1 INTRODUCTION

## 1.1 GEOTHERMAL ECOSYSTEMS

Terrestrial geothermal ecosystems are widespread throughout the modern natural world. They are found along tectonic boundaries or at continental hot spots, such as Yellowstone National Park, USA (Bock and Goode, 1996). They represent a surface manifestation of areas of instability within the Earth's crust and provide a central focus for water, heated at depth, to interact with a predominantly mesophilic biosphere. The water-heat-rock interaction results in alteration of fluid chemistry, which creates geothermal vents with fluids that, exhibit an array of exotic mineral species. The disequilibria that are generated by geothermal energy sources, whether the end product is a submarine or terrestrial system, can provide the energy requirement for many chemical reactions, either biotic or abiotic. The dynamics of this interaction between the hydrosphere, geosphere and biosphere results in the formation of many micro-niches and is demonstrated by the rich diversity of life colonising the vent fluids and surrounding locality (Brock, 1978). When water, altered by geothermal processes in deep aquifers in the Earth's crust reaches the surface, a new set of reactions take place, usually involving deposition of the dissolved mineral content. Examples exist in modern environments such as carbonate chimneys from deep-sea systems, such as the Lost City Hydrothermal Field (e.g. Kelley *et al.*, 2005), or as the formation of silica-sinters observed in terrestrial vents from the Taupo Volcanic Zone, New Zealand (e.g. Mountain *et al.*, 2003) or Yellowstone National Park, USA.

Modern ecosystems that harbour organisms which require, or are adapted to, high-temperature conditions are important with respect to studies of the evolution and diversification of life on an early Earth. Evidence from the geological record indicates that colonisation of an early Earth would have suited thermophilic (Greek: *Thermos*, Heat; *Philos*; Loving) organisms (Nisbet and Sleep, 2001) and this can be further evidenced by molecular phylogenetic analysis

## Introduction

based on 16S rRNA of extant life and the close position of hyperthermophiles and thermophiles to the root of the tree of life (e.g. Stetter, 1996). However, the notion of a universal tree of life itself is open to debate (e.g., Baptiste and Boucher, 2007), and may only provide information regarding the position of the last common ancestor and not necessarily the true common ancestor, or first life on Earth. Whether the observation that thermophilic phyla dominate the branches closest to the root of the tree is representative of a true common ancestor or a manifestation of a bottleneck in evolutionary biology remains a subject of debate (e.g. Schwartzman and Lineweave, 2004). Nonetheless, investigations of the microbial diversity associated with geothermal systems will allow inference of some information regarding evolutionary history.

Terrestrial geothermal systems provide an interesting locus with which to investigate the diversification and early evolution of life as in particular terrestrial geothermal environments represent the intersection of biotic populations that are predominantly thermophilic with a mesophilic biosphere. The proximity of these two biospheres is probably representative of a 'jump' in evolution between ecosystems based on chemosynthesis to those based upon photosynthesis.

The ability of life to survive in the most extreme of conditions on Earth has proven to be a catalyst for research concerning the ability of extra-terrestrial bodies to sustain life. Preservation of biosignatures associated with geothermal systems has become useful in the development of protocols for investigation of life, living or extinct, on other planets, such as Mars or Europa. Evidence suggests that Mars once contained liquid water at its surface (Carr, 1996; Squyers *et al.*, 2004; Jakosky *et al.*, 2005). Recent evidence also points to the presence of silica-rich deposits similar to those observed in and around terrestrial geothermal vents (Squyers *et al.*, 2008). The investigations of the ecological diversity of modern geothermal systems and the deposition and preservation of biosignatures contained therein is therefore not only relative

to the story of the evolution and limits of life on Earth but, and perhaps more importantly, the story of life throughout the Universe.

### 1.2 BIOMINERALISATION AND THE PRESERVATION OF (PALEO)BIOLOGICAL RECORDS

The investigation of biomineralisation in modern terrestrial geothermal ecosystems proceeds along two vectors: field studies from various sites around the world concerning various mineral phases (Ferris *et al.*, 1987; Pentecost, 1996; Cady and Farmer, 1996; Jones and Renault, 1996; Renault *et al.*, 1998; Konhauser *et al.*, 2001; Jones *et al.*, 2001; Mountain *et al.*, 2003; Inagaki *et al.*, 2003; Geptner *et al.*, 2005; Phoenix *et al.*, 2006; Jones and Renault, 2007) or laboratory based studies (Oehler and Schopf, 1971; Westall, 1997; Cady and Farmer, 1996; Phoenix *et al.*, 2000; Toporski *et al.*, 2002; Yee *et al.*, 2003; Lalonde *et al.*, 2005, 2008a, 2008b). The major aim of this body of research is to provide knowledge concerning the fossilisation processes that occur in modern terrestrial geothermal settings that ultimately will allow more reliable interpretation of ancient hydrothermal deposits. This work relies upon identification of microfossils and determining the biogenic nature of these artefacts. Much of what we know from Archean and Proterozoic geothermal ecosystems derives from morphological assessment of ancient depositions and metasediments (e.g. Schopf, 1993). However the correlation of ancient and contemporaneous micro-fossils is much debated (e.g. Brasier *et al.*, 2002) and relies upon better knowledge of the processes governing biomineralisation and even then little can be construed about cell physiology from morphological assessment.

Microbially-mediated precipitation of mineral phases can proceed via two main mechanisms, active and passive. Active mediation involves pathways where microbial life is directly responsible for mineralisation either by osmotic uptake of geothermal fluid (Lynne and Campbell, 2003) or as a consequence of metabolism (e.g. Birnbaum and Wireman, 1984; Ferris *et al.*, 1987; Birnbaum *et al.*, 1989; Pentecost, 1996). Passive mediation relies upon the micro

## Introduction

organism providing a site for nucleation via complexation of metal ions such as  $\text{Fe}^{2+}$  (e.g. Ferris *et al.*, 1988) or through providing a template for silica deposition through hydrogen bonding interactions between amorphous silica and terminal hydroxyl and amino groups of cell membranes or cell tissue (e.g. Knoll, 1985).

### 1.2.1 SILICA SINTERS

Silica-depositing hot-spring systems are widespread throughout the modern natural world and the ancient geological record. They are characterised by the reaction of hot-water from deep aquifers with surface and near-surface rocks which results in the formation of alkali-chloride waters that are super-saturated with respect to amorphous silica (Benning *et al.*, 2005).

Sinter is mainly composed of silica and is formed as a consequence of geothermal waters reaching the surface, then the combination of a sharp decrease in temperature and pressure results in the formation of striking sinter terraces. Silica precipitation proceeds rapidly and results in the deposition of successions of amorphous silica. Sinters usually contain a number of other minerals in lower concentrations; which usually result in the formation of uniquely coloured sinter formations (Figure 1.1).



*Figure 1.1 Silica-depositing terrestrial geothermal vents of the Taupo Volcanic zone. Top left: Artist's palette (Wai-o-tapu). Top right: Western margin of Champagne Pool (Wai-o-tapu). Bottom left: Artist's palette (Orakei Korako). Bottom right: Map of Africa (Orakei Korako). The yellow and orange colours observed at wai-o-tapu geothermal features are a consequence of a high content of sulphur containing minerals. The pearlescent blue colour observable in Orakei Korako springs is caused by the refractive properties of silica in water. A lower concentration of sulphur at this site allows the formation of orange and brown-coloured photosynthetic mat-forming microbial communities.*

There are numerous studies concerning the role of microbial biosilification (e.g. Phoenix *et al.*, 2000; Mountain *et al.*, 2003; Benning *et al.*, 2005). However, the formation of silica sinters is thought to proceed via abiotic processes such as cooling, evaporation or surface modulations, such as wave effects in large systems or splashing in turbid systems. It is likely microbial life play a role in the textural development of silica sinters (e.g. Mountain *et al.*, 2003). A

combination of abiotic and biotic factors leads to the incorporation of microbial colonies into the matrix of the sinter, facilitating preservation of recognisable artefacts including morphological remains (Cady and Farmer, 1996), ultra-fine extra-cellular structure (Phoenix *et al.*, 2005) and microbial membrane lipids (Pancost *et al.*, 2005).

### 1.3 LIPIDS PRESERVED IN SILICA SINTERS

Organic geochemical studies of modern terrestrial geothermal ecosystems can proceed via a number of approaches (Summons *et al.*, 1996; van der Meer *et al.*, 2008). Lipid biomarkers that derive from microbial consortia colonising vent localities that become preserved in mineral deposits associated with geothermal processes provide tools which allow correlations between extinct and extant biota and provide a means to investigate biologically-mediated processes and populations occurring in-situ.

Recent studies on the lipid composition contained within silica sinters from the Taupo Volcanic Zone, North Island, New Zealand (TVZ) have shown that preservation of organic compounds that are directly indicative of precursor organisms are abundant, and incorporation of organic matter into the silica matrix appears to facilitate molecular preservation (Pancost *et al.*, 2005, 2006; Talbot *et al.*, 2005; Gibson *et al.*, 2008; Kaur *et al.*, 2008). Initial reports adopted a holistic approach to lipid analyses (Pancost *et al.*, 2005, 2006; Talbot *et al.*, 2005) and demonstrated an abundance of well preserved bacterial and archaeal lipids in silica sinters from the TVZ. Subsequent reports have shown that silica sinters contain identifiable organic biosignatures indicative of cyanobacteria and methane-oxidising bacteria (Gibson *et al.*, 2008) and investigations over temporal scales of sinter successions have demonstrated the utility of microbial lipids to investigate past changes in the physico-chemical conditions of the vent (Kaur *et al.*, 2008). The application of lipid analysis to geothermal mineral deposits appears to be fruitful; however, the long-term fate of biomarkers in sinter successions is yet to be determined. For instance, investigations concerning the Devonian Rhynie chert, a well-known ancient

geothermal system from which much flora and fauna has been characterised (Trewin, 1996) shows an absence of recognisable chemical fossils (Summons *et al.*, 1996; Mountain, personal communication). Analysis of biomarker distributions preserved within inactive sinters of Champagne Pool, TVZ, has shown that polyfunctionalised biomarkers are present in sinters that formed around the time of the pool, ca ~ 900 years (Kaur *et al.*, 2008). However, the amount of preservation in truly ancient sinters is probably constrained by the timing of diagenesis of amorphous silica (Opal – A) to crystalline silica (Opal – CT), and ultimately quartz (Lynne and Campbell, 2004). Nevertheless, analysis of lipid distributions sheds light on the variety of organisms that are likely to become incorporated into a mineral matrix and also provides a means with which to investigate uncharacterised microbial populations and biogeochemical processes occurring in-situ. Initial studies of the lipid distribution of silica sinters have shown the presence of a number of novel lipids and indicated the presence of uncharacterised groups of micro organisms (e.g. Pancost *et al.*, 2005; Talbot *et al.*, 2005).

### 1.4 BACTERIOHOPANEPOLYOLS

The work in this thesis investigates the distribution of BHPs and corresponding diagenetic derivatives associated with terrestrial geothermal ecosystems. BHPs (Figure 1.2) have been shown to be abundant in a range of environmental conditions and are known to be important components of organic matter that enable reconstructions of bacterial populations contributing to preserved biogeochemical records (Talbot *et al.*, 2003c; Talbot *et al.*, 2005; Blumenberg *et al.*, 2007, 2009; Cooke *et al.*, 2008b; Coolen *et al.*, 2008; Xu *et al.*, 2009). The following section introduces the origin of BHPs in bacteria (Section 1.5) and discusses the source of BHPs observed in recent sedimentary material (Section 1.6). Occasionally, misunderstanding and misrepresentations can occur when one term has been used in a number of contexts. To avoid confusion throughout this introduction and the rest of the thesis, a brief overview of fundamental terminology used throughout will be introduced at this point; traditionally, the term ‘hopanoid’

## Introduction

refers to a class of compounds belonging to a wide range of C<sub>30</sub> natural products, the triterpenoids, but is mainly used when referring to BHPs, biohopanoids and geohopanoids (e.g. Blumenberg *et al.*, 2009).

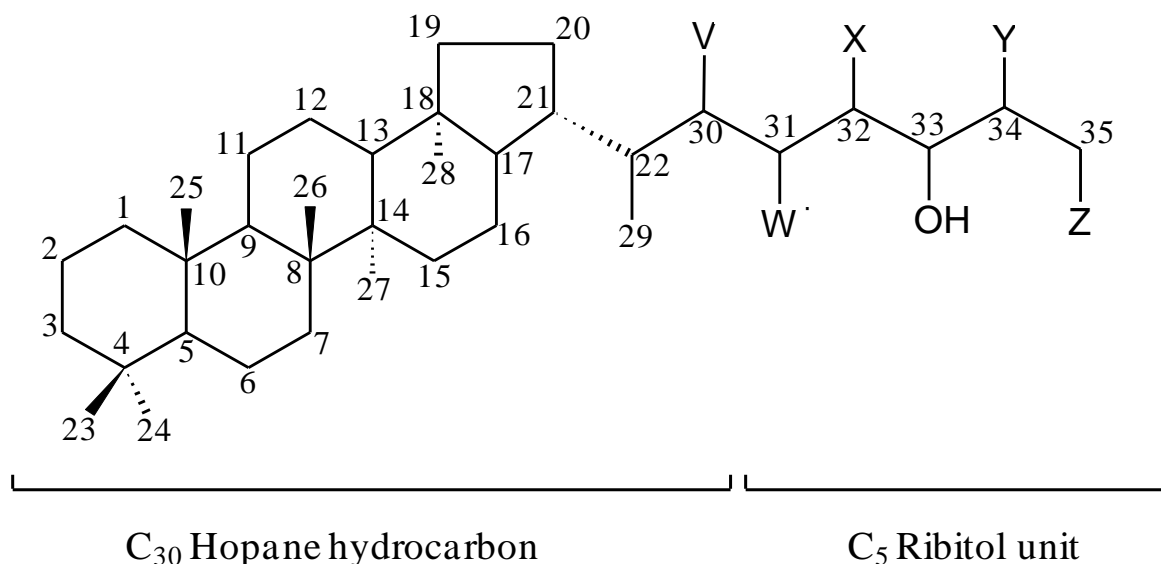


*Figure 1.2 Generic BHP structure. Standard numbering system for hopanoids. C<sub>30</sub> hopane hydrocarbon component and ribose derived n-alkyl polyfunctionalised side chain. V – Z represent different functional groups.*

For the purpose of this thesis, BHP refers to extended C<sub>35</sub> hopanoids that contain more than one hydroxyl group. A generic BHP is shown in (Figure 1.2) and the most reported BHP is BHT (**1**), which contains four hydroxyl groups within the C<sub>5</sub> ribitol unit. The term BHP, encompasses most C<sub>35</sub> hopanoid compounds including 32,35 anhydroBHT (**2**) and 31-hydroxy 32,35 anhydroBHP (**3**) but excludes homohopanols, diploptene (**4**) and diplopterol (**5**). An inventory of chemical names and abbreviations used throughout this Thesis is presented in the preface (see section ‘Structures and nomenclature used throughout this thesis’). The origin of BHPs in bacteria and their distribution throughout bacterial lineages can be found in Section 1.5.

## 1.4.1 BIOHOPANOID

The term ‘biohopanoid’ encompasses all polyfunctionalised compounds with the exception of 32,35 anhydrobacteriohopanetetrol (**2**) and 31-hydroxy 32,35 anhydrobacteriohopanepentol (**3**). Although these compounds are true ‘polyols’, they are produced via diagenetic pathways and a biological precursor remains elusive (e.g. Bednarczyk *et al.*, 2005; Talbot *et al.*, 2005; Schaeffer *et al.*, 2008). This term includes diplopterol and diploptene as they are known to be biologically produced but cannot be classed as ‘polyols’. Biohopanoids generally contain the stereochemical configuration  $17\beta(\text{H}),21\beta(\text{H})$  and geohopanooids  $17\beta(\text{H}),21\alpha(\text{H})$  or  $17\alpha(\text{H}),21\beta(\text{H})$ . There are a few exceptions to this rule, Rosa-Putra *et al.* (2001) identified  $17\alpha(\text{H}),21\beta(\text{H})$  C<sub>32</sub> homohopanol, likewise Talbot *et al.* (2008b) detected  $17\alpha(\text{H}),21\beta(\text{H})$  BHT (**1**) in sediments of Ace lake, Vestfold hills, Antartica (Figure 1.3).

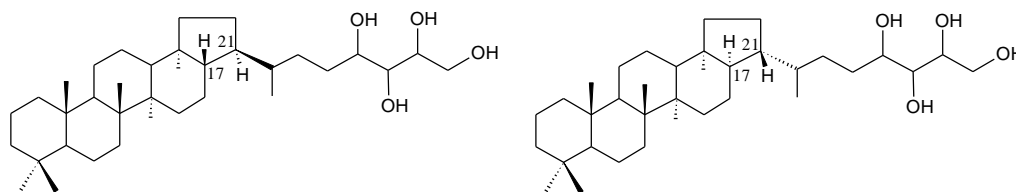


Figure 1.3 Isomeric forms observed at C<sub>17</sub> and C<sub>21</sub> in bacteriohopanetetrol. Left:  $17\beta(\text{H}), 21\beta(\text{H})$  BHtetrol.

Right:  $17\alpha(\text{H}), 21\beta(\text{H})$  BHtetrol.

## 1.4.2 GEOHOPANOID

Post-depositional chemical alteration of organic matter results in a series of recognisable molecular fossils which can be used to assess precursor biota, environmental conditions at the time of deposition and any structural alteration driven by a variety of parameters such as temperature, pH, or the presence or absence of oxygen (e.g. Simoneit, 1996). BHPs are known to be the biological precursor to the hopanoid-class of compound found throughout sedimentary

## Introduction

regimes (Ageta *et al.*, 1987; Reis-Kautt *et al.*, 1989; Sinninghe Damsté *et al.*, 1995; Summons *et al.*, 1999; Brocks *et al.*, 1999; Farrimond *et al.*, 2000). Hopanoids are known to be ubiquitous constituents of sediments, an observation that has led to this class of compound regularly being classed as the ‘most abundant natural product on Earth’ (e.g. Ourisson, 1987; Ourisson and Albrecht, 1992). Although the side-chain of the BHP compound is thermally labile, the hopane hydrocarbon is relatively stable and is observed in sediments, shales and bitumens dating back to the Archean and (Eigenbrode *et al.*, 2008). Numerous reports exist detailing the presence of hopanes in Archean sedimentary material. However recent advancement in analytical methodology (e.g. Rasmussen *et al.*, 2008) has brought into question the authenticity of these biomarkers for truly ancient biospheres. Hopanes carrying diagnostic additional methylations at C-2 (Section 1.5.5.1) and C-3 (Section 1.5.5.2) provide information regarding the antiquity of oxygenic photosynthesis (Summons *et al.*, 1999) and methane-oxidation (Eigenbrode *et al.*, 2008), two processes central to the modern carbon cycle. The distribution of non-methyl hopanes is also used to infer the presence of aerobic conditions as, excluding a few exceptions (Sinninghe Damsté *et al.*, 2004; Hartner *et al.*, 2005; Blumenburg *et al.*, 2006; Section 1.5.5.4), BHPs and hopanoids are produced by aerobic or facultative anaerobic bacterial taxa (e.g. Rohmer *et al.*, 1984).

### 1.5 BHPs: ORIGIN AND DISTRIBUTION IN BACTERIA

#### 1.5.1 THE DISCOVERY OF EXTENDED BACTERIAL HOPANOIDS

The first reported C<sub>35</sub> extended poly-functionalised hopanoid was bacteriohopanetetrol (**1**; Figure 1.2) isolated from *Acetobacter xylinum* (Forster *et al.*, 1973; now *Gluconoacetobacter xylinus*). Fundamental work concerning the biological function of BHPs conducted by Langworthy *et al.* (1976) and Poralla *et al.* (1984) showed that certain BHPs were produced by *Alicyclobacillus acidocaldarius* (formerly *Bacillus acidocaldarius*) in response to decreasing pH

## Chapter 1

and increasing temperature. Rohmer *et al.* (1984) described for the first time the apparent widespread distribution of BHP biosynthesis in bacterial species, although no clear pattern emerged distinguishing certain BHPs between different taxonomic groups of bacteria. In nearly one hundred species tested, including representatives of the archaea, BHP biosynthesis occurred in mainly aerobic bacterial taxa and did not occur at all in the archaea. Subsequently, Bringer *et al.* (1985) and Schmidt *et al.* (1986) showed that BHPs were produced in cultures of *Zymomonas mobilis* grown under anaerobic conditions. Like Langworthy and co-authors before had reported, BHP biosynthesis was apparently stimulated by incubation at increased temperature and elevated ethanol concentrations suggesting that BHP production was a reaction to weakening of the cell membrane. The biosynthesis of BHPs in response to changes in the lipid structure of the cellular membrane is now widely accepted (e.g. Poralla *et al.*, 1980; Kannenburg *et al.*, 1980; Poralla *et al.*, 1984; Bringer *et al.*, 1985; Schmidt *et al.*, 1986; Stroeve *et al.*, 1998; Poralla *et al.*, 2000). However, the evolutionary distribution of BHP-producing bacteria and the nature and complexity of BHP-compounds produced by bacterial species is currently the subject of great interest. Reports of side-chain moieties containing adenosine (**6**), amino acids (**7** and **8**), carbohydrates (**9**, **10**, **11** and **12**) and also ‘non-extractable BHPs’ (C  $\Delta^6$ **9**; e.g. Neunlist *et al.*, 1985; Renoux and Rohmer, 1985; Herrmann *et al.*, 1996a; Duvold and Rohmer, 1999) has led authors to suggest an alternative or additional function to that of molecular re-enforcement. Reports of biosynthesis in specific groups of bacteria, such as methylotrophic bacteria (Neunlist and Rohmer, 1985b), cyanobacteria (Bisseret *et al.*, 1985), purple non-sulphur bacteria (Neunlist and Rohmer, 1985a; Neunlist *et al.*, 1988), acetic acid bacteria (Herrmann *et al.*, 1996a), methanotrophic bacteria (Neunlist and Rohmer, 1985c; Talbot *et al.*, 2001), planctomycetes (Sinninghe Damsté *et al.*, 2004) and sulphate-reducing bacteria (Blumenberg *et al.*, 2006) has demonstrated some chemotaxonomic value throughout phylogenies. However, intrinsic difficulties are commonly noted when analysing bacterial cultures for the presence of BHPs;

## Introduction

firstly, BHPs have been shown to be bound to other cellular components (Benz *et al.*, 1983; Herrmann *et al.*, 1996a) and therefore may be overlooked by insufficient extraction methods. Secondly, the expression of BHP-lipids has been shown to be regulated by growth phase (Bringer *et al.*, 1985; Flesch and Rohmer, 1989; Summons *et al.*, 1994; Poralla *et al.*, 2000; Joyeux *et al.*, 2004) indicating that some bacterial species can produce different BHP and hopanoid assemblages under varying culturing conditions. The measurement of BHP distributions expressed under different environmental conditions provides information regarding the significance of BHP producing organisms in natural settings.

Improvements in screening and detection of BHP-producing bacteria in cultures and environmental settings has led to an increasingly detailed picture of the distribution throughout bacterial lineages, for instance, BHPs methylated at C-2 (**II**) appear to be indicative of autotrophic bacteria (Bisseret *et al.*, 1985; Summons *et al.*, 1999; Rashby *et al.*, 2007; Talbot *et al.*, 2008a) and BHPs methylated at C-3 (**III**) appear to indicate a heterotrophic source organism (Neunlist and Rohmer, 1985b; Zundel and Rohmer, 1985b; Summons and Jahnke, 1993; Cvejic *et al.*, 2000a). Screening of genomic databases for genes encoding for enzyme activity central to BHP biosynthesis has also further demonstrated the ability of obligate anaerobic organisms to produce BHPs (Fischer *et al.*, 2005).

### 1.5.2 BIOCHEMISTRY OF BACTERIOHOPANEPOLYOLS

The hydrocarbon component of a BHP-lipid is formed by intramolecular cyclisation of squalene by the enzyme squalene-hopene-cyclase (SHC; Figure 1.4). The structural similarity between the pentacyclic moiety in hopanes and the tetracyclic moiety in sterols (Figure 1.5) has led many to consider that hopanes are the evolutionary precursor to the sterols, which are essential to life in all eukaryotes and some bacteria (e.g. Pearson *et al.*, 2003, Volkman, 2005; Summons *et al.*, 2006 and references therein). Squalene is known to be formed from C<sub>5</sub> components derived from isoprene; isoprenoid pyrophosphate (IPP) is a universal building block

## Chapter 1

found through all three domains of life (Lange *et al.*, 2000). Two modes of formation of IPP are now well documented in bacteria, green algae and higher plants; the Bloch-Lynen pathway where IPP is formed from 3 molecules of Acetyl-CoA via the mevalonate pathway (MVA pathway; Rohmer *et al.*, 1993; Figure 1.6). Alternatively, Rohmer *et al.* (1993) postulated that bacteria can produce IPP via the reduction of 1-deoxyxyulose 5-phosphate, formed from pyruvate and glyceraldehyde, to 2-methylerythritol 4 phosphate (MEP; MEP Pathway; Figure 1.7).

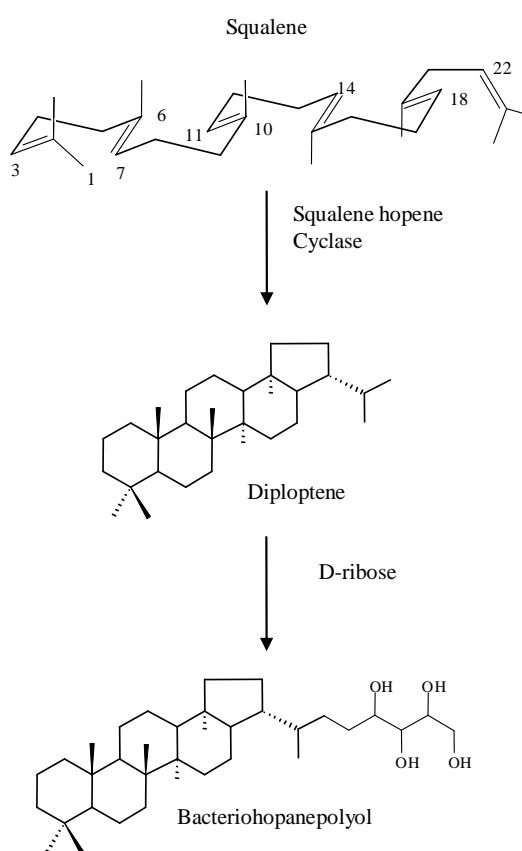


Figure 1.4 Formation of hopane hydrocarbon via intramolecular cyclisation of squalene.

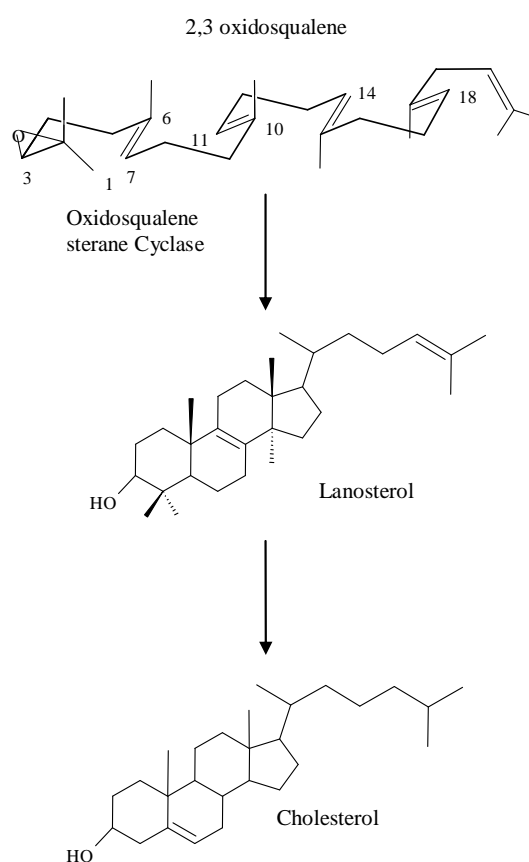


Figure 1.5 Formation of sterane hydrocarbon via intramolecular cyclisation of oxidosqualene.

## Introduction

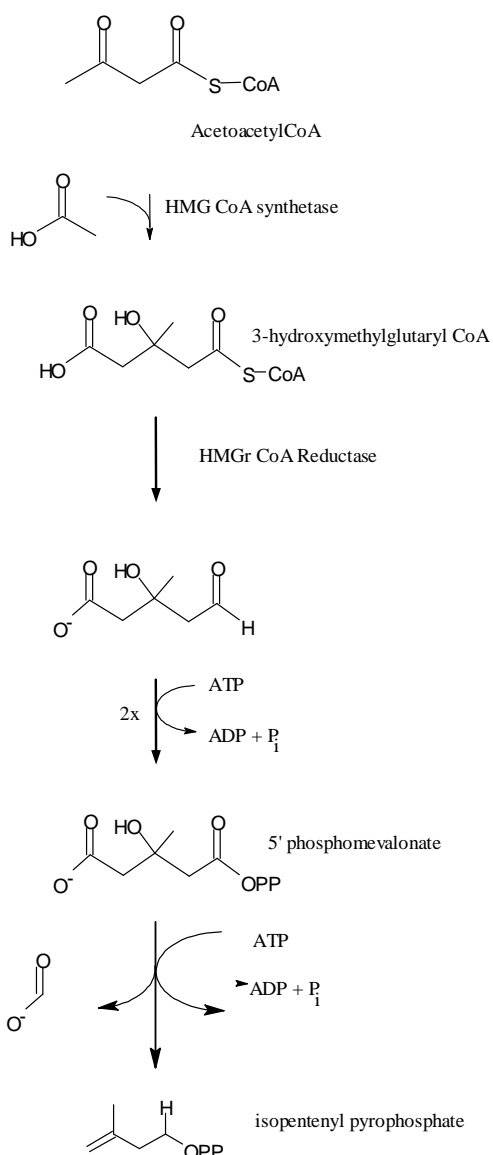


Figure 1.6 Formation of isoprene units via Mevalonate pathway (MVA pathway).

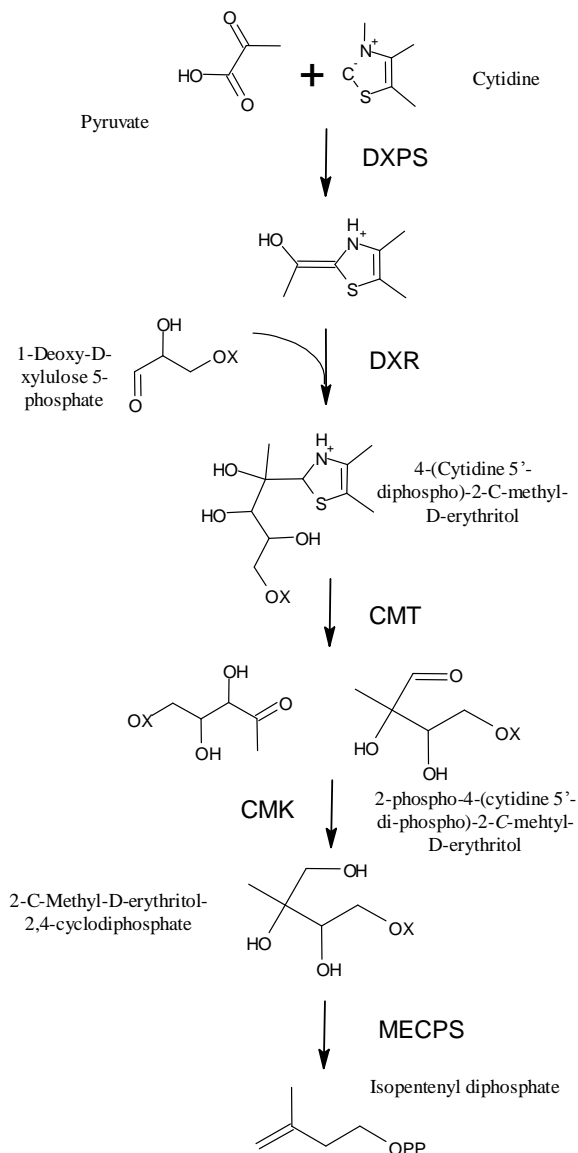


Figure 1.7 Formation of isoprene units via Methylerythritol Pathway (MEP pathway).

### 1.5.3 THE ORIGIN OF THE SIDE CHAIN

C<sub>30</sub> hopane (**I**) has been detected in many ferns, mosses, lichens, fungi and symbiotic bacteria of various marine sponges (Corbett and Young, 1966; Eijk *et al.*, 1986; Shatz *et al.*, 2000; Costantino *et al.*, 2001). The observation of C<sub>35</sub> polyfunctionalised hopanoids appears to be confined to bacterial lineages (e.g. Rohmer *et al.*, 1984, Farrimond *et al.*, 1998; Kannenburg

and Poralla, 1999). The n-alkyl polyfunctionalised C<sub>5</sub> unit is covalently attached via a carbon-carbon bond to C-29 of the hopane skeleton (Figure 1.2). Investigations using isotopically labelled metabolites demonstrated the origin of the side chain was a D-pentose precursor (Flesch and Rohmer, 1988) or in the case of BHPs produced by *Acetobacter* or *Nostocales*, D-arabinose (Rohmer, 1993). Based upon the stereochemistry of the side-chain which is usually present as a D-ribose configuration, i.e. 3<sup>2</sup>R 3<sup>3</sup>R 3<sup>4</sup>S, (Bisseret and Rohmer, 1989) a universal precursor was proposed. Adenosylhopane (**2**) has been suggested as a putative precursor as the ribose component contains the correct stereochemistry contained within the BHP side-chain (Bisseret *et al.*, 1994). Although a compound containing a heterocyclic moiety was unknown at the time, subsequent reports of adenosylhopane (**2**) in cultures of *Rhodopsuedomonas acidophila* (Rohmer, 1993), *Nitrosomonas sp.* (Seeman *et al.*, 1999) and *Bradyrhizobium japonicum* (Bravo *et al.*, 2001) suggest that this hypothesis may be correct although *Gluconoacetobacter xylinus* has been reported to produce a variety of epimeric forms of the C<sub>5</sub> unit (Pieseler and Rohmer, 1991).

Additional functionality linked via an ether bond or amino link to C-35 have also been reported in a wide variety of bacterial sources (e.g. Talbot *et al.*, 2007a). BHPs containing an extra functionality at C-35 are known as ‘composite BHPs’ and recent reports suggest these compounds may play a role in the formation of lipid rafts within the cell membrane (Saenz, 2010).

#### 1.5.4 STRUCTURAL VARIATIONS

Another feature of the biosynthesis of BHPs is the occurrence of additional methyl groups on the A-ring. A series of 2 $\beta$ -methylhopanoids (**II-1**, **13** and **II-14**) and 3 $\beta$ -methylhopanoids (**III**) were first isolated from *Methylococcus capsulatus* (**III-15**) and *Acetobacter pasteurianus* (**III-1**, **III-13**; Zundel and Rohmer, 1985b; Bisseret *et al.*, 1985). Bisseret *et al.* (1985) also identified  $\Delta^2$  pentahydroxybacteriohopane ( $\Delta^2$ -**13**) and postulated that this could be an

## Introduction

intermediate in the formation of C-2 and C-3 methylated BHPs and that the methyl group was donated from L-methionine (Figure 1.6; Zundel and Rohmer, 1985b). Detection of methylated precursors to BHPs, diploptene (**4**) and diplopterol (**5**) methylated in the A or B ring in cultures of *Bradyrhizobium japonicum* (Kannenburg *et al.*, 1996) and then a subsequent negative result of homologous elongated C<sub>35</sub> BHPs containing any characteristic methylations led the authors to conclude that the addition or removal of methyl groups could be an indication that the cyclisation reaction is a multi-step processes involving numerous enzymes. However, key enzymes involved in this process have yet to be discovered and attempts to further understand this mechanism by stimulating aerobic sterol desaturase and sterol methyl-transferase homologues in *Methylobacterium extorquens* have yielded inconclusive results (Bradley *et al.* 2007). Additional methylations on the 'A'-ring at C-2 and C-3 produce easily identifiable structural variants of the hopane hydrocarbon that are stable over geological timescales. Cyanobacteria are known to be producers of significant quantities of 2 $\beta$ -methyl BHPs, likewise, methane-oxidising bacteria and acetic acid bacteria are known to produce 3 $\beta$ -methyl BHPs. The detection of 3 $\beta$ -methyl hopanoids in sediments is usually attributed to a methanotrophic source especially where supported by a highly depleted isotopic  $\delta^{13}\text{C}$  composition (e.g. Summons and Jahnke, 1993; Burhan *et al.*, 2002; Pancost *et al.*, 2005; Eigenbrode *et al.*, 2008). It should be noted that additional methylations at C-31 are also known from a strain of acetic acid bacteria (**16**; Simonin *et al.*, 1994).

## Chapter 1

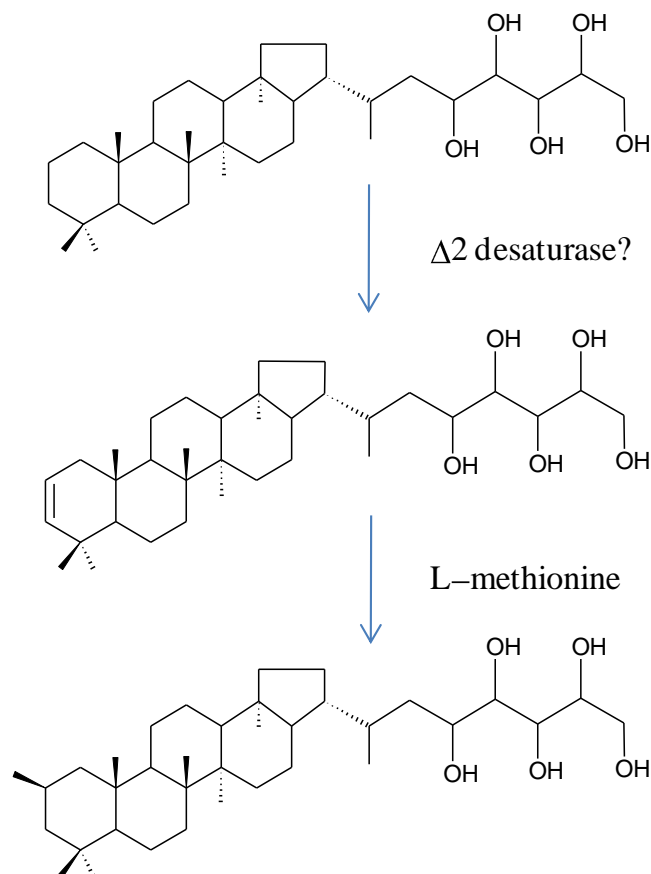


Figure 1.8 Hypothetical formation of 2β-methylbacteriohopanepolyols (Adapted from Zundel and Rohmer, 1985b).

### 1.5.5 DISTRIBUTION OF BHPs IN BACTERIA

BHP and hopanoid biosynthesis has been observed in many diverse bacterial taxa (Rohmer, 1993 and references therein; Farrimond *et al.*, 1998; Sinnighe Damsté *et al.*, 2004, Hartner *et al.*, 2005; Blumenberg *et al.*, 2006). The direction that this research has taken has been, in part, dictated by the initial findings of Rohmer *et al.* (1984). Investigations detailing the distribution of BHP-producing organisms are inevitably biased towards those species that are available in culture and likely represent a small fraction of total BHP and hopanoid producing organisms. Rather fortuitously, organisms that could be regarded as evolutionarily ‘significant’ are known to produce distinctive structures and this becomes a driver for research into BHP production in these organisms. On the whole, this body of research covers, but is not confined to,

## Introduction

cyanobacteria, planctomycetes and the proteobacteria including methanotrophic bacteria, acetic acid bacteria and purple non-sulphur bacteria. Many other reports exist detailing BHP biosynthesis in various Gram positive and Gram-negative bacteria (Figure 1.9).

In an attempt to demonstrate the chemotaxonomic value of BHPs and hopanoids throughout bacterial taxa, a survey of BHP-producing organisms is introduced: the main criteria for the groupings are based upon the major groups of bacteria for which BHP-biosynthesis has been documented. Observations of BHP biosynthesis in cultures of obligate anaerobic bacteria, although few in number, merit inclusion as these reports are directly juxtaposed to the traditional view of BHP and hopanoid distribution in the bacteria (e.g. Rohmer *et al.*, 1984).

### 1.5.5.1 CYANOBACTERIA

Cyanobacteria are known to be producers of significant quantities of characteristic BHPs and hopanoids (Bisseret *et al.*, 1985; Summons *et al.*, 1999; Talbot *et al.*, 2008a) in particular, cyanobacteria have the capability to produce BHPs containing additional methylations at C-2 and are thought to be the major contributors of this class of compound to modern and ancient sedimentary organic matter (Summons *et al.*, 1994).

Cyanobacteria can be divided into 6 orders: *Oscillatoriales*, *Nostocales*, *Choorococalles*, *Stigonometales*, *Pleurocapsales* and *Prochlorales*. Talbot *et al.* (2008a) offers a complete review of current knowledge concerning BHP-producing cyanobacteria.

# Chapter 1

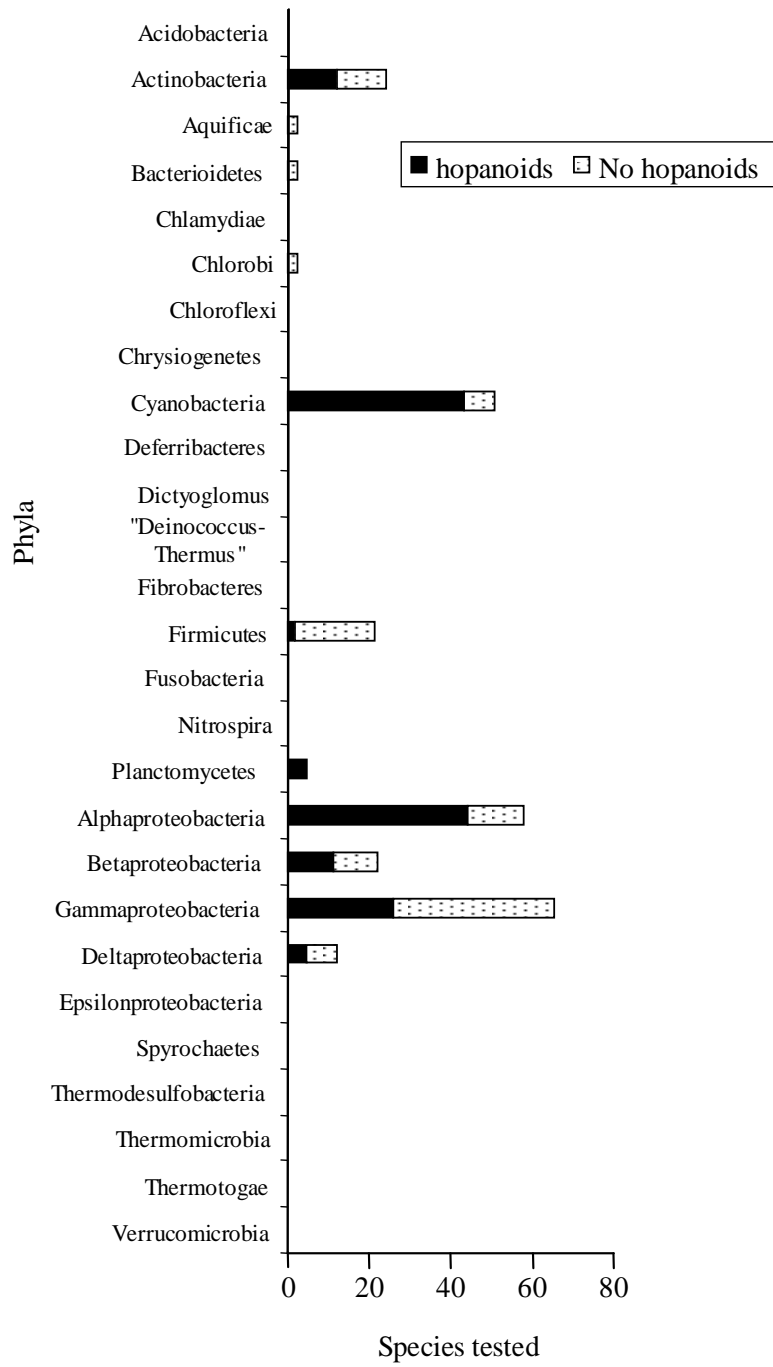


Figure 1.9 Phyla tested for BHP biosynthesis.

## Introduction

At this stage, little correlation of BHP-producing capability and respective structural variation is clear although certain trends are emerging, i.e. production of BHPs containing a pentahydroxylated side-chain seems to be confined to the orders *Nostocales* and *Oscillatoriales*. BHP producing organisms belonging to the order *Chroococcales* appear to be sources of ‘composite-type’ BHPs (**9**, **II-9**, **11**, **17**, **II-19**; Simonin *et al.*, 1992; Talbot *et al.*, 2003b; Talbot *et al.*, 2008a). Composite-BHPs are those that contain an ether-linked functionality at C-35 (e.g. Talbot *et al.*, 2007a). This may suggest that different groups of cyanobacteria produce very different BHP compounds. Relationships between the ratio of desmethyl to C-2 methylated BHP compound appears to vary within species and environmental conditions, apparently confusing any real conclusions about what biological function, if any, this additional methylation may serve. However, it has been shown that BHPs carrying an extra methylation can be harder to extract from sedimentary material (Allen, 2006). The presence of cyanobacteria in a particular ecological niche can usually be determined by the presence of a BHP together with a C-2 methylated homologue, although other intact BHPs such as BHT-pentose ether (PE-BHT; **17**) and 2-methyl BHT-pentose ether (2-me PE-BHT; **II-17**; Herrmann *et al.*, 1996b), which have only been detected in cultures of cyanobacteria provide a more definitive biomarker. Other sources of C-2 methylated BHPs and hopanoids have been reported from *Methylobacterium organophilum*, *Bradyrhizobium japonicum*, and *Rhodospseudomonas palustris*. (Renoux and Rohmer, 1985; Bisseret *et al.*, 1985; Knani *et al.*, 1994; Bravo *et al.*, 2001; Rashby *et al.*, 2007; Talbot *et al.*, 2007a). *Anabaena variabilis* and *Nocton muscorum* are the only known species of cyanobacteria to produce unsaturated composite BHPs (Rohmer *et al.*, 1984). O- $\alpha$ -D-galacturopyranosylbacteriohopanetetrol (**18**) and alturogalacturopyranosylbacteriohopanetetrol (**19**) previously isolated from *Rhodospirillum rubrum* (Llopiz *et al.*, 1992), was also isolated from *Prochlorothrix hollandica* (Simonin *et al.*, 1996) and in thermophilic strains of *Synechococcus* PCC 6907 along with a 2-methylated homologue (**II-19**). *Prochlorothrix*

*hollandica* has also been shown to produce 35-O- $\beta$ -3,5-Anhydrogalacturonopyranosylbacteriohopanetetrol (**20**) with a C-2 methylated homologue (**II-20**).

#### 1.5.5.2 METHANE-OXIDISING BACTERIA

Oxidation of methane by aerobic methanotrophic bacteria is thought to be a truly ancient physiological trait (e.g. Eigenbrode *et al.*, 2008). Aerobic methanotrophy is mediated by two distinct groups of bacteria: Type I methanotrophic bacteria, that typically inhabit low CH<sub>4</sub>, high O<sub>2</sub> environments and require fixed nitrogen, belong to the gammaproteobacteria and Type II methanotrophic bacteria that typically inhabit environments with high CH<sub>4</sub> and low O<sub>2</sub> partial pressures and form a phylogenetically distinct group among the alpha-proteobacteria (Hanson and Hanson, 1996).

Type I methanotrophs tested for BHP-biosynthesis, such as *Methylocaldum szegediense*, *Methylocaldum tepidum*, *Methylomonas methanica* and *Methylococcus capsulatus* belong to the gamma-proteobacteria. Type II Methanotrophs such as *Methylosinus trichosporium* and *Methylocystis parvus* have been shown to produce different assemblage of BHP compounds (Neunlist and Rohmer, 1985b, c; Cvejic *et al.*, 2000a).

Variations in the complexity observed in the side-chain contribute to a distinct distribution of structures between groups of methanotrophic bacteria. For example, *Methylococcus sp.* and the thermotolerant *Methylocaldum sp.* are phylogenetically related Type I methanotrophs and are known to produce Aminobacteriohopanepentol along with a 3 $\beta$ -methylated homologue (**15**, **III-15**; Neunlist and Rohmer, 1985b). Whereas, *Methylosinus sp.* and *Methylocystis sp.* are known to typically produce large amounts of aminobacteriohopanetetrol (**21**) and aminobacteriohopanetriol (**22**; Neunlist and Rohmer, 1985c; Talbot *et al.*, 2001). Although recent reports suggest that a symbiotic Type I methanotroph produces **21** and **22** and not **15** (Jahnke *et al.*, 1999; Coolen *et al.*, 2008).

## Introduction

It is important to differentiate between methanotrophic bacteria and methylotrophic bacteria as methylotrophic bacteria are known to grow on many substrates such as methylamine and methanol, whereas methanotrophs utilise methane monooxygenase enzymes (MMOs) to convert methane to methanol (e.g. Hakemian and Rosenzweig, 2007). Methylotrophs are also known to produce distinctive BHPs: *Methylobacterium fujisawaense* (Renoux and Rohmer, 1985) and *Methylobacterium organophilum* (Knani *et al.*, 1999) have been demonstrated to produce a unique guanidine-substituted cyclitol ether derivatives of bacteriohopanetetrol (**23**).

### 1.5.5.3 ACETIC ACID BACTERIA

Acetic acid bacteria such as *Acetobacter pastuerianus*, *Acetobacter europaeus* (now *Gluconobacter europaeus*) or *Gluconacetobacter xylinus* are known to be producers of large quantities of polyfunctionalised BHPs. In particular they are known to produce significant quantities of  $\Delta^6$  and  $\Delta^{11}$  unsaturated BHPs ( $\Delta^6$ ,  $\Delta^{11}$ ; e.g. Rohmer and Ourisson, 1986; Talbot *et al.*, 2007b) and also C-3 methylated BHPs (**III-1** and **III-13**; Zundel and Rohmer, 1985b; Talbot *et al.*, 2007b) and C-31 methylated BHPs (**16**; Simonin *et al.*, 1994). Many species may produce a combination of structural variations such as *Gluconobacter xylinus* which is known to produce mono- and di- unsaturated homologues of **1**, **9**, **11** (e.g. Rohmer and Ourisson, 1986; Talbot *et al.*, 2007b).

Other sources of unsaturated BHPs include *Methylocaldum szegediense*, *Burkholderia cepacia* (formerly *Pseudomonas cepacia*), *Anabeana variabilis*, *Nostoc muscorum*, *Rhodospseudomonas palustris*, and *Methylosinus* sp. (Rohmer *et al.*, 1984; Bisseret *et al.*, 1985; Cvejic *et al.*, 2000a; b; Talbot *et al.*, 2007a). *Nostoc muscorum* has been shown to produce both  $\Delta^2$  and  $\Delta^6$  unsaturated BHPs ( $\Delta^2$ **13**,  $\Delta^6$ **13**) although it should be noted that  $\Delta^2$  unsaturation observed was identified as a putative intermediate in the formation of 2 $\beta$ -methyl bacteriohopanepentol (**13**, Zundel and Rohmer, 1985b). *R. palustris* and *M. szegediense* are the only known sources of unsaturated homologues of aminobacteriohopanetriol and

aminobacteriohopanepentol, producing unsaturated aminobacteriohopanetriol and  $\Delta^{11}$  aminobacteriohopanepentol (Cvejic *et al.*, 2000a; Talbot *et al.*, 2007b). There is little evidence to suggest what advantage to a biological system incorporation of unsaturation into a BHP structure would possess. One possibility is that the unsaturation may be an intermediary step in BHP anabolism or catabolism (e.g. Zundel and Rohmer, 1985b) also one may consider a steric rearrangement to maintain the lipid bi-layer under certain environmental or culturing conditions. Comparisons of bacterial species known to biosynthesise unsaturated BHP compounds and consideration of the occurrence of unsaturated BHPs and hopanoids in environmental samples, ranging from arctic epilithic cyanobacteria (Talbot *et al.*, 2008a) to aerobic methanotrophic bacteria from the Haakan mud volcano (Elvert and Niemann, 2008) provide little clues.

#### 1.5.5.4 OBLIGATE ANAEROBIC BACTERIA - THE O<sub>2</sub> PARADOX

Although traditionally regarded as biomarkers for aerobic bacteria, e.g. methanotrophs, heterotrophs and cyanobacteria; BHP biosynthesis proceeds independently of the presence of molecular oxygen. BHP biosynthesis has been observed in a number of facultative anaerobic organisms such as purple non-sulphur bacteria and fermentative bacteria (Neunlist and Rohmer, 1985b; Neunlist *et al.*, 1985; Neunlist *et al.*, 1988; Flesch and Rohmer, 1989; Moreau *et al.*, 1995). Bringer *et al.* (1985) and Schmidt *et al.* (1986) showed that *Zymomonas mobilis* grown under anaerobic conditions was a prolific producer of BHPs. Facultative anaerobes *Rhodoblastus acidiphilia* (formerly *Rhodopsuedomonas acidophila*) and *Rhodopseudomonas palustris* (Neunlist *et al.*, 1988) are known to produce high quantities of extended and complex C<sub>35</sub> polyols. Flesch and Rohmer (1989) showed that under micro-aerated conditions, *Zymomonas mobilis* produces quite distinctive ketone-containing BHPs (**24**) suggesting that growth conditions may exert an effect on the nature of the BHP that is produced. Several subsequent reports have shown presence of hopanoids derived from bacteria inhabiting anoxic environmental conditions (Elvert *et al.*, 2001; Thiel *et al.*, 2003; Jahnke *et al.*, 2004; Pancost *et*

## Introduction

*al.*, 2005; Blumenberg *et al.*, 2006; Blumenberg *et al.*, 2007). However, few reports exist demonstrating BHP-biosynthesis in cultures of obligate anaerobes. Planctomycetes capable of annamox metabolism represent a group of bacteria defined as ‘missing’ in nature (Broda, 1977). BHP biosynthesis in *planctomycetales* has been observed in enrichment cultures of *Brocadia* and *Scalinidua* spp. when grown under anaerobic conditions (Sinninghe Damsté *et al.*, 2004). Fe(III) reducers, *Geobacter* sp. and *Magnetospirillum* sp. have been shown to anaerobically produce BHPs (Hartner *et al.*, 2005), although in this case BHP-biosynthesis was inferred by the presence of periodic acid cleavage products and no intact BHP compounds were detected. Blumenberg *et al.* (2006) demonstrate BHP-biosynthesis by sulfate-reducing bacteria belonging to the genus *Desulfivibrio* sp. isolated from mat-forming microbial consortia from the black sea. The occurrence of BHPs and hopanoids in anoxic sediments cannot be solely explained by the presence of these organisms, suggesting that “BHP-producing capability of obligate anaerobes is currently under estimated” (e.g. Pancost *et al.*, 2000; Elvert *et al.*, 2001; Thiel *et al.*, 2003; Talbot *et al.*, 2005; Blumenberg *et al.*, 2006).

### 1.5.5.5 PURPLE NON-SULPHUR BACTERIA

Purple non-sulphur bacteria belonging to the group *Rhodospirillales* are known to be prolific producers of C<sub>35</sub> polyols including amino-containing BHPs, composite BHPs containing ornithine (**7**) and tryptophan (**8**) residues and mono- and di-substituted carbamoyl (**25** and **26**) moieties (Table 3; Rohmer *et al.*, 1984; Neunlist *et al.*, 1985; Neunlist and Rohmer, 1985b; Neunlist *et al.*, 1988; Talbot *et al.*, 2007a). Most purple non-sulphur bacteria tested, if not all, are known to produce very distinctive side-chain structures. Species tested include *R. palustris*, *Rhodoblastus Acidophilus* (formerly *Rhodopsuedomonas acidophilus*), *Rhodomicrobium vanielii*, *Rhodopsuedomonas sphaeroides* and *Rhodospirillum rubrum* (Neunlist *et al.*, 1985; Ourisson *et al.*, 1987; Neunlist *et al.*, 1988; Llopiz *et al.*, 1992). Isolation of adenosylhopane from *R. palustris* led the authors to suggest that BHPs may be involved with secondary cellular

functions and also that adenosylhopane (**6**) could be a putative intermediate in the formation all BHP compounds. It was recently reported that cultures of *R. palustris* were also shown to produce BHPs containing C-2 methylations (**II-1**, **II-22**; Rashby *et al.*, 2007).

### 1.6 DISTRIBUTION AND SIGNIFICANCE OF BHPs AND HOPANOIDS IN ENVIRONMENTAL SETTINGS

#### 1.6.1 SEDIMENTARY BIOHOPANOIDS

Initial reports concerning the distribution of BHPs or biohopanoids in sedimentary material were confined to observations of BHT (e.g. Rohmer *et al.*, 1980; Mycke *et al.*, 1987; Ries-Kautt and Albrecht, 1989; Innes *et al.*, 1997) or inferred by the presence of homohopanol produced during reductive cleavage of more functionalised precursors (e.g. Innes *et al.*, 1998; Farrimond *et al.*, 2000; Watson, 2002). Initial investigations concerning the ecological and environmental distribution of BHPs and hopanoid highlighted the influence of environmental situation on the distribution of biohopanoids in any given setting. Fox *et al.* (1998) and Talbot *et al.* (2003a) showed the presence of composite BHPs from sedimentary material using High Performance Liquid Chromatography-Mass Spectrometry (HPLC-MS). Talbot *et al.* (2003c) revisited these earlier studies employing APCI-HPLC-MS methodology and augmented the sample suite with more diverse environmental settings and were able to elaborate on the structural diversity that was hinted upon in previous studies. Subsequent reports detailing BHP and hopanoid distributions in other environmental situations (Talbot *et al.*, 2005; Pancost *et al.*, 2006; Zhang *et al.*, 2007; Blumenberg *et al.*, 2007; Talbot and Farrimond, 2007; Cooke *et al.*, 2008a, b; Talbot *et al.*, 2008a, b; Blumenberg *et al.*, 2009) have established BHPs as an important class of compounds in a range of recent environments. This has extended our understanding of the extent of BHP-producing bacteria in environmental settings and has also led to the development of inventories of BHPs for different settings. The distribution of

sedimentary BHPs and hopanoids is relevant not solely to ecological and geochemical investigations as a complete survey of BHP-producing bacteria is unfeasible. Therefore, the occurrence of BHP and hopanoids in a variety of natural samples is directly applicable to assess the extent of bacteria capable of biosynthesising this class of compound and contributing to the sedimentary record.

### 1.6.2 BHPs AND GEOHOPANOIDS AS SOURCE INDICATORS

The BHP distribution observed throughout different sedimentary regimes is a product of different species of bacteria inhabiting different ecological niches. Any chemotaxonomic information contained within BHP structural diversity can be complicated by environmental factors or a physiological response exerting an influence on lipid expression. Also the preservation potential of BHPs in any given environment must be considered as polyfunctionalised, ‘composite-type’ BHPs which contain a labile chemical functionality, such as guanidine-substituted cyclitol ethers (**23**) observed in *M. fujisawaense* (Section 1.5.5.2), will likely degrade quicker than less functionalised counterparts. The distribution of hopanols, hopanoic acids and hopanes in sedimentary material can also be used to investigate precursor organisms contributing to the lipid pool. However, loss of chemical complexity in many cases reduces any source-specificity. This degradation can be used to assess post-depositional alteration to the organic matter (Figure 1.10; Peters and Moldowan, 1993; Simoneit, 1996 and references therein; Schaeffer *et al.*, 2006; Schaeffer *et al.*, 2008). In order to reflect upon the abundant literature concerning the environmental distribution of BHPs and their utility as markers for different depositional settings a short summary has been compiled (Table 1.1).

A few reports exist detailing exceptional preservation of polyfunctionalised hopanoids in sediments (e.g. van Dongen *et al.*, 2006) however in general the side-chain component and any unsaturations occasionally observed in certain bacterial species are rapidly degraded or altered

## Chapter 1

upon deposition (Rodier *et al.*, 1999). Product-precursor type investigations demonstrate that a variety of degraded products are possible from a particular biological precursor (e.g. Bisseret *et al.*, 1997; Tritz *et al.*, 1999), with the end-product determined by intermediary geological and possibly biological alteration (Moldowan and McCaffery, 1995; Bennett *et al.*, 2006). These investigations help correlate geohopanoids to their biological precursor.

## Introduction

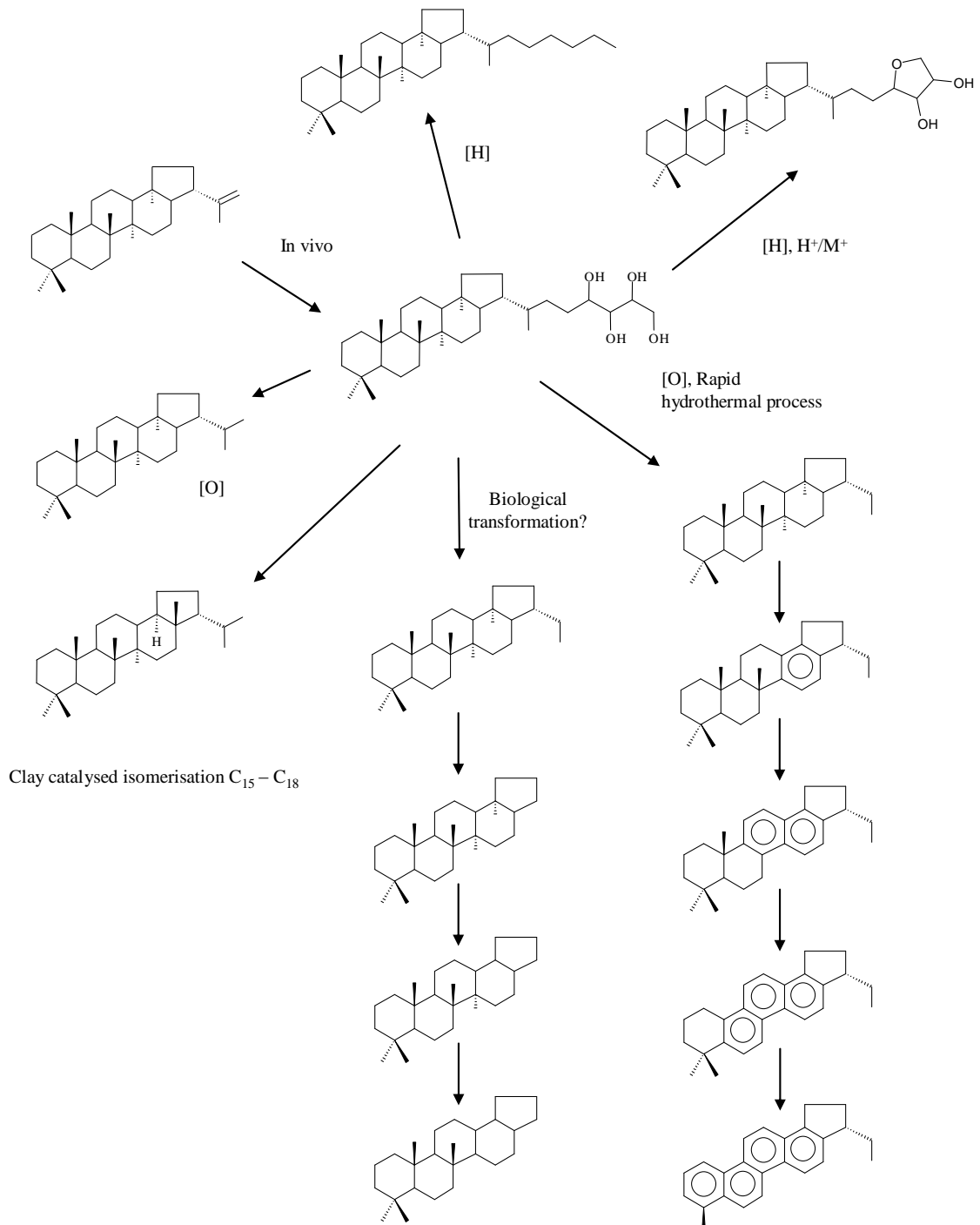


Figure 1.10 Pathways of post-depositional alteration of BHPs (Adapted from Simoneit, 1996).

## Chapter 1

*Table 1.1 BHPs and polyfunctionalised hopanoids as source indicators in bacteria and observations from environmental settings.*

BHP	Source	Environmental Occurrences	References
Tetra-functionalised	Many sources, low specificity	Many	Talbot <i>et al.</i> , 2007 and refs therein
Penta-functionalised	Few sources, mainly cyanobacteria. Observations in <i>Desulfovibrio</i> sp. Type II methanotrophs and some Acetic acid bacteria	Vary significantly. Dependant upon contribution of source organisms	Neunlist and Rohmer, 1985a, Zundel and Rohmer, 1985b, Blumenberg <i>et al.</i> , 2006, Talbot <i>et al.</i> , 2008,
Hexa-Functionalised	Type I methanotrophs	Shown to be low in marine settings. High in stratified water bodies. Silica sinter from TVZ.	Neunlist and Rohmer 1985c, Farrimond <i>et al.</i> , 2000, Talbot <i>et al.</i> , 2003c, Blumenberg <i>et al.</i> , 2007, Gibson <i>et al.</i> , 2008.
	BHHcyc appears to derive from unknown soil BHP-producing bacteria	Soil	
2 $\beta$ Methyl BHPs	Usually cyanobacteria, also <i>R. palustris</i>	Can vary significantly, usually oxic environments	Summons and Jahnke 1994, Rashby <i>et al.</i> , 2007
3 $\beta$ Methyl BHPs	Type I methanotrophs, Acetic acid bacteria	Usually associated with oxic/anoxic transition and micro-aerophilic settings.	Zundel and Rohmer 1985b; Blumenberg <i>et al.</i> , 2007.
Unsaturated BHPs	Limited sources, usually Acetic acid bacteria. Also documented in some cyanobacteria and methanotrophs, <i>R. palustris</i>	Rare but wide-ranging. Peat. Haakan mud volcano. Arctic epilith.	Rohmer and Ourrison, 1986, Quirk <i>et al.</i> , 1984, Talbot <i>et al.</i> , 2008, Elvert and Niemann, 2008.
AnhydroBHT	None currently known. Possibly derives from Adenosylhopane	Many, associated with reductive diagenesis.	Bednarczyk <i>et al.</i> , 2003. Talbot <i>et al.</i> , 2005, Schaeffer <i>et al.</i> , 2008

## Introduction

Table 1.2 Geohopanoids as source indicators.

Compound	Source/observation	Reference
17 $\alpha$ (H), 21 $\beta$ (H) C <sub>32</sub> hopanol <sup>a</sup>	Frankia spp.	Rosa-Putra <i>et al.</i> , 2001
17 $\alpha$ (H), 21 $\beta$ (H) BHT <sup>a</sup>	Sediments of meromictic Antarctic lake	Talbot <i>et al.</i> , 2008
C <sub>31</sub> – C <sub>35</sub> homohopanols	Bacteria	
2 $\alpha$ C <sub>31</sub> – C <sub>36</sub> homohopanols	Autotrophic bacteria	Summons <i>et al.</i> , 1999 Rasbhy <i>et al.</i> , 2007
3 $\alpha$ C <sub>31</sub> – C <sub>36</sub> homohopanols	Heterotrophic bacteria	Zundel and Rohmer, 1985b
32,35 AnhydroBHT,	Reducing/acidic environments	Bednarczyk <i>et al.</i> , 2005
31-hydroxy-32,35 AnhydroBHP		Talbot <i>et al.</i> , 2005 Schaeffer <i>et al.</i> , 2008
C <sub>30</sub> hopanes	Mainly bacteria, some ferns, mosses, lichens.	Peters and Moldowan, 1993
C <sub>35</sub> hopane	Reducing to anoxic conditions	Peters and Moldowan, 1993
28,30-bisnorhopane	Prominent in euxinic conditions	Peters and Moldowan, 1993
25,28,30-trisnorhopane	Anoxic marine, upwelling	Peters and Moldowan, 1993
Diahopanes	Carbonate/clastic	Peters and Moldowan, 1993
Mono - tetra aromatic hopanes	Hydrothermal (formation)	Simoneit <i>et al.</i> , 1996.

<sup>a</sup>BHPs with 17 $\alpha$ (H),21 $\beta$ (H) are known to be produced by certain bacteria (e.g. Talbot *et al.*, 2008b) but are included for completeness

## 2 SAMPLES, LOCATIONS AND METHODOLOGY

### 2.1 SAMPLES

#### 2.1.1 SINTERS

The samples analysed in this study were collected on sampling trips to the Taupo Volcanic Zone, North Island, New Zealand (TVZ) during field expeditions of May 2005 and September 2006. The TVZ samples were collected and provided by Gurpreet Kaur and Richard Pancost (University of Bristol), and Bruce Mountain (GNS science, New Zealand).

The El-Tatio Geysir Field (ETGF) sinters were collected by Vernon Phoenix (University of Glasgow).

#### 2.1.2 MICROBIAL MATS

A microbial mat from the sinter terrace at Orakei Korako (OK) geothermal field in the (TVZ) was collected by Gurpreet Kaur and Bruce Mountain during the sampling expedition of September, 2006.

A number of additional microbial mats were collected by Chuanlun Zhang (University of Athens, Georgia, USA). Microbial mats were sampled from the outflow channels of several geothermal springs in the Paradise Valley geothermal region of Nevada (USA) and the Surprise Valley and Egeville areas of California (USA).

### 2.2 SAMPLE SUITE AND LOCATIONS

Silica sinter samples have been analysed from terrestrial geothermal vents from two separate geothermal locations, the Taupo Volcanic Zone, North Island, New Zealand and the El-Tatio Geysir field, Chile.

## Chapter 2

### 2.2.1 TAUPO VOLCANIC ZONE, NORTH ISLAND, NEW ZEALAND

The Taupo Volcanic Zone (TVZ) is known to be one of the most active volcanic areas in the modern natural world. The TVZ is situated on the North Island of New Zealand and covers an area of around 200000 km<sup>2</sup> and spreads from Mount Ruapehu in the south to White Island in the North.

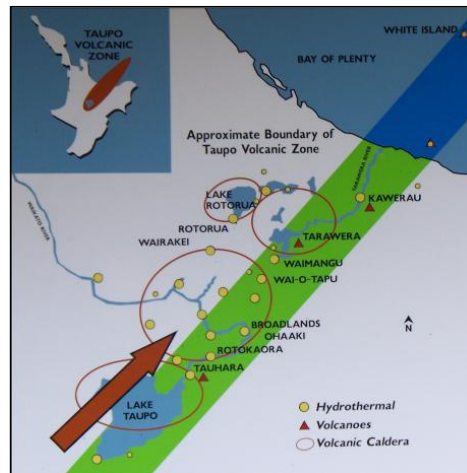


Figure 2.1 Taupo Volcanic Zone.

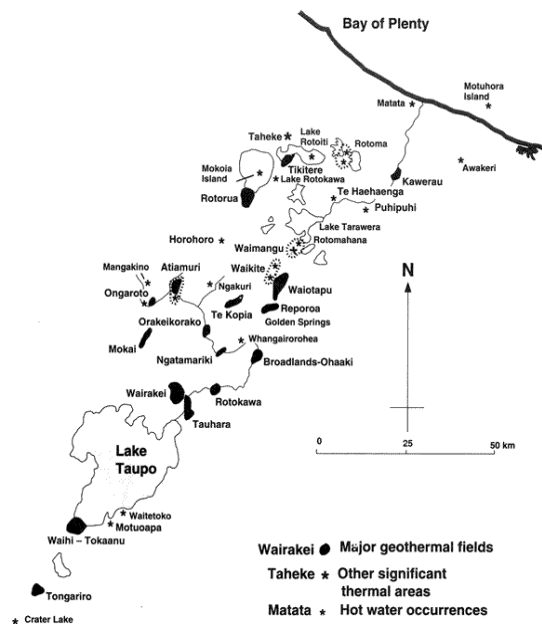


Figure 2.2 Geothermal areas of the Taupo Volcanic Zone. Picture courtesy of New Zealand geothermal association.

## Samples and methods

### 2.2.1.1 CHAMPAGNE POOL

A range of sinter samples have been analysed from Champagne Pool (CP). Samples were collected in a putative time sequence, i.e. the oldest, non-active sinter was taken from the furthest distance from the pool (Table 2.3). A series of eight sinters make up a suite of samples that derive from the most active (CP1 and Floc material) to sinter deposited around the time of the formation of the vent (CP11), ca 900 years ago (Kaur *et al.*, 2008). Further information regarding the nature of silica sinters and depositions at CP can be found in Chapter 3, section 3.1.



*Figure 2.3 Photographs of Champagne Pool. Left: Sinter terrace (grey) and sub-aqueous sinter covered in orange sulphidic floc material. Right: Artist's palette. Picture used to illustrate the scale of the Champagne Pool outflow region.*

### 2.2.1.2 ORAKEI KORAKO

Located in the TVZ, Orakei Korako (OK) geothermal field consists a number of active features including silica-depositing hot-springs, geysers, fumaroles and mud pools. Chloride concentrations at OK are relatively low for fluid that originates from deep-aquifers at TVZ (Mountain *et al.*, 2003). Samples were collected from Fred and Maggie Pool (FMP; Figure 4.1), the discharge channel from FMP and a series of inactive sinters from Golden Fleece terrace (GFT) and the now inactive Wairiri geyser. The temperature at sampling of FMP was 97.8°C and

## Chapter 2

the sample taken from the outflow channel was 68°C. The pH remained constant at pH = 7. A microbial mat collected from the sinter terrace was also analysed, the water temperature was 70°C (Kaur, 2009).

*Table 2.1 Chemical composition of vent fluid of FMP (Kaur, 2009).*

Species	Concentration (ppm)
Na	312
K	45
Li	4.0
Ca	1.7
Mg	0.04
As	0.51
Cl	301
F	11
SiO <sub>2</sub>	269
Fe	0.02
Al	<0.1
SO <sub>4</sub>	203
HCO <sub>3</sub>	228
H <sub>2</sub> S	0.20

Inactive sinters were sampled from the Golden Fleece Terrace (GFT) which is around 10 metres in a general north-westerly direction from FMP (Figure 2.5). GFT, also known as 'Te Kapua', formed during the 131 AD eruption and run-off from the Artist's Palette springs at the northern tip of the OK geothermal field cover its surface. Artist's palette was formed at least 8000 years before present and exhibits an unpredictable cycle of activity. When at its most active

## Samples and methods

the springs discharge vent fluids that support the growth of microbial mats throughout the OK geothermal area.



*Figure 2.4 Photographs of Fred and Maggie's Pool (FMP), Orakei Korako. Outflow channel observable in photograph on left-hand side (Photograph taken Nov, 2007 by the author).*



*Figure 2.5 Photograph of Golden Fleece Terrace (GFT; Photograph taken Nov, 2007 by the author).*



Figure 2.6 Panoramic view of the Orakei Korako Geothermal Field (Photograph taken Nov, 2007 by the author).

### 2.2.1.3 LOOP ROAD

Situated ~3 km south of the Wai-O-tapu geothermal area are the Loop Road (LR; Figure 2.7) hot-springs. Over the past 100 years, anthropogenic factors including attempts to harness geothermal power and artificial drainage for farmland have resulted in a number of hydrological changes to this particular setting. These include variations in water depth of the vents and biosilification of much fauna resulting in the formation of rhizolith (Jones *et al.*, 1998).

Seven samples have been analysed, including three actively precipitating sinters from the air-water interface, two non-actively precipitating sinters from a sinter flat and two samples associated with a rhizolith. During the formation of rhizolith concretions, plant tissues act as a template for silica precipitation. Rhizoliths form porous and solid laminae which contain fossilised microbial biomass (Jones *et al.*, 1998). At the time of sampling the water temperature was 70°C and pH 5.6 (Kaur, 2009).

### 2.2.1.4 OPAHEKE POOL

The spring is located in the Reporoa caldera and at the time of sampling the water was 98°C and pH 7.6 (Figure 4.2). The sample suite from Opaheke Pool (OP) comprised of five sinters, two active and three non-active samples, which were taken from increasing distance from the pool ledge to reflect an increase in age. The active sinters comprised of a spicular sinter

## Samples and methods

removed from the pool wall and a ‘pavlova’ sinter that was removed from the outflow channel. The term ‘pavlova sinter’ is a colloquialism used because of similarities between the textural development of the sinter facie and a common desert thought to have originated in NZ.

### 2.2.1.5 ROTOKAWA

The Rotokawa geothermal field (RK) is composed of a number of small vents that combine to form a small thermal lake that has a surface area of around 70 m<sup>2</sup>. Geothermal activity in this area is thought to date back to 20,000 years before present (Krupp and Seward, 1990). Oxidation of surficial acid-sulphate waters results in high sulphate concentrations and low pH (Table 2.2). The mixing of acid-chloride and acid-sulphate geothermal waters has resulted in a sinter flat that is composed of laminated amorphous silica and interbedded mud-deposits. Two non-actively precipitating sinters were removed from the north-east margin of the spring. The water temperature at the vent (Figure 4.2) was 85°C and pH 2. The temperature reduced significantly towards the discharge aprons where microstromatolites can be observed. Initial investigations have shown the lipid distributions of the micro-stromatolites, including the presence of BH*pentol*, BH*tetrol* and anhydroBHT (**13, 1, 2**; Pancost *et al.*, 2005; Talbot *et al.*, 2005).

## Chapter 2



*Figure 2.7 Sample locations. Top left: Rotokawa. Top Right: Loop Road. Bottom left: Opaheke Pool, Bottom right Terrace spring, ETGF.*

## Samples and methods

Table 2.2 Composition of vent fluid from Rotokawa vent (Kaur, 2009).

Species	Concentration (ppm)
Li	6.8
Na	824
K	88
Mg	3.6
Ca	31
B	41
Al	4.9
Fe	0.33
Mn	0.58
SiO <sub>2</sub>	333
As	0.64
Cl	1198
HCO <sub>3</sub>	<1
H <sub>2</sub> S	16
SO <sub>4</sub>	622
NO <sub>3</sub>	<0.02
PO <sub>4</sub>	<0.04
F	3.2
Br	2.2
NH <sub>3</sub>	n.m <sup>a</sup>

<sup>a</sup>n.m indicates not measured.

### 2.2.2 EL-TATIO GEYSER FIELD, CHILE

The El-Tatio geyser field (ETGF) is located in Chile at 4300 metres above sea-level and  $\sim 22^\circ$  latitude (Fernandez-Turiel *et al.*, 2005; Phoenix *et al.*, 2006). It is situated in the northern Atacama Desert near the Chile-Bolivia border (Figure 2.7). It is exposed to a high flux of solar radiation,  $\sim 35\%$  more than that at sea level (Piazena, 1996). Sinter formation at this hyper-arid site proceeds via rapid cooling and evaporation of vent waters.

#### 2.2.2.1 TERRACE SPRINGS

A number of samples were known to contain viable cyanobacterial communities inhabiting up to 10mm below the surface of the rock (Phoenix *et al.*, 2006). The source of the hot-spring water is run-off from the Andes Mountains that becomes heated by a geothermal source; most of the springs discharge water at  $\sim 86^\circ\text{C}$ , which is close to local boiling point temperature (Phoenix *et al.*, 2006). Figure 2.5 shows the sinter terrace at ETGF, a microbial mat can be seen covering the surface (Photo courtesy of V. Phoenix).



Figure 2.8 Geographical location of the El-Tatio Geyser Field, Chile.

## Samples and methods

Table 2.3 Lithographical setting and notes of sinter samples used in this study.

Sample Site	Area	Sample	Source
Champagne Pool	TVZ <sup>a</sup>	CPf	Suspended 'floc' material from vent fluid
		CP1A	Active Sinter from air-water interface. Includes orange floc material.
		CP3	Non-active sinter.
		CP5	Non-active sinter. Composed of Fissile sinter material.
		CP6	Non-active sinter. Older than CP3
		CP7	Non-active sinter. Older than CP6
		CP8	Non-active sinter. Older than CP6
		CP11	Non-active sinter. Oldest sample from CP11
Loop Road	TVZ	LR2A	Active Sinter from air-water interface
		LR2AS	Spicules from top of LR2A
		LR3A	Active Sinter from air-water interface
		LR3N	Non-active sinter
		LR4N	Non-active sinter
		LR5R	Rhizolith with silicified core
		LR6R	Hard sinter from top of rhizolith
Opaheke Pool	TVZ	OP2A	Active sinter taken from pool wall
		OP7A	Active 'Pavlova' sinter taken from outflow channel
		OP4N	Non-active sinter taken ~20 cm from Pool
		OP5N	Non-active sinter taken ~50 cm from Pool**
		OP6N	Non-active sinter taken ~4 m from Pool
Orakei Korako	TVZ	OK1-TA	Top layer of active sinter collected from Pool Wall
		OK1-MA	Middle layer of active sinter collected from Pool Wall
		OK1-BA	Bottom layer of active sinter collected from Pool Wall
		OK3A	Active sinter taken from outflow channel ~ 20m from vent
		OK4N	Non-active sinter collected from Golden Fleece Terrace
		OK5N	Non-active sinter collected from Golden Fleece Terrace
		OK6N	Non-active sinter collected from mound of inactive geyser
Rotokawa	TVZ	RK2N	Non-active sinter
		RK3N	Non-active sinter
Terrace Springs	ETGF <sup>b</sup>	ET1A	Fibrous sinter
		ET25A	Older sinter material which contained cryptoendolithic cyanobacteria*
		ET26A	Stromatolite which contained viable layers of bacteria and a cyanobacterial film on top*

<sup>a</sup>TVZ, Taupo Volcanic Zone, North Island New Zealand. <sup>b</sup>ETGF, El-Tatio Geyser Field, Chile. \* used in Pheonix et al., 2006. \*\* used in Gibson et al., 2008.

### 2.2.3 GEOTHERMAL AREAS OF CALIFORNIA AND NEVADA

A number of microbial mats were collected from geothermal springs in the USA. Samples were collected from the Egeville (EV) and Surprise Valley (SV) geothermal systems in California and the Great Boiling Springs (GBS) and Paradise Valley (PV) geothermal systems in Nevada.

The SV region includes a number of geothermal springs including the Cedarville springs, Glenn's hot spring and Applegate hot springs (not part of this Thesis). The water temperature of the SV spring is 65°C (Table 2.4) at the source and cools significantly as the water follows a small creek. South of Surprise Valley region is the EV spring where the water temperature is 55°C at the source (Table 2.4). The spring emanates from the side of a hill and at a point has been covered by construction of an access road. The Paradise Valley spring is a large travertine-depositing system with water temperature of 55°C at the source. A number of samples were provided from the Great Boiling Springs, which include samples from GBS and Rick's Hot Creek springs (RHC). Water temperature of the source of the GBS spring is 95.2°C and water at the source of RHC is 95.3°C (Table 2.4). The springs are well known tourist attractions and the spring waters are diverted into bathing pools.

## Samples and methods

*Table 2.4 Location and environmental conditions of microbial mats analysed during this study.*

Sample Site	Area	Sample	Temp	pH
Paradise Valley	California, USA	PV1*	54.0	
Eagleville	California, USA	EV1*		
		EV47	41.0	9.0
Great Boiling Spring	Nevada, USA	GBS03	23.7	7.6
		GBS08	51.1	7.3
		GBS12	59.7	6.8
		GBS18	30.9	7.5
		GBS19	95.2	7.0
Surprise Valley	Nevada, USA	Sv2 Con Source	86.0	6.4
		Sv2 Con1	63 – 70	6.1
		Sv2 Con2	69.2	6.2
		Sv2 Con3	60.4	6.0
		Sv2 Con4	53.1	8.1
		Sv2 Con5	42.0	8.8
Ricks' Hot Creek	Nevada, USA	RHC Source	95.3	6.4
		RHC04	62.9	6.0
		RHC05	53.6	8.2
		RHC06	47.7	8.3
		RHC07	41.3	8.5
Orakei Korako	TVZ <sup>a</sup>	OK-Mat	71.0	7.0

<sup>a</sup>TVZ, Taupo Volcanic Zone, North Island, New Zealand. \* used in Zhang et al., 2007.

### 2.3 CHEMICAL METHODS

An overview of analytical methodology and chemical procedures is given in Figure 2.4.3.

#### 2.3.1 EXTRACTION PROCEDURES

##### 2.3.1.1 BLIGH AND DYER EXTRACTION

The Bligh and Dyer extraction method (Bligh and Dyer, 1959) has been widely utilised for rapid and reproducible extraction of lipidic material from tissues and environmental matrices (Bligh, 1978). The extraction technique used throughout this study is that of Summons *et al.*, (1994) and is based upon the Kates' modified Bligh and Dyer extraction technique (Kates, 1975).

Sinters were freeze-dried and powdered using a Tema mill. The mill was cleaned thoroughly with DCM (distilled in-house) between samples. Microbial mats were freeze-dried and ground with a pestle and mortar that had been pre-cleaned with (DCM). Duplicate aliquots of powdered sample material were extracted as detailed below. Prior to starting an extraction all glassware, i.e. syringes, round-bottom flasks, measuring cylinders and 50 ml Teflon centrifuge tubes are cleaned thoroughly with DCM and MeOH:chloroform (2:1; v/v; MeOH distilled in house, GLC grade chloroform purchased from Fisher Scientific, UK).

Sinter material (ca. 3 g) or microbial mats (ca. 3 g) was placed into a pre-cleaned, 50 ml Teflon centrifuge tube. To this a water (4 ml; MilliQ 18 M $\Omega$ .cm<sup>-1</sup>) was added and the vial shaken to suspend the dry sinter material. A methanol/chloroform mixture (10 ml:5 ml; v/v) was added to make a solvent ratio of 0.8/2/1 (v/v/v). The sample was extracted via ultra-sonication (1 h) and left to shake for 4 h. The tube was then centrifuged for 15 min at 12,000 rpm. The solvent mixture was removed via glass syringe to another 50 ml Teflon centrifuge tube whereby phase separation was initiated via addition of a 1:1 water/chloroform mixture. The resultant chloroform phase was transferred to a pre-cleaned 100 ml round-bottomed flask (rbf).

## Samples and methods

The remaining sinter or cell material was re-extracted a further two times as above. However, the water phase from the previous extraction was further extracted via addition of the chloroform fraction separated from the second extraction and additional phase separation was achieved using a 1:1 water/chloroform mixture. The lipid extract from each extraction was combined in a 100ml rbf and evaporated to dryness under reduced pressure. The dried lipid extract was removed from the rbf via pipette using warm chloroform/methanol (2:1; v/v) and transferred to a sample vial. The lipid extract was blown down under a stream of N<sub>2</sub> and stored in a refrigerator.

### 2.3.1.2 SOXTHERM EXTRACTION

Freeze-dried sinter (5 g) was extracted using a Gerhardt soxtherm extraction apparatus with MeOH/chloroform (2:1; v/v). Pre-extracted, activated copper turnings were added to the soxtherm beaker prior to extraction to remove elemental sulphur. The extracts were transferred to rbf using warm MeOH/chloroform (2:1; v/v). Warm solvents were necessary during this procedure to prevent loss of BHPs and geohopanoids via amphiphilic attraction to the surface of the glassware. The extracts were dried under reduced pressure, transferred to samples and dried under a stream of N<sub>2</sub>. The vials were stored in a refrigerator.

### 2.3.1.3 ACCELERATED SOLVENT EXTRACTION

Sediment (8 g) was mixed with pre-extracted sand in a 5:1 ratio (sand: sample). This was then extracted with a mixture of dichloromethane/isopropanol of varying relative volumes.

### 2.3.1.4 COMPARISON OF EXTRACTION TECHNIQUES

Recent reports of BHP distributions from environmental matrices have employed the modified Bligh and Dyer extraction process (e.g. Talbot and Farrimond, 2007; Cooke *et al.*, 2008a, b; Gibson *et al.*, 2008; Coolen *et al.*, 2008; Talbot *et al.*, 2008b). However during initial studies on sinters (e.g. Talbot *et al.*, 2005), organic material was extracted using the soxtherm

apparatus (Section 2.3.1.2). In order to ensure the most efficient method of extraction was used during this study, a series of tests were carried out to investigate the most suitable method of extracting maximum amounts of polyfunctionalised lipidic material from silica sinters. Three methods were assessed: the Kates' modified Bligh and Dyer method (Section 2.1.1.1), Soxtherm extraction (Section 2.1.1.2) and an Accelerated Solvent Extraction system (ASE; Section 2.3.1.3). Extraction using the ASE system was unsuccessful and no results will be presented in the thesis.

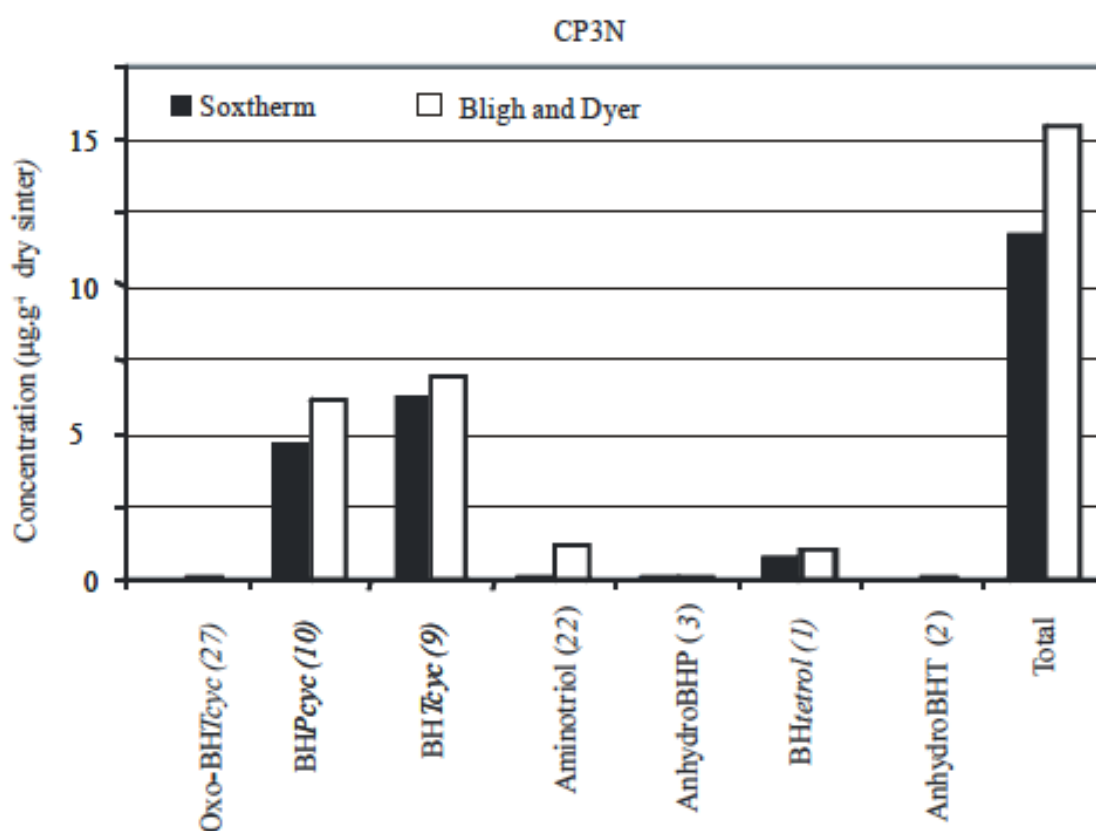


Figure 2.9 Comparison of Extraction Procedure 1: concentration of selected BHPs extracted from sample CP3N.

## Samples and methods

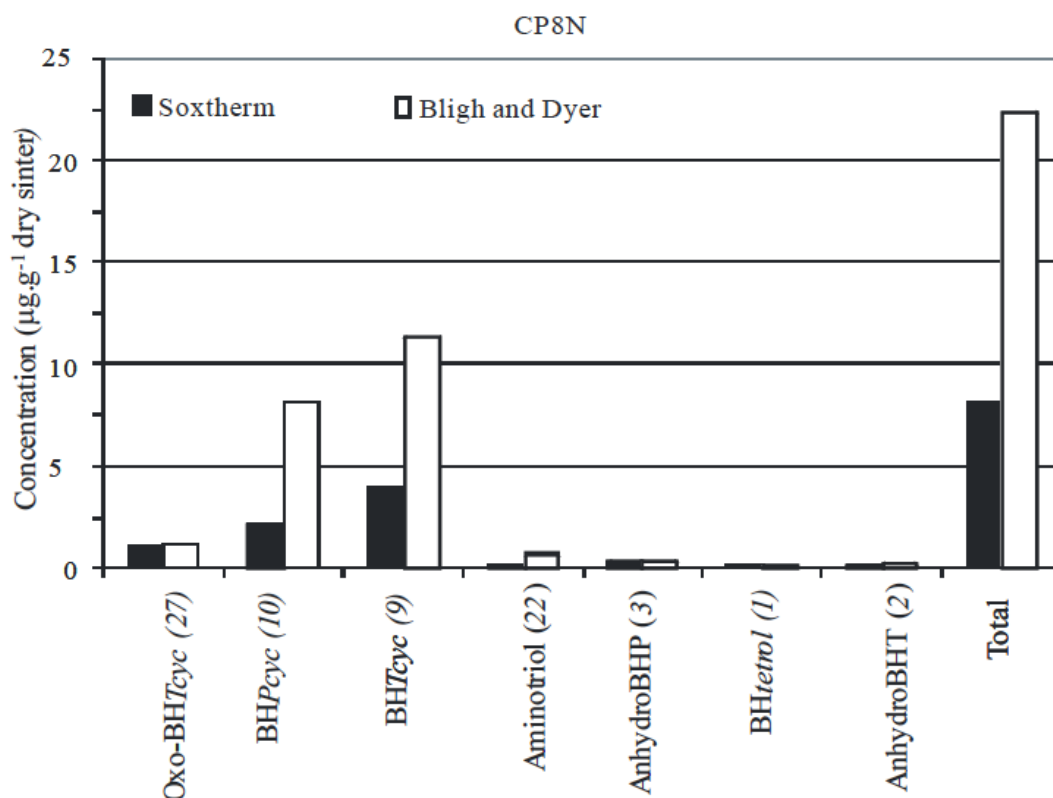


Figure 2.10 Comparison of Extraction Procedure 2: concentration of selected BHPs extracted from sample CP8N.

In both cases, the highest abundance of BHPs were extracted using the modified Bligh and Dyer extraction technique. Differences in abundances are thought to be a consequence of loss of chemical functionality caused by prolonged heating during soxtherm extraction. It should be noted that further comparison between the modified Bligh and Dyer and soxtherm extraction techniques was not possible due to the failure of the soxtherm apparatus.

### 2.3.2 DERIVITISATION

#### 2.3.2.1 ACETYLATION

An aliquot of total lipid extract (~ ¼ of the TLE) was transferred to a 10ml vial and dried under N<sub>2</sub>. The extract was re-dissolved in 4ml of Acetic Anhydride and Pyridine (1:1; v/v; reagents from Fisher Scientific, UK), recapped and heated at 50°C for 1 hour and left to stand over night. The extract was transferred to a 100ml rbf via pipette and evaporated to dryness. A

## Chapter 2

pre-cleaned splash-head was fitted to the rotary evaporator to prevent condensed acetic anhydride/pyridine returning to the rbf. Excess acetic anhydride/pyridine was removed by adding a small volume of isopropyl alcohol (IPA; ca. 5 ml; Fisher Scientific, UK). Prior to analysis, derivitised extracts were filtered using a 0.45  $\mu\text{m}$  PTFE filter.

### 2.3.2.2 METHYLATION OF HOPANOIC ACIDS

This procedure esterifies any carboxylic acids to methyl esters. An aliquot of total lipid extract ( $\sim \frac{1}{4}$  of the TLE) was transferred to a 50 ml rbf and dried under  $\text{N}_2$ . The extract was then refluxed with 15 ml boron trifluoride/methanol solution ( $\text{BF}_3 \cdot \text{MeOH}$  14%; Sigma-Aldrich, UK) and 10 ml chloroform/methanol (2:1; v/v) for 1 h. The resultant mixture was transferred to a 100ml separating funnel and a phase separation initiated via addition of chloroform (15 ml) and water (25 ml). The organic layer (bottom) was removed via the tap to a 100 ml rbf. Re-extraction was repeated 2 more times and the extracts combined and evaporated to dryness. The extract was transferred via glass pipette using warm DCM to a small vial, dried under a stream of  $\text{N}_2$  and stored in a refrigerator. For extracts that are particularly low (i.e. less than 5  $\mu\text{g}$ ), less  $\text{BF}_3$  should be added to the reflux as an excess of derivation agents can polymerise and affect the performance of the GC column and ion source of the GC-MS.

### 2.3.2.3 PERIODIC ACID/SODIUM BOROHYDRIDE CLEAVAGE OF POLYFUNCTIONALISED BHPS

The periodic acid/sodium borohydride cleavage procedure ( $\text{PA}/\text{NaBH}_4$ ; PA, Sigma Aldrich, UK) produces monofunctionalised hopanoid-aldehydes which are then subsequently reduced to homohopanols using sodium borohydride ( $\text{NaBH}_4$ ; Fisher Scientific, UK). This procedure results in the formation of monofunctionalised hopanols that are directly indicative of polyfunctionalised precursors and enables indirect quantification of hopanoids that are not amenable to GC-MS analysis (e.g. Rohmer *et al.*, 1984).

## Samples and methods

An aliquot of total lipid extract (~ ¼ of the TLE) was transferred to a small conical flask and dried under N<sub>2</sub>. To the dried extract, periodic acid (300 mg) and tetrahydrofuran/water solution (3 ml; 8:1; v:v) were added and the solution stirred for 1 hr. Distilled water (10ml) was added and the rinsing transferred to 100ml separating funnel. The conical flask was rinsed with petroleum ether (15 ml) and transferred to the separating funnel. After separation of phases, the organic layer (top) was removed via pipette to a 100 ml rbf. The conical flask was washed with petroleum ether (15 ml) and the phase separation repeated a further two times, each time washing the flask with petroleum ether (15 ml). The combined extracts in the rbf were evaporated to dryness, re-dissolved in a small amount of acetone (ca. 3 ml) and dried under N<sub>2</sub>. This concentrated the extract into the bottom of the rbf. Sodium borohydride (100mg) and ethanol (3ml) were added to the rbf and stirred for 1 hr. Potassium dihydrogen phosphate (KH<sub>2</sub>PO<sub>4</sub>; 15 ml; AnalaR, UK) was then carefully added to the rbf. After effervescence had ceased, petroleum ether (15 ml) was added to the flask and the contents transferred to a separating funnel. Further petroleum ether was added to the separating funnel (15 ml) and phases separated. The organic layer (top) was removed via pipette to a clean 100ml rbf. Phase separation was repeated a further two times. The combined extracts were evaporated to dryness under reduced pressure and transferred to a 10ml vial via pipette using warm DCM. DCM was removed under a stream of N<sub>2</sub> and the vial was stored in a refrigerator. Prior to analysis this extract required acetylating as discussed in Section 2.3.2.1.

### 2.3.2.4 SILYLATION

All of the fractions to be analysed using GC-MS required further derivitisation with a small amount of N,O-bis(trimethylsilyl)-trifluoroacetamide (BSTFA; ca. 3 – 5 drops; Fluka, UK). After addition of BSTFA, the capped vial was heated at 50°C for 1 hour. This procedure silylated any underivitised functional groups and increased the volatility of the compound, improving chromatographic performance. Excess reagent was removed by drying under N<sub>2</sub>.

### 2.3.3 PURIFICATION OF LIPID EXTRACTS FROM SINTER SAMPLES

It has been suggested previously that the employment of a clean-up step prior to analyses benefits the analysis of hopanoids and prolongs the life time of the analytical equipment (e.g. Innes, 1998; Watson, 2002). In previous studies, problems concerning sample clean up have been alleviated either passing the fraction over activated  $\text{Al}_2\text{O}_3$  (e.g. Innes, 1998) or by employment of a GC-MS with a split/splitless injector (Watson, 2002). However, during this study a number of problems were encountered when analysing hopanoid distributions, particularly when analysing using GC-MS. Firstly, low abundances of organic matter versus high quantities of sulfidic and other inorganic species resulted in a number of difficult problems to overcome. Removal of elemental sulphur using pre-extracted, activated copper turnings (VWR) proved unsuccessful and leaving a suspension of copper sulfide which then required removal via filtration. Instead, prior to derivitisation, total lipid extracts were re-dissolved in warm methanol (ca – 3-5 ml) and placed in the freezer for 30 min which caused the elemental sulfur to precipitate out of solution. The supernatant methanol was carefully removed via pipette to a clean 5 ml vial and the sample dried under  $\text{N}_2$ . The resultant extract was re-dissolved in warm methanol (ca. 3- 5 ml) and the sample placed in the freezer for 30 mins, allowing the sulphur to precipitate out of solution. This was repeated one more time.

Derivitisation of extracts to methyl esters and during  $\text{PA}/\text{NaBH}_4$  cleavage resulted in the production of extracts which exhibited very poor chromatographic performance. This has been assumed to be caused by low quantities of organic matter resulting in excess polymerisation of  $\text{BF}_3\cdot\text{MeOH}$  or periodic acid or interaction with high quantities of dissolved mineral content that remained in the TLE after extraction. In order to circumvent this issue the derivitised fraction was passed over a short column of  $\text{Al}_2\text{O}_3$  (pre-activated in oven at  $150^\circ\text{C}$  for 1 h; BHD, UK) and anhydrous sodium sulphate ( $\text{Na}_2\text{SO}_4$ ; purchased from BDH, UK) in a 10:1 mix ( $\text{Al}_2\text{O}_3$ :  $\text{Na}_2\text{SO}_4$ ). The extracts were eluted with dichloromethane/methanol (3:1; v/v). Inclusion of  $\text{Na}_2\text{SO}_4$  was

## Samples and methods

necessary to remove excess acid from the methyl ester fraction. Samples were then passed through a 0.45 $\mu$ m PTFE filter (VWR international).

### 2.4 ANALYTICAL METHODS

#### 2.4.1 APCI-HPLC-MS<sup>N</sup>

The acetylated extract was dissolved in 500  $\mu$ l of methanol/propanol (60/40; v/v) for injection onto the High Performance Liquid Chromatography Column (HPLC). Reversed phase (rp) HPLC analysis was carried out using a Thermo Surveyor HPLC system equipped with a Phenomenex C<sub>18</sub> column (5 $\mu$ m; 150 mm x 3 mm i.d.) with an inline Phenomenex guard column made from the same material (Macclesfield, UK). Separation was achieved at 1 mL.min<sup>-1</sup> using the following gradient profile: A = 90%, B = 10 %, C = 0 % (0 – 5 mins); A = 59 %, B = 40, C = 1% (at 45 mins; where A= MeOH, B = Water, C = IPA; HPLC grade solvents, Fisher Scientific, UK), then isocratic till to 70 mins.

LC/MS<sup>n</sup> was performed using a ThermoFinnigan LCQ ion trap mass spectrometer equipped with an atmospheric pressure chemical ionisation (APCI) source. The LC-MS<sup>n</sup> settings were: capillary temperature 155°C, APCI vaporiser temperature 400°C, corona discharge current 8  $\mu$ A, sheath gas flow 40 and auxiliary gas flow 10 (arbitrary units). The APCI source was operated in positive ion mode.

LC-MS<sup>n</sup> was carried out in data-dependant scan mode; Scan event 1 – full mass spectrum, range m/z 400 – 1200; Scan event 2 – data dependant MS<sup>2</sup> product ion spectrum of the most abundant ion from Scan 1; Scan event 3 – data-dependant MS<sup>3</sup> product ion spectrum of the largest from Scan 2.

A semi-quantitative estimate of BHP-abundance was calculated by comparison of individual base peak area relative to the [M+H – AcOH]<sup>+</sup> = m/z 345 base peak area of acetylated 5 $\alpha$ -pregnane-3 $\beta$ , 20 $\beta$ -diol (Sigma-Aldrich, UK), used as an internal standard. Calibration of

response factors was done using a suite of five standard BHP peak areas whereby N containing BHPs were found to give a response roughly 12 times that of the internal standard and BHPs with no N atoms were found to give a response factor roughly eight times that of the internal standard.

### 2.4.2 GAS CHROMATOGRAPHY-MASS SPECTROMETRY (GC-MS)

Aliquots of derivitised samples were dissolved in 100  $\mu\text{L}$  of DCM prior to injection onto the GC-MS column. Acetylated fractions were run on a DB5-HT column and PA/ $\text{NaBH}_4$  and methyl ester fractions were run on a DBX-LB column. In many cases due to the small quantities of lipid extract, samples had to be concentrated into 30  $\mu\text{L}$  in order to improve peak intensity for identification. Ions were identified in full scan mode and quantified in selected ion monitoring mode (SIM). The SIM program consisted of eight ions,  $m/z$  189, 191, 203, 205, 243, 245, 258 and 260. Hopanoids were identified from the  $m/z$  191 chromatogram and ring A methylated hopanoids were identified using the  $m/z$  205 chromatogram relative to androstane ( $m/z$  245; Sigma-Aldrich, UK) and androstanol ( $m/z$  243; Sigma-Aldrich, UK) standards. GC-MS analysis was carried out on a Hewlett-Packard 5890 II GC (Split/Splitless injector) linked to a Hewlett-Packard 5872 MSD (electron voltage 70eV; Filament current 220  $\mu\text{A}$ ; Source temperature 270°C; Multiplier voltage 2000V; interface temperature 350°C). For separation and analysis of the acetylated fraction, a DB5-HT column (15m x 0.25  $\mu\text{m}$  i.d.; 0.1 mm film thickness) was used with helium carrier gas. The oven temperature was programmed from 50 – 200°C at 15°C/min (held for 1 min), 200 – 250°C at 10°C/min (held for 1 min) and 250 – 350°C at 5°C/min (held for 8 min). Selected samples were run in full scan mode ( $m/z$  50 – 700) to obtain mass spectra of compounds. Semi-quantitative estimation of hopanoid abundances were measured by comparison of their peak areas with those of an internal standard, 5 $\alpha$ -androstane (for hopanes and hopanoic acids) and 5 $\alpha$ -androstan-3 $\beta$ -ol (for hopanols) with a relative response factor of 1.

## Samples and methods

Peak identification was based upon comparison of spectra with authentic standards, previously reported spectra (e.g. Philp, 1985) and relative retention times. Analyses were carried out between January and May, 2008. To check the reproducibility of results a sample (From Priest Pot analysed by Watson, 2002) of known composition was run during the analysis of acetylated fractions (Figure 2.11).

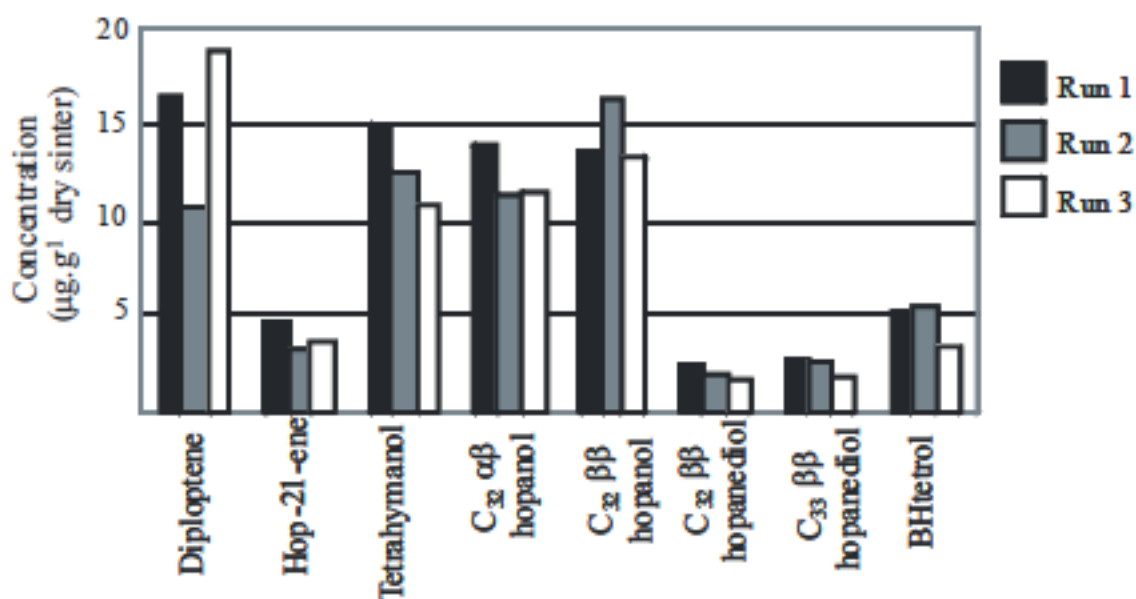


Figure 2.11 Comparison of the abundances of selected hopanoids during re-runs of the acetylated fraction of sample from Priest Pot (e.g. Watson, 2002).

For separation and analysis of the PA/NaBH<sub>4</sub> and methylated fractions a DB-XLB column (cf. Jahnke *et al.*, 2004; 30 m x 0.25 µm i.d.; 0.25 µm film thickness) was used with helium carrier gas. The oven temperature was programmed at 60 – 200°C at 10°C/min (held for 1 min), 200 – 340°C 4°C/min held for 30 min. Selected samples were run in full scan mode (m/z 50 – 700) to obtain mass spectra of compounds. Peak identification was based upon comparison of spectra with authentic standards, previously reported spectra (e.g. Philp, 1989) and relative retention times. Semi-quantitative estimation of hopanoid abundance was measured by comparison of peak areas with those of an internal standard, 5α-androstane (for hopanes and

hopanoic acids) and  $5\alpha$ -androstan- $3\beta$ -ol (for hopanols) with a relative response factor of 1. Analyses were carried out between April and November, 2008. To check the reproducibility a sample of known composition (sample CP11a) was run during the analysis of PA/ $\text{NaBH}_4$  fractions (Figure 2.12).

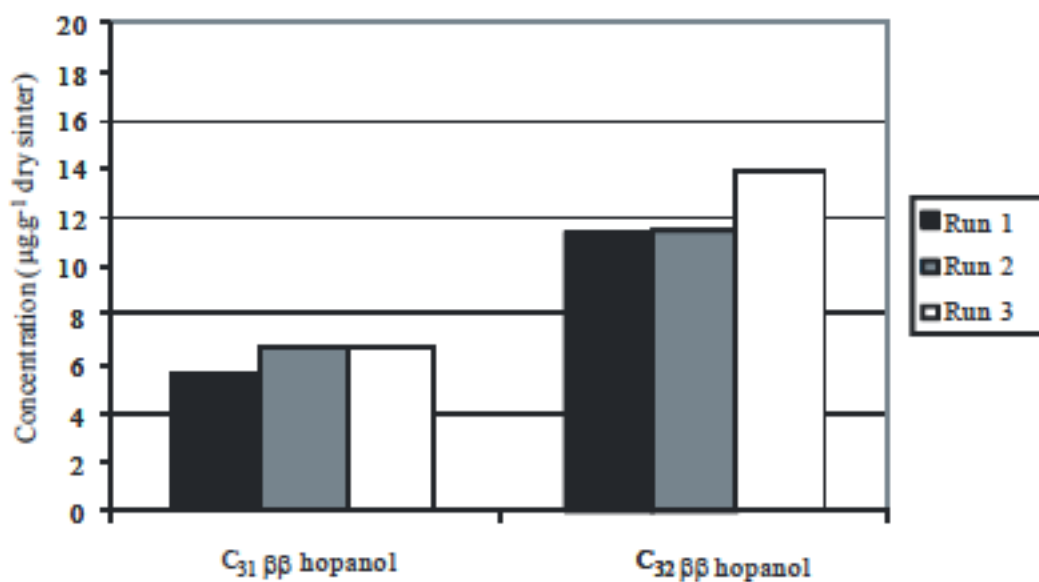


Figure 2.12 Comparisons of abundances of hopanols detected during series of sample runs of PA/ $\text{NaBH}_4$  fraction of sample CP11a.

## Samples and methods

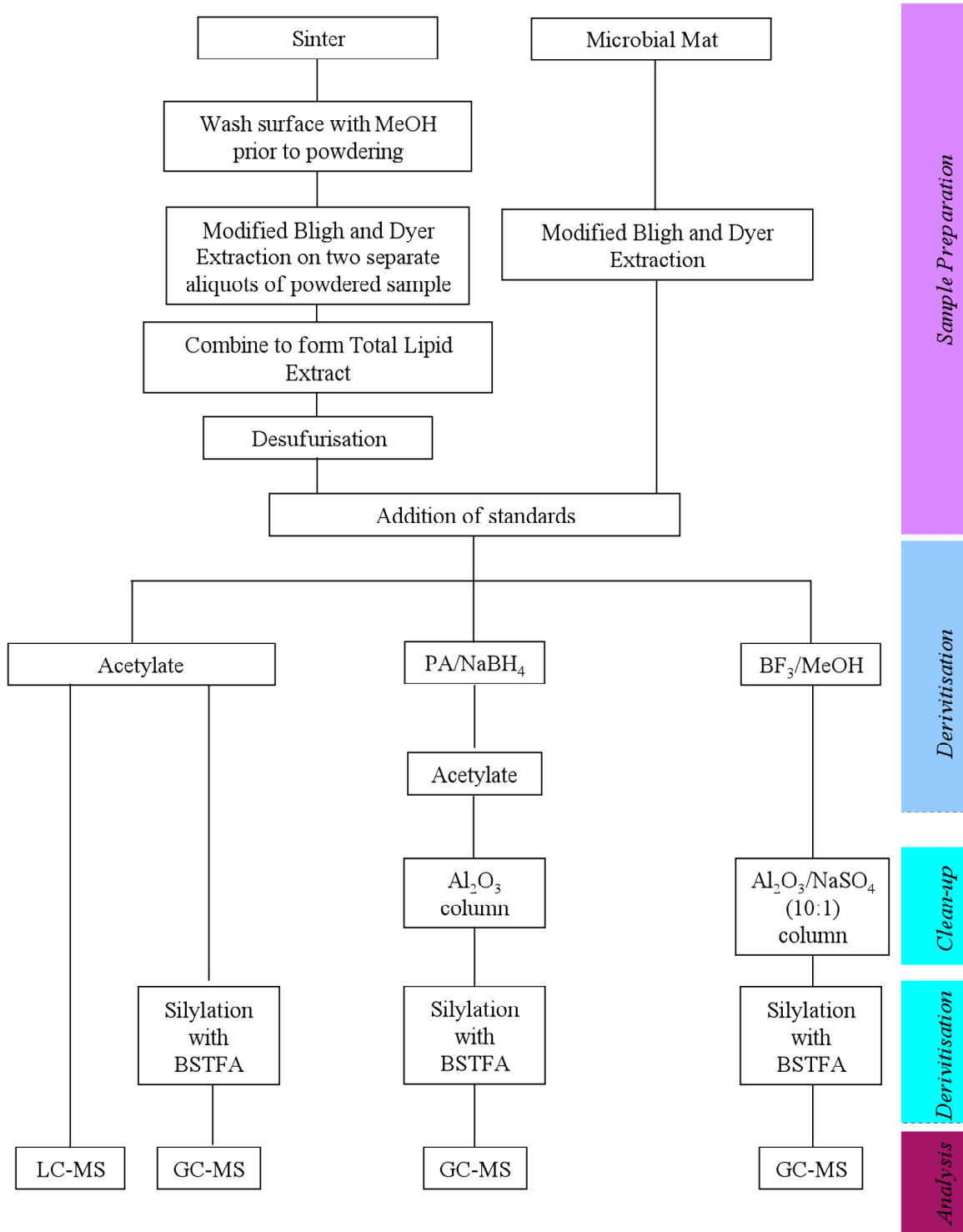


Figure 2.11 Schematic of methodology.

### 3 DISTRIBUTIONS OF INTACT BHPs IN ACTIVE BIOFACIES OF TERRESTRIAL GEOTHERMAL SYSTEMS

#### 3.1 INTRODUCTION

This study presents the analysis of distributions of BHPs derived from bacteria that colonise actively precipitating sinter formations and form microbial mats of terrestrial geothermal vents. The sample suite consists of a number of active sinters from the Taupo Volcanic Zone (TVZ), North Island, New Zealand and the El-Tatio Geyser Field, Chile (ETGF). The BHP distributions of microbial mats collected from outflow regions of geothermal areas in TVZ and Nevada and California, USA have also been investigated and provide complimentary information regarding depositional environment.

For the purpose of this study, active biofacies include actively-precipitating silica sinters and microbial mats from the outflow channels of silica-depositing vents. Floc material composed of sulfidic minerals with incorporated biomass sampled from the vent waters have also been investigated. Bacterial cultures of *Thermoanaerobacter tencongenensis* (Phylum: Firmicutes) and *Venenivibrio stagnispumantis* (Phylum: aquificales) were also tested for the presence of BHPs, however, both cultures did not produce BHPs or hopanoids (samples kindly provided by Adrian Hetzer, University of Waikato, New Zealand). The BHP distributions in the samples of this particular study are regarded to most closely resemble the bacterial community of the vent source and of the outflow regions of these terrestrial vents.

The sites investigated during this study have received little, or in some cases no, prior investigations regarding possible microbial populations or biogeochemical processes occurring *in-situ*. The most famous and well-studied site is Champagne Pool (CP; e.g. Jones *et al.*, 2001; Mountain *et al.*, 2003; Pheonix *et al.*, 2005; Pancost *et al.*, 2005; Kaur *et al.*, 2008; Childs *et al.*, 2008; Hetzer *et al.*, 2008). This site in particular has been the focus of

many investigations concerning biomineralisation of microbial life and the biogenic nature of silica sinters (Mountain *et al.*, 2003; Phoenix *et al.*, 2005; Hetzer, 2009). Investigations concerning the microbiology of the vent water and surrounding vicinity have shown a diverse microbial assemblage that is highly variable and dependant upon depositional regime (e.g. Jones *et al.*, 2001; Hetzer *et al.*, 2007; Childs *et al.*, 2008). The remnants of microbial colonisation recorded in CP sinters are well documented (Mountain *et al.*, 2003; Phoenix *et al.*, 2005; Kaur *et al.*, 2008).

Much work has centred upon the morphological and geochemical nature of the sinter formations at CP (e.g. Jones *et al.*, 2001; Mountain *et al.*, 2003; Phoenix *et al.*, 2005). The sinter deposits at CP consist of a sub-aerial sinter formation that encompasses the pool, except for the margin that is directly adjacent to Artist's Palette. The grey sinter rim reaches around 15 cm over the ledge of the pool in some places (Figure 3.1). Scanning electron microscopy has shown that the sinters are laminated and contain abundant low-diversity microbial consortia that consist of either filamentous or coccoid bacteria (Jones *et al.*, 2001). A subaqueous sinter shelf is also observable around the entire pool. This sinter formation is covered by orange filamentous floc material which is suspended throughout the pool water and accumulates over the surface of sub-aqueous domal stromatolites. The flocs are composed of As-Sb silicified filaments and are thought to be thermophilic anaerobic bacteria or archaea (Jones *et al.*, 2001), possibly *Thermoplasmatales* (Reysenbach and Cady, 2001; Childs *et al.*, 2008). Recent studies using culturing-independent and culture based studies have elaborated on previous estimates and indicated a predominance of thermophilic microbiota that utilise hydrogen-oxidising and sulphur-respiring metabolic pathways (Hetzer *et al.*, 2007; Hetzer *et al.*, 2008; Childs *et al.*, 2008). However, gene sequences that exhibit low similarity to known bacterial and archaeal phylotypes suggest that a proportion of the microbiota associated with CP remains to be characterised.

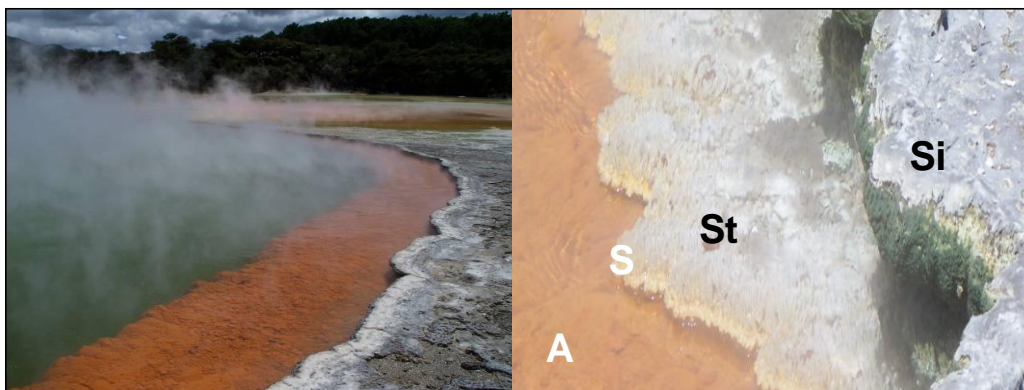


*Figure 3.1 Sinter formations at Champagne Pool. Left: Photograph showing sub-aqueous sinter shelf covered with orange floc material. Right: Sinter formation zone. A = anoxic vent water. S = Sulphur formed via abiotic oxidation of  $H_2S$ . St = Spicular stromatolites. Si = Sinter formation.*

The sinter formations of ETGF have provided a natural setting in which to investigate the effect that biomineralisation has upon the ability of cyanobacteria to colonise environments that are exposed to high levels of solar radiation (Phoenix *et al.*, 2006). In this example, specific BHPs that are diagnostic of cyanobacteria were targeted. This investigation of the distribution of BHPs appears to be the first organic geochemical study of sinters from ETGF. Analysis of sinters from ETGF were chosen to determine if common BHP-signatures are observed in sinter material from a geographically distinct location. ETGF is an important addition to the sample suite as the hyper-arid, high altitude and low-latitude conditions of the site allow further evaluation of the environmental limits of BHP-producing bacteria.

Microbial mats can be considered to be a truly ancient form of life, as observed in stromatolites (Schopf, 1993) and Banded Iron Formations (BIFs). Stromatolites are known to have been vastly more abundant during Archean and Proterozoic successions and were confined to intertidal settings, saline lakes and thermal springs during the Palaeozoic (Walter, 1996). BIFs are often associated with lithified microbial mats thought to consist of iron reducing phototrophs (Kappler *et al.*, 2005). Microbial mats from modern terrestrial geothermal environments have lipid distributions that are known to be similar to preserved

hydrocarbons from Archean and Proterozoic successions (Summons *et al.*, 1996). Low molecular weight, simple and branched alkyl chains, acyclic polyprenoids such as phytanes, phytol and carotenoids are abundant (Ward *et al.*, 1985; Dobson *et al.*, 1988; Robinson and Eglinton, 1990; Shiea *et al.*, 1991; Zeng *et al.*, 1992; Summons *et al.*, 1996; Jahnke *et al.*, 2004; Zhang *et al.*, 2004). Intrinsic differences are also present; primarily the lipid distributions in modern mat-forming consortia reflect the distribution of living biota and are therefore polyfunctionalised lipids such as phospho- and glycerol fatty acids, alcohols, wax esters, bacterial diethers, glycerol diphytanyl glycerol tetraethers and polyfunctionalised bacterial hopanoids (e.g. Shiea *et al.*, 1990; Pearson *et al.*, 2004; Jahnke *et al.*, 2004; Zhang *et al.*, 2007; van der Meer *et al.*, 2008). In order to complement the results of the studies on active sinters, a survey of the lipid distributions of mat-forming bacteria colonising outflow regions of a number of terrestrial vents has been conducted. Previous work concerning BHP and hopanoid distributions of mat-forming bacteria from Yellowstone National Park showed the presence of a few non-specific BHPs (Talbot *et al.*, 2008a) whilst mat-forming consortia from the Paradise Valley geothermal area (Nevada) showed a diverse BHP-assemblage including specific cyanobacterial and methanotrophic bacterial signatures (Zhang *et al.*, 2007) similar to those detected in a non-active sinter from Opaheke Pool (OP; Gibson *et al.*, 2008).

Microbial mats situated in outflow channels that originate from terrestrial vents allow determination of changes in microbial populations and observed lipid distributions down a temperature gradient. This should give insight into how temperature can affect BHP-distributions in a natural setting. Other factors such as pH and solute concentration measured at the time of sampling will allow similar investigations.

Numerous geothermal settings exist in the TVZ, yet relatively little is known regarding the microbiology and biogeochemistry of the vents and outflow regions. The BHP distributions of sinters collected from a number of other sites are also reported in this study. Silica sinters from Loop Road (LR), Orakei Korako (OK) and Opaheke Pool (OP) have only

been subjected to organic geochemical analyses where a holistic approach to lipid analysis was adopted (e.g. Kaur, 2009).

Lipid biomarkers have been shown to be powerful tools in characterising microbial populations colonising geothermal vents and outflow regions (e.g. van der Meer *et al.*, 2001; Pancost *et al.*, 2005; Talbot *et al.*, 2005; Pancost *et al.*, 2006, Kaur *et al.*, 2008; Kaur, 2009). In this study, assessment of distributions of intact Bacteriohopanepolyols (BHPs) have been employed to investigate bacterial populations, bacterially-mediated processes and the preservation of this class of biomarker in active facies of terrestrial geothermal systems.

### 3.1.1 AIMS AND SCOPE OF THIS STUDY

This study aims to investigate the BHP composition associated with actively-precipitating silica sinters from terrestrial geothermal vents of TVZ and ETGF. The aims of this study are to:

- Investigate the BHP composition of active silica sinters, organo-sedimentary depositions and microbial mats associated with a modern terrestrial geothermal vent
- Document variations observed between depositional regimes
- Assess the potential for BHPs to characterise any bacterial populations in the vents studied

## 3.2 RESULTS

The distribution of BHPs have been analysed from ‘active’ settings (facies) of terrestrial geothermal vents including microbial mats, sulphide-precipitate and actively precipitating silica sinters from the air-water interface. Distributions of polyfunctionalised BHPs have been analysed using LC-MS<sup>n</sup> methodology (Chapter 2) and partial LC-MS chromatograms illustrating the diversity of structures observed are presented below. The identification and (partial) structural characterisation of novel BHP compounds in these samples is detailed in Chapter 5.

### 3.2.1 RESULTS: ANALYSIS OF BHP DISTRIBUTIONS FROM ACTIVE FACIES OF CHAMPAGNE POOL

The ‘active facies’ can be further divided by the fact they consist of flocculation (floc) material from a sub-aqueous environment (CPf) and sub-aerial actively precipitating sinter (CP1A) from the air-water interface.

#### 3.2.1.1 FLOC MATERIAL (SUB-AQUEOUS)

Four BHPs were identified during LC-MS<sup>n</sup> analysis of sample CPf. The distribution consists entirely of known BHPs. These were BHP<sub>cyc</sub>, BHT<sub>cyc</sub>, aminotriol, BH<sub>tetrol</sub> (**10**, **9**, **22**, **1**; Figure 3.2222). BH<sub>tetrol</sub> was the least abundant compound detected and aminotriol was the most abundant with concentrations ranging from 0.88 to 3.1 µg.g<sup>-1</sup> dry sinter (Table 3.1).

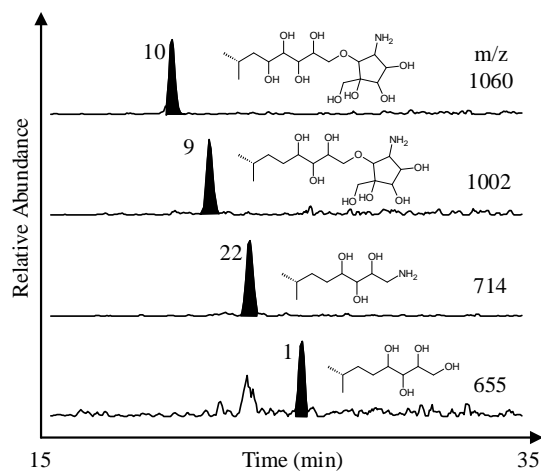


Figure 3.2 Partial mass chromatogram (15 – 35 min) showing BHP distribution observed in floc material from CP (Sample CPf). Structures and structure numbers related to underivitisised parent compounds but note compounds are analysed as peracetate derivatives.

### 3.2.1.2 ACTIVE SINTER (SUB-AERIAL)

An actively precipitating sinter from the air-water interface (CP1A) was found to contain six BHPs: BHP<sub>cyc</sub>, BHT<sub>cyc</sub>, BHT<sub>gly</sub>, Aminotriol and BH<sub>tetrol</sub> (**10**, **9**, **11**, **22**, **1**; Figure 3.33). Abundances of known BHPs range from 0.37 to 1.6  $\mu\text{g}\cdot\text{g}^{-1}$  dry sinter (Table 3.1). Oxo-BHT<sub>cyc</sub> (**34**) has been tentatively-identified as a novel BHP (See section 5.2.2), was detected in this sample and was present in a concentration of 0.1  $\mu\text{g}\cdot\text{g}^{-1}$  dry sinter. Total BHP abundances in this sample were 4.34  $\mu\text{g}\cdot\text{g}^{-1}$  dry sinter. Structural characterisation of novel compounds and interpretation of their APCI MS<sup>2</sup> and MS<sup>3</sup> spectra can be found in Chapter 5 (Section 5.5.2)

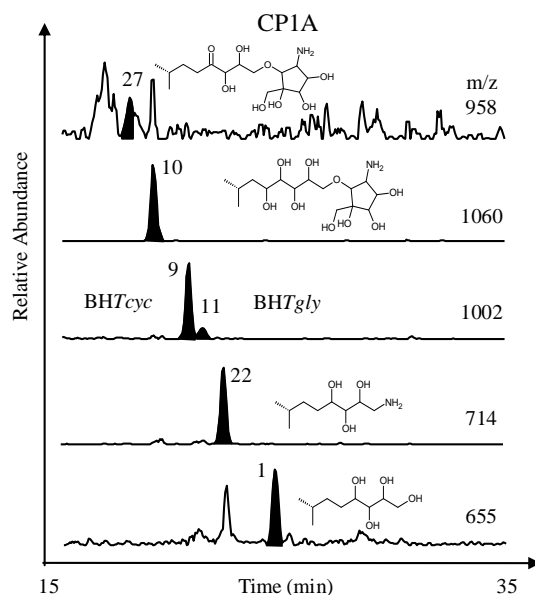


Figure 3.3 Partial mass chromatograms (15 – 35 min) showing distribution of BHPs in sinter from air-water interface from Champagne Pool (Sample CP1A).

### 3.2.2 BHP DISTRIBUTIONS OF ACTIVE SINTERS FROM OK

Active sinters were collected from the pool edge of Fred and Maggie's Pool (FMP; samples OK1A) and from the edge of the outflow channel (OK3A), around 20 m from FMP.

#### 3.2.2.1 FRED AND MAGGIE'S POOL: VENT

The BHP distribution observed in the 'top' and 'bottom' layers of OK1A (samples OK1-TA and OK1-BA) were similar and consist of BH*pentol*, 2-me BH*pentol*, BH*tetrol* and anhydroBHT (**13**, **II-13**, **1**, **2**; Figure 3.44). In the top layer, anhydroBHT (**2**) was the least abundant BHP and BH*pentol* (**13**) was the most abundant BHP, with concentrations ranging from 0.01 to 0.04  $\mu\text{g}\cdot\text{g}^{-1}$  dry sinter (Table 3.1). In the bottom layer, anhydroBHT (**2**) was present in trace amounts and 2-me BH*pentol* (**II-13**) was the most abundant BHP (0.03  $\mu\text{g}\cdot\text{g}^{-1}$  dry sinter; Table 3.1).

The 'middle' layer of the sinter (Figure 3.44; sample OK1-MA) showed a more diverse BHP distribution consisting of eight BHPs, of which seven are previously known and

one is tentatively assigned here as a novel BHP. The distribution of known BHPs consists of *BHP<sub>cyc</sub>*, *BH<sub>pentol</sub>*, *2-me BH<sub>pentol</sub>*, *2-me aminotriol*, *BH<sub>tetrol</sub>*, *2-me BH<sub>tetrol</sub>* and anhydroBHT (**10**, **13**, **II-13**, **II-22**, **1**, **II-1**, **2**). *BHP<sub>cyc</sub>* (**10**) was the least abundant BHP detected and *BH<sub>pentol</sub>* (**13**) was the most abundant BHP detected, with concentrations ranging from 0.04 to 0.2  $\mu\text{g}\cdot\text{g}^{-1}$  dry sinter (Table 3.1). A tentatively assigned novel BHP with an acetylated parent ion of  $[\text{M}+\text{H}]^+ = m/z$  1256 (**28**) was also present in this sample in a concentration of 0.1  $\mu\text{g}\cdot\text{g}^{-1}$  dry sinter. (See Chapter 5 for interpretation of novel  $\text{MS}^2$  spectra.)

The total abundance of BHPs in each sample was 0.20, 0.27 and 0.16  $\mu\text{g}\cdot\text{g}^{-1}$  dry sinter for samples OK1-TA, OK1-MA and OK1-BA respectively (Table 3.1).

Active Biofacies

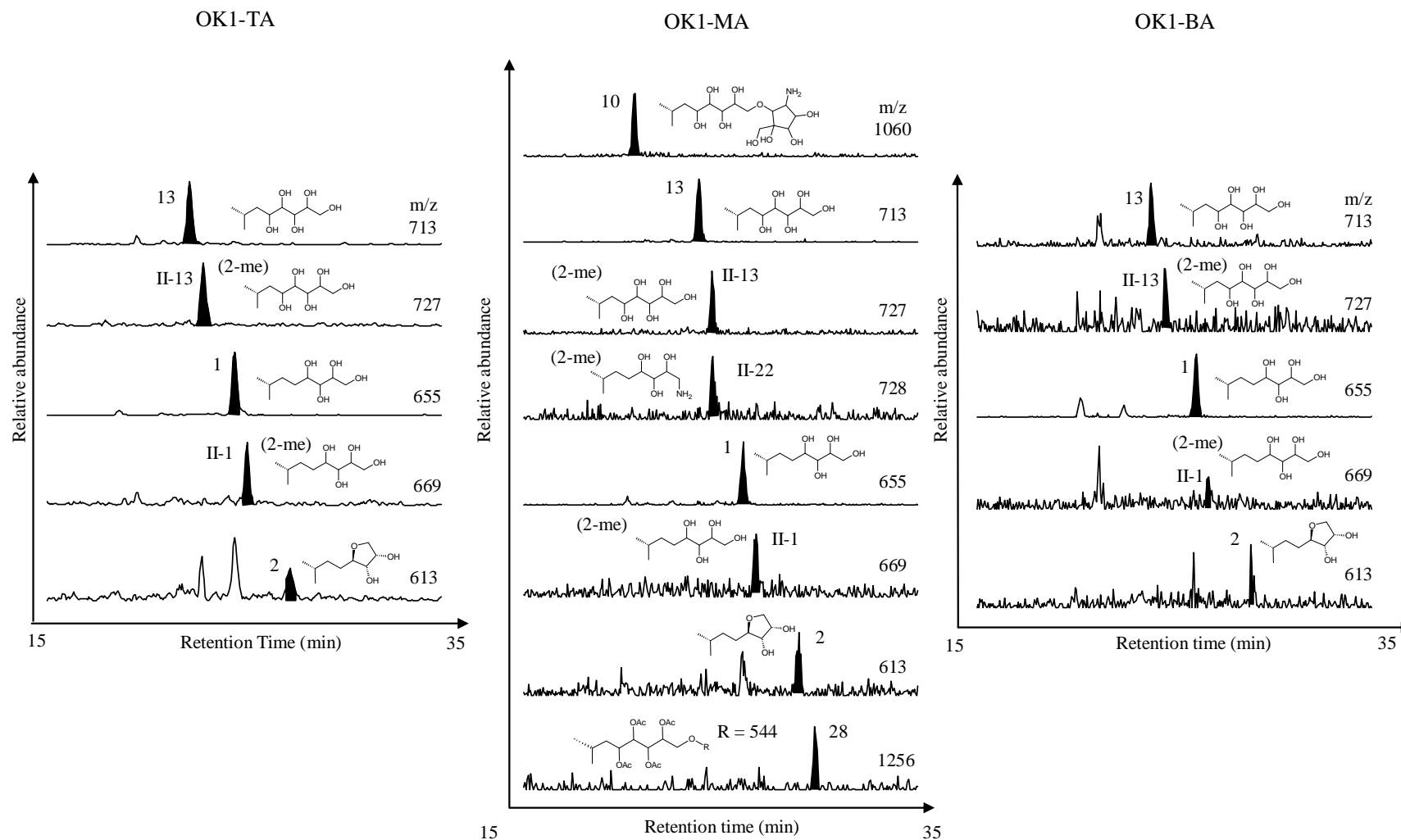


Figure 3.4 BHP distributions of active sinter collected from the vent of Fred and Maggie's Pool. Partial mass chromatograms (15 – 35 min) showing BHPs detected in the top (left), middle (centre) and bottom (right) layer of the sinter collected from FMP

## 3.2.2.2 FRED AND MAGGIE'S POOL: OUTFLOW CHANNEL

The BHP distribution of a silica sinter (OK3A) taken from the outflow channel of FMP (~ 20 m from vent source) showed a different BHP assemblage than that observed in the sinter from the source. Seven BHPs were detected (Figure 3.5) in sample OK3A. The distribution consists of five BHPs that have previously been characterised (*BHP<sub>cyc</sub>*, *BHT<sub>cyc</sub>*, aminotriol, *BHtetrol* and anhydroBHT; **10**, **9**, **22**, **1**, **2**) and two compounds that have been tentatively assigned as novel BHPs during this study with  $[M+H]^+ = m/z$  958 (**27**; oxo-*BHT<sub>cyc</sub>*; See Chapter 5, Section 5.3.2.1 for structural assignment) and  $m/z$  1018. anhydroBHT (**2**) was the least abundant and aminotriol (**22**) was the most abundant BHP detected, with concentrations ranging from 1.18 to 420  $\mu\text{g}\cdot\text{g}^{-1}$  dry sinter (Table 3.1). Aminotriol accounts for over 77% of the total BHP abundance in this sample. The two novel BHPs tentatively identified in this sample, oxo-*BHT<sub>cyc</sub>*, and a compound with parent ion mass  $[M+H]^+ = m/z$  1018 (**27**, **29**; Figure 3.5) are each present in abundances of 0.34  $\mu\text{g}\cdot\text{g}^{-1}$  dry sinter.

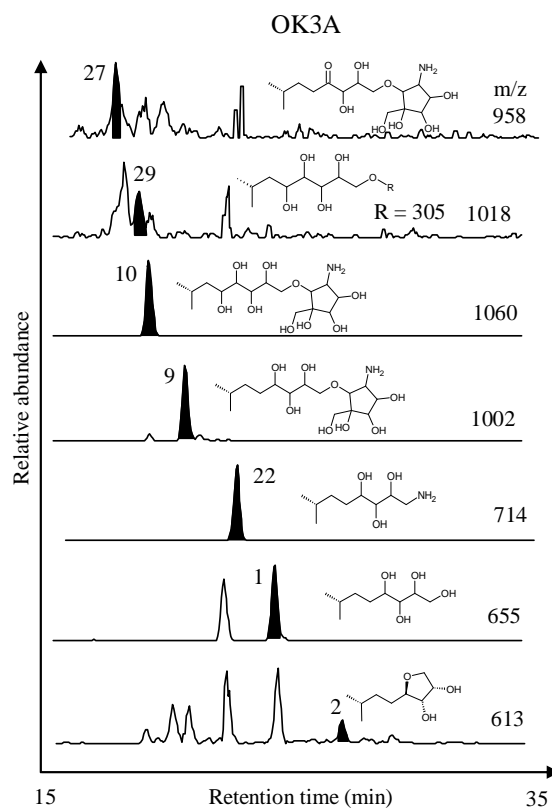


Figure 3.5 Partial mass chromatogram (15 – 35 min) showing BHPs detected in active sinter taken from outflow channel of FMP.

### 3.2.2.3 ACTIVE SINTER FACIES FROM LOOP ROAD

Eight BHPs were detected during analysis of sample LR2A (Figure 3.6666), of which seven have been previously characterised (BHP<sub>cyc</sub>, BHT<sub>cyc</sub>, 2-me BHT<sub>cyc</sub>, BH<sub>pentol</sub>, aminotriol, BH<sub>tetrol</sub> and anhydroBHT; **10**, **9**, **II-9**, **13**, **22**, **1**, **2**) and one compound has been tentatively assigned as a novel BHP. Known BHPs detected in this sample were BHP<sub>cyc</sub>, BHT<sub>cyc</sub>, 2-me BHT<sub>cyc</sub>, BH<sub>pentol</sub>, aminotriol, BH<sub>tetrol</sub> and anhydroBHT (**10**, **9**, **II-9**, **13**, **22**, **1**, **2**). 2-me BHT<sub>cyc</sub> (**II-9**) was the least abundant BHP while aminotriol (**22**) was the most abundant BHP detected in this sample with concentrations ranging from 0.02 to 1.3  $\mu\text{g}\cdot\text{g}^{-1}$  dry sinter (Table 3.1). Isomeric versions of BHT<sub>cyc</sub> (**9**) were observed on the mass chromatogram of m/z 1002, however, it was not possible to positively identify the species from the MS<sup>2</sup> spectrum (Figure 3.6). The novel BHP identified in sample LR2A has  $[\text{M}+\text{H}]^+ = \text{m/z } 958$  (**27**) and was present in a concentration of 0.03  $\mu\text{g}\cdot\text{g}^{-1}$  dry sinter.

Seven BHPs were detected during analysis of sample LR2AS (Figure 3.6), of which six are known BHPs and one BHP has been tentatively assigned as a novel BHP. The distribution of BHPs that have been previously characterised consisted of *BHP<sub>cyc</sub>*, *BHT<sub>cyc</sub>*, *BH<sub>pentol</sub>*, aminotriol, *BH<sub>tetrol</sub>* and anhydroBHT (**10**, **9**, **13**, **22**, **1**, **2**). AnhydroBHT (**2**) was the least abundant BHP detected and *BHP<sub>cyc</sub>* (**10**) was the most abundant BHP detected with concentrations ranging from 0.08 to 0.51  $\mu\text{g}\cdot\text{g}^{-1}$  dry sinter (Table 3.1). A novel compound with  $[\text{M}+\text{H}]^+ = m/z$  958 (**27**) has been tentatively identified as oxo-*BHT<sub>cyc</sub>* and was found to be present in a concentration of 0.04  $\mu\text{g}\cdot\text{g}^{-1}$  dry sinter.

Ten BHPs were been detected during analysis of sample LR3A (Figure 3.6), of which seven are known BHPs and three have been tentatively assigned as novel BHPs during this study. The distribution of BHPs that have been previously characterised consists of *BHP<sub>cyc</sub>*, *BHT<sub>cyc</sub>*, aminotriol, *BH<sub>pentol</sub>*, anhydroBHP, *BH<sub>tetrol</sub>* and anhydroBHT (**10**, **9**, **22**, **13**, **3**, **1**, **2**). AnhydroBHP (**3**) was the least abundant BHP and aminotriol was the most abundant BHP, with concentrations ranging from 0.07 to 1.16  $\mu\text{g}\cdot\text{g}^{-1}$  dry sinter (Table 3.1). The novel BHPs detected in this particular sample consisted of oxo-*BHT<sub>cyc</sub>*,  $[\text{M}+\text{H}]^+ = m/z$  1018 and guanidine-substituted *BHP<sub>cyc</sub>* (**27**, **29**, **30**). Guanidine- substituted *BHP<sub>cyc</sub>* (**30**) was present in trace amounts; oxo-*BHT<sub>cyc</sub>* (**27**) and  $[\text{M}+\text{H}]^+ = m/z$  1018 (**29**) were present in concentrations of 0.01  $\mu\text{g}\cdot\text{g}^{-1}$  dry sinter respectively and trace amounts respectively (Table 3.1).

### Active Biofacies

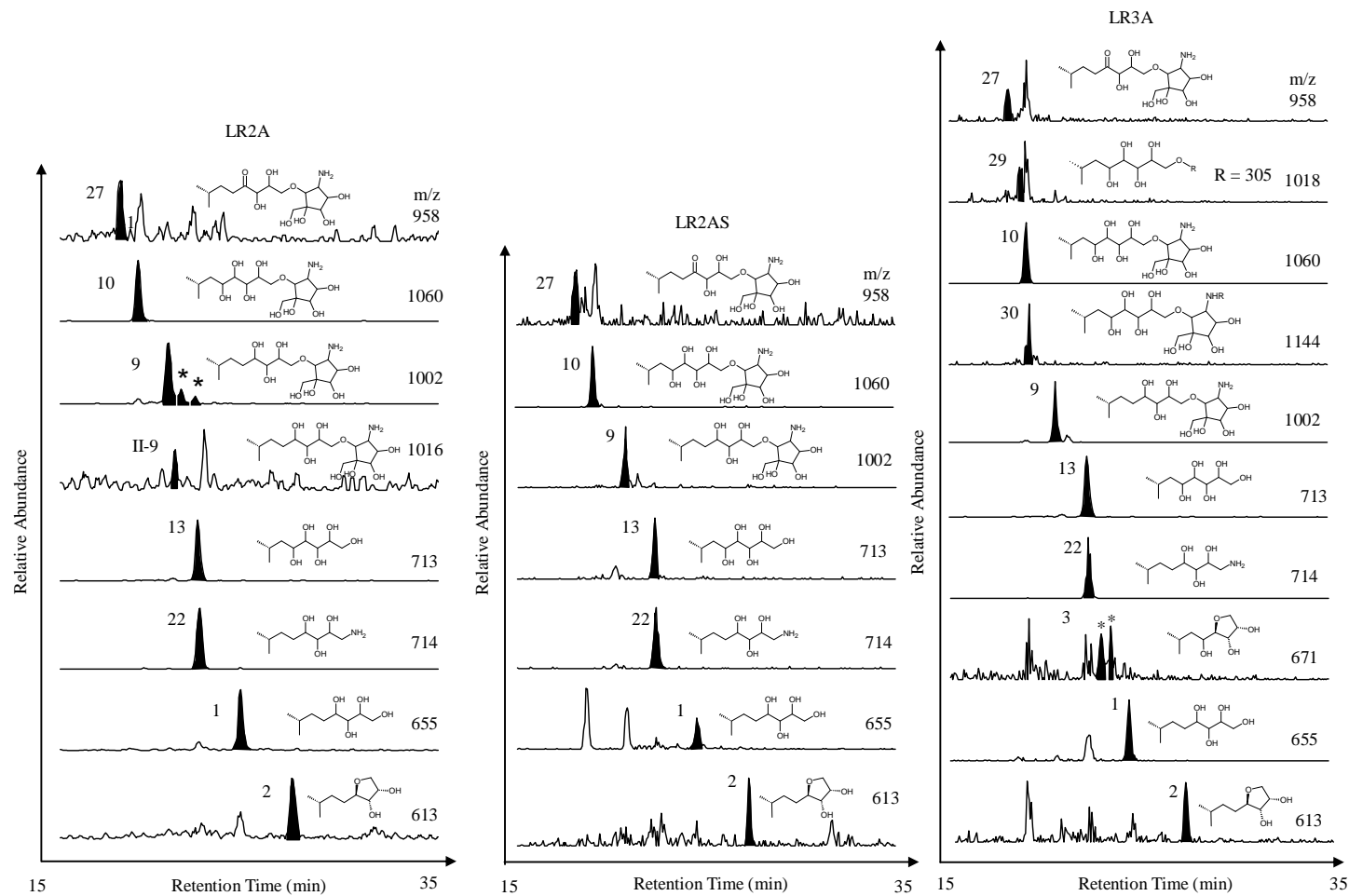


Figure 3.6 Partial mass chromatogram (15 – 35 min) showing BHPs detected in active sinters of Loop Road. \* indicate stereoisomers. 'R of m/z 1144 = 86 Da.

## 3.2.2.4 ACTIVE SINTER FACIES OF OPAHEKE POOL

Sample OP2A collected from the pool edge contained only *BHtetrol* and *BHTcyc* (**1**, **9**) in low amounts,  $0.01$  and  $0.04 \mu\text{g}\cdot\text{g}^{-1}$  dry sinter respectively (Chromatogram not shown; Table 3.1). The Pavlova sinter (sample OP7A) taken from the outflow channel (; Table 3.1) contained eight BHPs including six previously characterised BHPs (*BHPcyc*, *BHpentol*, *2-me BHpentol*, *BHtetrol*, *2-me BHtetrol* and anhydroBHT; **10**, **13**, **II-13**, **1**, **II-1**, **2**) and two novel compounds with  $[\text{M}+\text{H}]^+ = m/z$  1032 and 1046 (**31**, **32**) previously reported by Zhang *et al.*, (2007). The two novel compounds were also present with stereoisomers. AnhydroBHT (**2**) was the least abundant BHP and *BHpentol* (**13**) was the most abundant compound identified in this sample, abundances range from  $0.08$  to  $3.81 \mu\text{g}\cdot\text{g}^{-1}$  dry sinter. The novel BHPs were present in concentrations of  $0.02$  and  $0.52 \mu\text{g}\cdot\text{g}^{-1}$  dry sinter (Table 3.1) for  $[\text{M}+\text{H}]^+ = m/z$  1032 and 1046 respectively. The total abundance of BHPs in this sinter was  $13.48 \mu\text{g}\cdot\text{g}^{-1}$  dry sinter (Table 3.1).

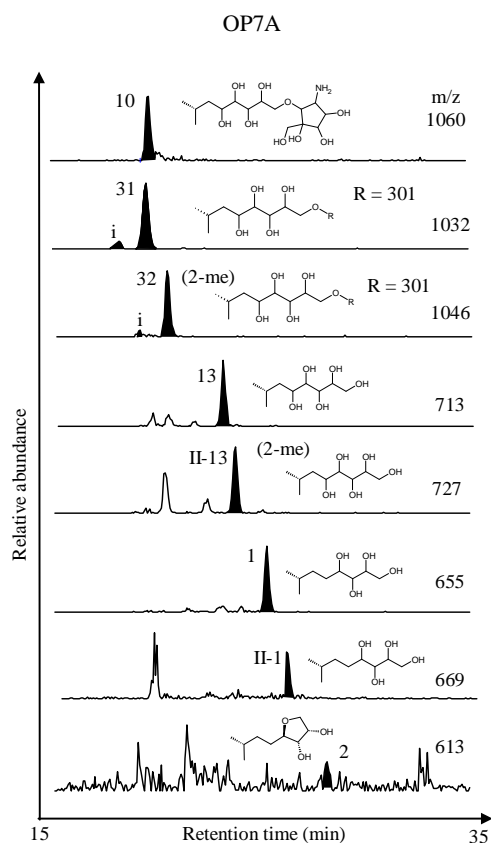


Figure 3.7 Partial mass chromatogram (15 – 35 min) showing BHPs detected in active sinter from Opaheke Pool (sample OP7A). 'i' indicates early eluting isomer.

### 3.2.3 EL-TATIO GEYSER FIELD, CHILE

The BHP distribution of active sinters collected from Terrace springs at ETGF is dominated by the presence of BHP signatures that are known to derive from cyanobacterial sources.

Six BHPs were identified in Sample ET1 including *BHT<sub>cyc</sub>*, *BHT<sub>gly</sub>*, PE-BHT, aminotriol, adenosylhopane and *BH<sub>tetrol</sub>* (**9**, **11**, **17**, **22**, **6**, **1**). *BHT<sub>cyc</sub>* (**9**) was the least abundant BHP detected and aminotriol (**22**) was the most abundant BHP detected with abundances ranging from 0.05 to 0.9  $\mu\text{g}\cdot\text{g}^{-1}$  dry sinter (Table 3.1).

Nine BHPs were identified in Sample ET25. The distribution consisted of nine known BHPs, *BHP<sub>cyc</sub>*, 2-me *BHP<sub>cyc</sub>*, AP-BHT, PE-BHT, *BHT<sub>cyc</sub>*, *BHT<sub>gly</sub>*, aminotriol, *BH<sub>tetrol</sub>* and 2-me *BH<sub>tetrol</sub>* (**10**, **II-10**, **20**, **9**, **11**, **1**, **II-1**). 2-me *BH<sub>tetrol</sub>* (**II-1**) was the least abundant BHP and PE-BHT (**17**) was the most abundant BHP detected with abundances ranging from 0.01 to 0.36  $\mu\text{g}\cdot\text{g}^{-1}$  dry sinter (Table 3.1).

Only two BHPs were detected during analysis of sample ET26 (Chromatogram not shown). Aminotriol (**22**) and *BH<sub>tetrol</sub>* (**1**) were present in abundances of 0.07 and 0.11  $\mu\text{g}\cdot\text{g}^{-1}$  dry sinter respectively (Table 3.1).

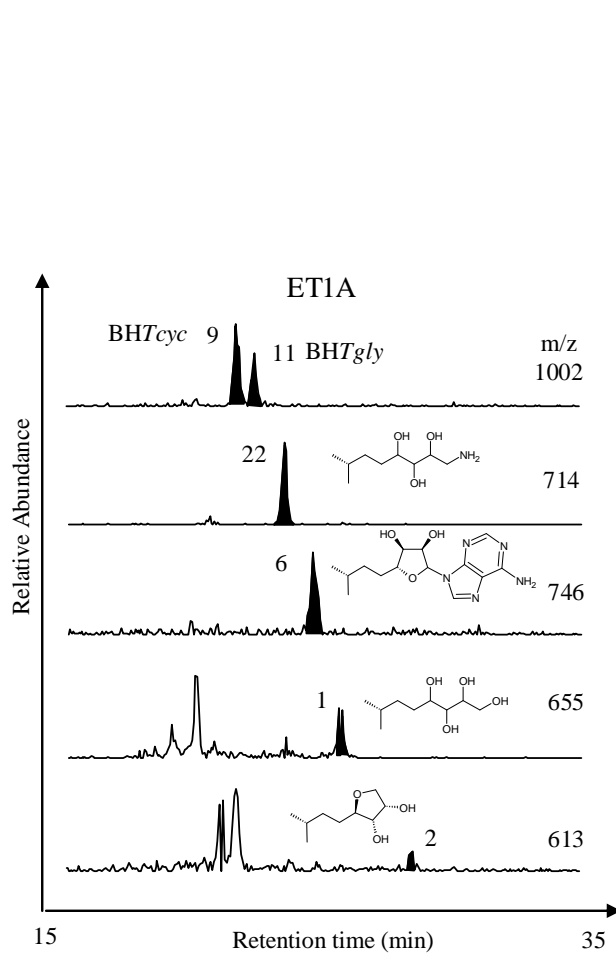


Figure 3.8 Partial mass chromatograms (15 – 35 mins) showing BHPs detected in active sinter (sample ET1A).

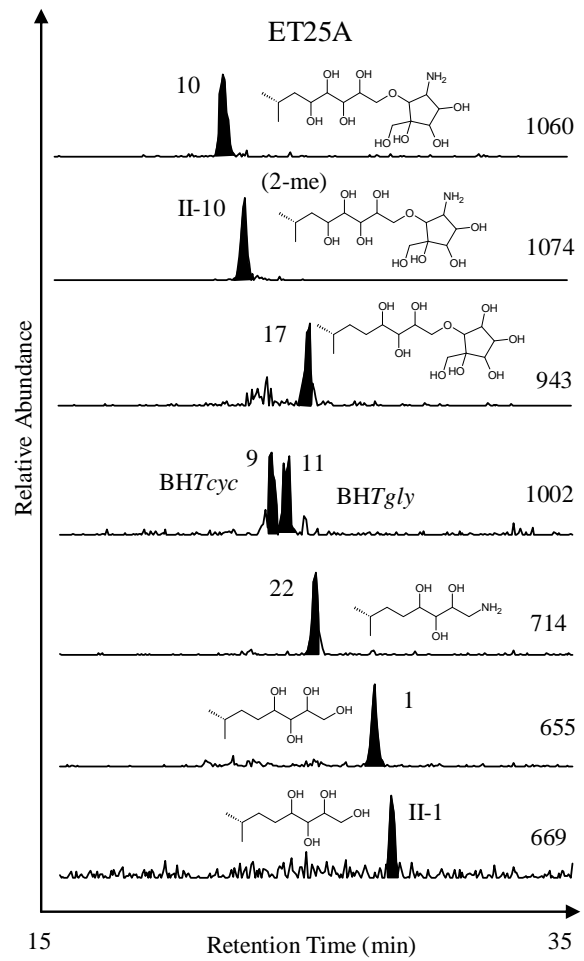


Figure 3.9 Partial mass chromatograms (15 – 35 mins) showing BHPs detected in active sinter (sample ET25A).

## Active Biofacies

Table 3.1 Abundances of BHPs ( $\mu\text{g}\cdot\text{g}^{-1}$  dry sinter) detected in active sinters from TVZ and ETGF.

BHP	Str <sup>b</sup>	CP <sup>f</sup>	CP1A	OK1TA	OK1MA	OK1BA	Sample <sup>a</sup>									
							OK3A	LR2A	LR2AS	LR3A	OP2A	OP7A	ET1A	ET25A	ET26A	
<i>Known BHPs</i>																
BHP <sub>cyc</sub>	<b>10</b>	1.7	<b>1.6</b>	- <sup>c</sup>	0.04	-	25	<b>1.2</b>	<b>0.51</b>	0.42	-	1.0	-	0.08	-	
2-me BHP <sub>cyc</sub>	<b>II-10</b>	-	-	-	-	-	-	-	-	-	-	-	-	<b>0.22</b>	-	
BHT <sub>cyc</sub>	<b>9</b>	1.1	0.83	-	-	-	9.3	0.43	0.27	0.27	<b>0.04</b>	-	0.06	0.05	-	
2-me BHT <sub>cyc</sub>	<b>II-9</b>	-	-	-	-	-	-	0.02	-	-	-	-	-	-	-	
BHT <sub>gly</sub>	<b>11</b>	-	0.15	-	-	-	-	-	-	-	-	-	-	0.04	-	
PE BHT	<b>17</b>	-	-	-	-	-	-	-	-	-	-	-	-	0.51	-	
2-me PE BHT	<b>II-17</b>	-	-	-	-	-	-	-	-	-	-	-	-	-	-	
Aminotriol	<b>22</b>	<b>3.1</b>	1.2	-	-	-	<b>420</b>	-	-	<b>1.2</b>	-	-	<b>0.13</b>	0.16	0.03	
2-me Aminotriol	<b>II-22</b>	-	-	-	0.01	-	-	-	-	-	-	2.8	-	-	-	
BH <sub>pentol</sub>	<b>13</b>	-	-	<b>0.04</b>	<b>0.20</b>	0.01	-	0.78	0.3	-	-	<b>3.8</b>	-	-	-	
2-me BH <sub>pentol</sub>	<b>II-13</b>	-	-	0.02	0.03	0.03	-	-	-	-	-	-	-	-	-	
BH <sub>tetrol</sub>	<b>1</b>	0.88	0.37	0.15	0.01	<b>0.12</b>	63	0.52	0.24	0.43	0.01	2.8	0.08	0.14	<b>0.05</b>	
2-me BH <sub>tetrol</sub>	<b>II-1</b>	-	-	Tr <sup>d</sup>	0.01	Tr	-	-	-	-	-	0.76	-	0.01	-	
AnhydroBHP	<b>2</b>	-	-	-	-	-	-	-	-	0.07	-	-	-	-	-	
AnhydroBHT	<b>3</b>	-	-	0.01	0.01	Tr	1.2	0.16	0.08	0.12	-	-	-	-	-	
<i>Novel BHPs<sup>f</sup></i>																
Oxo-BHT <sub>cyc</sub>	<b>27</b>	-	0.1	-	-	-	0.34	0.03	0.04	0.01	-	-	-	-	-	
Guanidine BHP <sub>cyc</sub>	<b>30</b>	-	-	-	-	-	-	-	-	0.06	-	-	-	-	-	
m/z = 1256	<b>28</b>	-	-	-	0.01	-	-	-	-	-	-	-	-	-	-	
m/z = 1198	<b>36</b>	-	-	-	-	-	-	-	-	-	-	-	-	-	-	
m/z = 1018	<b>29</b>	-	-	-	-	-	0.34	-	-	Tr	-	-	-	-	-	
m/z = 1032	<b>31</b>	-	-	-	-	-	-	-	-	-	-	0.02 <sup>e</sup>	-	0.01	-	
m/z = 1046	<b>32</b>	-	-	-	-	-	-	-	-	-	-	0.52 <sup>e</sup>	-	-	-	
Total		6.78	4.25	0.22	0.32	0.16	519	3.21	1.44	2.54	0.05	13.4	0.27	1.52	0.08	

<sup>a</sup>Sample sites, CP = Champagne Pool, OK = Orakei Korako, LR = Loop Road, OP = Opaheke Pool, Et = El Tatio. <sup>b</sup>Structure. <sup>c</sup>Not detected. <sup>d</sup>Trace amounts present ( $<0.005 \mu\text{g}\cdot\text{g}^{-1}$  dry sinter). <sup>e</sup>Combination of isomeric versions. <sup>f</sup>Spectra of novel BHPs can be found in Chapter 5. Bold text indicates most abundant BHP in a particular sample.

### 3.3 RESULTS: ANALYSIS OF THE BHP DISTRIBUTIONS OF MICROBIAL MATS

The BHP distribution of microbial mats is dominated by the presence of novel BHPs (e.g. Zhang *et al.*, 2007). This group of compounds consists of tetra- and penta-functionalised compounds with  $[M+H]^+ = m/z$  974 and 1032 (**33**, **31**) respectively and their 2-methyl homologues with  $[M+H]^+ = m/z$  988 and 1046 (**34**, **32**). Additional early eluting isomers of the penta-functionalised compounds have also been identified in some samples. A typical distribution of these novel compounds is given in Figure 3.10. Structural assignment of ions and fragmentations are given in Chapter 5 (Section 5.3.3).

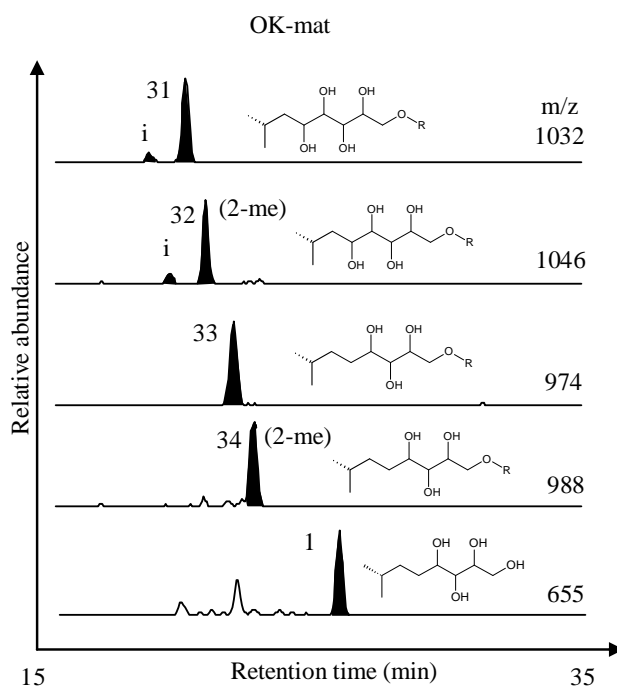


Figure 3.10 Typical distribution of novel BHPs from mat-forming microbial consortia (Sample OK-mat). 'i' indicates early eluting isomer. R group = 301 Da. BHTetrol (**1**) is also shown for comparison of retention time.

Part of this work has previously been published (Zhang *et al.*, 2007). As mentioned above, the detection of novel BHPs dominate the observed distributions; where relevant,

chromatograms of BHP distributions where the novel compounds are absent are also presented.

### 3.3.1 NEVADA HOT SPRINGS

#### 3.3.1.1 GREAT BOILING SPRING

Analysis of microbial mats collected from the Great Boiling spring showed the presence of BHPs in all samples analysed. The BHP distributions of samples GBS08, GBS12 and GBS 18 were dominated by the presence of four common novel compounds (31,32, 33, 34). Abundances can be found in Table 3.2. BH*tetrol* was also present in each sample (Table 3.2). Aminotriol (**22**) was detected in samples GBS08 and GBS12 and 2-me BH*tetrol* (**II-1**) in sample GBS12.

Sample GBS03 was found to contain two known BHPs: BH*tetrol* and aminotriol (**1**, **22**) at abundances of 2.33 and 2.31  $\mu\text{g}\cdot\text{g}^{-1}$  dry material respectively.

Sample GBS 19 also contained two known BHPs: BH*tetrol* and 2-me BH*tetrol* (**1**, **II-1**) at 0.04 and 0.05  $\mu\text{g}\cdot\text{g}^{-1}$  dry material respectively.

#### 3.3.1.2 RICK'S HOT CREEK (RHC)

The observed BHP distributions from the RHC site showed a different BHP assemblage to mat-samples collected from other geothermal sites in Nevada. The common group of six tentatively assigned novel BHPs (including 2 isomers) were not observed and BHP distributions are generally composed of known BHP compounds. A minor exception to this is the observation of other novel composite BHPs in a microbial mat collected from the source of RHC, however, these tentatively-assigned novel components are different from those observed at other sites and reported in Zhang *et al.* (2007). A description of these compounds and assignment of ions can be found in Chapter 5 (Section 5.4.1)

Five known BHPs (*BHP<sub>cyc</sub>*, *BHT<sub>cyc</sub>*, *BH<sub>pentol</sub>*, *BH<sub>tetrol</sub>* and 2-me *BH<sub>tetrol</sub>*; **10**, **9**, **13**, **1**, **II-1**) and two compounds tentatively assigned as novel BHPs have been identified in sample RHC-source. Abundances range from 0.02  $\mu\text{g}\cdot\text{g}^{-1}$  dry material for 2-me *BH<sub>tetrol</sub>* (**II-1**) to 0.17  $\mu\text{g}\cdot\text{g}^{-1}$  dry material for *BH<sub>tetrol</sub>* (**1**; Table 3.2). The two tentatively identified novel BHPs have  $[\text{M}+\text{H}]^+ = m/z$  1256 and 1198 (**28**, **35**).  $[\text{M}+\text{H}]^+ = m/z$  1256 has been identified in sinter material collected from the vent of Fred and Maggie's Pool (FMP; Section 3.2.2.2). It appears that a tetra functionalised counterpart of  $m/z$  1256 is also present in this sample with  $[\text{M}+\text{H}]^+ = m/z$  1198. Abundances are 0.02 and 0.01  $\mu\text{g}\cdot\text{g}^{-1}$  dry material for the penta- and tetra-functionalised components respectively.

Three known BHPs were identified in sample RHC07. The distribution consisted of *BH<sub>tetrol</sub>*, PE-BHT and 2-me PE-BHT (**1**, **17**, **II-17**). The BHPs were present in an abundance of 0.03, 0.19 and 0.05  $\mu\text{g}\cdot\text{g}^{-1}$  dry material respectively. Sample RHC06 contained four known BHPs; *BHT<sub>cyc</sub>*, PE-BHT, aminotriol and *BH<sub>tetrol</sub>* (**9**, **17**, **22**, **1**). Abundances are 0.16, 0.14, 0.02 and 0.04  $\mu\text{g}\cdot\text{g}^{-1}$  dry material respectively.

Four known BHPs were identified during analysis of sample RHC05; *BHT<sub>cyc</sub>*, PE-BHT, *BH<sub>tetrol</sub>* and 2-me *BH<sub>tetrol</sub>* (**9**, **17**, **1**, **II-1**). PE-BHT (**17**) was the most abundant BHP detected and was present in a concentration of 0.49  $\mu\text{g}\cdot\text{g}^{-1}$  dry material. *BH<sub>tetrol</sub>*, 2-me *BH<sub>tetrol</sub>* and *BHT<sub>cyc</sub>* (**1**, **II-1**, **9**) were present in concentrations of 0.06, 0.01 and 0.12  $\mu\text{g}\cdot\text{g}^{-1}$  dry material respectively.

### 3.3.1.3 PARADISE VALLEY (PV)

Nine BHPs were identified during analysis of a microbial mat collected from the Paradise Valley (PV) geothermal area (previously published in Zhang *et al.*, 2007). The distribution consisted of five known BHPs and the 4 major isomers of the novel compounds (**31**, **32**, **33**, **34**) The known compounds were aminopentol, aminotetrol, aminotriol, *BH<sub>tetrol</sub>*

and 2-me BH*tetrol* (**15**, **21**, **22**, **1**, **II-1**). Aminotetrol (**21**) was found to be the least abundant BHP and aminotriol (**22**) was found to be most abundant BHP with abundances ranging from 0.08 to 1.1  $\mu\text{g}\cdot\text{g}^{-1}$  dry material. Of the novel compounds, the methylated tetra functionalised compound  $[\text{M}+\text{H}]^+ = 988$  (**34**) was the least abundant and the methylated pentafunctionalised compound,  $[\text{M}+\text{H}]^+ = m/z 1046$  (**32**) was the most abundant novel compound identified. Abundances ranged from 1.92 to 4.67  $\mu\text{g}\cdot\text{g}^{-1}$  dry material (Table 3.2).

### 3.3.2 CALIFORNIA HOT SPRINGS

#### 3.3.2.1 SURPRISE VALLEY

Samples from Surprise Valley geothermal vent included six microbial mats collected from the source and various intervals at decreasing water temperature. Once again, the four novel BHPs mentioned above i.e. (**31**, **32**, **33**, **34**) were present in samples SV2 Con1, SV2 Con3 and SV2Con5 (Table 3.2).

Six known BHPs were identified in sample SV2Con4 (Figure 3.11). The distribution consisted of BHP*cyc*, BHT*cyc*, aminotriol, BH*tetrol*, 2-me BH*tetrol* and adenosylhopane (**10**, **9**, **22**, **1**, **II-1**, **5**). BHT*cyc* was the least abundant compound identified and BH*tetrol* the most abundant at concentrations ranging from 0.01 to 0.07  $\mu\text{g}\cdot\text{g}^{-1}$  dry material (Table 3.2).

In addition to the 4 novel compounds (**31**, **32**, **33**, **34**), analysis of sample SV2con5 also showed the presence of two known BHPs; BH*tetrol* and 2-me BH*tetrol* (**1**, **II-1**). Abundances were 0.1 and 0.25  $\mu\text{g}\cdot\text{g}^{-1}$  dry material respectively (Table 3.2).

BHPs were not observed during the analysis of sample SV2Con2 and SV2 Con Source.

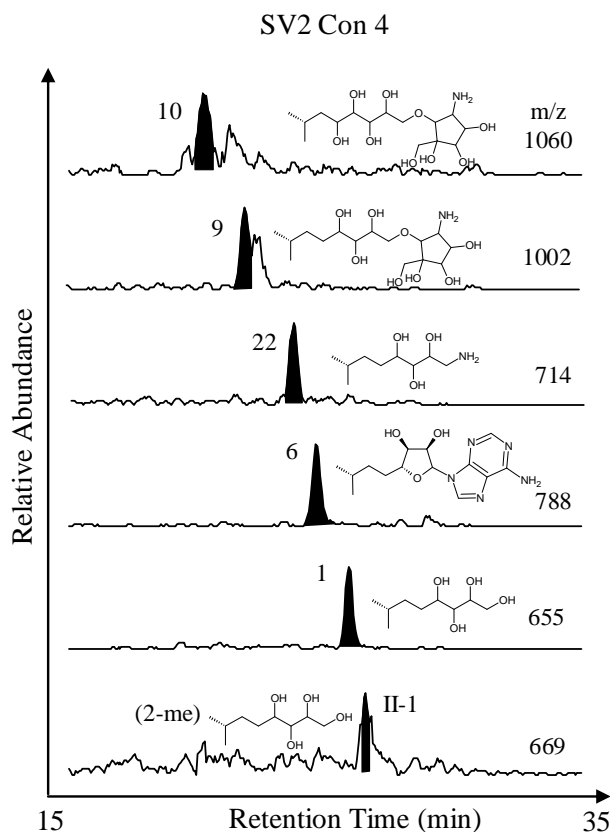


Figure 3.11 Distribution of known BHPs detected in a microbial mat from Surprise Valley vent.

### 3.3.2.2 EAGLEVILLE (EV)

One sample from the Eagleville (EV) hot-spring site was analysed previously (Zhang *et al.*, 2007) and found to contain 3 known BHPs: aminotriol, BHtetrol and 2-me BHtetrol (**22**, **1**, **II-1**) in abundances of 4.06, 42.1 and 5.4  $\mu\text{g}\cdot\text{g}^{-1}$  dry material respectively. One further sample (EV47) was provided for this study but was not found to contain any BHPs.

### 3.3.3 NEW ZEALAND HOT SPRINGS

Six BHPs were identified during analysis of a microbial mat collected from the sinter terrace of the Orakei Korako (OK) geothermal field. Four of the six BHPs have been tentatively identified as novel BHPs (e.g. Zhang *et al.*, 2007; **31**, **32**, **33**, **34**) and two known BHPs were also detected. Abundances of  $[\text{M}+\text{H}]^+ = 1032$  and  $1046$  were 1.52 and 1.39  $\mu\text{g}\cdot\text{g}^{-1}$

dry material respectively, while isomeric forms were both present in a concentration of 0.2  $\mu\text{g}\cdot\text{g}^{-1}$  dry material. *BHT<sub>cyc</sub>* and *BH<sub>tetrol</sub>* (**9**, **1**) were also detected at concentrations of 1.32 and 1.92  $\mu\text{g}\cdot\text{g}^{-1}$  dry material respectively.

Table 3.2 Abundances of BHPs ( $\mu\text{g}\cdot\text{g}^{-1}$  dry material) detected in microbial mats.

Sample site <sup>a</sup> BHP	Str <sup>b</sup>	Sample																			
		GBS					RHC					SV					EV		PV	OK	
		03	08	12	18	19	So <sup>c</sup>	4	5	6	7	So	1	2	3	4	5	1 <sup>d</sup>	47	1 <sup>d</sup>	
Known BHPs		- <sup>e</sup>	-	-	-	-	-	-	-	-	-	-	-	-	-	-	-	-	-	-	-
BHP <sub>cyc</sub>	10	-	-	-	-	-	<b>0.10</b>	-	-	-	-	-	-	-	-	0.01	-	-	-	-	-
BHT <sub>cyc</sub>	9	-	0.17	-	-	-	0.06	-	0.13	<b>0.17</b>	-	-	-	-	-	-	-	-	-	-	1.3
PE-BHT	17	-	-	-	-	-	-	-	<b>0.48</b>	0.14	<b>0.19</b>	-	-	-	-	-	-	-	-	-	-
2-me PE BHT	II-17	-	-	-	-	-	-	-	-	-	0.05	-	-	-	-	-	-	-	-	-	-
Adenosyl BHT	6	-	-	-	-	-	-	-	-	-	-	-	-	-	-	0.05	-	-	-	-	-
Aminotriol	22	<b>0.23</b>	-	0.4	0.17	-	-	-	-	0.03	-	-	-	-	-	0.02	-	4.1	-	<b>1.1</b>	-
Aminotetrol	23	-	-	-	-	-	-	-	-	-	-	-	-	-	-	-	-	-	-	0.08	-
Aminopentol	15	-	-	-	-	-	-	-	-	-	-	-	-	-	-	-	-	-	-	0.46	-
BH <sub>pentol</sub>	13	-	-	-	-	-	0.09	-	-	-	-	-	-	-	-	<b>0.07</b>	-	-	-	-	-
2-me BH <sub>pentol</sub>	II-13	-	-	-	-	-	-	-	-	0.04	-	-	-	-	-	Tr <sup>f</sup>	-	-	-	-	-
BH <sub>tetrol</sub>	1	0.21	-	-	0.29	0.04	0.02	-	0.06	-	0.03	-	-	-	-	0.02	0.11	<b>42</b>	-	0.65	<b>2.0</b>
2-me BH <sub>tetrol</sub>	II-1	-	-	-	0.14	<b>0.05</b>	0.02	-	0.1	-	-	-	-	-	-	-	0.24	5.4	-	0.18	-
Novel BHPs																					
m/z 1256	28	-	-	-	-	-	-	-	-	-	-	-	-	-	-	-	-	-	-	-	-
m/z 1032	31	-	0.29	2.8	0.28	-	-	-	-	-	-	-	0.04	-	0.01	-	0.36	-	-	3.9	0.21
m/z 1032 (iso) <sup>g</sup>	i-31	-	0.01	0.82	0.13	-	-	-	-	-	-	-	<b>0.14</b>	-	<b>0.02</b>	-	-	-	-	-	<b>1.5</b>
m/z 1046	32	-	<b>0.40</b>	<b>3.1</b>	<b>0.51</b>	-	-	-	-	-	-	-	0.03	-	Tr <sup>f</sup>	-	<b>0.81</b>	-	-	<b>4.7</b>	0.21
m/z 1046 (iso) <sup>g</sup>	i-32	-	0.07	0.34	0.1	-	-	-	-	-	-	-	0.13	-	0.01	-	-	-	-	-	1.4
m/z 974	33	-	-	-	-	-	-	-	-	-	-	-	-	-	-	-	-	-	-	1.9	-
m/z 988	34	-	-	-	-	-	-	-	-	-	-	-	-	-	-	-	-	-	-	2.4	-
Total BHP		0.44	0.94	7.46	1.62	0.09	0.29	-	0.77	0.38	0.27	-	0.34	-	0.04	0.17	1.52	51.5	-	16.02	6.62

<sup>a</sup> Sample sites: GBS = Great Boiling Spring, RHC = Ricks' Hot Creek, Sv = Surprise valley, EV = Eagleville, PV = Paradise Valley, OK = Orakei Korako; <sup>b</sup> Str = structure; <sup>c</sup> So = source; <sup>d</sup> previously published in Zhang et al. (2007); <sup>e</sup> - indicates not detected; <sup>f</sup> Tr = trace (< 0.005  $\mu\text{g}/\text{g}$ ); <sup>g</sup> iso = early eluting isomer (i).

### 3.4 DISCUSSION

The microbiology of terrestrial hot-springs is dominated by the presence of thermophilic photoautotrophs and chemolithoautotrophs. Populations are usually determined primarily by temperature, sulphide concentration and the presence of harmful mineral species. For instance, water temperatures that exceed 75°C eliminate the growth of cyanobacteria and other photosynthetic bacteria such as green-sulphur and green non-sulphur bacteria (Castenholz, 1969; Ward *et al.*, 1998). Growth of chemolithoautotrophs, such as members of the *Aquificales* is promoted (Reysenbach *et al.*, 1994). These organisms are usually found at temperatures that exceed the upper limit for photosynthesis. H<sub>2</sub>S also inhibits growth of cyanobacteria (Castenholz, 1979) but promotes growth of sulphur-respiring photosynthetic bacteria (e.g. van der Meer *et al.*, 2001). The sample sites in this study exhibit a wide variety of environmental conditions which therefore dictate that BHP distributions derive from a wide-range of bacterial species. This is reflected in the observed distributions which are now discussed.

#### 3.4.1 COMPOSITION OF BHP DISTRIBUTIONS OF ACTIVE SINTERS

##### 3.4.1.1 CHAMPAGNE POOL

The vent waters of CP are known to be anoxic (Temperature, 75°C; pH 5.5), whether this anoxia is prevalent at the surface (e.g. Jones *et al.*, 2001) is open to debate, however, the BHP-distribution observed from the suspended floc material must derive from anaerobic bacterial species due to the sub-aqueous formation of this particular facies. Although the compounds detected (BHT<sub>cyc</sub>, BHP<sub>cyc</sub>, aminotriol and BH<sub>tetrol</sub>; **9**, **10**, **22**, **1**) are produced by a wide range of bacteria taxa (e.g. Talbot and Farrimond, 2007), the presence of these compounds in the sample CPf suggests a currently unidentified anaerobic BHP-producing organism.

BHPs and hopanoids are thought to derive mainly from aerobic bacteria, however, this report builds upon recent accounts of the presence of BHPs and hopanoids from anaerobic environments and bacterial cultures that challenge the traditional view of the ecology of BHP-producing bacteria (e.g. Thiel *et al.*, 2003; Sinninghe Damsté *et al.*, 2004; Hartner *et al.*, 2005; Blumenberg *et al.*, 2006). BHT<sub>cyc</sub>, BHP<sub>cyc</sub>, aminotriol and BH<sub>tetrol</sub> (**9**, **10**, **22**, **1**) were present in the sinter taken from the air-water interface at CP (sample CPf), indicating that BHP distributions may contain input from organic matter derived from bacteria colonising the vent waters. Differences in the BHP distributions are also clear between samples CPf and CP1A; namely the presence of oxo-BHT<sub>cyc</sub> and BH<sub>tgly</sub> (**9**, **10**) in sample CP1A. The increased complexity of the BHP distribution observed in the sinter (Sample CP1A) compared to the floc material (Sample CPf) must derive from bacteria colonising the air-water interface.

#### 3.4.1.2 ORAKEI KORAKO GEOTHERMAL FIELD

BHPs were detected in all sinter facies collected from the Orakei Korako Geothermal Field (OK) and were also detected in a microbial mat collected from the sinter flat. A suite of 2-me BHPs were identified in samples OK1-TA, OK1-MA and OK1-BA. Interestingly, samples OK1-TA and OK1-BA did not appear to contain any composite-BHP structures. The water temperature of FMP is 97.8°C. Which exceeds the known upper temperature limit for all bacteria (e.g. Huber *et al.*, 1996). This suggests that the BHP distribution may originate from foreign sources or possibly from endolithic sources, whereby colonisation in the silica sinter may provide temporary refuge from the high-water temperature. BHP abundances are low in samples OK1-TA, OK1-MA and OK1-BA compared to other sinters analysed from TVZ and are of a similar order to BHPs observed in sample OP2A (water temperature 95°C; Section 3.4.1.4; Table 3.1). This is reflective of the high temperatures of the FMP vent which are more suited to archaeal phylotypes (Kaur, 2009). *Aquifex pyrophilus* can grow in waters

up to 95°C and this represents the known upper temperature limit for bacteria (Huber *et al.*, 1996). Kaur (2009) demonstrates a decrease of diethers and archaeol, derived from archaeal species, between sinters of FMP (OK1-TA, OK1-MA and OK1BA) and of the outflow channel (sample OK3A) of FMP representing a change in microbial community driven by a decrease in temperature. Since members of the *Aquificales* are not known to be BHP-producing organisms, an as yet currently uncharacterised BHP-producer must be present at this site. More surprising still is the presence of desmethyl and 2-methyl BHP homologues (2-methyl BHtetrol, 2-methyl BHpentol, 2-methyl aminotriol; **II-1**, **II-13**, **II-22**), which are indicative of the presence of cyanobacterial species, although other sources of 2-me BHtetrol and 2-me Aminotriol are now known (Rashby *et al.*, 2007).

A novel compound of  $[M+H]^+ = m/z$  1256 (**28**) has been detected here and has also been detected during analysis of sinter material from LR and during analysis of mat-forming cyanobacteria from geothermal areas in Nevada, USA. The water temperature of RHC was 95°C at the time of sampling, similar to that observed at FMP. Although, the structure remains uncharacterised, the occurrence of this particular BHP at two distinct high-temperature locations may provide a new and exciting expansion to the current understanding of the use of BHPs as biomarkers in thermophilic, or in this case, hyperthermophilic organisms (See Chapter 1, section 1.5 for explanation of differentiation of terminology).

The sinter taken from the outflow channel (Sample OK3A; Table 3.2) showed a more diverse BHP distribution indicating a more diverse bacterial assemblage at this point. Abundances of BHPs and hopanoids are 2-3 orders of magnitude higher (Table 3.1) than that of the vent source, 520  $\mu\text{g}\cdot\text{g}^{-1}$  dry sinter sampled from the outflow channel compared to  $\sim 0.1$   $\mu\text{g}\cdot\text{g}^{-1}$  dry sinter from the FMP source. This is reflective of a change in microbial population driven by a decrease in water temperature of around 30°C. This particular sample contained

oxo-BHT<sub>cyc</sub> (**27**) and a composite BHP with  $[M+H]^+ = m/z$  1018 (**29**), similar to that observed in sinters of CP and LR.

#### 3.4.1.3 LOOP ROAD HOT SPRINGS

The actively precipitating sinter from the air-water interface (Sample LR2A) showed the presence of a range of known and novel compounds which indicate the bacterial community occupying this particular zone of sinter formation include previously undetermined BHP-producing bacteria, and potentially uncharacterised bacterial species. The conditions of this particular vent are similar to those found at CP, i.e. mildly acidic, pH 5.5 – 5.6 and temperatures of 70°C (LR) compared to 75°C (CP). The compounds detected in the anaerobic floc material at CP (sample CPf; Table 3.1), BHP<sub>cyc</sub>, BHT<sub>cyc</sub>, aminotriol, BH<sub>tetrol</sub> and anhydroBHT (**10**, **9**, **22**, **1**, **2**) were also detected in the three actively precipitating sinters at LR suggesting the presence of anaerobic BHP-producing bacteria at this site, however it should be noted that these compounds are also known from a wide-range of bacteria (e.g. Talbot and Farrimond, 2007; Talbot *et al.*, 2008 and references therein) and have been detected in diverse samples (Talbot and Farrimond, 2007) The remaining BHPs that make up the lipid distributions likely derive from bacteria inhabiting the air-water interface or the direct vicinity of this redox boundary. Oxo-BHT<sub>cyc</sub> (**27**) is present in all three samples taken from the air-water interface, at present the only known source of an oxo-BHP is *Zymomonas mobilis* (Flesch and Rohmer, 1989) which produces oxo-BHT<sub>gly</sub> (**24**) when grown under micro-aerophilic conditions. This may indicate that at this site this particular group of compounds derive from bacteria colonising an oxygen-minimal environment.

BHP<sub>pentol</sub> (**13**) is known to be produced by cyanobacteria and was detected in samples LR2A and LR2AS. 2-me PE BHT (**17**) was detected in LR3A, suggesting that cyanobacteria may be colonising the sinter formation.

## 3.4.1.4 OPAHEKE POOL

An actively precipitating sinter from the pool ledge (Sample OP2A) showed only trace amounts of BH*tetrol* (**1**) and BH*Tcyc* (**9**); this is likely due to the elevated water temperature (95°C, pH 7.0 at the time of sampling) at this site, which is more likely to support hyperthermophilic archaeal phylotypes than bacteria. Kaur (2009) detected 1,2-dialkylglycerols in active sinters from this site, suggesting that the main groups of bacteria are *Aquificales*. Also, plant biomarkers were detected suggesting that lipid distributions can be influenced by input of foreign organic matter as mentioned in Section 3.2.2.4. Water temperature decreases as distance from the source increases and the BHP-distribution of the sinter collected from outflow channel at OP (Sample OP7A) would suggest a more diverse bacterial community including cyanobacteria.

The Pavlova sinter taken from the outflow channel contained novel pentafunctionalised BHPs with peracetylated  $[M+H]^+ = m/z$  1032 and 1046 (**31**, **32**) which have previously been detected in cyanobacterial mats from the Paradise Valley geothermal area in Nevada (Zhang *et al.*, 2007) and Orakei Korako (Section 3.3.3). Although these compounds have only recently been reported, they are usually present with a number of other compounds such as their tetrafunctionalised homologues with  $[M+H]^+ = m/z$  974 and 988 (**33**, **34**) respectively. The presence of the tetrafunctionalised was not detected during the analysis. The presence of these compounds along with 2-methyl BH*pentol* and 2-methyl BH*tetrol* (**II-13**, **II-1**) indicates a BHP-producing cyanobacterial community colonising the outflow channel.

## 3.4.1.5 EL-TATIO GEYSER FIELD

The sinters of ETGF have received little attention in the past with regard to geochemical investigations (Phoenix *et al.*, 2006). This study represents the first investigation of the organic geochemistry of this particular environmental setting. The presence of BHPs in

sinters from ETGF shows that those signatures observed in sinters from TVZ are common to geographically distinct locations and further demonstrates the use of BHPs as biomarkers in geothermal vents. The BHPs distributions observed in silica sinters collected from ETGF are dominated by the presence of BHPs that can be associated with a cyanobacterial precursor or a photosynthetic source. Adenosylhopane (**6**) was detected in sample ET1 (Figure 3.8) and has previously been detected in cultures of *Rhodopsuedomonas acidophila*, *Rhodopsuedomonas palustris*, *Rhodomicrobium vanielli*, *Nitrosomonas europaea* and *Bradyrhizobium japonicum* (Neunlist and Rohmer, 1985b; Neunlist *et al.*, 1988; Seeman *et al.*, 1999; Talbot *et al.*, 2007a). It has also been detected in an enrichment culture of *Chroococidiopsis sp.* (Talbot *et al.*, 2008a). Cyanobacteria that are morphologically similar to this *Chroococidiopsis sp.* were detected (Phoenix *et al.*, 2006) at this site and the BHP distribution provides consistent evidence for the presence of the organism in this particular facie. Aminotriol (**22**) has only ever been detected in cyanobacteria of the genus *Microcystis sp.* along with various other groups of BHP-producing bacteria. It therefore cannot be unambiguously linked to any particular precursor organism.

Sample ET25 (Figure 3.9; Table 3.1) contained the most diverse BHP assemblage containing a number of known BHP cyanobacterial signatures. In cyanobacteria, production of BHP-compounds that contain composite functionalities appear to be confined to the orders of *Chroococcales sp.* and *Stigonematales sp.* (Talbot *et al.*, 2008; see Chapter 1, section 1.8.4.1 for discussion). The presence of other BHP compounds and corresponding methylated counterparts builds a strong case for the cyanobacterial origin of these compounds in this particular sample location. The presence of cyanobacterial BHP-signatures at this geothermal field demonstrates the utility of BHP as biomarkers for bacterial populations and further extends our knowledge of the ecology of BHP-producing bacteria.

Abundances of BHPs were particularly low in sinters collected from ETGF compared to those observed from TVZ, with abundances ranging from 0.08 to 1.25  $\mu\text{g}\cdot\text{g}^{-1}$  dry sinter. This observation suggests that the BHP-producing bacterial community comprise a minor component of the total microbial community at ETGF. The elevation of this location (4300 m above sea level) results in the water of the vent being very close to local boiling point. As observed in sinters from other high temperature vents from TVZ (i.e. those expelling fluid at or close to 100°C) such as FMP or OP, abundances of BHPs appear to particularly low where temperature of the vent is high and have either been attributed to an allochthonous source (OP) or may derive from endolithic cyanobacteria (FMP). It is thought that the BHP distribution at this site also derives from endolithic communities similar to those at FMP. The high temperature of the vent coupled with intense solar radiation makes this location particularly inhospitable whereby refuge in pore spaces of silica sinters provides the necessary shelter to facilitate colonisation.

#### 3.4.2 COMPOSITION OF BHP DISTRIBUTIONS OF MICROBIAL MATS

Microbial mats from GBS, SV, EV and OK contain distributions that are dominated by the presence of novel BHP compounds (See Section 3.3; **31**, **32**, **33**, **34**). Other BHPs were also identified, such as BHT<sub>cyc</sub> (**9**; in samples GBS08 and OK), aminotriol (**22**; in samples GBS12 and GBS18) and BH<sub>tetrol</sub> (**1**; in samples GBS18 and OK). In samples SV2Con1, SV2Con3 and SV2Con5 the BHP distribution consisted of only the novel compounds. These compounds were first detected in microbial mats of EV and PV (Zhang *et al.*, 2007) where a combined approach of phylogenetics, carbon isotopes and lipid biomarkers was employed to investigate cyanobacterial populations, metabolic pathways and biogeochemical processes occurring *in situ*. The presence of this group of compounds indicates a similar microbial assemblage at these sites.

In samples from SV, the early-eluting isomer of  $[M+H]^+ = m/z$  1032 and 1046 (**31**, **32**) are the dominant compounds, whereas in samples from GBS and OK the late-eluting isomers are the more dominant compounds. The origin of this reversal is unclear and could be attributed to a physiological response to the conditions at each site, however, this requires further investigation.

Samples from RHC showed a different assemblage of BHPs but still consisted predominantly of cyanobacterial signatures. PE BHT (**17**) was present in samples RHC 05, 06 and 07. 2-methylated derivatives of PE BHT (**II-17**) and BH*tetrol* (**II-1**) were identified in samples RHC07 and RHC05 respectively. A novel compound with  $[M+H]^+ = m/z$  1256 (**28**) was also identified. Sample SV4 also showed a different assemblage of BHPs. BHP*cyc*, adenosylhopane, aminotriol, BH*pentol*, 2-me BH*pentol* and BH*tetrol* (**10**, **6**, **22**, **13**, **II-13**, **1**) were identified indicating a different bacterial consortia at this particular sampling interval. A number of sources of adenosylhopane have been identified (e.g. Neunlist and Rohmer, 1985b; Neunlist *et al.*, 1988; Talbot *et al.*, 2008a). It is possible that in this sample adenosylhopane (**6**) derives from cyanobacteria and the presence of BH*pentol* (**13**) would provide further evidence to support this assumption.

### 3.4.3 SOURCES OF BHPs IN SILICA SINTERS

#### 3.4.3.1 ANAEROBIC BACTERIA

Comparison of BHP distributions from sub-aqueous (anoxic) and sub-aerial (oxic) samples from CP show that a proportion of the BHPs incorporated into the silica matrix may derive from bacteria in the vent waters and not just the sinter formation zones. Previously reported strictly anaerobic sources of BHPs include members of the Planctomycete phylum: *Candidatus "Brocadia anammoxidans"*, "*K. stuttgartiensis*", "*Scalindua spp.*", *Pirella marina*, *Geobacter metallireducens* and *G. sulfurreducens* (Phylum: Proteobacteria, delta-subdivision; Sinninghe Damsté *et al.*, 2004; Hartner *et al.*, 2005). However, 16s rRNA

analysis showed an absence of *Planctomycetes* in sub-aqueous settings of CP (Childs *et al.*, 2008). Furthermore, Childs *et al.* (2008) show that the dominant bacterial species belong to the orders *Aquificales*, *Thermodesulfobacteriales* or *Bacillales* suggesting that there remains an undetermined BHP-producing organism associated with this depositional setting. As phylogenetic assessment using 16s rRNA does not produce a quantitative assessment it may be that species of *Planctomycetes* were missed in the analysis of this depositional setting. Whether or not the organism, or organisms, in question possess truly obligate anaerobic metabolism or are facultative anaerobes remains to be determined.

#### 3.4.3.2 OXIC-ANOXIC TRANSITION ZONE

As mentioned in Section 1.4 and Section 3.3.1.1, sinter formation proceeds more readily at or just above the air-water interface (Mountain *et al.*, 2003). Since the pool waters at CP are regarded as anoxic (Jones *et al.*, 2001) then this zone of sinter formation corresponds to an oxic-anoxic transition zone (OATZ). Incorporation of organic matter into sinter formations therefore records life at this redox boundary. One must consider that bacterial species known to thrive in oxygen minimal zones are likely the major contributors of organic matter to sinters collected from the air-water interface. Furthermore, one must consider these species to be thermophilic and tolerant to acidic pH. A survey of known BHP-producing organisms suggests that a currently unidentified BHP-producing organism must be colonising the OATZ of the locations studied. This is the first report of oxo-BHPs in any environmental sample, therefore this class of biomarker are likely diagnostic for bacteria colonising oxic-anoxic transitions in environmental samples. The only other report of an oxo-BHP was oxo-BHTgly (**24**) isolated in cultures of *Zymomonas mobilis* (Flesch and Rohmer, 1989) grown under micro-aerophilic conditions and it must be stressed that the oxo-BHPs detected in sinters contain the 'cyc' conformer of the terminal group moiety rather than the 'gly' conformer (see Chapter 5, section 5.5.2.2)

Culture independent surveys of the sinter formation zones at CP showed the presence of close relations of *Planctomycetes* in the ‘acid-organic layer’ which forms as a result of evaporation of vent waters and outgassing of H<sub>2</sub>S (Childs *et al.*, 2008) and these organisms may be involved with nitrogen cycling in CP. BH*tetrol* (1) was the only BHP detected in the study of this organism (Sinninghe Damsté *et al.*, 2004), future investigations concerning the occurrence of polyfunctionalised BHPs in this particular phyla will improve our understanding of the BHP and lipid distribution at this site. Phylogenetic analysis also showed close relations to *Burkholderiales* sp. several of which are known to produce BH*tetrol*, BH*Tcyc*, and  $\Delta^6$  BH*Tcyc* (Cvejic *et al.*, 2000b). Unsaturated BHPs were not observed in the sinter collected from CP, but as mentioned in section 1.8, the observation of unsaturated bacteriohopanepolyols is quite rare and usually attributed to acetic acid bacteria (e.g. Rohmer and Ourisson, 1986; Talbot *et al.*, 2007b). Other potential sources of BHPs at the oxic-anoxic transition could include *Magnetospirillum* sp. known to contain the machinery for BHP-biosynthesis (Pearson *et al.*, 2007) and to thrive in environments with low oxygen concentrations. BHP-production in facultative anaerobic bacteria such as *R. palustris* was first reported by Rohmer *et al.* (1984). Subsequent reports of BHP-biosynthesis in the facultative anaerobe *Zymomonas mobilis* showed BHP compositions were dependent upon O<sub>2</sub> concentrations during culturing (Bringer *et al.*, 1985; Schmidt *et al.*, 1986; Flesch and Rohmer, 1989). Thermophilic bacteria are known to gain energy through fermentative metabolic pathways (Rusch *et al.*, 2005) and the presence of novel, oxo-BHPs similar to those observed in cultures of *Z. mobilis* grown under micro-aerophilic conditions and present in older sinters provides evidence for the presence of a currently unidentified BHP-producing, thermophilic bacteria colonising micro-oxygenated portions of the pool.

Cyanobacterial BHP signatures have been detected in sinters of FMP, LR, OP and ET (Samples OK1-TA, OK1-MA and OK1-BA; LR2A and LR2AS; OP7A; ET25A). It is

possible that incorporation into the silica matrix and colonisation of pore spaces in sinter material provides protection from the otherwise lethal environmental conditions (e.g. Phoenix and Konhauser, 2008). Studies of sinters have demonstrated that biosilification facilitates cyanobacterial colonisation at ETGF (Phoenix *et al.*, 2006) where silica is found to act as a natural UV screen by allowing the transmission of photosynthetically-active light (PAL) but preventing harmful UV<sub>a</sub> and UV<sub>b</sub> radiation. This allows cyanobacteria to remain photosynthetically viable up to a depth of ~10 mm within sinter material (Phoenix *et al.*, 2000).

Guanidine-BHP<sub>cyc</sub> (**30**) was tentatively identified in sinter from LR (sample LR3A), this compound forms a more complex homologue of guanidine-BHT<sub>cyc</sub> (**24**) which is known to be produced by facultative methylotrophs (Bisseret *et al.*, 1985; Knani *et al.*, 1994; See Chapter 5, section 5.3.1).

#### 3.4.4 SOURCES OF BHPs IN MICROBIAL MATS

##### 3.4.4.1 CYANOBACTERIA

The microbial mat sampled from OK showed an almost identical BHP distribution to that observed in cyanobacterial mats from geothermal areas in GBS, PV and SV. The cyanobacteria assemblage at the EV and PV site is thought to consist mainly of uncharacterised cyanobacteria (Zhang *et al.*, 2007). However, *Synechococcus* sp. cyanobacteria are known to be the dominant mat-building cyanobacteria in springs above 55°C from North America, New Zealand and Japan (Papke *et al.*, 2003). The temperature of the vents where the novel BHPs were not detected outside the range at which *Synechococcus* sp. could be expected to grow. Thermophilic *Synechococcus* PCC6907 has been shown to produce distinctive BHPs containing hexasuronic acid composite functionalities (**19**, **20**; Llopiz *et al.*, 1996), however, LC-MS based methods to reliably interpret the presence of BHPs containing carboxylic acid moieties need to be developed. Llopiz *et al.* (1996) also

reported the presence of two further BHP compounds but concluded that structural identification was not possible due to the low amounts of extracted compound. *Chlorogloeopsis* sp., a known BHP-producing organism (e.g. Talbot *et al.*, 2008a) and *Mastigocladus* sp. are known to be present at OK and other New Zealand springs (Shiea *et al.*, 1991; Mountain, personal communication). *Mastigocladus* sp. have also been shown to grow within the temperature range of the water at the sites investigated (Miller *et al.*, 2009), suggesting another possible source of BHPs. However, BHP production in *Mastigocladus* sp. is still unconfirmed.

It appears that the source of the novel BHPs grows at temperatures between 42.8 – 71.0°C and between pH 6.0 to 8.8 (Table 3.3). However, only m/z 1046 and 1032 peaks were detected in sample SV2 Con5 (Temperature 42.8°C, pH 8.8; Table 3.2), discounting this from the sample set redefines the temperature and pH limits at which this set of BHPs are produced to between 51.1 – 70.0°C and pH 6.0 – 7.8 (Table 3.3).

*Synechococcus* sp. cyanobacteria are thought to have evolved from an ancestral precursor inhabiting mesophilic temperature environments which then diversified into thermophilic species able to colonise geothermal springs (Miller and Castenholz, 2000). Cyanobacterial BHPs are present in microbial mats collected from GBS, SV and PV (California and Nevada, USA) and OK (New Zealand) show almost identical distributions and consist of between four and six novel BHPs compounds. This suite of novel compounds consists of two isomers of pentafunctionalised BHP with  $[M+H]^+ = m/z$  1032, a 2-methylated homologue that is also present with an isomeric version with  $[M+H]^+ = m/z$  1046, a tetrafunctionalised BHP with  $[M+H]^+ = m/z$  974 and a 2-methyl homologue with  $[M+H]^+ = m/z$  988.

If the BHP distributions derive from geographically distinct *Synechococcus* sp., this suggests that the biosynthetic pathway responsible for the production of these specific

compounds evolved before the radiation of *Synechococcus* cyanobacteria. Furthermore, as BHPs are considered to increase membrane stability at elevated temperatures, it is possible that this group of BHPs contributes towards the thermal tolerance of *Synechococcus* sp. enabling colonisation of high-temperature environments.

*Table 3.3 Occurrence of novel BHPs with  $[M+H]^+ = m/z$  1046, 1032, 988 and 974 observed during analysis of microbial mat samples*

Sample	Region	Novel BHPs	Temp (°C)	pH
GBS03	Nevada	No	23.7	7.6
GBS08	Nevada	Yes	51.1	7.3
GBS12	Nevada	Yes	59.7	6.8
GBS18	Nevada	Yes	50.9	30.9
GBS19	Nevada	No	95.2	95.2
SV2 Con Source	Nevada	No	86.0	6.4
SV2 Con 1	Nevada	Yes	63.7	6.1
SV2 Con 2	Nevada	No	69.2	6.2
SV2 Con 3	Nevada	Yes	60.4	6.0
SV2 Con 4	Nevada	No	53.1	8.1
SV2 Con 5	Nevada	Yes	40.2	8.8
RHC 07	Nevada	No	41.3	8.5
RHC 06	Nevada	No	47.7	8.3
RHC 05	Nevada	No	53.6	8.2
RHC 04	Nevada	No	62.9	6.0
RHC Source	Nevada	No	95.3	6.4
EV1	California	No	41.0	
EV47	California	No	41.0	9.0
PV	Nevada	Yes	54.0	
OK	New Zealand	Yes	71.0	7.0

#### 3.4.4.2 METHANOTROPHIC BACTERIA

The presence of Aminopentol and Aminotetrol (**21**, **22**) in microbial mats from PV (Sample PV, section 3.3.1.3) indicate the presence of methanotrophic bacteria in this setting (e.g. Zundel and Rohmer, 1985b; Talbot *et al.*, 2001). No 16S rRNA gene sequences were observed that matched known methanotrophic bacteria suggesting the presence of novel methane-oxidising consortia at this site (e.g. Zhang *et al.*, 2007).

#### 3.4.5 SIMILARITIES AND GENERAL TRENDS

The BHP distributions detected in silica sinters are clearly distinct from those detected from samples of microbial mats. In general BHP distributions of sinters are more complex whereas distributions from microbial mats are dominated by the presence of a few BHPs including a novel family of BHPs. *BHtetrol* (**1**) is present in each sample analysed. Sintors deposited in from pools with acidic vent fluids, i.e. CP and LR, appear to have a slightly different assemblage to those sinters deposited under neutral conditions such as OP, OK and ET. *BHP<sub>cyc</sub>* and *BHT<sub>cyc</sub>* (10, 9) are abundant in samples from CP and LR and *BHP<sub>cyc</sub>* is the most abundant BHP in CP and LR sinters excluding sample LR3A. This suggests that these compounds are produced in response to elevated temperature and acidic pH and is in good agreement with Poralla *et al.* (1984), where cultures of *Bacillus acidocaldarius* (now *Alicyclobacillus acidocaldarius*) were shown to produce high quantities of composite BHPs in response to increasing incubation temperature and decreasing pH. Furthermore, Joyeux *et al.* (2004) showed an increased abundance of pentafunctionalised BHPs via PA/NaBH<sub>4</sub> cleavage-reduction at higher temperature when cultures of *Fratueria aurantia* were grown over a range of temperatures. Oxo-*BHT<sub>cyc</sub>* (**27**) was also present in these sinters, suggesting that this compound derives from an acidophilic thermophile. Interestingly, where these compounds are not the most dominant BHPs, distributions contain many diagnostic cyanobacterial BHP signatures. Apart from a few exceptions (e.g. Rashby *et al.*, 2007), 2-

methyl BHPs are robust indicators of cyanobacterial colonisation (Talbot *et al.*, 2008a). 2-methyl BHPs have been detected in sinters from FMP, OP and ET suggesting the presence of cyanobacteria populations at these sites. 2-me BHT<sub>cyc</sub> was also present in small amounts in material from LR (sample LR2A), where cyanobacteria likely contribute to the textural development of sinters, leading to the formation of spicular sinters such as sample LR2AS.

Sinters collected from the outflow channels of the vents studied, such as samples OK3A and OP7 contain a far greater abundance of BHPs of 2-3 orders of magnitude higher than that contained within sinters from the vent source. This indicates that BHP-producing bacteria are more dominant at intermediate thermophilic temperature regimes (e.g. 40 – 75°C) rather than hyperthermophilic temperatures (e.g. > 75°C). Kaur (2009) demonstrated a transition away from lipids that indicate the presence of archaeal phylotypes as sample distance increased from the vent source. This indicates that the amount of BHPs detected along a temperature gradient can be used to determine changes in microbial populations within a geothermal ecosystem (see Section 3.4.6.1 for further discussion). The conditions of the outflow channels may be more conducive to colonisation by BHP-producing bacteria, where distance between high temperature, acidic, solute-enriched and turbid waters provides a more suitable environment for habitation.

Comparison of the BHP distributions observed in sinters and microbial mats show marked differences. This is primarily an indication of different biological input and highlights the utility of BHPs to distinguish between bacteria colonising vent waters and sinter formation zones with those colonising outflow channels and mat-forming consortia. Certain similarities are observable, namely a high-proportion of penta-functionalised BHPs are present in both settings. Although certain cyanobacteria are known to be sources of penta-functionalised BHPs (Bisseret *et al.*, 1985; Talbot *et al.*, 2008a), biosynthesis of more

functionalised compounds is likely a physiological response in order to maintain membrane integrity at elevated temperature (e.g. Poralla *et al.*, 1984; Joyeux *et al.*, 2004).

### 3.4.6 THE NATURAL LABORATORY

In order to assess the physiological response of BHP-producing bacteria to a number of environmental factors such as temperature, acidity and UV-exposure, comparisons of physico-chemical parameters and observed BHP-distributions at each site are now discussed. Relatively little published work exists concerning the effect of environmental or growth condition on the biosynthesis of BHPs in BHP-producing bacterial species. This, as discussed in Section 1.5, is due mainly to the sensitive nature of BHP-biosynthesis to culturing conditions and growth phase (Bringer *et al.*, 1985; Flesch and Rohmer, 1989; Summons *et al.*, 1994; Poralla *et al.*, 2000; Joyeux *et al.*, 2004). The range of conditions at the terrestrial vents in this study provides an ideal focus for conducting such an investigation in a natural setting. This is a putative investigation as many other factors, such as the specific biological input to a particular system have yet to be determined.

#### 3.4.6.1 TEMPERATURE

Comparisons of the temperature at each vent site and the BHP-distributions contained within actively-precipitating sinter facies is shown in Figure 3.12. The BHP-distributions of actively precipitating sinters were selected as they are most representative of the in-situ bacterial population at the temperature measured at the time of sampling. Active sinters from ETGF have also been excluded as the elevation of the geothermal field reduces the boiling point of water which may affect in-situ bacterial populations.

At the upper temperature limit for bacterial thermophiles (95°C, Huber *et al.*, 1992; Sample OP2A, OK1-TA, Ok1-MA and OK1-BA) the abundances of BHPs in the samples are lower than those from mid-range thermophiles (samples CP1f, CP1A, OK3A, LR2A, LR2AS,

LR3A, OP7A). It is clear that the bacterial population associated with the outflow channel of FMP (Sample OK3A) is exceptional with regard to BHP-production, disregarding this sample from the investigation shows an overall decrease in BHP-abundance with increasing temperature (Figure 3.12).

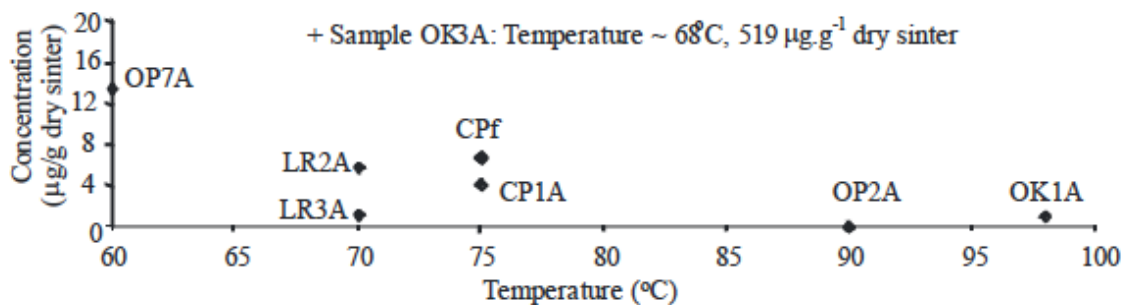


Figure 3.12 Graph showing BHP-abundance of active sinters from TVZ plotted as a function of temperature. For easier interpretation, sample OK3A has been removed from sample suite for this investigation.

The decrease in BHP-abundance observed as a function of temperature is reflective of the upper-temperature limit of bacteria and not a physiological response to the conditions (e.g. Kannenburg *et al.*, 1980). Archaeal phylotypes which do not produce BHPs are known to be more common at hyper-thermophilic temperature ranges, reflected in the lower abundances of BHPs. Although, sample OK1 showed the presence of BHPs, the distribution in this case if indigeneic (see 4.4.2.1), would appear to derive from cryptoendolithic photosynthetic organisms that have become incorporated into the silica-matrix where temperatures would be greatly reduced. The upper temperature limits for life in general are likely to be extended with the discovery of new microorganisms from new extreme temperature settings.

#### 3.4.6.2 pH

Comparisons of pH values of sample locations and associated BHP-distributions of active silica sinters should indicate any physiological response and/or bacterial-community change driven by low pH conditions.

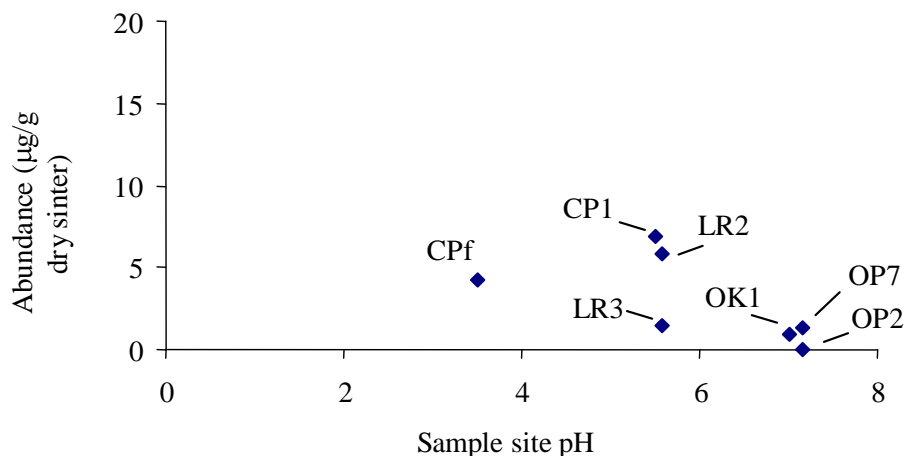


Figure 3.2 BHP abundance as function of sample environment pH.

From Figure 3.13, little relationship is obvious between BHP-abundance and environmental pH. There is a general increase of BHP abundance as pH decreases but FMP and OP are high temperature sites and BHP-producing bacteria are expected to be lower at these locations (see 4.4.3.1). However, comparisons of the compositions of the BHP-distributions, i.e. the chemical nature of the compounds from acidic vent sites and depositional environments show marked similarities. Namely the high relative abundances of ‘composite-BHPs’ (Table 3.1), Anhydro-type BHPs and the presence of ‘oxo-BHPs’ seem to be common signatures observed in sinters deposited from acidic geothermal vents. The acid-catalysed formation of Anhydro-type BHPs is discussed in Section 1.1. The upper temperature limit for thermophilic acidophiles currently lies at 63°C for bacteria (M. Stott, GNS science, personal communication), however, the BHP-distributions observed throughout this study suggest that this may need re-evaluating.

#### 3.4.6.3 UV INTENSITY

ETGF is exposed to large amounts of solar radiation for extended periods of time, however, no clear response is observed in the BHP distributions between this particular

setting and those observed from TVZ. BHP abundances are relatively low compared to sites from TVZ. This may be a consequence of the harsh conditions at ETGF. The BHP-distributions observed in sample ET25A consist of a number of cyanobacterial signatures, it is known that the sinters of ETGF harbour endolithic cyanobacterial colonies that are adapted to growth under high UV radiation.

### 3.5 CONCLUSIONS

This study represents the first comprehensive analysis of BHPs from the active facies of terrestrial geothermal environments. This study has encompassed precipitated sulphide minerals from the vent fluids of CP (sample CPf), a range of sinters from the air-water interface (Samples CP1A, OK1-TA, OK1-MA, OK1-BA, LR2A, LR3A OP2A; Section 3.2) and a suite of microbial mats (Section 3.3). Two bacterial isolates from CP were analysed but BHPs were not detected in either sample and future geochemical investigations of terrestrial geothermal ecosystems would benefit from the inclusion of a parallel culture-based or phylogenetic investigation. However, it is clear that any geochemical analyses could provide an informative tool with which to begin microbiological investigations. For instance, BHP-signatures have been detected that highlight the presence of cyanobacteria and methylotrophic bacteria in samples from FMP (Samples OK1-TA, OK1-MA, OK1-BA, LR2A, LR3A, OP7A). Analysis of floc material (Sample CPf) from the vent waters of CP demonstrates that a currently unidentified BHP-producing organism inhabits the anoxic vent fluids in this system. Therefore a proportion of the BHPs identified in other sinters collected from the air-water interface could also include a contribution from bacteria colonising the vent source. As discussed in Section 3.1, sinters form more readily at the air-water interface which can be considered analogous to an oxic-anoxic boundary and incorporation of organic material is thought to record life at this redox boundary (Gibson *et al.*, 2008). Therefore, the majority of BHPs identified in sinters from CP, FMP, LR and ET are thought to derive from bacteria that

survive in oxygen-depleted zones. Sinters that were collected from the outflow channels, such as sample OK3A and OP7A most likely record input of bacteria that survive in cooler conditions than the vent source. The sinter from the outflow channel of FMP (OK3A) showed an increased abundance of BHPs which is thought to derive from a more prolific BHP-producing bacterial community at this temperature setting. The active sinter taken from the outflow channel of OP (OP7A) displayed a BHP distribution that indicates the presence of cyanobacteria which are thought to be contributing to the unique sinter formations at this site via a phototrophic response.

The novel BHP distribution observed in the microbial mats is thought to derive from *Synechococcus* sp. or *Mastigocladus* sp. cyanobacteria. *Synechococcus* sp. are known to be the dominant mat-forming cyanobacteria in geothermal areas of the USA, New Zealand and Japan (Papke *et al.*, 2003). Whereas *Mastigocladus* sp. are known to survive at temperatures within the sample set investigated in this study (Miller *et al.*, 2009) and have been observed at OK (Mountain, personal communication), however, it is unknown at present whether *Mastigocladus* sp. produce BHPs.

Overall, the distributions measured in this analysis demonstrate that chemical functionality of BHPs is retained upon incorporation into the silica matrix. Although relatively little is known about precursor bacterial populations, upon consideration of the complexity of the distributions, environmental conditions and previously characterised BHP-producing bacteria, it is highly probable that the BHP-distributions observed within active sinters are frequently recording novel and undetermined bacterial assemblages. The distributions observed here contribute further insight to the ecology and biogeochemistry of the springs investigated.

Analyses of BHP distributions preserved within silica sinters, microbial mats and organo-sedimentary depositions have shown:

- Polyfunctionalised BHP structures are sufficiently well-preserved leading to the identification of recognisable biosignatures.
- A number of novel polyfunctionalised BHPs have been detected that imply the presence of currently undetermined BHP-producing bacterial species.
- Detection of BHPs from active facies from anoxic depositional settings at Champagne Pool indicates novel anaerobic BHP-producing organism(s) contribute to lipid distribution observed from this site.
- A novel cyanobacterial-BHP signature has been identified and is present in geographically-distinct geothermal regions.
- BHPs appear to be less abundant or absent from active sinters where water temperatures exceed 75°C.
- BHP-distributions appear more complex where environmental pH is acidic.

## 4 INTACT BHPs OF NON-ACTIVE SINTER FORMATIONS IN TERRESTRIAL GEOTHERMAL ECOSYSTEMS

### 4.1 INTRODUCTION

This study presents the analysis of BHP distributions that are preserved in non-active silica sinters of terrestrial geothermal vents. Chapter 3 detailed the distribution of BHPs in ‘active geothermal settings’ such as floc material, microbial mats or sinters collected from the vent perimeter that are in direct contact with vent fluid. The focus of this study, non-active sinter material, is that which has been deposited at an earlier interval in the life-time of the vent in question. Sinter formation resulting in contraction of the pool surface or hydro-geological changes that render the vent inactive mean that these particular samples are no longer in contact with the vent itself.

It has been shown that the remnants of microbial colonisation can be well preserved into mineral depositions and can be used to reconstruct past processes in ancient material (e.g. Thiel *et al.*, 2003; Orcutt *et al.*, 2005; Bouloubassi *et al.*, 2006; Birgel *et al.*, 2006; Blumenberg *et al.*, 2007; Kaur, 2009). Previous reports detailing the distribution of microbial lipids in silica sinters have shown that organic geochemical signatures are sufficiently well preserved (e.g. Pancost *et al.*, 2005, 2006; Talbot *et al.*, 2005). Variations in lipid distributions over time, that form as a result of a physiological change to adapt to changing conditions or reflective of changing microbial populations driven by a change in physico-chemical conditions of the pool have also been described (Kaur *et al.*, 2008). By analysing the BHP distributions of non-active sinters, we hope to assess the long-term preservation potential of BHPs in sinter material with a view to document changing bacterial populations and biogeochemistry of a particular vent over time.

Previous work on the distribution of BHPs in non-active silica sinter depositions showed the presence of anhydroBHT, BH*tetrol* and BH*pentol* (Structures **2**, **1**, **13**) in sinters from

Rotokawa (RK). Samples from CP and OK have also been previously analysed by GC-MS methodology (Talbot *et al.*, 2005; Pancost *et al.*, 2006). These initial experiments showed little diversity of BHP-assemblages but did highlight the possibility that BHPs and hopanoids likely derive from currently uncharacterised sources.

#### 4.1.1 AIMS

- Identify and quantify the BHP distribution of non-active silica sinters
- Assess the long-term preservation of BHPs in silica sinters
- Investigate the utility of BHPs to record changing microbiology and geochemistry of a vent over time.

#### 4.2 LOCATIONS AND SAMPLE SUITE

Multiple samples have been analysed from the TVZ. Descriptions of samples and sample locations can be found in Chapter 2 (See Section 2.3). Briefly, the BHP distributions of non-active sinter samples from Champagne Pool (CP), Orakei Korako Geothermal Field (OK), Loop Road (LR), Opaheke Pool (OP) and two non-active samples from the Rotokawa (RK) geothermal field have been included in this particular sample set.

#### 4.3 RESULTS

##### 4.3.1 BHP DISTRIBUTIONS OF NON-ACTIVE SINTERS FROM CHAMPAGNE POOL (CP)

The non-active sinters of CP were collected from increasing distances from the pool edge. This constitutes a putative time-sequence where CP3N was closest to the pool edge and is therefore the youngest non-active sinter and CP11N was collected from the furthest distance and is therefore the oldest sinter sample. Sample CP5N was collected out of sequence from a position where the sinter terrace has been raised due to geological processes. This sample has been included for completeness.

## 4.3.1.1 CP3N

Ten BHPs were detected during LC-MS<sup>n</sup> analysis of sample CP3N (Figure 4.1) of which seven are previously known and three others have been tentatively assigned during this study. The distribution of previously known BHPs consists of BHP<sub>cyc</sub>, BHT<sub>cyc</sub>, aminotriol, BH<sub>pentol</sub>, BH<sub>tetrol</sub>, anhydroBHP and anhydroBHT (**10**, **9**, **22**, **13**, **1**, **3** and **2**). BHT<sub>cyc</sub> (**9**) was the most abundant BHP detected and anhydroBHP (**2**) was the least abundant known BHP detected, with concentrations ranging from 0.01 to 0.39 µg.g<sup>-1</sup> dry sinter (Table 4.1). Three compounds tentatively assigned as novel BHPs were detected in this sample, oxo-BHT<sub>cyc</sub> (**27**), oxo-BH<sub>pentol</sub> (**37**) and oxo-BH<sub>tetrol</sub> (**38**). Oxo-BHT<sub>cyc</sub> (**27**) was present in trace amounts (i.e. < 0.005 µg.g<sup>-1</sup> dry sinter); abundances of oxo-BH<sub>pentol</sub> (**38**) and oxo-BH<sub>tetrol</sub> (**44**) were 0.01 and 0.06 µg.g<sup>-1</sup> dry sinter respectively (Table 4.1). The total abundance of BHPs in sample CP3 was 1.07 µg.g<sup>-1</sup> dry sinter (Table 4.1).

## 4.3.1.2 CP6N

Eight BHPs were detected in sample CP6N (Figure 4.2), of which five BHPs have been previously characterised and three have been tentatively identified as novel BHPs in this study. Known BHPs detected were BHP<sub>cyc</sub>, BHT<sub>cyc</sub>, aminotriol, BH<sub>tetrol</sub> and anhydroBHT (**10**, **9**, **22**, **1**, **2**). Aminotriol (**22**) was found to be the most abundant BHP representing 68% of the total BHP composition and BH<sub>tetrol</sub> (**1**) was the least abundant with concentrations ranging from 0.27 to 4.65 µg.g<sup>-1</sup> dry sinter (Table 4.1). Three compounds that have been tentatively assigned as novel BHPs were detected are oxo-BHT<sub>cyc</sub> (**27**), oxo-BH<sub>tetrol</sub> (**44**) and a compound with parent ion mass [M+H]<sup>+</sup> = m/z 1018 (**29**). Structural assignment of [M+H]<sup>+</sup> = m/z 1018 (**29**) is based upon characteristic BHP-fragmentations observed in the MS<sup>2</sup> Spectrum (e.g. Talbot *et al.*, 2003a, b; Talbot *et al.*, 2007a; b). In this case however, it has not been possible to complete a full structural characterisation as ions in the MS<sup>2</sup> spectrum only provide evidence of the presence

of a terminal group with a mass of 306 Da (See Chapter 5, Section 5.3 for further discussion and MS<sup>2</sup> spectrum) and no further structural information. Abundances of the novel compounds range from 0.09 µg.g<sup>-1</sup> dry sinter for [M+H]<sup>+</sup> = m/z 1018 (**29**) to 0.33 µg.g<sup>-1</sup> dry sinter for oxo-BH*tetrol* (**37**; Table 4.1). Overall abundances of BHPs in sample CP6 were 6.80 µg.g<sup>-1</sup> dry sinter (Table 4.1).

#### 4.3.1.3 CP7N

Nine BHPs were detected in sample CP7N (Figure 4.3), seven of which have previously been characterised and another is tentatively identified as a novel BHP during this study. The known BHPs detected in this sample are BHP*cyc*, BHT*cyc*, aminotriol, BH*pentol*, BH*tetrol*, 2 isomers of anhydroBHP and anhydroBHT (**10**, **9**, **22**, **13**, **1**, **2** and **3**). From the distribution of BHPs that have been previously characterised, BHP*cyc* and BHT*cyc* (**10** and **9**) were found to be the most abundant (0.54 µg.g<sup>-1</sup> dry sinter each) and anhydroBHP was the least abundant (0.06 µg.g<sup>-1</sup> dry sinter; Table 4.1). Oxo-BHT*cyc* (**27**) was present in an abundance of 0.15 µg.g<sup>-1</sup> dry sinter. The total abundance of BHPs in this sample was 1.74 µg.g<sup>-1</sup> dry sinter (Table 4.1).

#### 4.3.1.4 CP8N

Fourteen BHPs were detected in sample CP8N (Figure 4.4), of which seven have been previously characterised and 5 have been tentatively assigned as novel BHPs during this study. The distribution of previously reported BHPs consisted of BHP*cyc*, BHT*cyc*, guanidine-substituted BHT*cyc*, aminotriol, BH*pentol*, BH*tetrol* and two isomers of anhydroBHP (**10**, **9**, **23**, **22**, **13**, **1**, **2**). BHT*cyc* (**9**) was the most abundant BHP and guanidine-substituted BHT*cyc* (**23**) was the least abundant BHP, with concentrations ranging from 0.01 to 4.2 µg.g<sup>-1</sup> dry sinter (Table 4.1). Of the novel compounds that have been tentatively identified during this study, oxo-BHP*cyc* (**36**), oxo-BHT*cyc* (**27**), oxo-BH*pentol* (**37**), oxo-BH*tetrol* (**38**) and a compound with a protonated parent ion [M+H]<sup>+</sup> = m/z 1018 (**29**) were detected in this sample. Oxo-BHT*cyc* (**27**)

was the most abundant novel BHP and oxo-BHP<sub>cyc</sub> (**36**) and  $[M+H]^+ = m/z$  1018 (**29**) were the least abundant with concentrations ranging from 0.02 to 0.53  $\mu\text{g}\cdot\text{g}^{-1}$  dry sinter (Table 4.1). The total abundance of BHPs in this sample was 10.87  $\mu\text{g}\cdot\text{g}^{-1}$  dry sinter (Table 4.1).

#### 4.3.1.5 CP11N

Fourteen BHPs were detected in sample CP11N (Figure 4.5), of which eight of the BHPs have been previously characterised and the remaining five have been tentatively assigned as novel BHPs during this study. The distribution of previously reported BHPs consisted of BHP<sub>cyc</sub>, BHT<sub>cyc</sub>, guanidine-substituted BHT<sub>cyc</sub>, aminotriol, BH<sub>pentol</sub>, BH<sub>tetrol</sub>, two isomers of anhydroBHP and anhydroBHT (**10**, **9**, **23**, **22**, **13**, **1**, **3**, **2**). AnhydroBHP (**3**) was found to be the least abundant and BHP<sub>cyc</sub> (**10**) was the most abundant BHP with concentrations ranging from 0.02 to 6.44  $\mu\text{g}\cdot\text{g}^{-1}$  dry sinter. BHP<sub>cyc</sub> and BHT<sub>cyc</sub> (**10** and **9**) were considerably more abundant than the other BHPs detected, with abundances of 6.4 to 4.3  $\mu\text{g}\cdot\text{g}^{-1}$  dry sinter respectively. Aminotriol, BH<sub>pentol</sub> and BH<sub>tetrol</sub> (**22**, **13**, **1**) were detected in lower abundances ranging from 1.49 to 2.08  $\mu\text{g}\cdot\text{g}^{-1}$  dry sinter (Table 4.1) Compounds that have been tentatively assigned as novel BHPs (oxo-BHP<sub>cyc</sub>, guanidine-BHP<sub>cyc</sub>, oxo-BHT<sub>cyc</sub>, oxo-BH<sub>pentol</sub>, oxo-BH<sub>tetrol</sub>; **36**, **30**, **27**, **36**, **37**) during this study were present in considerably lower amounts, ranging from trace amounts of guanidine-BHP<sub>cyc</sub> (**30**) to 0.22  $\mu\text{g}\cdot\text{g}^{-1}$  dry sinter of oxo-BHT<sub>cyc</sub> (**27**). Overall abundance of total BHPs in sample CP11N was 17.01  $\mu\text{g}\cdot\text{g}^{-1}$  dry sinter (Table 4.1).

#### 4.3.1.6 CP5N

Nine BHPs were detected in sample CP5N (Figure 4.6) of which six have been previously characterised and three have been tentatively identified as BHPs during this study. From the distribution of known BHPs, BHP<sub>cyc</sub>, BHT<sub>cyc</sub>, and aminotriol (**10**, **9**, **22**) were the most abundant with abundances ranging from 28.83 to 66.95  $\mu\text{g}\cdot\text{g}^{-1}$  dry sinter (Table 4.1) BH<sub>tetrol</sub>, anhydroBHP and anhydroBHT (**1**, **2**, **3**) were present in lower amounts ranging from

0.52 to 7.45  $\mu\text{g}\cdot\text{g}^{-1}$  dry sinter. Three compounds that have been tentatively identified as novel BHPs are oxo-BHT<sub>cyc</sub> (**27**), oxo-BHT<sub>tetrol</sub> (**37**) and a novel BHP with  $[\text{M}+\text{H}]^+ = m/z$  1018 (**29**). Abundances were 2.97, 10.63 and 17.74  $\mu\text{g}\cdot\text{g}^{-1}$  dry sinter respectively. The total abundance of BHPs in sample CP5N was 193  $\mu\text{g}\cdot\text{g}^{-1}$  dry sinter (Table 4.1).

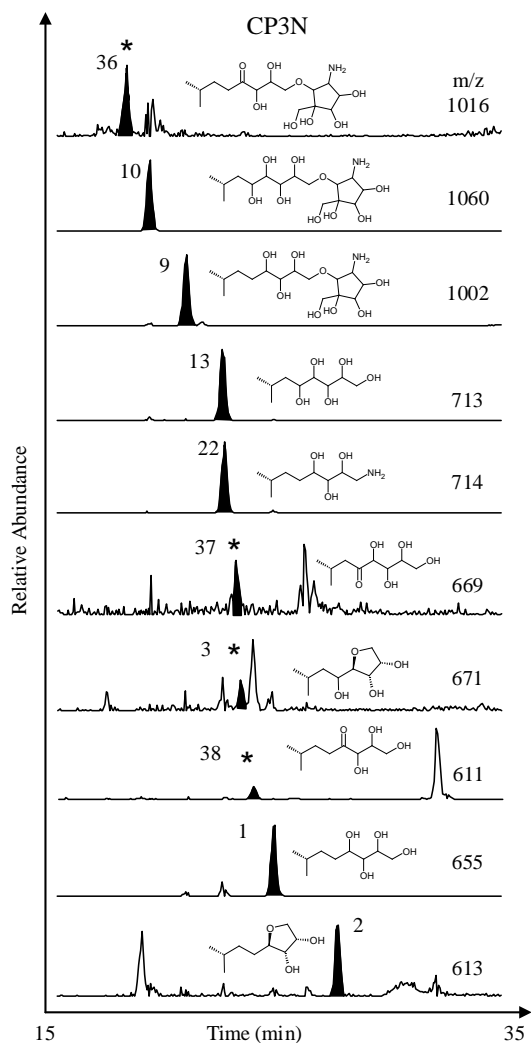


Figure 4.1 Partial mass chromatograms (15 – 35 min) showing BHP distributions observed in sample CP3N. \*Indicates correct peak.

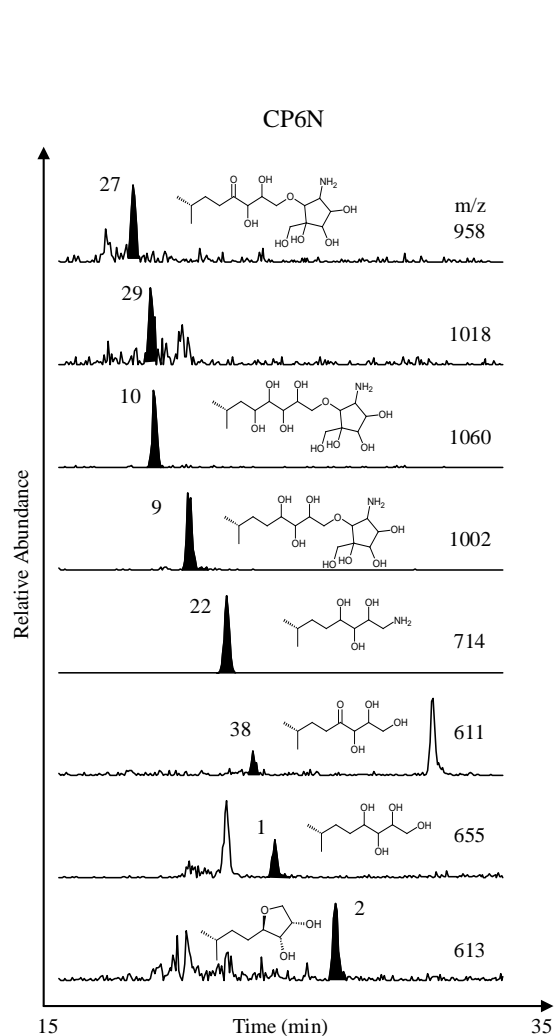


Figure 4.2 Partial mass chromatograms (15 – 35 min) showing BHP distributions observed in sample CP6N. \*Indicates correct peak.

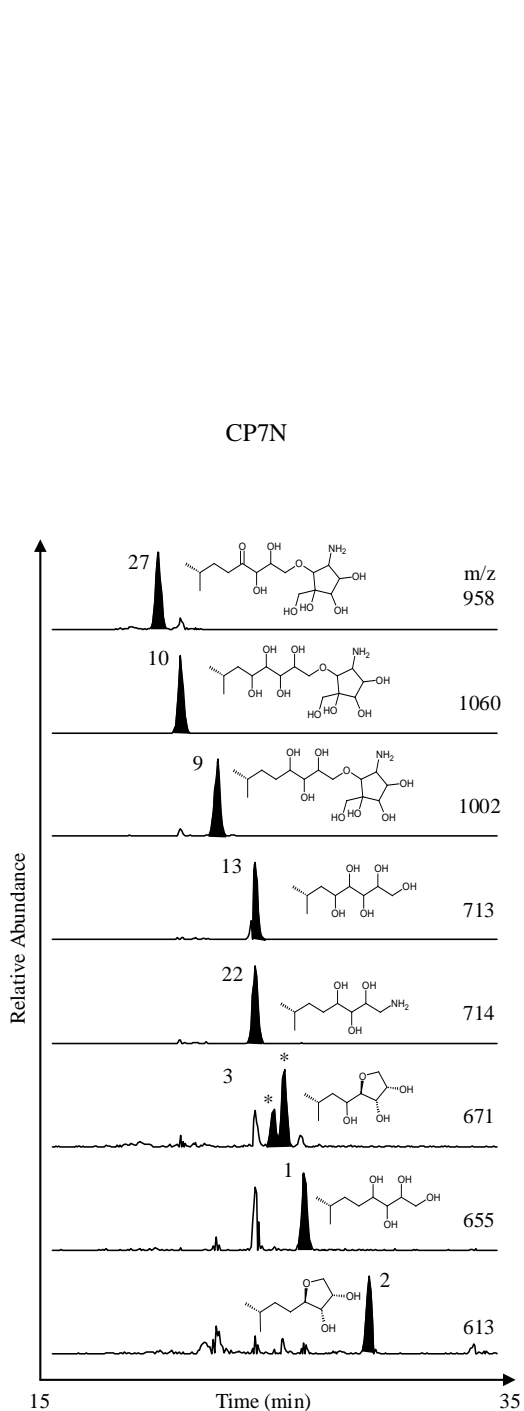


Figure 4.3 Partial mass chromatograms (15 – 35 min) showing BHP distributions observed in sample CP7N. \*Indicates correct peak.

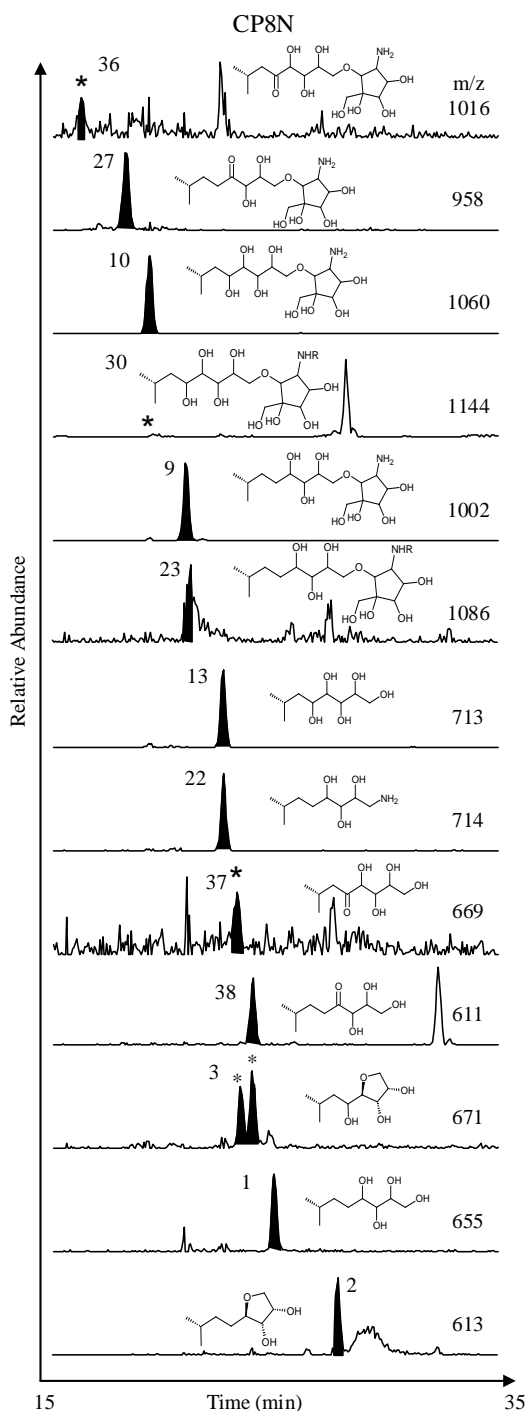


Figure 4.4 Partial mass chromatograms (15 – 35 min) showing BHP distributions observed in sample CP8N. \*Indicates correct peak.

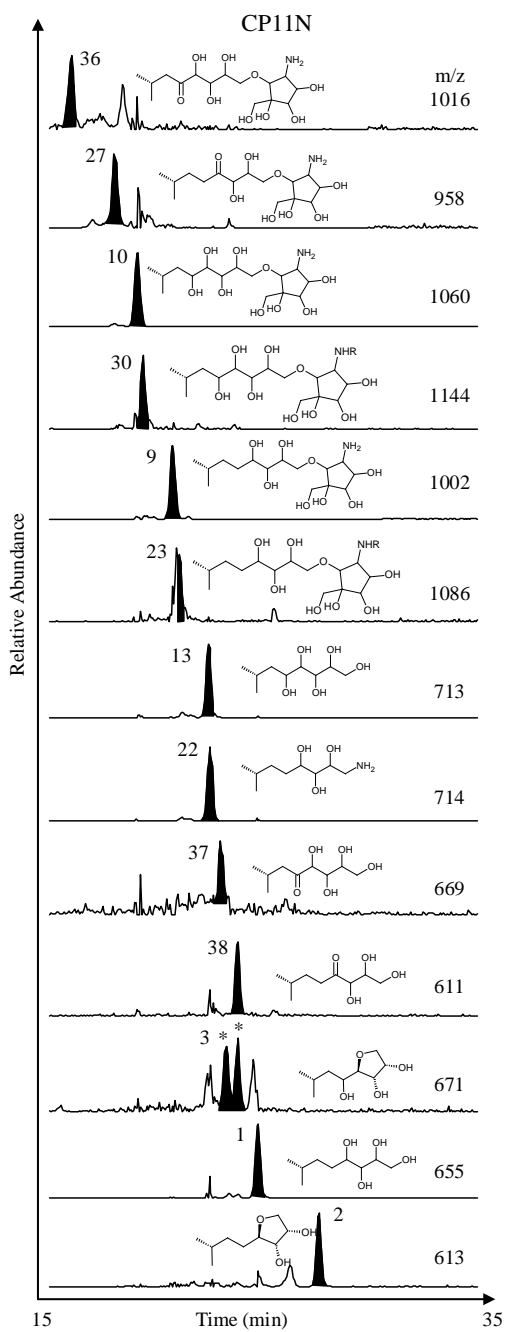


Figure 4.5 Partial mass chromatograms (15 – 35 min) showing BHP distributions observed in sample CP11N. \*Indicates correct peak.

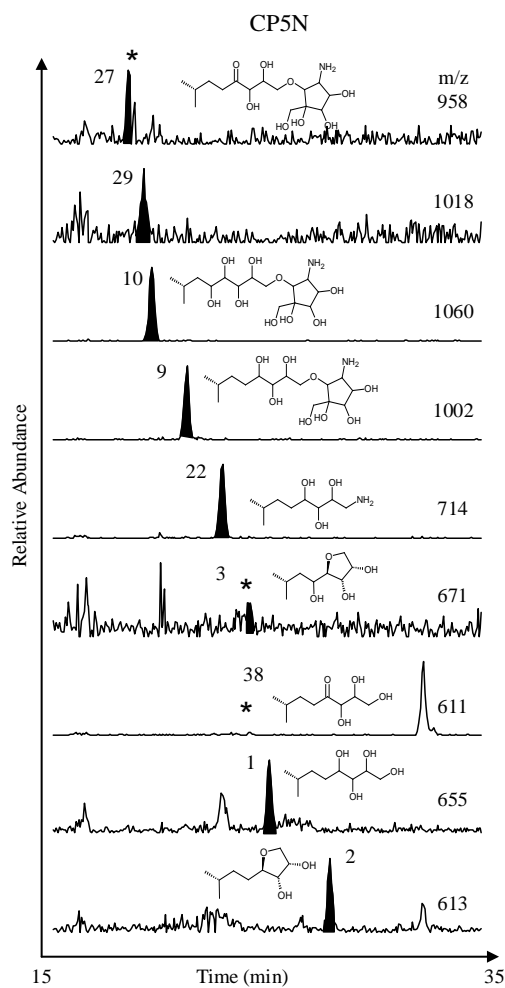


Figure 4.6 Partial mass chromatograms (15 – 35 min) showing BHP distributions observed in sample CP5N. \*Indicates correct peak.

## 4.3.2 BHP DISTRIBUTIONS OF NON-ACTIVE SINTERS FROM ORAKEI

## KORAKO

## 4.3.2.1 OK4N

Eight BHPs were detected in sample OK4N (Figure 4.7), of which six are BHPs that have been previously characterised and four are compounds that have been tentatively assigned as novel BHPs during this study. The distribution of previously known BHPs consists of *BHHcyc*, *BHPcyc*, *BHTcyc*, aminotriol, adenosylhopane and *BHtetrol* (**39**, **10**, **9**, **22**, **6**, **1**). Adenosylhopane (**6**) was the least abundant BHP and aminotriol (**22**) was the most abundant BHP detected, with concentrations ranging from 0.24 to 1.05  $\mu\text{g}\cdot\text{g}^{-1}$  dry sinter (Table 4.1). Two tentatively identified novel BHPs with parent ion of  $[\text{M}+\text{H}]^+ = m/z$  1190 and 1205 were observed (Figure 4.7). The abundance of each compound is 0.33 and 0.05  $\mu\text{g}\cdot\text{g}^{-1}$  dry sinter respectively (Table 4.1). Compounds with  $[\text{M}+\text{H}]^+ = m/z$  1146 and 1204 form penta- and hexa-functionalised homologues of a new series of BHPs with terminal group ion  $m/z$  434 (Chapter 5). The overall abundance of BHPs in this sample is 3.39  $\mu\text{g}\cdot\text{g}^{-1}$  dry sinter (Table 4.1).

## 4.3.2.2 OK5N

Five known BHPs were detected in sample OK5N (Figure 4.8). The distribution consisted of *BHHcyc*, *BHPcyc*, *BHTcyc*, aminotriol and *BHtetrol* (**39**, **10**, **9**, **22**, **1**), of which *BHHcyc* (**39**) was the least abundant and aminotriol (**22**) was the most abundant BHPs detected, with values ranging from 0.05 to 0.7  $\mu\text{g}\cdot\text{g}^{-1}$  dry sinter (Table 4.1). The total abundance of BHPs in this sample was 1.2  $\mu\text{g}\cdot\text{g}^{-1}$  dry sinter (Table 4.1).

## 4.3.2.3 OK6N

Six BHPs were detected in sample OK6N (Figure 4.9). The distribution consists of BHP<sub>cyc</sub>, 2-me BHP<sub>cyc</sub>, BHT<sub>cyc</sub>, 2-me BHT<sub>cyc</sub>, aminotriol and BHtetrol (**10**, **II-10**, **22**, **II-22**, **1**). 2-me BHT<sub>cyc</sub> (**II-9**) was the least abundant BHP detected and aminotriol was the most abundant BHP detected, with concentrations ranging from 0.03 to 0.2  $\mu\text{g}\cdot\text{g}^{-1}$  dry sinter (Table 4.1). The total abundance of BHPs in this sample was 0.55  $\mu\text{g}\cdot\text{g}^{-1}$  dry sinter (Table 4.1).

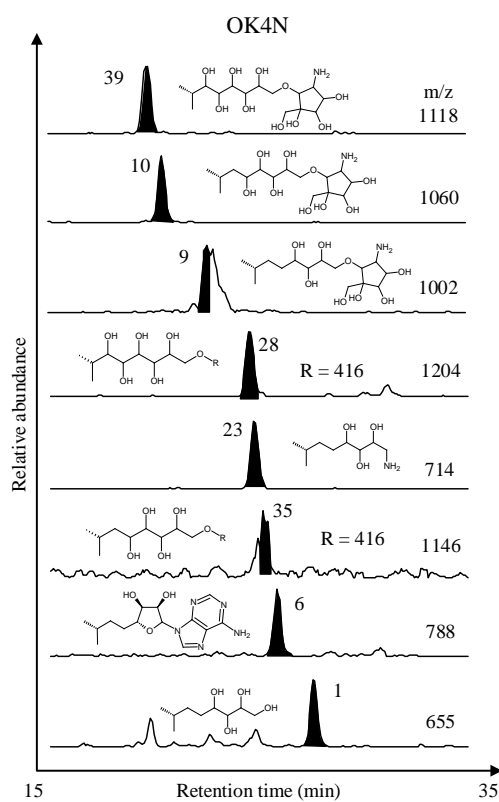


Figure 4.7 Partial mass chromatograms (15 – 35 min) showing BHP distributions observed in sample OK4N.

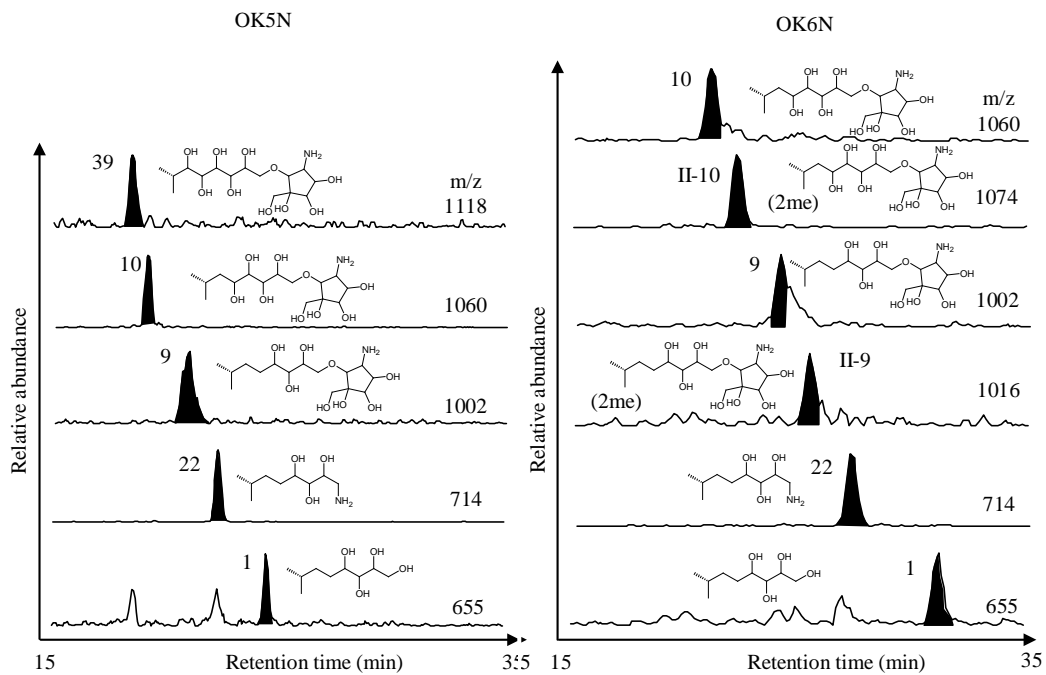


Figure 4.8 Partial mass chromatograms (15 – 35 min) showing BHP distributions observed in sample OK5N.

Figure 4.9 Partial mass chromatograms (15 – 35 min) showing BHP distributions observed in sample OK6N.

### 4.3.3 BHP DISTRIBUTIONS OF NON-ACTIVE SINTERS FROM LOOP ROAD

Four non-active sinter samples from Loop Road were collected from two different depositional settings. Samples LR3N and LR4N are non-active sinters taken from the pool ledge, whilst sample LR5R and LR6R were taken from a silicified rhizolith.

#### 4.3.3.1 LR3N

Twelve BHPs were detected during analysis of sample LR3N (Figure 4.10), of which eight BHPs have previously been characterised and four are tentatively assigned as novel BHPs during this study. The previously characterised BHPs consisted of *BHP<sub>cyc</sub>*, *BHT<sub>cyc</sub>*, pentose-ether BHT, *BH<sub>pentol</sub>*, anhydroBHP, 2-me pentose-ether BHT, *BH<sub>tetrol</sub>* and anhydroBHT (**10**, **9**, **17**, **13**, **3**, **II-17**, **1**, **2**). Of these compounds, 2-me PE BHT (**II-17**) was the least abundant and *BHT<sub>cyc</sub>* was the most abundant, with concentrations ranging from 0.34 to 1.76  $\mu\text{g}\cdot\text{g}^{-1}$  dry sinter (Table 4.1). Four compounds tentatively assigned as novel BHPs were also present, these consisted of oxo-*BHT<sub>cyc</sub>*, oxo-*BH<sub>pentol</sub>*, oxo-*BH<sub>tetrol</sub>* (**27**, **37**, **38**) and a compound with a protonated parent ion  $[\text{M}+\text{H}]^+ = m/z$  984 (**42**). Oxo-*BH<sub>pentol</sub>* (**27**) was the least abundant novel BHP and oxo-*BH<sub>tetrol</sub>* (**38**) was the most abundant, with concentrations ranging from 0.02 to 0.98  $\mu\text{g}\cdot\text{g}^{-1}$  dry sinter (Table 4.1). Aminotriol was not observed during the analysis of this sample.

#### 4.3.3.2 LR4N

Eight BHPs were detected during analysis of sample LR4N (Figure 4.11), of which seven are BHPs that have previously been characterised and one compound has been tentatively assigned as a BHP during this study. The distribution of BHPs that have been previously characterised consists of *BHP<sub>cyc</sub>*, *BHT<sub>cyc</sub>*, aminotriol, anhydroBHP, 2-me PE BHT, *BH<sub>tetrol</sub>* and anhydroBHT (**10**, **9**, **22**, **3**, **II-17**, **1**, **2**). Of the BHP which have been previously characterised, anhydroBHT was the least abundant BHP detected and *BHP<sub>cyc</sub>* was the most

abundant compound detected in this sample, with concentrations ranging from 0.13 to 14.47  $\mu\text{g}\cdot\text{g}^{-1}$  dry sinter (Table 4.1). The tentatively assigned novel BHPs detected in this sample are oxo-BHT<sub>cyc</sub> (**27**),  $[\text{M}+\text{H}]^+ = m/z$  1018 (**29**) and guanidine-substituted BHP<sub>cyc</sub> (**30**). Each compound was present in concentrations of 0.18, 0.14 and 0.16  $\mu\text{g}\cdot\text{g}^{-1}$  dry sinter respectively (Table 4.1). In this sample BHP<sub>cyc</sub> and BHT<sub>cyc</sub> (**10**, **9**) were significantly more abundant than other BHPs detected, comprising 90 % of the total BHP composition.

#### 4.3.3.3 LR5R

Eight BHPs were detected during analysis of sample LR5R (Figure 4.12), including six that have previously been characterised and two tentatively assigned as novel BHPs during this study. The distribution of previously characterised BHPs consists of BHP<sub>cyc</sub>, BHT<sub>cyc</sub>, aminotriol, 2-me PE BHT, BH<sub>tetrol</sub> and anhydroBHT (**10**, **9**, **22**, **II-17**, **1**, **2**). Of the BHPs that have been previously characterised, 2-me PE BHT (II-17) was the least abundant compound detected and aminotriol was the most abundant compound detected, with concentrations ranging from 0.19 to 22.72  $\mu\text{g}\cdot\text{g}^{-1}$  dry sinter (Table 4.1). The two tentatively assigned novel BHPs detected in this sample are compounds with parent ion masses of  $[\text{M}+\text{H}]^+ = m/z$  1018 and 960 (**29**, **43**).  $[\text{M}+\text{H}]^+ = m/z$  1018 (**29**) was the least abundant compound and  $[\text{M}+\text{H}]^+ = m/z$  960 (**29**) was the most abundant, with concentrations ranging from 0.06 to 0.81  $\mu\text{g}\cdot\text{g}^{-1}$  dry sinter (Table 4.1).

#### 4.3.3.4 LR6R

Nine BHPs were detected during analysis of sample LR6R (Figure 4.13) of which five are BHPs that have previously been characterised and four have been tentatively assigned as novel BHPs during this study. The previously characterised BHPs include BHP<sub>cyc</sub>, BHT<sub>cyc</sub>, aminotriol, BH<sub>tetrol</sub> and anhydroBHT (**10**, **9**, **22**, **1**, **2**). Of the known BHPs detected in this sample, anhydroBHT was the least abundant BHP and aminotriol was the most abundant BHP,

with concentrations ranging from 0.11 to 5.66  $\mu\text{g}\cdot\text{g}^{-1}$  dry sinter (Table 4.1). The distribution of novel BHPs consists of oxo-BHT<sub>cyc</sub> (**27**) and oxo-BHT<sub>tetrol</sub> (**30**). Of these compounds oxo-BHT<sub>tetrol</sub> (**30**) was the least abundant compound and oxo-BHT<sub>cyc</sub> (**27**) was the most abundant compound detected, with concentrations ranging from 0.01 to 0.25  $\mu\text{g}\cdot\text{g}^{-1}$  dry sinter. Two other late-eluting compounds with parent mass ion  $[\text{M}+\text{H}]^+ = m/z$  1100 and 1114 (**44**, **45**), have also been tentatively identified as novel BHPs by observing characteristic fragmentations in the MS<sup>2</sup> and MS<sup>3</sup> spectra of these particular compounds. The abundance of both of these novel compounds was 0.01  $\mu\text{g}\cdot\text{g}^{-1}$  dry sinter (Table 4.1).

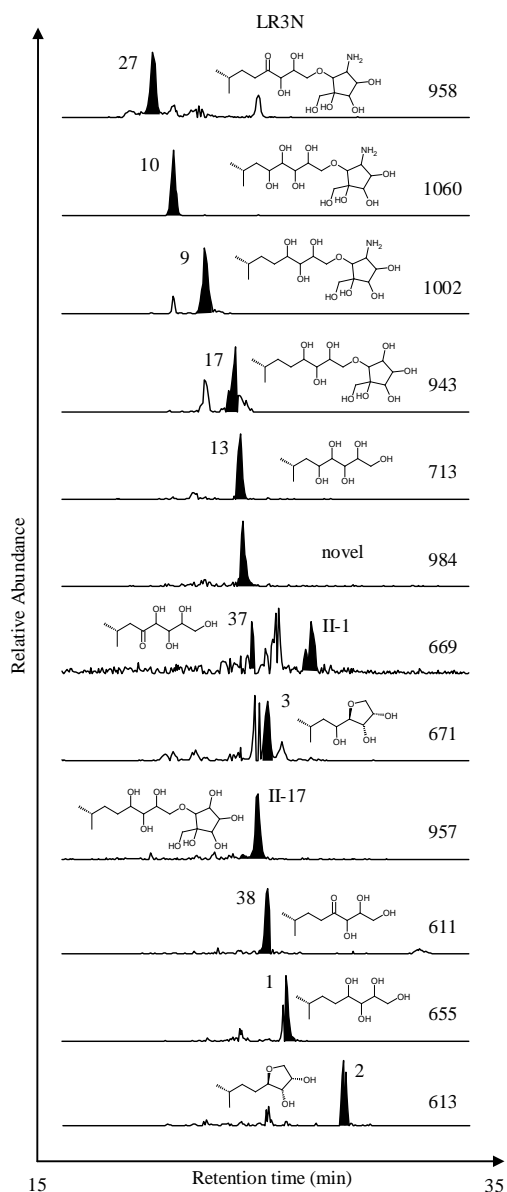


Figure 4.10 Partial mass chromatograms (15 – 35 min) showing BHP distributions observed in sample LR3N.

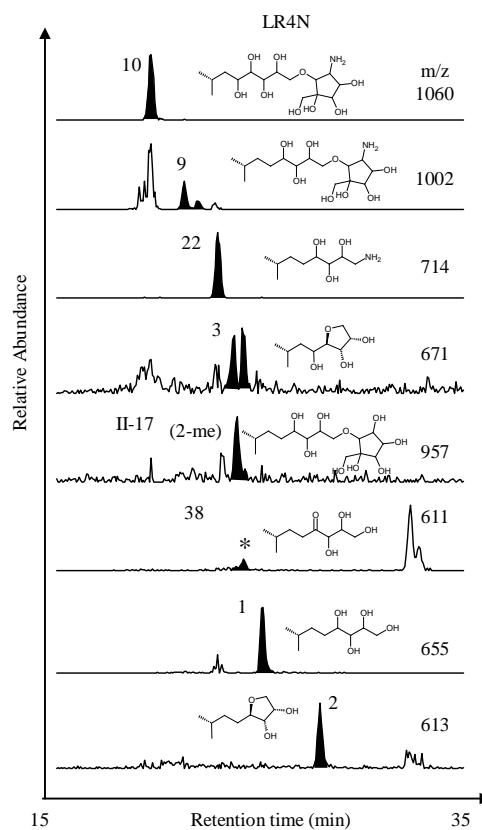


Figure 4.11 Partial mass chromatograms (15 – 35 min) showing BHP distributions observed in sample LR4N.

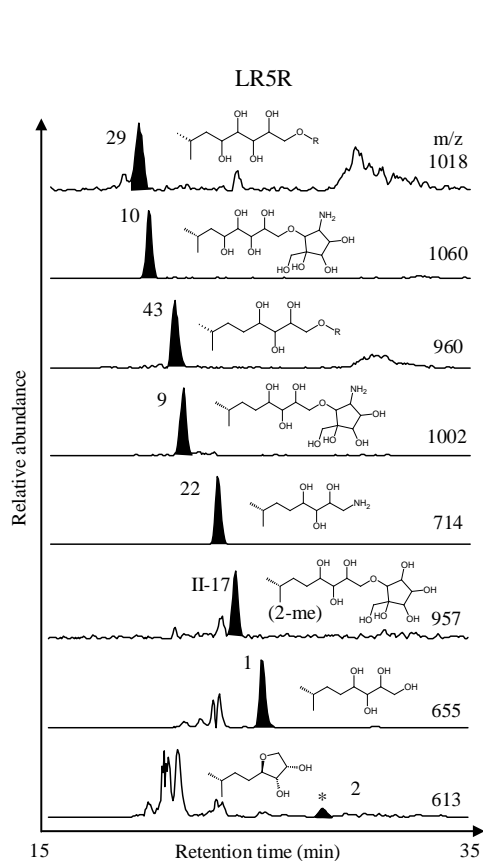


Figure 4.12 Partial mass chromatograms (15 – 35 min) showing BHP distributions observed in sample LR5R

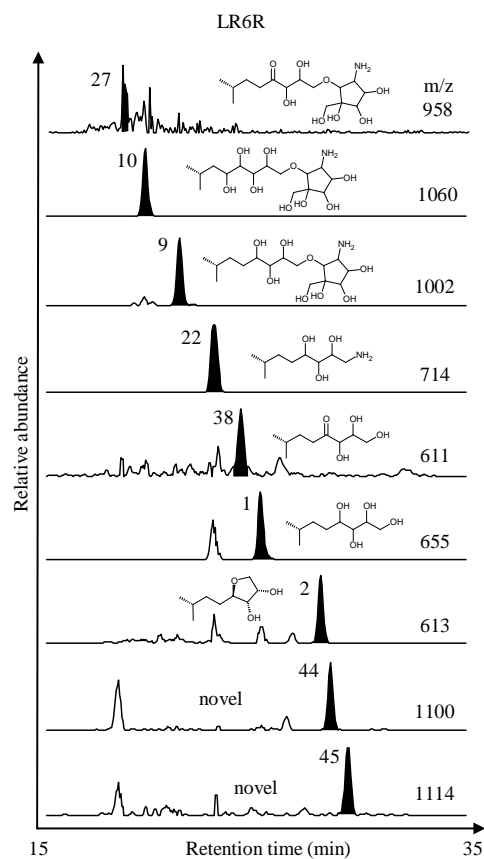


Figure 4.13 Partial mass chromatograms (15 – 35 min) showing BHP distributions observed in sample LR6R

#### 4.3.4 BHP DISTRIBUTIONS OF NON-ACTIVE SINTERS FROM OPAHEKE

##### POOL

The BHP-distributions of three inactive sinter samples taken from increasing distances from the pool ledge were analysed (OP4N, OP5N and OP6N).

##### 4.3.4.1 OP4N

The BHP distribution of a sample taken closest to the pool edge OP4N (Figure 4.14; Table 4.1) contained seven BHPs. The distribution consists of an early eluting isomer of anhydroBHP (18.44 min), BHP<sub>cyc</sub>, BHT<sub>cyc</sub>, BH<sub>pentol</sub>, aminotriol, BH<sub>tetrol</sub> and

anhydroBHT (**3**, **10**, **9**, **13**, **22**, **1**, **2**). AnhydroBHP (**2**) was the least abundant and aminotriol (**22**) was the most abundant BHP detected, with concentrations ranging from 3.47 to 30.59  $\mu\text{g}\cdot\text{g}^{-1}$  dry sinter (The overall abundance of BHPs in this sample was 79.21  $\mu\text{g}\cdot\text{g}^{-1}$  dry sinter (Figure 4.14; Table 4.1). AnhydroBHP (**2**) was detected as an early eluting isomer.

#### 4.3.4.2 OP5N

The BHP distribution of a sample taken around 50 cm from the pool ledge (OP5 Figure 4.15; Table 4.1). The distribution in this sample included a number of known BHPs that can be attributed to particular groups of organisms such as Type I methanotrophic bacteria and cyanobacteria. The distribution consists of twelve BHPs that been previously characterised. In this sample aminotriol (**22**) and BH*tetrol* (**1**) were significantly more abundant than all other BHPs detected and were present in abundances of 13.68 and 4.26  $\mu\text{g}\cdot\text{g}^{-1}$  dry sinter (Table 4.1). The remaining distribution of ten BHPs consisted of BHP*cyc*, aminopentol, 3-me aminopentol, BHT*cyc*, BH*pentol*, 2-me BH*pentol*, 2-me aminotriol, 2-me BH*tetrol* and anhydroBHT (**10**, **15**, **III-15**, **9**, **13**, **II-13**, **II-22**, **II-1**, **2**) and were present in amounts ranging from 0.06  $\mu\text{g}\cdot\text{g}^{-1}$  dry sinter for 2-me BH*tetrol* (**II-1**) to 0.47  $\mu\text{g}\cdot\text{g}^{-1}$  dry sinter (Table 4.1) for anhydroBHT (**2**). The overall abundance of BHPs in this sample was 19.08  $\mu\text{g}\cdot\text{g}^{-1}$  dry sinter (Table 4.1).

#### 4.3.4.3 OP6N

The sinter taken from around 4m from the pool edge (OP6N; Figure 4.16; Table 4.1) is assumed to be the oldest sample. Seven BHPs which have been previously characterised were identified during analysis of sample OP6N. The distribution of known BHP compounds consists of BHP*cyc*, BHT*cyc*, unsaturated aminotriol, BH*pentol*, aminotriol, anhydroBHP, BH*tetrol* and anhydroBHT (**10**,  $\Delta$ -**22**, **13**, **1**, **2**). BH*pentol* (**13**) was present in the lowest amount (0.38  $\mu\text{g}\cdot\text{g}^{-1}$  dry sinter; Table 4.1) and aminotriol (**22**) was the most abundant BHP

detected ( $65.18 \mu\text{g.g}^{-1}$  dry sinter; Table 4.1). Total abundances of BHPs in sample OP6 were  $88.46 \mu\text{g.g}^{-1}$  dry sinter (Table 4.1).

Aminotriol was the most abundant BHP detected in all three inactive sinters, with abundances ranging from  $13.68 \mu\text{g.g}^{-1}$  dry sinter in sample OP5N, to  $65.18 \mu\text{g.g}^{-1}$  dry sinter in sample OP6 (Table 4.1). Overall abundances ranged from  $19.08 \mu\text{g.g}^{-1}$  dry sinter in sample OP5 to  $88.45 \mu\text{g.g}^{-1}$  dry sinter in sample OP6N (Table 4.1).

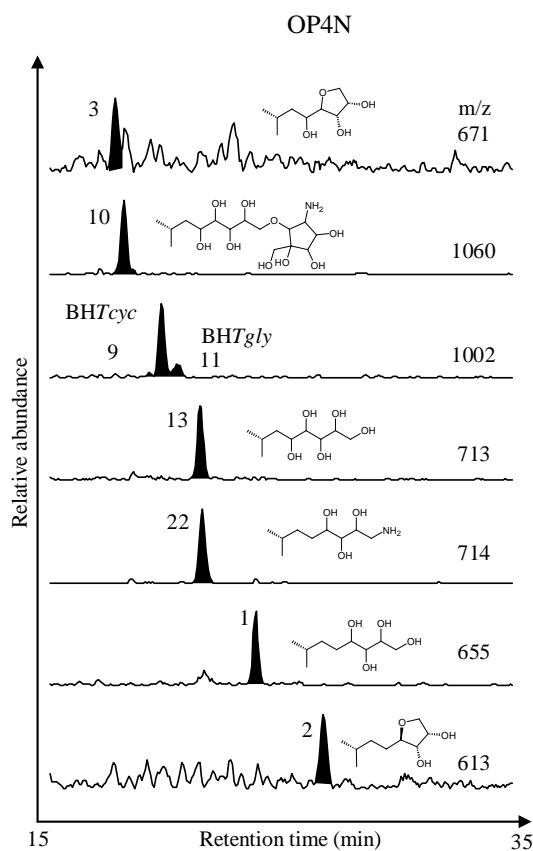


Figure 4.14 Partial mass chromatograms (15 – 35 min) showing BHP distributions of inactive sinter OP4N.

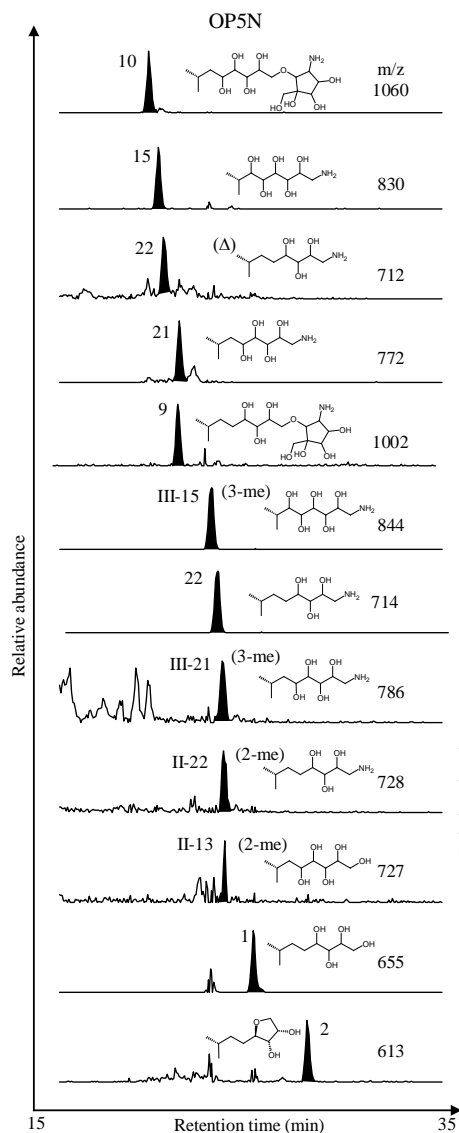


Figure 4.15 Partial mass chromatograms (15 - 35 min) of BHP distributions taken from inactive sinter from OP5.

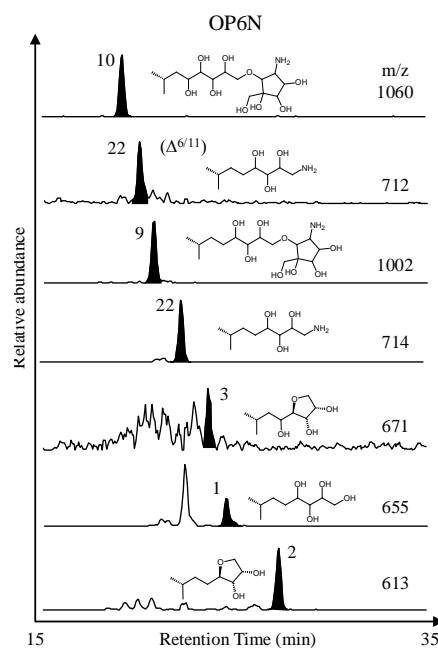


Figure 4.16 Partial mass chromatograms (15 - 35 min) of BHP-distributions of inactive sinter OP6.

#### 4.3.5 BHP DISTRIBUTIONS OF NON-ACTIVE SINTERS FROM ROTOKAWA

##### 4.3.5.1 RK2N

A total of sixteen BHP structures were detected in sample RK2N (Figure 4.17). The distribution consists of eleven BHPs with previously characterised structures and five compounds that have been tentatively assigned as novel BHPs during this study. The

distribution of known BHPs consists of *BHP<sub>cyc</sub>*, *BHT<sub>cyc</sub>*, guanidine-substituted *BHT<sub>cyc</sub>*, *BHPentol*, aminotriol, anhydroBHP, PE-BHT, 2-me PE-BHT, *BHtetrol* and anhydroBHT (**10**, **9**, **23**, **13**, **22**, **3**, **17**, **II-17**, **1**, **2**). 2-me PE-BHT (**II-17**) was the least abundant BHP and *BHP<sub>cyc</sub>* (**10**) was the most abundant BHP detected ranging from 0.26 to 14.47  $\mu\text{g}\cdot\text{g}^{-1}$  dry sinter (Table 4.1). The tentatively assigned novel BHPs includes oxo-*BHP<sub>cyc</sub>*, oxo-*BHT<sub>cyc</sub>*, guanidine-substituted *BHP<sub>cyc</sub>*, oxo-*BHtetrol* (**36**, **30**, **27**, **38**) and a compound with parent ion mass  $[\text{M}+\text{H}]^+ = m/z$  984 (**42**). Oxo-*BHP<sub>cyc</sub>* (**27**) is the least abundant and oxo-*BHT<sub>cyc</sub>* (**27**) is the most abundant compound, with abundances ranging from 0.07 to 2.64  $\mu\text{g}\cdot\text{g}^{-1}$  dry sinter (Table 4.1). In this particular sample *BHP<sub>cyc</sub>* and *BHT<sub>cyc</sub>* (**10**, **9**) are the most abundant compounds detected with abundances ranging from 8.7 to 14.47  $\mu\text{g}\cdot\text{g}^{-1}$  dry sinter (Table 4.1). Composite-BHPs, account for 71% of the total abundance of BHPs in this sample.

#### 4.3.5.2 RK3N

Eleven BHPs were detected in sample RK3N (Figure 4.18). The distribution consists of eight BHPs with previously characterised structures and three compounds that have been tentatively assigned as novel BHPs during this study. The known BHPs include *BHP<sub>cyc</sub>*, *BHT<sub>cyc</sub>*, *BHPentol*, aminotriol, 2-me PE-BHT, *BHtetrol*, 2-me *BHtetrol* and anhydroBHT (**10**, **9**, **13**, **22**, **II-17**, **1**, **II-1**, **2**). 2-me *BHtetrol* (**II-2**) was present in the lowest amount (0.04  $\mu\text{g}\cdot\text{g}^{-1}$  dry sinter) and *BHT<sub>cyc</sub>* (**9**) was the most abundant compound detected (2.63  $\mu\text{g}\cdot\text{g}^{-1}$  dry sinter; Table 4.1). The three tentatively assigned novel components are oxo-*BHT<sub>cyc</sub>*, oxo-*BHPentol*, oxo-*BHtetrol* (**27**, **37**, **38**) (Figure 4.18). The abundances of the tentatively assigned BHPs ranged from 0.12 for oxo-*BHPentol* (**37**) to 1.26  $\mu\text{g}\cdot\text{g}^{-1}$  dry sinter (Table 4.1) for oxo-*BHT<sub>cyc</sub>* (**27**).

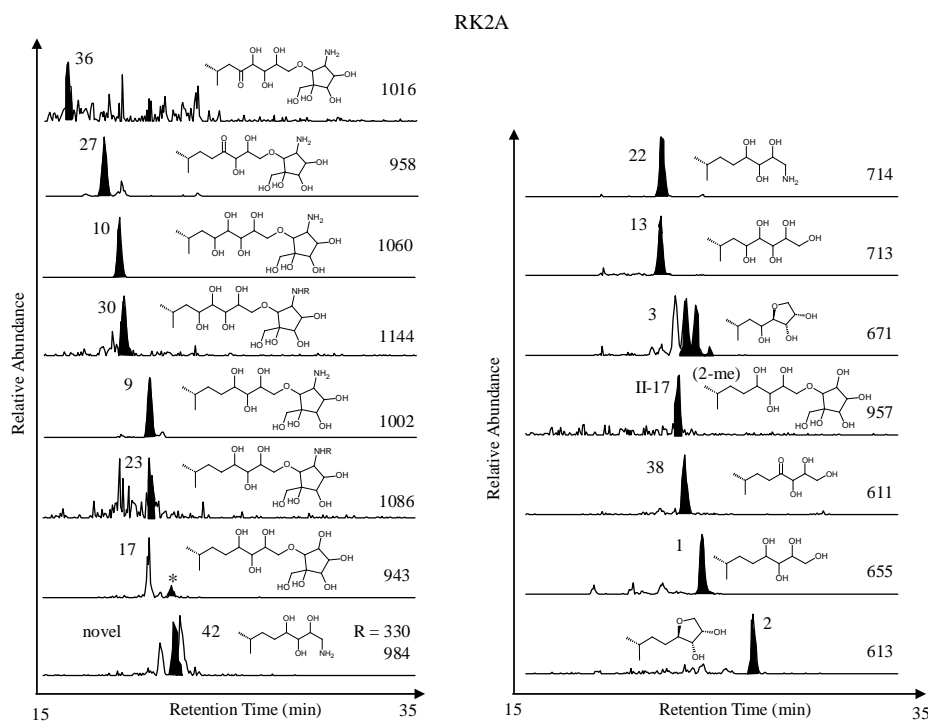


Figure 4.17 Partial mass chromatograms (15 – 35 min) showing BHP structures observed in sample RK2N. R group indicated in chromatograms of  $m/z$  1144 and 1086 refers to  $C(NH_2)NH$ .

BHPs in non-active sinters

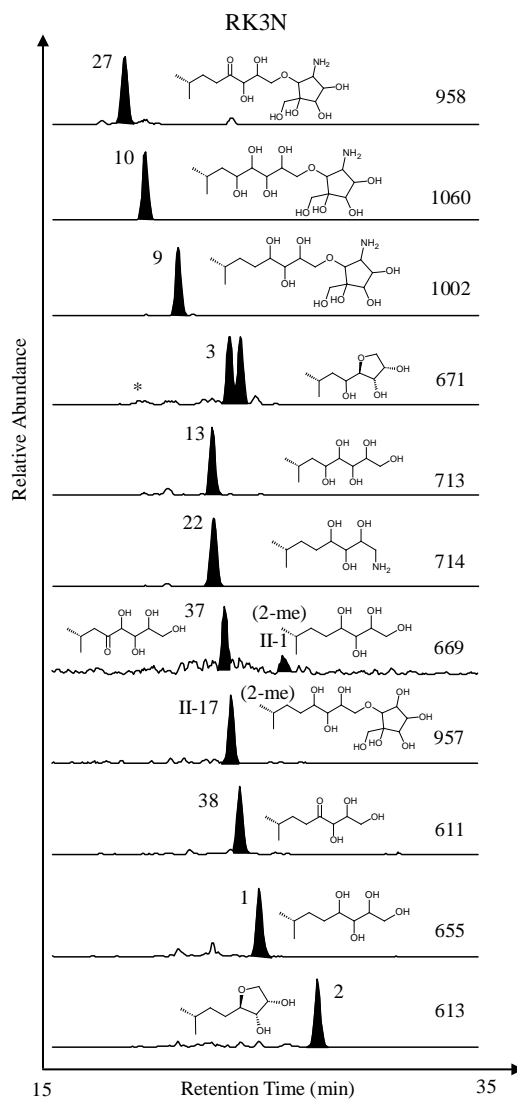


Figure 4.18 Partial mass chromatograms (15 – 35 min) showing BHP structures observed in sample RK3N (arrow indicates early eluting isomer).

## Chapter 4

Table 4.1 Abundances of BHPs identified in non-active sinters of TVZ.

BHP	Str <sup>b</sup>	Sample <sup>a</sup>																	
		CP3N	CP6N	CP7N	CP8N	CP11N	CP5N	OK4N	OK5N	OK6N	LR3N	LR4N	LR5R	LR6R	OP4N	OP5N	OP6N	RK2N	RK3N
BHH <sub>cyc</sub>	39	- <sup>c</sup>	-	-	-	-	-	0.29	0.05	-	-	-	-	-	-	-	-	-	-
BHP <sub>cyc</sub>	10	0.16	0.32	<b>0.54</b>	<b>3.3</b>	<b>6.1</b>	<b>67</b>	0.45	0.22	0.05	1.0	<b>15</b>	1.6	1.5	14	0.16	13	<b>14</b>	<b>2.7</b>
2-me BHP <sub>cyc</sub>	II-10	-	-	-	-	-	-	-	-	0.10	-	-	-	-	-	-	-	-	-
BHT <sub>cyc</sub>	9	<b>0.39</b>	0.73	0.54	4.2	4.2	56	0.08	0.11	0.08	<b>1.8</b>	5.4	-	1.2	-	0.11	-	8.7	2.6
2-me BHT <sub>cyc</sub>	II-9	-	-	-	-	-	-	-	-	0.03	-	-	-	-	-	-	-	-	-
Guanidine BHT	23	-	-	-	0.01	0.21	-	-	-	-	-	-	-	-	-	-	-	0.10	-
Aminotriol	22	0.14	<b>4.6</b>	-	0.38	1.9	29	<b>1.05</b>	<b>0.7</b>	<b>0.2</b>	-	0.67	<b>22</b>	<b>5.7</b>	<b>31</b>	<b>14</b>	<b>65</b>	3.8	0.83
2-me Aminotriol	II-22	-	-	-	-	-	-	-	-	-	-	-	-	-	-	0.17	-	-	-
Δ-Aminotriol	Δ-22	-	-	-	-	-	-	-	-	-	-	-	-	-	-	-	1.0	-	-
Aminotetrol	21	-	-	-	-	-	-	-	-	-	-	-	-	-	-	0.04	-	-	-
2-me Aminotetrol	II-21	-	-	-	-	-	-	-	-	-	-	-	-	-	-	0.05	-	-	-
3-me Aminotetrol	III-21	-	-	-	-	-	-	-	-	-	-	-	-	-	-	0.11	-	-	-
Aminopentol	15	-	-	-	-	-	-	-	-	-	-	-	-	-	-	0.15	-	-	-
3-me Aminopentol	III-15	-	-	-	-	-	-	-	-	-	-	-	-	-	-	0.05	-	-	-
Adenosylhopane	6	-	-	-	-	-	-	0.24	-	-	-	-	-	-	-	-	-	-	-
PE-BHT	17	-	-	-	-	-	-	-	-	-	1.2	-	-	-	-	-	-	0.75	-
2-me PE-BHT	II-17	-	-	-	-	-	-	-	-	-	0.34	-	0.19	-	-	-	-	0.26	0.38
BH <sub>pentol</sub>	13	0.09	-	0.20	1.2	1.5	-	-	-	-	-	-	-	16	0.40	0.38	2.1	1.0	
BH <sub>tetrol</sub>	1	0.19	0.27	0.06	0.29	2.1	7.4	0.47	0.12	0.09	0.5	0.83	2.6	1.4	12	4.3	7.2	2.0	0.67
2-me BH <sub>tetrol</sub>	II-1	-	-	-	-	-	-	-	-	-	-	-	-	-	-	0.06	-	-	0.04
AnhydroBHP	3	0.01	-	0.06	0.70	0.12	0.52	-	-	-	-	0.18	-	-	-	-	-	1.0	-
AnhydroBHT	2	0.02	0.33	0.09	-	0.26	1.4	-	-	-	1.0	0.13	2.3	0.11	3.5	0.47	4.1	0.86	0.97
<i>Novel Structures<sup>e</sup></i>																			
Guanidine-BHP	30	-	-	-	-	Tr <sup>d</sup>	-	-	-	-	-	0.16	-	-	-	-	-	0.16	-
Oxo-BHP <sub>cyc</sub>	36	-	-	-	0.02	0.06	-	-	-	-	0.02	-	-	-	-	-	-	0.07	-
Oxo-BHT <sub>cyc</sub>	27	Tr	0.10	0.10	0.53	0.22	3.0	-	-	-	0.60	0.18	0.17	0.25	-	-	-	2.6	1.3
Oxo-BHP <sub>pentol</sub>	37	Tr	-	-	0.03	0.06	-	-	-	-	-	-	-	-	-	-	-	-	0.12
Oxo-BHT <sub>tetrol</sub>	38	0.06	-	0.15	0.26	0.15	11	-	-	-	0.98	-	-	0.01	-	-	-	1.0	0.90
[M+H] <sup>+</sup> <sup>f</sup>																			
m/z 1018	29	-	-	-	0.02	-	18	-	-	-	-	0.14	0.06	-	-	-	-	-	-
m/z 960	43	-	0.09	-	-	-	-	-	-	-	-	-	0.81	-	-	-	-	-	-
m/z 1204	40	-	-	-	-	-	-	-	0.27	-	-	-	-	-	-	-	-	-	-
m/z 1146	41	-	-	-	-	-	-	0.14	-	-	-	-	-	-	-	-	-	-	-
m/z 984	42	-	-	-	-	-	-	-	-	-	0.27	-	-	-	-	-	-	0.73	-
m/z 1100	44	-	-	-	-	-	-	-	-	-	-	-	-	0.01	-	-	-	-	-
m/z 1114	45	-	-	-	-	-	-	-	-	-	-	-	-	0.01	-	-	-	-	-
Total BHP		1.06	6.44	1.74	10.94	16.88	193	2.29	1.20	0.55	7.71	22.69	29.7	10.19	76.5	20.07	90.69	38.16	11.55

<sup>a</sup>Samples: CP = Champagne Pool, LR = Loop Road, OK = Orakei Korako, RK = Rotokawa. <sup>b</sup>Structures. <sup>c</sup> – not detected. <sup>d</sup>trace amounts. <sup>e</sup>tentatively-assigned novel BHP structures, discussed in Chapter 5. <sup>f</sup>full structural identification not possible, see chapter 5 for discussion of spectra. Abundances given as  $\mu\text{g}\cdot\text{g}^{-1}$  dry material, bold text indicates most abundant BHP.

## 4.4 DISCUSSION

### 4.4.1 ORIGINS OF BHPs DETECTED IN NON-ACTIVE SINTERS

BHPs have been shown to be abundant throughout sinter facies and display complex distributions that vary between sample location. Many BHPs that have been detected, such as *BHP<sub>cyc</sub>*, *BHT<sub>cyc</sub>*, aminotriol and *BH<sub>tetrol</sub>* (**10**, **9**, **22**, **1**), are known to be produced by a wide-range of bacteria (e.g. Rohmer, 1993). Conversely, some BHPs have been detected and, as mentioned in Chapter 1, are known to exhibit a high degree of chemotaxonomic information and are specific to a group of organisms or appear to be produced in response to particular environmental conditions, such as guanidine-*BHT<sub>cyc</sub>*, aminopentol and 3-me aminopentol (**23**, **15**, **III-15**), and also 2-me *BH<sub>pentol</sub>* (**II-13**; See Table 1.1, Chapter 1). The variety observed in the BHP distributions of non-active sinters is reflective of the dynamic nature and ever-changing conditions at each site which affect microbial diversity and the biogeochemistry of the vents studied.

#### 4.4.1.1 CHAMPAGNE POOL (CP)

The BHP distributions observed in depositions from CP are unique compared to those observed from any other environmental situation (e.g. Talbot *et al.*, 2003c; Talbot and Farrimond, 2007; Coolen *et al.*, 2008; Cooke *et al.*, 2008b; Blumenberg *et al.*, 2009). The suite of well preserved, known and novel BHP compounds is reflective of environmental situations, bacterial populations and depositional settings that have received little attention in the past. BHP distributions are dominated by the presence of composite BHPs; *BHP<sub>cyc</sub>* (**10**) and *BHT<sub>cyc</sub>* (**9**) are the dominant compounds identified in each non active sinter with the exception of CP6N (Figure 4.2). For example, in samples CP8N and CP11N, composite BHPs account for >60% of BHPs observed in the sinter material (Figure 4.19). Previous reports

concerning BHP biosynthesis in *Alicyclobacillus acidocaldarius* (formally, *Bacillus acidocaldarius*) have shown an increase in the amount of composite BHPs when cultures were incubated at higher temperatures (e.g. Poralla *et al.*, 1984). Therefore, higher percentage abundance of composite BHPs in older sinters may indicate higher vent temperatures in the past (e.g. Kaur *et al.*, 2008; See also Section 4.4.3.1 for further discussion).

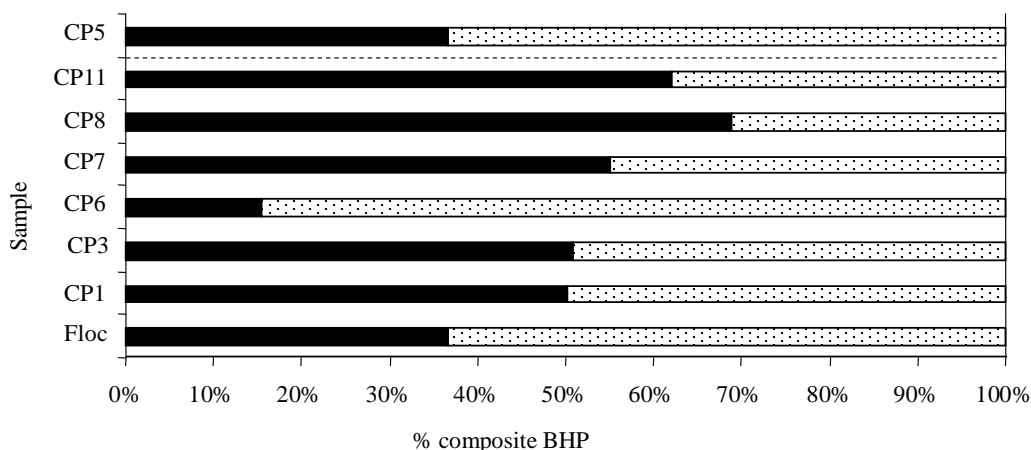


Figure 4.1 Percentage of BHP assemblage as BHPs containing C-35 ether linked composite functionality (shaded area) of total BHPs detected in CP study.

Aminotriol, BH*tetrol* and anhydroBHT (**22**, **1**, **2**) were also observed in each non-active sinter. BH*tetrol* and aminotriol, along with BHP*cyc* (**10**) and BHT*cyc* (**9**), are known to be produced by a wide-variety of BHP-producing bacteria and therefore cannot be assigned to any particular group of bacteria. They were also identified in sample CPf and may therefore derive from bacteria colonising the vent waters at CP. The production of anhydroBHT (**2**) via intramolecular cyclisation of BH*tetrol* has been reported by Schaeffer *et al.* (2008), and its presence in non-active sinter material likely derives from such a diagenetic processes mediated by the presence of acidic vent waters (pH 5.5 at the time of sampling; Mountain, Personal communication) or in the presence of metal ions (e.g. Bednarczyk *et al.*, 2005). Loss

of an adenine moiety from adenosylhopane has been proposed as a potential source; however, adenosylhopane (**6**) was not detected in sinters from CP.

AnhydroBHP (**3**) was also identified in all non-active sinter samples from CP with the exception of CP8N; this compound is thought to be produced via a similar pathway to anhydroBHT. BH*pentol* was identified in non active samples CP3N, CP7N, CP8N and CP11N (Figures 4.1, 4.3, 4.4 and 4.5). BH*pentol* (**13**) was first isolated from *Nostoc* sp. (Bisseret *et al.*, 1985) and is a good indicator of cyanobacterial populations, however, without the presence of a C-2 methylated homologue (e.g Summons *et al.*, 1999; Talbot *et al.*, 2008a) it is difficult to definitively conclude that cyanobacteria are present at this site as this BH*pentol* (**2**) could be formed via loss of C-35 composite functionality from BHP*cyc* (**10**). Acetic acid bacteria are also known to produce BHPs with a pentafunctionalised side-chain (Zundel and Rohmer, 1985b; Talbot *et al.*, 2007b and references therein). Other specific non-composite BHPs such as aminotetrol which is diagnostic for Type II methanotrophs (e.g. Neunlist and Rohmer, 1985c; Talbot *et al.*, 2001) and some sulphate-reducing bacteria of the genus *Desulfovibrio* (Blumenberg *et al.*, 2006), were not detected at CP.

A tentatively-assigned novel BHP, oxo-BHT*cyc* (**27**) was identified in each non-active sinter sample (Table 4.1). The origin of this novel compound is unclear, however, it is thought to derive from bacteria colonising oxygen-depleted zones (See Chapter 3, section 3. and Chapter 5, Section 5.3.2.3 for further discussion). A non-composite, tetra-functionalised homologue, oxo-BHT*tetrol* (**38**) was identified in each non-active sinter sample with the exception of sample CP6N. This compound could be produced during loss of the cyclitol ether (*cyc*) terminal group from oxo-BHT*cyc* (**27**). Other novel BHPs containing an ‘oxo’ functionality were also present in non-active sinters from CP, these comprise, oxo-BHP*cyc* (**36**; present in samples CP8 and CP11), oxo-BH*pentol* (**37**; present in samples CP3N, CP8N and CP11N).

The observation of a suite of novel compounds (See Chapter 5, Section 5.3.2) may demonstrate the utility of BHPs as biomarkers for uncharacterised bacterial populations and further suggests that BHP-producing bacteria are currently underestimated in natural settings. Samples CP8N (Figure 4.4) and CP11 (Figure 4.5) contained a tentatively assigned novel BHP, guanidine BHP<sub>cyc</sub> (**30**). This is a more functionalised homologue of guanidine BHT<sub>cyc</sub> (**23**) which is known to be produced by methylotrophic bacteria (e.g. Renoux and Rohmer, 1985; Knani *et al.*, 1994) and was also identified in samples CP8N and CP11N. The presence of a more functionalised counterpart of an already known BHP may represent a physiological response by which methylotrophic bacteria at CP adapt to the environmental conditions at CP, such as higher temperatures or acidic pH (e.g.. Joyeux *et al.*, 2004).

The BHP distribution of sample CP6N (Figure 4.2) appears to be different to the other samples from CP, a high concentration of aminotriol (**22**) is observed and accounts for 86% of the total BHP abundance (Figure 4.2; Table 4.1). The BHP distribution of Sample CP6N shows the greatest abundance of non-composite BHPs (>80 % of total BHP composition), this may indicate a periodic change in bacterial populations of the vent or air-water interface, or it may suggest that a bacterial population known to produce large amounts of aminotriol was particularly abundant in at the time of deposition of this sinter.

Sample CP5N was collected from the underside of an area of sinter terrace that has been raised by geological activity (Jones *et al.*, 2001; Lynne and Campbell, 2003; Mountain *et al.*, 2003). It is therefore likely that this particular sinter has accumulated organic material from other sources and, due to the sheltered location, was colonised by different groups of bacteria. This is reflected in the total abundances of BHPs in this particular sinter (125  $\mu\text{g}\cdot\text{g}^{-1}$  dry sinter) which is an order of magnitude higher than abundances observed in an actively precipitating sinter (e.g. Sample CP1: 7.0  $\mu\text{g}\cdot\text{g}^{-1}$  dry sinter; Chapter 3, Section 3.3.1).

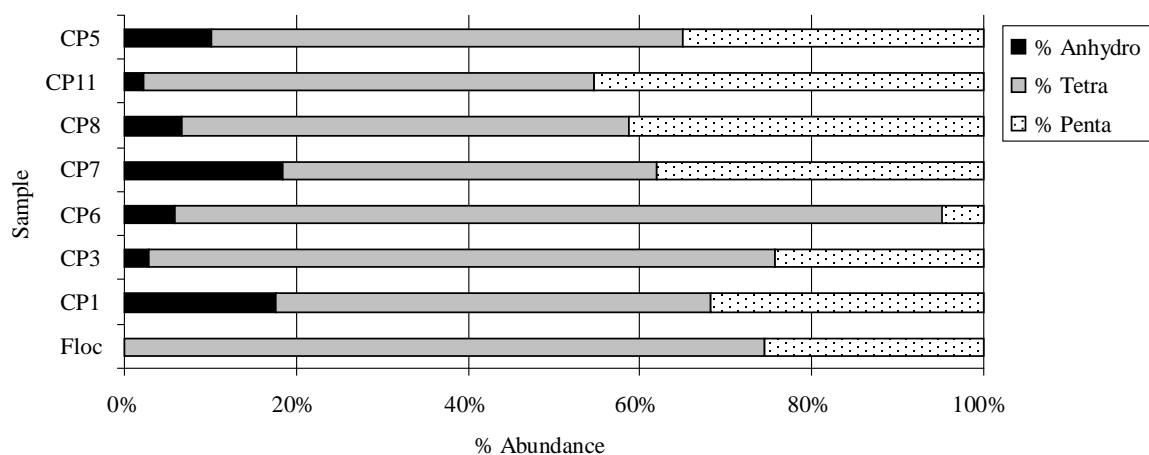


Figure 4.2 Composition of BHP assemblage detected in CP sinters. Includes BHP distribution of active sinters from Chapter 3.

#### 4.4.1.2 ORAKEI KORAKO GEOTHERMAL FIELD (OK)

The Orakei Korako geothermal field is situated in the midst of the Waikato forest, and the sinter terrace forms as outflow from vents situated above the Paeroa fault scarp traverse down the hillside to Lake Ohakuri. As is observable in Figure 4.21, the sinter terrace itself has in places vegetation cover. It is not surprising therefore that the BHP distribution of older sinters collected from the sinter terrace (samples OK4N and OK5N; Figure 4.9 and Figure 4.10) and an extinct geyser mound (sample OK6N; Figure 4.11) were overprinted by the presence of compounds usually detected in soil bacterial communities, such as adenosylhopane (**6**) and BHHcyc (**39**; Cooke *et al.*, 2008b). BHHcyc (**39**) was present in samples OK4N and OK5N whilst adenosylhopane (**6**) was present in sample OK4N. The source of the soil marker BHPs could be either the surrounding forest or a subterranean bacterial population. Adenosylhopane (**6**) has been previously detected in several purple non-sulphur bacteria including *Rhodopseudomonas palustris* (e.g. Neunlist and Rohmer, 1985b; Talbot *et al.*, 2007a) and it could be argued that a thermophilic relative of this organism could

be the source of this lipid. However co-occurrence of *BHHcyc* suggests that, on current knowledge at least, the source of these compounds lies outside the thermophilic milieu.

*BHPcyc*, *BHTcyc*, aminotriol and *BHtetrol* (**10**, **9**, **22**, **1**) were present in each non-active sinter (Table 4.1). AnhydroBHT or anhydroBHP (**2**, **3**), however, were not identified in non-active sinters from this site. Tentatively assigned novel ‘Oxo-BHPs’ such as those detected at LR, CP, RK and active sinter sample OK3A (Chapter 5, section 5.3.2) were also absent. However, two tentatively-assigned novel composite-BHP compounds with  $[M+H]^+ = m/z$  1204 and 1146 were identified in sample OK4N (Figure 4.9). BHP abundances are higher than those observed at FMP and range from 0.5 to 2.6  $\mu\text{g}\cdot\text{g}^{-1}$  dry sinter (Table 4.1).



*Figure 4.3 Sinter terrace and flat with vegetation protruding to the surface. In the background, the Paeroa fault (formed 131 AD) and the Waikato forest. In the foreground a small eruption crater.*

Different BHP-distributions from different depositional settings from OK appear to reflect different bacterial populations. It has been shown previously that microbial populations were

confined by temperature and depositional facie despite flow of water throughout the locations (Fouke *et al.*, 2003).

#### 4.4.1.3 LOOP ROAD HOT SPRINGS (LR)

Four inactive sinters were analysed which can be separated into two groups, non-active sinters from the sinter flat and two inactive sinters associated with a rhizolith sinter (defined above). Inactive sinter samples LR3N (Figure 4.10) and LR4N (Figure 4.11) from the sinter flat showed similar BHP-distributions. *BHP<sub>cyc</sub>*, *BHT<sub>cyc</sub>*, PE-BHT, oxo-BHT, anhydroBHP, *BH<sub>tetrol</sub>*, and anhydroBHT (**10, 9, 17, 27, 3, 1, 2**) were present in both samples. Composite BHPs, such as *BHP<sub>cyc</sub>*, *BHT<sub>cyc</sub>* and PE-BHT, were significantly more abundant (89%) than other non-composite BHPs (Table 4.1, See Section 4.2.2 for further discussion).

Sample LR3N showed the presence of a number of BHPs previously identified in cyanobacteria, PE-BHT, 2-me PE-BHT and *BH<sub>pentol</sub>* (**17, II-17, 1**; Talbot *et al.*, 2008a). Three of the novel oxo-BHPs were identified alongside a tentatively-assigned novel composite-BHP with  $[M+H]^+ = m/z$  984 (**42**).

Two further inactive sinters associated with a rhizolith deposition were analysed; one rhizolith with a silicified core (LR5R; Figure 4.12) and a sinter removed from the top of the rhizolith (LR6R; Figure 4.13). *BHP<sub>cyc</sub>*, *BHT<sub>cyc</sub>*, aminotriol, *BH<sub>tetrol</sub>* and anhydroBHT (**10, 9, 22, 1, 2**) were present in both samples. Tentatively assigned novel BHPs with  $[M+H]^+ = m/z$  1018 and 960 (**29, 43**; See Chapter 5) were present in LR5R along with 2-me *BHT<sub>cyp</sub>*. The sinter removed from the top of the rhizolith contained the aforementioned distribution plus, oxo-*BHT<sub>cyc</sub>*, oxo-*BH<sub>tetrol</sub>* (**27, 38**) and two further novel high molecular weight compounds with  $[M+H]^+ = m/z$  1100 and 1114 Da (**44, 45**; Chapter 5, section 5.4.3).

#### 4.4.1.4 OPAHEKE POOL (OP)

Three non-active sinters were collected from the sinter terrace at Opaheke Pool. BHP<sub>cyc</sub>, BHT<sub>cyc</sub>, aminotriol, BHT<sub>tetrol</sub> and anhydroBHT (**10**, **9**, **22**, **1**, **2**) were detected in each sample. The most complex assemblage at this site is sample OP5N (Figure 4.15), which contained a suite of highly source-specific BHP compounds (Figure 4.15). Aminotriol (**22**) was the most abundant BHP identified (14 µg.g<sup>-1</sup> dry sinter) and comprised around 70% of the total BHP abundance (Table 4.1). 2-me aminotriol (**II-22**) was also present along with 2-me BH<sub>pentol</sub> (**II-13**; Figure 4.15) suggesting the presence of cyanobacteria at this site, although other sources of 2-me aminotriol are now known (e.g. Rashby *et al.*, 2007). Other highly specific BHPs observed here such as aminopentol and 3-methyl aminopentol (**15**, **III-15**) have only been detected in Type I methane-oxidising bacteria (Bisseret *et al.*, 1985; Cvejic *et al.*, 2000a), but have also been detected in methanotrophs occupying the oxic-anoxic transition of the Black Sea (Blumenberg *et al.*, 2007).

The structural assignment of the additional methyl groups is based upon relative retention times with desmethyl and C-3 methylated counterparts (Figure 4.15) as observed in cultures of the type I methanotroph, *Methylococcus capsulatus* (Neunlist *et al.*, 1985; Summons and Jahnke, 1993). Aminotetrol and 3-me aminotetrol were also present (**21**, **III-21**; Figure 4.15). An unsaturated BHP with an m/z of 712 was detected in sample OP5N. Δ<sup>11</sup> unsaturated BHPs have previously been observed in thermophilic methanotrophs of the genus *Methylocaldum* (Cvejic *et al.*, 2000a), however, it is not possible to deduce the position of the unsaturation using the methodology applied here (Talbot *et al.*, 2007b).

Sample OP4N (Figure 4.14) contained a very early eluting isomer of anhydroBHP and also showed the presence of BHT<sub>gly</sub> and BH<sub>pentol</sub> which were not observed in samples

OP5N and OP6N. It is difficult to determine the origin of an early eluting isomer of anhydroBHP as such a large difference in retention time is observed (~19 mins as compared to ~23 mins). Variations in stereochemistry are not known to produce such large variations in retention time during liquid-chromatographic separation. The observed compound may be a fragment of a larger, currently unknown BHP.

#### 4.4.1.5 ROTOKAWA (RK)

The BHP distributions observed in inactive sinters of RK were found to be the most complex analysed during this study (Table 4.1; Figure 4.18). A suite of known and novel structures were detected and included the presence of cyanobacterial signatures, methylotrophic bacteria signatures and other structures that have also been detected at other geothermal sites, such as OK, LR and CP (Chapter 3).

The signatures from cyanobacterial sources at RK likely derive from endolithic species colonising pore spaces in the sinter formations where water temperature has cooled sufficiently to allow cyanobacterial colonisation (water temperature of vent, 85°C at the time of sampling). The observation of micro-stromatolites in the outflow channels of the RK vents provides further evidence of cyanobacterial colonisation at this site (e.g. Pancost *et al.*, 2006). Previous attempts to investigate the microbial assemblage at RK showed the presence of a low-diversity microbial assemblage (Stott, personal communication). The presence of novel oxo-BHPs at this site suggests a similar BHP-producing bacterial community to that colonising CP. The pH of the vent waters of RK have the lowest pH of all the sites investigated in this study (pH 2) and the increased diversity of BHPs at this site likely as consequence of the acidic pH.

#### 4.4.2 GENERAL TRENDS AND SIMILARITIES

Previous studies detailing the presence of BHPs and hopanoids in environmental settings have been confined to distributions that derive from soil bacteria or bacteria inhabiting non-thermophilic, aquatic settings. With the exception of the reports of Talbot *et al.* (2005) and Gibson *et al.* (2008) which form part of this study (Chapter 4), the high-temperature, low pH, mineral-enriched settings, such as those observed in vents from the TVZ have received little attention relative to other previously studied environmental settings. This is reflected in the rather unusual distribution of known and novel BHPs and hopanoids that have been detected at this site and throughout this study.

BHP<sub>cyc</sub>, BHT<sub>cyc</sub>, aminotriol, BHT<sub>tetrol</sub>, and anhydroBHT (10, 9, 22, 1, 2) are present in the majority of samples analysed and represent the five most commonly occurring compounds throughout the analysis of active (Chapter 3) and non-active silica sinters. However, BHP<sub>cyc</sub>, BHT<sub>cyc</sub>, aminotriol, and BHT<sub>tetrol</sub> are known to be produced by a wide-range of bacterial species (Talbot and Farrimond, 2007; Talbot *et al.*, 2008a and references therein) and anhydroBHT has been detected in a number of environmental settings (e.g. Talbot *et al.*, 2005; Bednarczyk *et al.*, 2005; Cooke *et al.*, 2008a). These five BHPs cannot be attributed to any particular group of organisms or processes. However, in this instance the high ratio of composite BHPs relative to non-composite BHPs is a new observation (Figure 4.22).

Particularly high percentage abundances of composite-BHPs have been detected in samples LR4 and RK2, where 92 % and 74% respectively of the compounds detected were composite BHPs. The elevated abundance of composite BHPs draws parallels with the work of Poralla *et al.* (1984), who demonstrated increased abundances of composite BHPs when incubation temperature was increased and pH decreased during studies based upon cultures of *Alicyclobacillus acidocaldarius*. *Zymomonas mobilis* is known to produce up to 49% of

the total hopanoids as composite BHPs (Hermans *et al.*, 1991). Similar distributions have been observed in sulphide-oxidising bacteria occupying subterranean caves (Albrecht and Freeman, personal communication).

Throughout the investigations of the BHP distributions of non-active sinters, the observed BHP distributions are dominated by tetra-, and penta-functionalised components (Figure 4.22) and known hexafunctionalised BHPs have only been identified in one sample (OP5N; Figure 4.15) previously reported by Gibson *et al.* (2008). Tetra-functionalised BHPs are known to be produced by a wide variety of bacterial groups (e.g. Rohmer *et al.*, 1984; Farrimond *et al.*, 1998). Pentafunctionalised BHPs are known to be produced by cyanobacteria (e.g. Summons *et al.*, 1999; Talbot *et al.*, 2008a), acetic acid bacteria in response to increasing temperatures (e.g. Joyeux *et al.*, 2004; Talbot *et al.*, 2007b and references therein) and sulphate-reducing bacteria belonging to the genus *Desulfovibrio* sp. (Blumenberg *et al.*, 2006). The observation of high abundances of pentafunctionalised BHPs contrasts with previous reports of the presence of BHPs in recent environments, either by analysis of intact-BHPs (Talbot *et al.*, 2003c; Talbot and Farrimond, 2007; Coolen *et al.*, 2008; Cooke *et al.*, 2008b; Blumenberg *et al.*, 2009) or by inference via PA/NaBH<sub>4</sub> methodology (e.g. Innes, 1998; Farrimond *et al.*, 2000). This may indicate that BHPs observed in non-active sinters derive mainly from cyanobacterial sources (See Section 4.4.2.1) with a minor contribution from methanotrophs in certain cases (sample OP5N; Figure 4.15). This is in contrast to other previously studied environmental settings where sediments from lacustrine settings showed a predominance of data indicating input from Type I methanotrophic organisms utilising methane produced by anaerobic methanogens in anoxic sediments (Farrimond *et al.*, 2000; Talbot *et al.*, 2003c; Blumenberg *et al.*, 2007). In marine settings, high abundances of tetra-functionalised BHPs have previously been observed (Farrimond *et al.*, 2000). The distributions of BHPs from silica sinters show a

distinct trend towards the tetra- and penta-functionalised apex of the ternary diagram shown in Figure 4.22, indicating that photosynthetic bacteria may be providing fixed carbon and possibly nitrogen to the microbial community at the vents in question.

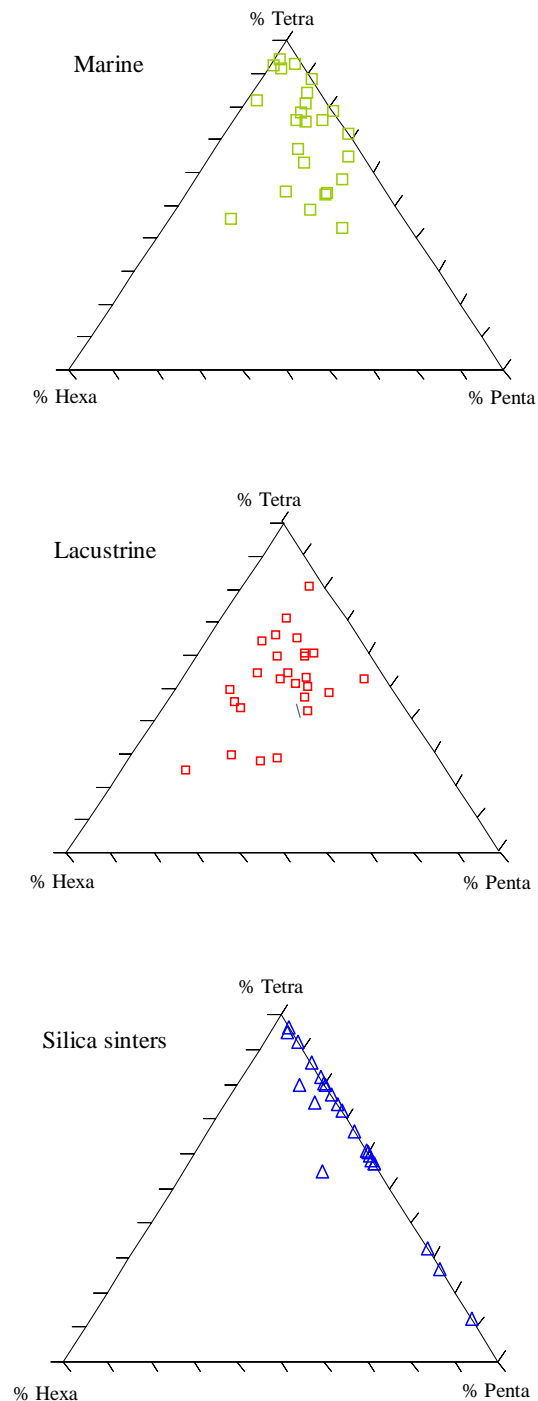


Figure 4.4 Relative distribution of Tetra-, Penta-, and hexafunctionalised BHPs from certain environmental conditions. Top – marine sediments, middle – lacustrine sediments, lower – silica sinters. Data on marine and Lacustrine settings adapted from Watson, 2002.

#### 4.4.2.1 BHP-SIGNATURES OF CYANOBACTERIA

The detection of cyanobacterial BHP-signatures, such as BH*pentol*, 2-me BH*pentol*, PE BHT and 2-me PE BHT (**13**, **II-13**, **17**, **II-17**) is a common theme throughout this study (See also Section 3.4.4.1, Chapter 3) and at first their presence in sinters from CP (see Section 4.4.1.1), LR (samples LR3N, LR4N and LR5R), OP (sample OP5N) and RK (sample RK2N) seems to be an erroneous observation. LR and RK have been described as 'barren' to obvious photosynthetic microbes (Mountain, *Pers. comm.*), and the water temperature at OP (98°C) render this site as inhospitable to cyanobacteria. The cyanobacterial BHP-distributions of non-active sinters from LR (Sample LR, OP (sample OP5N) and RK (sample RK2N) therefore likely derive from endolithic or cryptoendolithic cyanobacterial species. Colonisation of pore-spaces of sinter material or incorporation into the silica matrix provides a temporary refuge that excludes many detrimental environmental conditions such as acidity or out-gassing of H<sub>2</sub>S from the vent source. It could also be suggested that the cyanobacterial BHP-signatures may derive from an allochthonous source; however, the detection of similar BHP distributions in sinters from ETGF (Chapter 3, Table 3.1; Figure 3.8 and Figure 3.9) demonstrates the ability of known endolithic cyanobacterial populations ( e.g. Phoenix *et al.*, 2006) to biosynthesise specific BHPs.

#### 4.4.2.2 DISTRIBUTION OF BHPs OVER SPATIAL AND TEMPORAL SCALES

The active and non-active samples from CP were collected from an increasing distance from the pool edge. As sinter formation results in contraction of the pool surface, this provides a putative time sequence which includes sinters deposited at around the time of formation of the vent and actively-precipitating sinters from the air-water interface. CP formed around 900 years ago (Mountain *et al.*, 2003) and investigations concerning the distribution of microbial lipids have demonstrated the potential of preserved organic matter

to document changing microbial populations over time (Kaur *et al.*, 2008). Comparison of active depositional facies from Chapter 3 (sample CPf and CP1A) with the distributions identified in non-active sinters presented in this chapter (section 4.3.1 to 4.3.6) shows a similar trend to that observed by Kaur *et al.* (2008). An overall decrease in the abundance of BHPs is observed over the course of the sample suite, however, an increase in the complexity of the BHP distribution is also observed as sinter age increases. The origin of this relationship requires much thought as the trend may be indicating that BHP-producing bacterial populations at this site were more diverse in the past. However, BHP production in particular bacteria has been shown to be influenced by changing environmental temperatures. Since higher temperatures have been proposed in the past (Kaur *et al.*, 2008) at CP, the trend may also indicate a physiological response to a decrease in temperature (e.g. Joyeux *et al.*, 2004). This raises two questions: Are changing BHP distributions reflective of changing BHP-producing bacterial communities which may be induced by a decrease in temperature over time? Alternatively, are BHP-producing bacterial communities remaining static in which case, are changing BHP distribution reflecting a physiological response to changing environmental conditions?

A decrease in BHP abundance is observed from the oldest to the youngest sinters (samples CP11 to CP3), the exception to this trend is sample CP6 (Figure 3.34), from which high abundances of tetra-functionalised BHPs, in particular high amounts of aminotriol (**22**) which account for 84% of the total BHP abundance. This suggests that the BHP distribution of this sinter sample may have been influenced by some other processes that resulted in this particular sinter forming at a time where a bacterial colony that produced large amounts of aminotriol was colonising the vent water or sinter formation zones. Abundances of BHPs increase in samples CP1A and CPf and this is likely reflective of input from living bacterial communities in each particular setting.

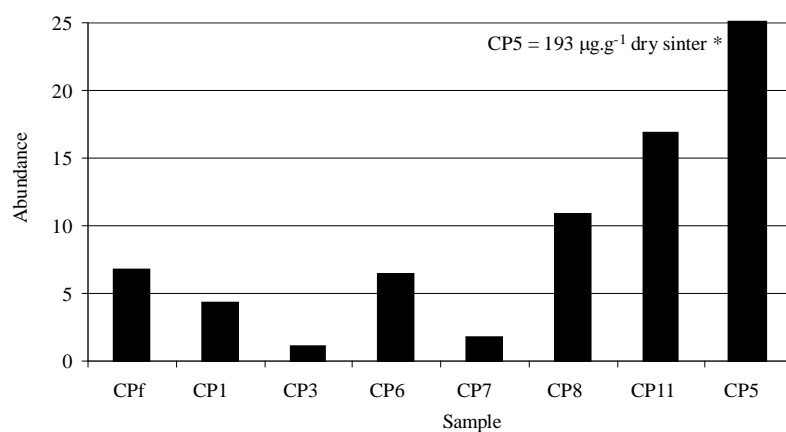


Figure 4.5 Total abundance of BHPs in silica sinters of Champagne Pool.

The decrease in abundance of organic matter has previously been attributed to changes in physical parameters of the pool (Kaur *et al.*, 2008). In particular, a higher temperature, consistent with a thermal eruption, has been invoked as a possible reason for higher temperatures in the past. CP is thought to harbour a low diversity microbial assemblage (Jones *et al.*, 2001; Ellis *et al.*, 2005) and changes in BHP distribution indicate a more diverse bacterial population in the past. It is also worthwhile to consider that the temperature may not be the only limiting factor affecting microbial colonisation as the relatively large size of Champagne pool and long-residence time of pool water (Hetzer *et al.*, 2007), may lead to a lack of metabolic substrate and an accumulation of toxic sulfidic species such as orpiment ( $As_2S_3$ ), stibnite ( $Sb_2S_3$ ), carlinite ( $Tl_2S$ ) and methyl and hydride homologues such as  $AsH_3$ ,  $CH_3AsH_2$ ,  $(CH_3)_2AsH$  (Hirner *et al.*, 1998) may also be driving any changes in microbial assemblages.

#### 4.4.2.3 DISTRIBUTIONS OF BHPs IN ACTIVE VS NON-ACTIVE SINTERS

It appears that within a sample site, non-active sinters contain a greater abundance of BHPs than actively-precipitating counterparts. Previously, a greater abundance of organic material from CP has been attributed to a changing microbial population driven by a decrease in temperature consistent with geothermal eruption leading to formation of the

pool. However, the transient nature of geothermal environments, driven by non-uniform heat source, biotic and abiotic changes in water chemistry, hydrological and geological changes suggest that changes in microbial population can be driven by a large number of factors. It is unclear therefore if the variation in BHP distributions are reflective of changing bacterial populations or contain an overprint by a physiological response to changing conditions at the pool

A more diverse BHP assemblage is observed in non-active vents from CP, LR, OK and OP. This could be due to bacteria colonising pore-spaces or remaining viable after incorporation into the silica matrix. Colonising the pore spaces in sinter material may provide relief from the strongly sulphidic vent outgassing and also can provide a means of trapping certain nutrients (e.g. Phoenix and Konhauser, 2008). Diffuse flow of nutrients (CH<sub>4</sub>, NH<sub>4</sub>) through sinter material may provide the necessary nutrients that allow the growth of a diverse range of bacterial species and may provide an explanation for the increased diversity of BHP structures observed in older sinter material. However, BHP distributions of older sinter material show that recognisable chemical functionalities are retained upon deposition and incorporation in the silica matrix.

The preservation of microbial lipids in silica sinters has been previously reported (e.g. Pancost *et al.*, 2005, 2006; Talbot *et al.*, 2006; Kaur *et al.*, 2008; Gibson *et al.*, 2008), however, incorporation into the silica matrix is likely to be an oversimplification as this does not account for silification of biomass in non-actively precipitating sinters. Therefore it may be worthwhile to consider the inhibitory effect of dissolved mineral and metal content on autolytic enzymes (e.g. Ferris *et al.*, 1988). Autolytic enzymes rapidly decompose cellular components upon cell death and inhibition of this 'self-destruct' mechanism may result in the deposition of complex BHP distributions.

#### 4.4.2.4 NOVEL BACTERIOHOPANEPOLYOLS

One striking observation of the BHP-distributions that derive from bacteria colonising terrestrial vents is the frequent occurrence of novel BHPs and although many of the compounds remain to be fully characterised (See Chapter 5, Section 5.36) they go some way to signifying the observed BHP-distribution as indigenous.

The structures of five novel BHPs have been tentatively assigned throughout this study and are reported in Chapter 5, guanidine-substituted BHP<sub>cyc</sub> (Section 5.3.1), oxo-BHP<sub>cyc</sub> (Section 5.3.2), oxo-BHT<sub>cyc</sub> (Section 5.3.3), oxo-BHP<sub>pentol</sub> (Section 5.3.4) and oxo-BHT<sub>tetrol</sub> (5.3.5). BHP-compounds containing a ketone functionality appear to be common throughout sinter-depositions. Other compounds with parent ions of  $[M+H]^+ = m/z$  1018 and 960 (Chapter 3, Section 3.2.2.4 and Section 3.2.2.5) have also been detected throughout analysis of BHPs distributions of LR, OP and RK. Structural assignment and further discussion of these compounds can be found in Chapter 5.

#### 4.5 CONCLUSIONS

The BHP distributions contained within non-active silica sinters have been shown to be composed of complex and unique BHP-signatures. Known BHP compounds have been detected that indicate the presence of cyanobacteria, Type I methanotrophic bacteria and methylotrophic bacteria in sinter material. The presence of novel BHPs indicates that uncharacterised BHP-producing bacterial species are widespread in this environmental setting and elaborates upon the environmental distribution of bacterial species contributing the sedimentary record. Investigation of older sinter material dating back to the origin of pool formation (e.g Kaur *et al.*, 2008) demonstrates that preservation of BHPs is sufficient to detail the changing bacterial populations and physico-chemical conditions of the pool over time. However, the efficacy of this class of compounds as biomarkers can be limited by

a lack of knowledge regarding precursor biota and the distributions reported here will benefit from future work concerning the ability of extremophilic bacteria to produce BHPs. The BHPs preserved in sinter material retain chemical functionalities that should provide a detailed inventory of bacterial species colonising any geothermal vent.

## 5 NOVEL BHPs: NEW BIOMARKERS FOR BIOGEOCHEMISTRY AND INSIGHTS INTO THE EXTENT OF BHP-PRODUCING BACTERIA

### 5.1 INTRODUCTION

The utilisation of intact polar lipids, including BHPs, has improved our understanding of the microbial ecology and biogeochemistry of modern environments (e.g. Hinrichs *et al.*, 1999; Zink *et al.*, 2003; Sturt *et al.*, 2004; Blumenberg *et al.*, 2004; Ortcutt *et al.*, 2005; Biddle *et al.*, 2006; Talbot and Farrimond, 2007; Talbot *et al.*, 2008a; Rossel *et al.*, 2008; van Mooy *et al.*, 2009). BHPs represent a class of intact polar lipid that are produced by certain types of bacteria, and sufficient evidence exists to support the use of BHPs as biomarkers for certain groups of bacteria (e.g. cyanobacteria, aerobic methanotrophs and methylotrophs) inhabiting any particular environmental niche. Expanding our knowledge by investigating BHP distributions over a range of environmental conditions will improve our understanding regarding the ecology of BHP-producing bacteria and the biogeochemistry of the environments they inhabit. The work in this thesis represents the first detailed investigation of BHPs in depositional environments of terrestrial geothermal vents. It also shows the use of BHPs as biomarkers for bacteria colonising extreme environmental conditions and bacterially mediated processes occurring therein.

Silica sinters and microbial mats have been shown to be a rich a source of novel and unusual BHP compounds (Chapter 3 and Chapter 4; Zhang *et al.*, 2007). In some cases it has been possible to assign structural characteristics to these by comparison to the MS<sup>2</sup> spectra of structurally similar compounds i.e. compounds of similar mass or where particular chemical functionalities are known. Proposed novel structures are discussed below. However, by observing particular fragmentations it is clear that many of these compounds belong to the BHP-

family but which as yet cannot be fully determined without further structural qualification, e.g.  $^1\text{H}$  or  $^{13}\text{C}$  NMR.

Repeated occurrence of a particular compound or group of compounds during this study merits further discussion and the  $\text{MS}^2$  and  $\text{MS}^3$  spectra of the compounds in question have been included in the following sections. In certain cases it has been possible to tentatively assign a novel BHP structure in full. In other cases, a BHP compound has been identified via  $\text{MS}^2$  fragmentations but the full structure of the chemical functionality proposed as a C-35 ether linked ‘terminal group’ (TG from herein) remains to be determined (see below).

Cleavage of the  $\text{C}_{35}\text{-(O-TG)}$  ether bond in composite BHPs can produce a number of fragments. Charge retention on the pentacyclic component allows determination of the degree of functionalisation, i.e. a tetra-, penta- or hexafunctionalised BHP (e.g. Talbot *et al.*, 2003a, b). This also produces a neutral fragment (TGOH) which is not detected and effectively ‘lost’. Charge retention on the C-35 ether linked functionality results in an ion corresponding to  $[\text{TG}(\text{OH}_2)]^+$ . Alternatively the ether bond can be cleaved between the terminal group and the ether oxygen which produces the  $[\text{TG}]^+$  fragment. Although the full terminal group is everything attached to C-35 and therefore should be represented as  $[\text{TGO}]$ , it is simpler to describe the compounds presented here in terms of the neutral loss fragment, TGOH, as this provides an easier method of identifying and comparing with  $[\text{TG}(\text{OH})_2]^+$  ions on the  $\text{MS}^n$  spectra. The TGOH fragment is actually a product of ionisation.

## 5.2 AIMS

The aims of this chapter are as follows;

- Describe a new group of BHPs, termed ‘oxo-BHPs’ that have been identified during investigations of the BHP distributions preserved within silica sinters including discussion of the environmental distribution and likely origins of this class of BHP
- Report other tentatively-assigned BHPs that occur in several silica sinter samples or that form part of a homologous series of BHPs
- Discuss the bio- and geochemical implications associated with finding significant structural diversity of BHP compounds within an environmental setting that has received little attention in the past

## 5.3 STRUCTURAL ASSIGNMENT OF NOVEL BHPs BASED UPON INTERPRETATION OF APCI MS<sup>2</sup> SPECTRA

Five novel compounds, the structure of which have been fully assigned are presented first. These compounds form a more functionalised homologue of an already known compound (Section 5.3.1) or contain readily identifiable functional groups (Section 5.3.2). Interpretation of spectra from novel composite-BHPs can be found in Section 5.3.3

### 5.3.1 GUANIDINE-SUBSTITUTED CYCLITOL ETHER BHPs

Guanidine-BHT (**23**) contains a C-35 ether linked cyclitol ether where the 1' amine group is linked to a guanidine moiety. Compounds that match the acetylated mass and retention time have been identified in sinter samples LR3A (Chapter 3, Figure 3.6), CP8N, CP11N and RK2N (Chapter 4; Figure 4.4, Figure 4.5 and Figure 4.17). Ions indicating the presence of a guanidine substituted terminal group i.e.  $m/z$  414 (TG) and 432 ([TGOH<sub>2</sub>]<sup>+</sup>) were not observed

in the MS<sup>2</sup> spectra reported by Talbot *et al.* (2007a). However, analysis of silica sinters showed the presence of two compounds that produce MS<sup>2</sup> spectra with ions at m/z 414 and 432 (Figure 5.1). These compounds have been identified as peracetylated guanidine-BHT and a tentatively assigned peracetylated guanidine-BHP with [M+H]<sup>+</sup> = m/z 1144. The presence of ions indicating the presence of guanidine substituted terminal groups is assumed to be the result of different stereochemistry to that reported in Talbot *et al.* (2007a).

The MS<sup>2</sup> spectra (Figure 5.1) of a novel compound with parent ion [M+H]<sup>+</sup> = m/z 1144 shows multiple losses of CH<sub>3</sub>COOH (displayed as AcOH on the structure within Figure 5.2; neutral ion loss of 60 Da) from [M+H]<sup>+</sup>, i.e. m/z 1084, 1024, 964 and 904. Loss of penta-acetylated guanidine-substituted cyclitol ether moiety (terminal group ion [TG] with neutral fragment loss of 432 Da) from C-35 is observed by presence of an ion at m/z 713, a characteristic fragment of pentafunctionalised BHPs (Talbot *et al.*, 2003a; Talbot *et al.*, 2007a). Multiple losses of CH<sub>3</sub>COOH from [M+H – TG]<sup>+</sup> = m/z 713, i.e. m/z 653 and 473 which relate to neutral loss of 1 or 4 CH<sub>3</sub>COOH respectively are observed (Figure 5.1). Ions indicating losses of 2 and 3 CH<sub>3</sub>COOH from [M+H – TG]<sup>+</sup> = m/z 713, i.e. m/z 593 and 533 were not observed. Loss of guanidine-substitution from the amine functionality on the terminal sugar, i.e. HCNH(NHAc) results in a mass loss of 86 Da and is observable by the presence of ions m/z 1060, commonly identified as the parent ion of the MS<sup>2</sup> spectra for BHP<sub>cyc</sub> (**10**; Talbot *et al.*, 2003a; 2007a). Ions which are usually observed for BHT<sub>cyc</sub> (**9**) and BHP<sub>cyc</sub> (**10**), i.e. m/z 348 and 330, are present as minor ions in the spectrum and provide further evidence of an ether-linked C-35 cyclitol moiety (Figure 5.1). Relative retention times of guanidine-BHT and guanidine-BHP with BHT<sub>cyc</sub> (**9**) and BHP<sub>cyc</sub> (**10**) (Figure 5.3) and are in good agreement with retention times reported by Talbot *et al.* (2007a).

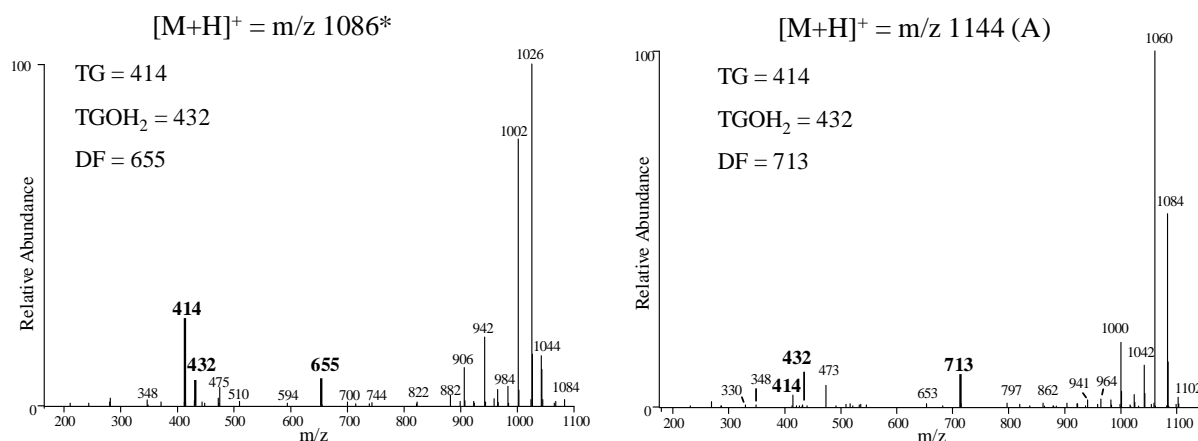


Figure 5.1 MS<sup>2</sup> Spectrum of  $[M+H]^+ = m/z 1086$  (left) and  $m/z 1144$  (right). TG = terminal group, TGOH<sub>2</sub> = terminal group plus ether linkage, DF = diagnostic fragmentation that allows identification of the degree of functionalisation contained within the side-chain component of the BHP. \* Original structural characterisation by Renouox and Rohmer, 1985. (A) 35-O- $\beta$ -guanidine-substituted cyclitol bacteriohopane-31,32,33,34,35-ol

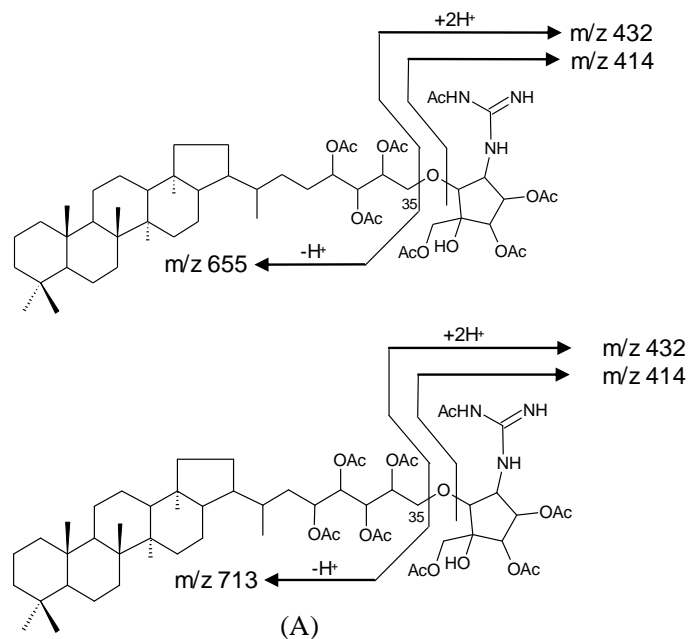


Figure 5.2 Peracetylated structures of Guanidine-BHT (top) and Guanidine-BHP (bottom). Arrows indicate fragmentation pathways that allow identification of these compounds during APCI-MS<sup>n</sup> analysis. (A) 35-O- $\beta$ -Guanidine-substituted cyclitol bacteriohopane-31,32,33,34,35-ol.

## Novel BHPs

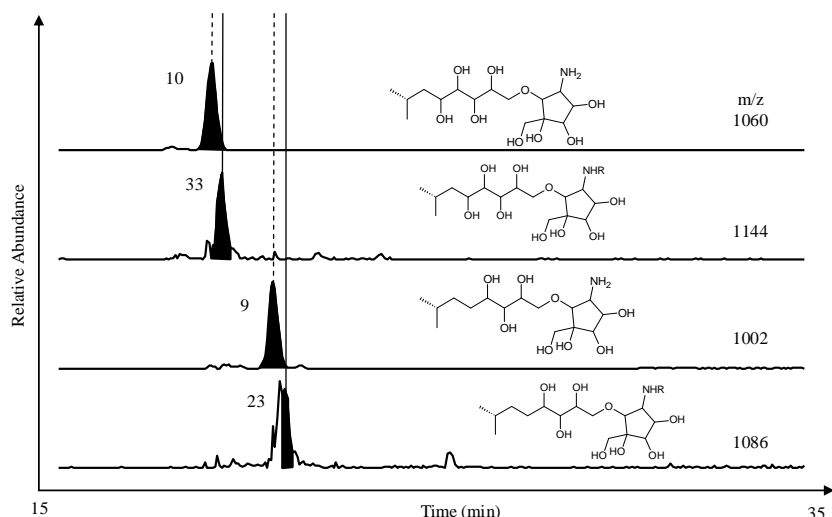


Figure 5.3 Partial mass chromatograms (15 – 35 min) showing retention time of guanidine-substituted BHTcyc and guanidine-substituted BHPcyc relative to retention times of BHTcyc and BHPcyc. R group on structure for  $[M+H]^+ = m/z$  1144 and 1086 = CNH(NH).

Table 5.1 Assignment of ions for guanidine-substituted BHPs

Ion/compound <sup>a</sup>	Guanidine BHT	Guanidine BHP
$[M+H]^+$	1086 <sup>b</sup>	1144 <sup>b</sup>
$[M+H - \text{AcOH}]^+$	1026	1084
$[M+H - 2\text{AcOH}]^+$	966	1024
$[M+H - 3\text{AcOH}]^+$	906	964
$[M+H - 4\text{AcOH}]^+$	- <sup>c</sup>	904 <sup>d</sup>
$[M+H]^+ - (\text{TG})$	655	713
$[M+H]^+ - (\text{TG} + \text{AcOH})$	595	653
$[M+H]^+ - (\text{TG} + 2\text{AcOH})$	535 <sup>d</sup>	593 <sup>d</sup>
$[M+H]^+ - (\text{TG} + 3\text{AcOH})$	475	533 <sup>d</sup>
$[M+H]^+ - (\text{TG} + 4\text{AcOH})$	- <sup>c</sup>	473
TG	414	414
TG(OH <sub>2</sub> )	432	432
TG(OH <sub>2</sub> ) – HCNH(NHAc)	348	348
TG – HCNH(NHAc)	330 <sup>d</sup>	330

<sup>a</sup>Compounds: Guanidine BHT (23) is Guanidine-substituted Bacteriohopanetetrol cyclitol ether (Renoux and Rohmer, 1985). Guanidine-BHP (30) is guanidine-substituted bacteriohopanepentol cyclitol ether, tentatively assigned during this study. <sup>b</sup>base peak or precursor ion for MS<sup>2</sup> spectrum. <sup>c</sup>not applicable. <sup>d</sup>ion not observed on MS<sup>2</sup> spectrum AcOH = CH<sub>3</sub>COOH, TG = C<sub>35</sub> ether-linked terminal group

### 5.3.2 'OXO'-BHPs

Oxo-BHTgly (**24**; Figure 5.26) was originally isolated from *Zymomonas mobilis* (Flesch and Rohmer, 1989). Original structural characterisation identified the presence of a ketone functionality at C-32 and a ether-linked composite functionality at C-35. Compounds identified throughout the analysis of BHP distribution of sinters from TVZ show a compound with the same peracetylated protonated molecule mass as that reported by Flesch and Rohmer (1989) i.e.  $[M+H]^+ = m/z$  958. BHPs that contain carbonyl oxygen (C=O) functionalities can be identified in  $MS^n$  spectra via neutral loss of 18 Da, which corresponds to cleavage of the C=O bond and loss of the oxygen atom as  $H_2O$ . This could also correspond to neutral loss of a hydroxyl group (C-OH) via cleavage of the C-O bond. However, consideration of the masses of the parent compound shows that the presence of a C=O or C-OH group can be determined by the fact that a C=O containing compound would be 2 mass units less than a compound containing an unacetylated OH group. Retention times can also provide clues to the nature of functional groups as the more polar carbonyl-containing compound would be expected to elute earlier than corresponding hydroxyl-containing counterpart in reverse-phase liquid chromatography. Based upon these comparisons it has been possible to identify a number of other novel compounds containing a ketone functionality.

#### 5.3.2.1 Oxo-BHTcyc

A compound with  $[M+H]^+ = m/z$  958 has been identified in a number of active and non-active sinters from TVZ (Table 5.8). This compound has been found to be the most common novel BHP and is present in 55% of sinter samples analysed. Parent ion and fragmentation pathways appear to be similar to that reported for BHTcyc (**9**; Talbot *et al.*, 2003a), however, the compounds appear to contain distinct differences in the C-35 linked composite functionality and elute earlier during chromatographic separation (Figure 5.6) suggesting a more polar structure. The low intensity of the ions at  $m/z$  330 (TG) and 348 (TGOH<sub>2</sub>) in the  $MS^2$  spectrum indicate

the presence of a cyclitol ether moiety (Figure 5.4) as opposed to the glucosamine moiety described in Flesch and Rohmer (1989). Losses of  $\text{CH}_3\text{COOH}$  from  $[\text{M}+\text{H}]^+$  are observable at  $m/z$  898, 838. Loss of tetra-acetylated ether-linked aminocyclopentitol moiety results in a fragment of  $m/z$  611. Further loss of  $\text{CH}_3\text{COOH}$  giving ions of  $m/z$  551 and 491 are accompanied by an additional loss of 18 (i.e. loss of the O from a C=O as  $\text{H}_2\text{O}$ ) ( $m/z$  473) which confines the ketone to the n-alkyl side-chain component (Figure 5.4; Table 5.2). The position of the ketone has yet to be determined but is tentatively assigned to C-32 as previously reported by Flesch and Rohmer (1989). The compound is tentatively assigned as 35-O- $\beta$ -cyclitol bacteriohopane-32-oxo-33,34-ol (**27**; oxo-BHT<sub>cyc</sub>; Figure 5.5).

#### 5.3.2.2 OXO-BHP<sub>CYC</sub>

A compound with  $[\text{M}+\text{H}]^+ = m/z$  1016 has been detected in samples CP3, CP8, CP11 and RK2N. Comparisons with previously published APCI fragmentation pathways (e.g. Talbot *et al.*, 2003a, b; Talbot *et al.*, 2007a, b) and the proposed novel tetra-functionalised BHP (Section 5.3.2.1 above) suggest that this compound is penta-functionalised and related to previously determined penta-functionalised composite BHPs, such as BHP<sub>cyc</sub> (**10**) although comparison of retention times shows that this compound forms a more polar derivative than that of BHP<sub>cyc</sub> (**10**; Figure 5.6). Peaks in the  $\text{MS}^2$  mass spectra relate to multiple loss of  $\text{CH}_3\text{COOH}$  from  $[\text{M}+\text{H}]^+$  i.e.  $m/z$  956, 896, 836. The presence of an ion at  $m/z$  669 indicates loss of ether linked terminal group (TGOH; 347 Da). Multiple losses of  $\text{CH}_3\text{COOH}$  from  $m/z$  669, i.e.  $m/z$  669, 549 and 489 followed by an additional loss of 18 Da suggest the presence of a penta-functionalised component with a C-35 composite functionality (Figure 5.4; Table 5.2). The position of the ketone cannot be determined without further spectroscopic analysis although based upon the structure reported in Flesch and Rohmer (1989) it is assumed that the ketone group is located at C-31. The compound has been tentatively assigned as 35-O- $\beta$ -cyclitol bacteriohopane-31-oxo-32,33,34,35-ol (**28**; oxo-BHP<sub>cyc</sub>).

## 5.3.2.3 OXO-BHTRIOL

A compound with a base peak of  $m/z$  611 has been identified in active and non-active samples from TVZ (Table 5.8). This compound is the second most common novel BHP identified during this study and is present in 35% of sinter samples analysed. Compounds with odd mass usually indicate an absence of a nitrogenous functional group. Furthermore BHPs without a N-containing group usually readily fragment under APCI conditions resulting in the observation of a parent ion of the  $MS^2$  spectrum of  $[M+H - AcOH]^+$  (Talbot *et al.*, 2003a, b; Talbot *et al.*, 2007a, b). Multiple loss of  $CH_3COOH$  from  $[M+H - AcOH]^+$  i.e.  $m/z$  551 and 491 followed by neutral loss of 18, i.e.  $m/z$  473, have been used to indicate a tetra-functionalised BHP containing an unacetylated ketone functionality (Figure 5.4; Table 5.2). C-ring cleavage of BHPs can result in neutral fragment loss of 192 (AB) with charge retention on the side chain containing portion of the molecule. The  $MS^2$  spectrum shows multiple loss of  $CH_3COOH$  from  $[M+H - AcOH - AB]^+$  i.e.  $m/z$  479, 419 and 359. The position of the ketone functionality is yet to be determined but is tentatively assigned to C-32, on the basis of the aforementioned oxo-BHT<sub>cyc</sub> (Section 5.3.2) and structural assignment of oxo BHT<sub>gly</sub> made by Flesch and Rohmer (1989). This compound has been tentatively assigned 32-oxo-bacteriohopane-33,34,35 triol (Figure 5.5).

## 5.3.2.4 OXO-BHTETROL

A compound with  $[M+H - AcOH]^+ = m/z$  669 has been identified in samples CP3N, CP8N, CP11N and RK3N. Early elution time and differences in  $MS^2$  spectrum indicate that this compound is different to C-2 or C-3 methylated BHT<sub>etrol</sub> (**II-1** or **III-1**) which has the same parent ion. This compound appears to be related to the tentatively assigned oxo-BHT<sub>cyc</sub> (**41**; Section 5.3.2). Three losses of  $CH_3COOH$  from  $[M+H - AcOH]^+$  i.e.  $m/z$  609, 549 and 489 followed by neutral loss of 18, i.e.  $m/z$  471, suggest a pentafunctionalised BHP containing a ketone functionality (Figure 5.4; Table 5.2). C-ring cleavage of BHPs results in neutral fragment

loss of 192 (AB). The MS<sup>2</sup> spectrum shows 2 losses of CH<sub>3</sub>COOH from [M+H – AcOH – AB]<sup>+</sup> i.e. m/z 477 and 417. The position of the ketone functionality is yet to be determined but is tentatively assigned to C-31, as in the aforementioned oxo-BHP<sub>cyc</sub> (Section 5.3.3) and structural assignment of oxo-BHT<sub>gly</sub> made by Flesch and Rohmer (1989). This compound has been tentatively assigned 31-oxo-bacteriohopane-32,33,34,35 tetrol (**29**; Figure 5.5).

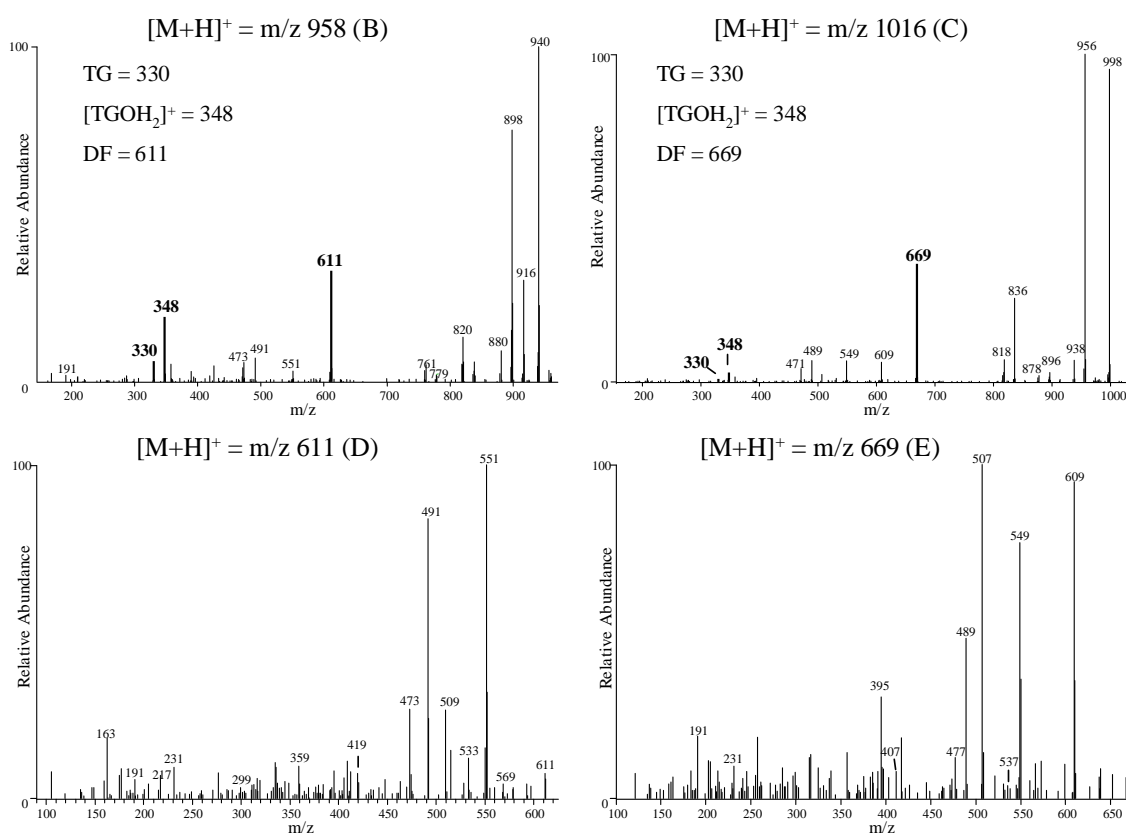


Figure 5.4 Figure showing MS<sup>2</sup> spectra of proposed novel 'oxo-BHPs' detected in silica sinters. [M+H]<sup>+</sup> = m/z 958 (top left), m/z 1016 (top right), m/z 611 (bottom left) and m/z 669 (bottom right). (B) 35-O-β-cyclitol bacteriohopane-31-oxo-32,33,34,35-ol. (C) 35-O-β-cyclitol bacteriohopane-32-oxo-33,34,35-ol. (D) 32-oxo-bacteriohopane-33,34,35 triol. (E) 31-oxo-bacteriohopane-32,33,34,35 tetrol.

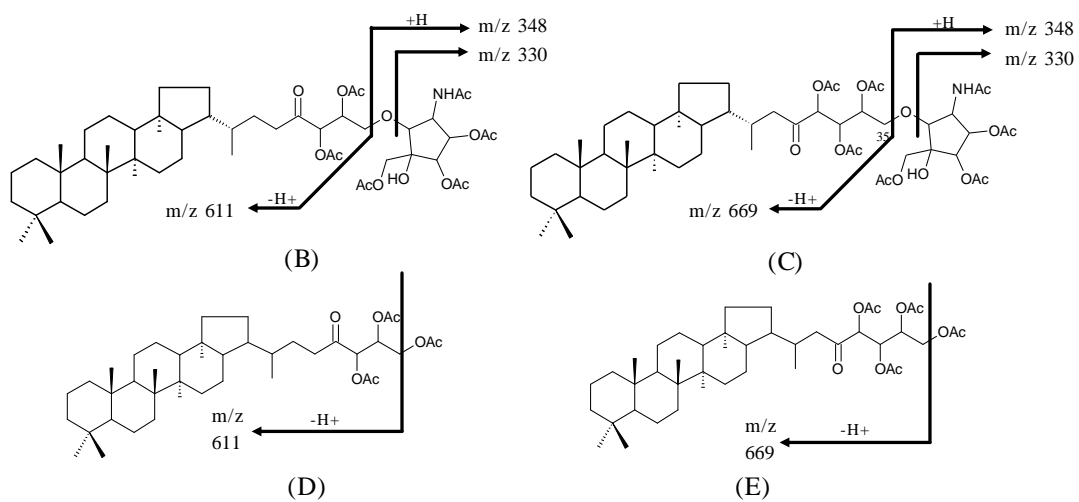


Figure 5.5 Tentatively-assigned structures of novel 'oxo-BHPs' detected throughout silica sinters of TVZ. Arrows show key fragmentations of peracetylated compounds

Novel BHPs

Table 5.2 Assignment of ions observed in APCI-MS<sup>2</sup> spectra of proposed novel Oxo-BHPs

Ion/Compound	Oxo-BHP <sub>cyc</sub>	Oxo-BHT <sub>cyc</sub>	Oxo-BH <sub>pentol</sub>	Oxo-BHT <sub>tetrol</sub>
[M+H] <sup>+</sup>	1016 <sup>a</sup>	958 <sup>a</sup>	729	671
[M+H - AcOH] <sup>+</sup>	956	898	669 <sup>a</sup>	611 <sup>a</sup>
[M+H - 2AcOH] <sup>+</sup>	896	838	609	551
[M+H - 3AcOH] <sup>+</sup>	836	778	549	491
[M+H - 4AcOH] <sup>+</sup>	-	-	489	-
TG	330	330	-	-
TGOH	347	347	-	-
TG(OH <sub>2</sub> )	348	348	-	-
[M+H - TGOH] <sup>+</sup>	669	611	-	-
[M+H - (AcOH + TG)] <sup>+</sup>	609	551	-	-
[M+H - (2AcOH + TG)] <sup>+</sup>	549	491	-	-
[M+H - (3AcOH + TG)] <sup>+</sup>	489	-	-	-
[M+H - (2AcOH + TG + oxo)] <sup>+</sup>	531 <sup>b</sup>	473	-	-
[M+H - (3AcOH + TG + oxo)] <sup>+</sup>	471	-	-	-
AB	191	191	191	191
[M+H - (AcOH + AB)] <sup>+</sup>	764 <sup>b</sup>	706 <sup>b</sup>	477	419
[M+H - (2AcOH + AB)] <sup>+</sup>	704 <sup>b</sup>	646 <sup>b</sup>	407	359

<sup>a</sup> Parent ion of MS<sup>2</sup> spectrum. <sup>b</sup> expected ion not observed on MS<sup>2</sup> spectra. TG = C<sub>35</sub>-linked Terminal group, AcOH = CH<sub>3</sub>COOH, AB = neutral fragment loss of the A + B rings via C-ring cleavage (192 Da), oxo = ketone functionality

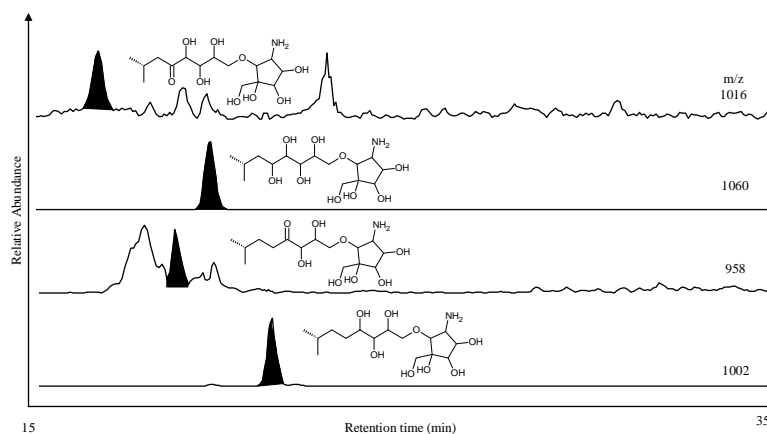


Figure 5.6 Partial mass chromatograms showing relative retention times of tentatively-assigned novel composite Oxo-BHPs compounds to BHPcyc and BHTcyc

### 5.3.3 NOVEL COMPOSITE BHPs

Novel composite-BHPs can be identified by the presence of ions in  $MS^2$  spectra that indicate a tetra-, penta- or hexafunctionalised BHP precursor (i.e. diagnostic fragments, DF) plus an ether linked component (TGOH) that would indicate a neutral loss of sufficient mass to make up the mass difference observed between the parent ion and the diagnostic fragment (Figure 5.7 and Figure 5.8). During the tentative-assignment of novel BHPs, ions that indicate the mass of the terminal group sometimes co-occur with an ion of +18 Da. This ion corresponds to cleavage of the C<sub>35</sub>-O-TG bond between carbon and oxygen and retention of charge on the terminal group ( $[TGOH_2]^+$ ). Based upon previous structural characterisations (e.g. Langworthy *et al.*, 1976; Rohmer *et al.*, 1984; Bisseret *et al.*, 1985) and previously published APCI fragmentation pathways (Talbot *et al.*, 2003a, b; Talbot *et al.*, 2007a, b) it is assumed that this chemical functionality forms an ether-linkage to C-35 of the side-chain component. Other composite-type BHPs have been reported, i.e. ornithine-BHT (**7**) and tryptophan-BHT (**8**; e.g. Neunlist *et al.*, 1988; Talbot *et al.*, 2007a), these compounds contain an N-acylated C-35 linkage and produce fragments of identifiable by the presence of an ion at m/z 672 (not shown). These compounds were not identified during this study.

## Novel BHPs

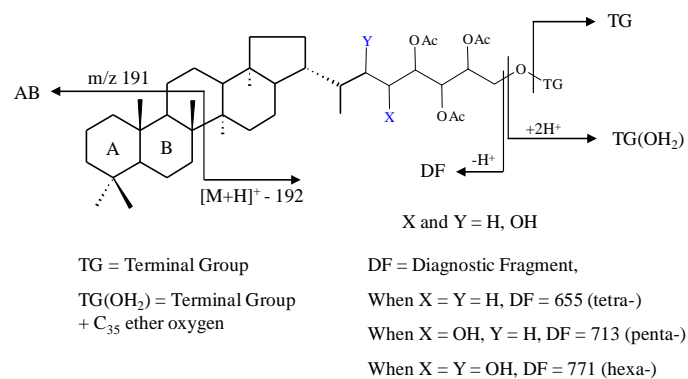


Figure 5.7 Characteristic fragmentation pathways expected in composite BHPs

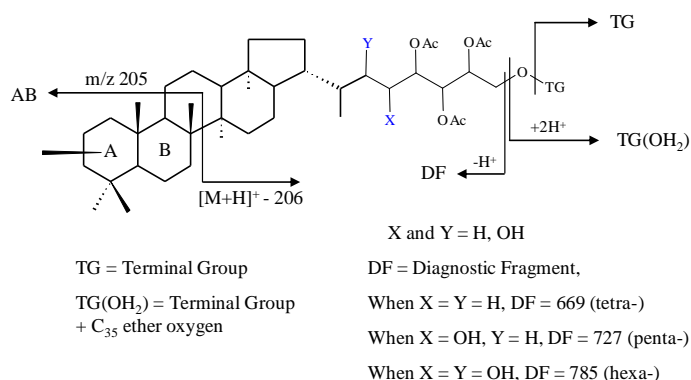


Figure 5.8 Characteristic fragmentation pathways expected in composite BHPs containing an A-ring methylation

### 5.3.3.1 NOVEL BHPs WITH A TERMINAL GROUP OF MASS 305 DA

Two compounds with parent ions of  $[M+H]^+ = m/z$  1018 and 960 have been identified in silica sinters of CP, LR and RK during this study (Table 5.1). Interpretation of the MS<sup>2</sup> spectra (Figure 5.9) indicates that both of these particular compounds contain a chemical functionality that produces ions at  $m/z$  288 (TG) and 306 ( $[TGOH_2]^+$ ) (Figure 5.10). These ions indicate neutral mass loss of 287 Da and 305 Da (TGOH) from the peracetylated parent ion. Loss of TGOH fragment from the parent ion produces ions at  $m/z$  713 and 655 in the MS<sup>2</sup> spectra of  $[M+H]^+ = 1018$  and 960 indicating the presence of penta- and tetrafunctionalised BHPs respectively (Figure 5.10; Talbot *et al.*, 2003a, b; Talbot *et al.*, 2007a). Assignment of other ions that provide further evidence of the presence of novel BHP can be found in Table 5.3. For example, ions observed in the MS<sup>2</sup> spectrum of  $[M+H]^+ = m/z$  1018 indicate neutral

loss of 18 Da which suggests the presence of an unacetylated hydroxyl group, and is observed by the presence of an ion at  $m/z$  1000. Multiple losses of  $\text{CH}_3\text{COOH}$  from  $[\text{M}+\text{H}]^+$ , i.e.  $m/z$  958, 898, 818. Loss of TGOH (305 Da) produces an ion at  $m/z$  713, from this fragment multiple losses of  $\text{CH}_3\text{COOH}$  are observed, i.e.  $m/z$  653, 593, 533 and 473. An ion at  $m/z$  826 indicates loss of A+B rings during C-ring cleavage. Charge retention on the AB fragment produces the ion at  $m/z$  191 (Figure 5.9).

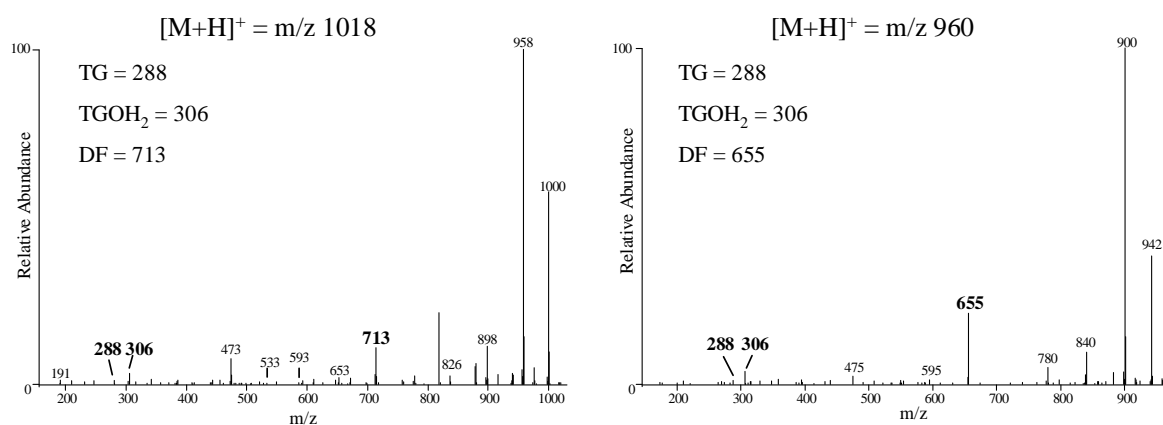


Figure 5.9  $\text{MS}^2$  spectra of novel composite BHPs with terminal group of mass 305 Da

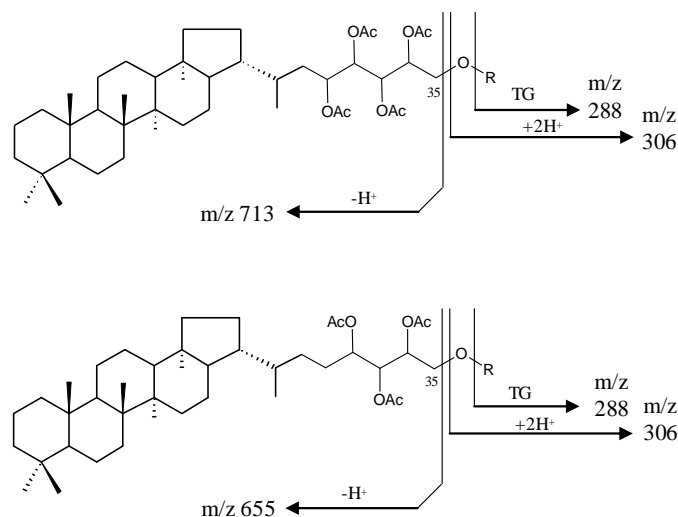


Figure 5.10 Characteristic fragmentations of novel BHPs with terminal group of mass 305. Top: Pentafunctionalised component with  $[\text{M}+\text{H}]^+ = m/z$  1018. Bottom: Tetra-functionalised BHP with  $[\text{M}+\text{H}]^+ = m/z$  960.

## Novel BHPs

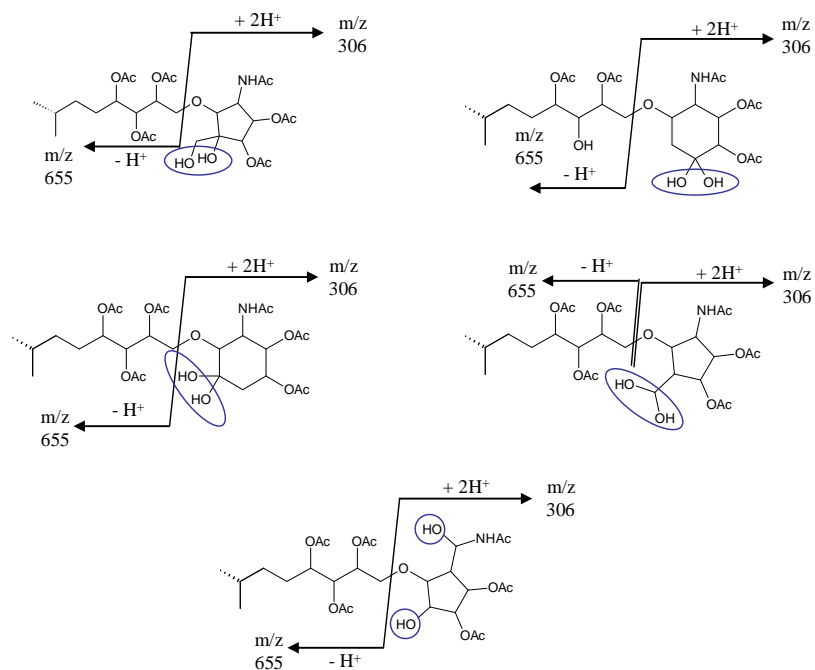


Figure 5.11 Possible structures of tentatively-assigned novel BHPs containing terminal group of mass 305 Da.

Circles indicate unacetylated hydroxyl groups

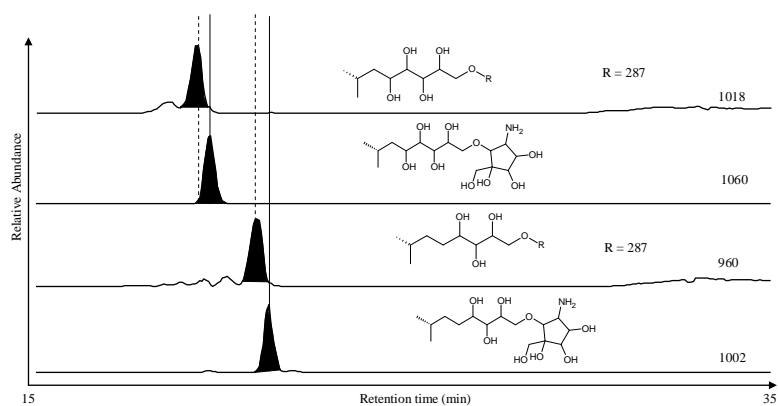


Figure 5.12 Partial mass chromatogram showing retention times of tentatively-assigned novel composite BHPs compounds relative to BHPcyc and BHTcyc. Structure of 'R' group on m/z 1018 and 960 remains undetermined

group ion and C-35 ether linkage, DF = 'diagnostic fragment'

## 5.3.3.2 NOVEL BHPs WITH TERMINAL GROUP OF MASS 433 DA

Two compounds with  $[M+H]^+ = m/z$  1204 and 1146 have been identified during analysis of non-active sinters from OK (sample OK4N; Table 5.8). The compounds are tentatively-assigned as BHPs on the basis that both compounds produce  $MS^2$  spectra (Figure 5.14) that show loss of terminal group with mass 433 Da, observable as ions at  $m/z$  416 (TG) and 434 ( $[TGOH_2]^+$ ). Loss of terminal group (TGOH) produces ions of  $m/z$  771 and 713 which are diagnostic fragments of hexa- and penta-functionalised BHPs respectively. This indicates the two compounds likely form part of a homologous series. Structural assignment remains tentative and is based upon comparisons with previously characterised fragmentation pathways (e.g. Talbot *et al.*, 2003a, b; Talbot *et al.*, 2007a, b) and assignment of major ions observed in the  $MS^2$  spectra of each compound can be found in Table 5.3. For example, multiple losses of  $CH_3COOH$  are observable from  $[M+H]^+ = m/z$  1146, i.e.  $m/z$  1086, 1026, 966, 906. The presence of an ion at  $m/z$  906 indicates four losses of  $CH_3COOH$  from  $[M+H]^+ = m/z$  1146. The presence of ions at  $m/z$  434 (TGOH) and 416 (TG) suggest loss of ether-linked composite functionality from C-35. Loss of terminal group ions from  $[M+H]^+ = m/z$  1146 results in the production of a fragment at  $m/z$  713, which corresponds to a penta-functionalised BHP (Talbot *et al.*, 2007a). Further losses of  $CH_3COOH$  from  $[M+H]^+$  are observable, i.e.  $m/z$  653 and 473. The presence of an ion of  $m/z$  471 indicates loss of four  $CH_3COOH$  groups from  $m/z$  713 and provides further evidence of a penta-functionalised component.

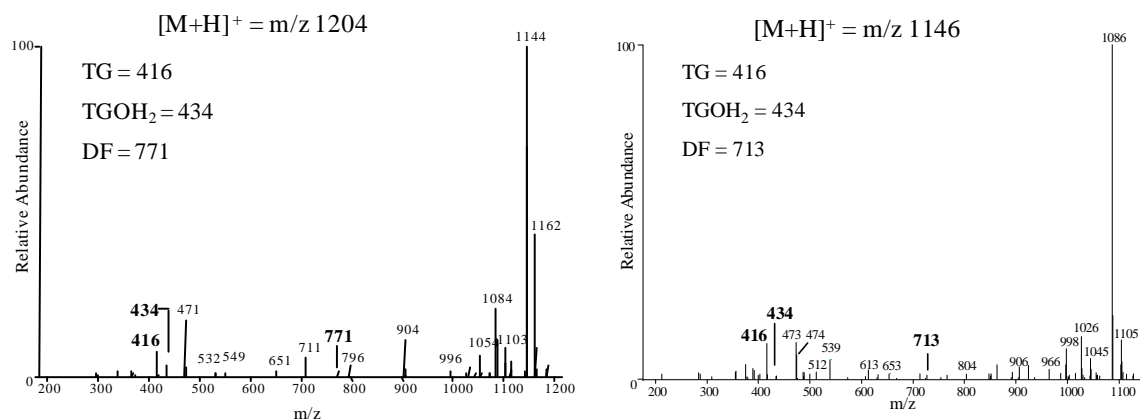


Figure 5.13 MS<sup>2</sup> spectra of  $[M+H]^+ = m/z$  1204 (left) and  $m/z$  1146 (right). Arrows indicate characteristic fragmentations. AcOH indicates  $CH_3COOH$

### 5.3.3.3 NOVEL BHPs WITH TERMINAL GROUP OF MASS 543 DA

Two compounds with  $[M+H]^+ = m/z$  1256 and 1198 have been identified during this study.  $[M+H]^+ = m/z$  1256 was identified in an active sinter of OK (sample OK1A middle; Chapter 3) and a microbial mat sampled from the vent source of RHC (Chapter 3).  $[M+H]^+ = m/z$  1198 was identified in a microbial mat sample from RHC. During APCI MS<sup>n</sup> analysis it is apparent that the two compounds contain a C-35 ether-linked functionality that has the same mass, 543 Da, which appears as an ion on the MS<sup>2</sup> spectra of both compounds as an ion at  $m/z$  544. This is the only fragmentation associated with the terminal group observed during APCI MS<sup>n</sup> analysis of  $[M+H]^+ = m/z$  1256 and 1198 and TG fragmentations are not observed. This could indicate that the terminal group contains chemical functionalities that are able to retain charge and therefore hinder fragmentation. Alternatively, the large mass of both compounds may require refinement of the factors controlling fragmentation in the ion trap. Assignment of ions that indicate  $[M+H]^+ = m/z$  1256 and 1198 are BHPs can be found in Table 5.3. Assignment of ions for  $[M+H]^+ = m/z$  1256 are given as an example, multiple losses of  $CH_3COOH$  from  $[M+H]^+$  are observable, i.e.  $m/z$  1196, 1136, 1076 and 1016. Loss of terminal group from  $[M+H]^+$  results in the formation of an ion at  $m/z$  713 and possibly

indicates this compound as a penta-functionalised BHP. Losses of  $\text{CH}_3\text{COOH}$  from  $[\text{M}+\text{H} - \text{TG}]^+ = m/z 713$ , i.e.  $m/z 653$  and  $473$  indicate the compound is a penta-functionalised BHP (Talbot *et al.*, 2003a, b; Talbot *et al.*, 2007a, b) with a composite functionality at C-35 with  $m/z 544$ .

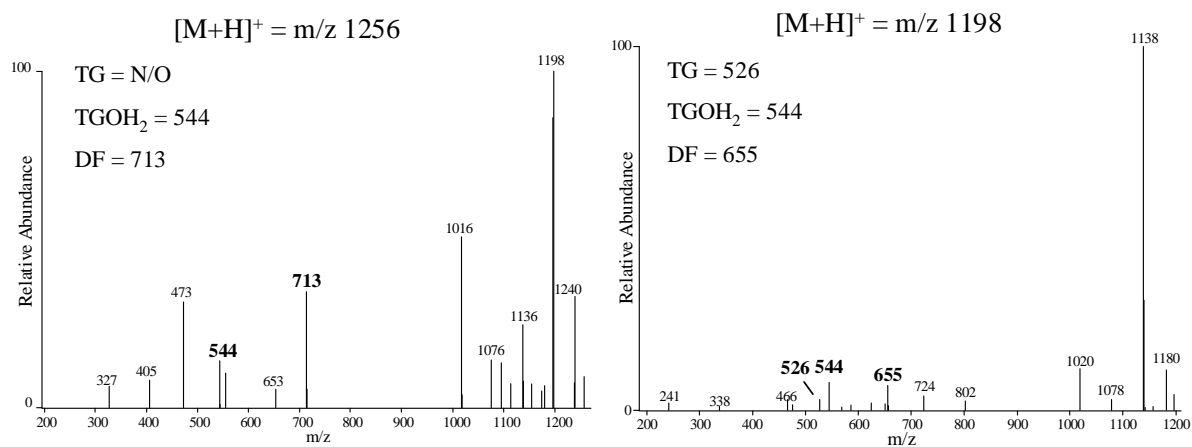


Figure 5.14 MS<sup>2</sup> spectrum  $[\text{M}+\text{H}]^+ = m/z 1256$  (left) and  $m/z 1198$  (right). N/O = not observed.

Table 5.3 Characteristic ions observed during APCI fragmentations of tentatively assigned novel BHPs.

Compound/Ion	Novel Compound <sup>a</sup>					
	F	G	H	I	J	K
[M+H] <sup>+</sup>	960 <sup>b</sup>	1018 <sup>b</sup>	1146 <sup>b</sup>	1204 <sup>b</sup>	1198 <sup>b</sup>	1256 <sup>b</sup>
[M+H - AcOH] <sup>+</sup>	900	958	1086	1144	1138	1196 <sup>c</sup>
[M+H - 2AcOH] <sup>+</sup>	840	898	1026	1084	1078	1136
[M+H - 3AcOH] <sup>+</sup>	780	838 <sup>c</sup>	966	1024 <sup>c</sup>	1018 <sup>c</sup>	1076
[M+H - 4AcOH] <sup>+</sup>	-	778 <sup>c</sup>	906	964 <sup>c</sup>	-	1016
[M+H - 5AcOH] <sup>+</sup>	-	-	-	904	-	-
TG	288	288	416	416	526 <sup>c</sup>	526 <sup>c</sup>
TGOH	305	305	433	433	543	543
TG(OH <sub>2</sub> )	306	306	434	434	544	544
[M+H - TG] <sup>+</sup>	655	713	713	771	655	713
[M+H - (TG(OH <sub>2</sub> ) + AcOH)] <sup>+</sup>	595	653	653	711	595 <sup>c</sup>	653
[M+H - (TG(OH <sub>2</sub> ) + 2AcOH)] <sup>+</sup>	535 <sup>c</sup>	593	593	651	535 <sup>c</sup>	593 <sup>c</sup>
[M+H - (TG(OH <sub>2</sub> ) + 3AcOH)] <sup>+</sup>	475	533	533	591 <sup>c</sup>	475 <sup>c</sup>	533 <sup>c</sup>
[M+H - (TG(OH <sub>2</sub> ) + 4AcOH)] <sup>+</sup>	-	473	473	531 <sup>c</sup>	-	493
[M+H - (TG(OH <sub>2</sub> ) + 5AcOH)] <sup>+</sup>	-	-	-	471	-	-
AB	192	192	192	192	192	192
[M+H - AB] <sup>+</sup>	768 <sup>c</sup>	826	954 <sup>c</sup>	1012 <sup>c</sup>	1006	1064 <sup>c</sup>
[M+H - (AB+ AcOH)] <sup>+</sup>	708	766	894 <sup>c</sup>	952 <sup>c</sup>	946 <sup>c</sup>	1004 <sup>c</sup>

<sup>a</sup> novel composite structures. F and G terminal group 305 Da (section 5.3.3.1). H and I terminal group 433 Da (Section 5.3.3.2). J and K terminal group 543 Da (Section 5.3.3.3). <sup>b</sup> Indicates parent ion of MS<sup>2</sup> spectrum. <sup>c</sup> indicates expected ion not present in MS<sup>2</sup> spectrum. TG = C<sub>35</sub> ether-linked Terminal Group ion. AB = A + B rings produced during C-ring cleavage. AcOH = CH<sub>3</sub>COOH.

## 5.4 STRUCTURAL ASSIGNMENT OF NOVEL BHPs BASED UPON INTERPRETATION OF APCI MS<sup>2</sup> AND MS<sup>3</sup> SPECTRA

In certain cases the MS<sup>2</sup> spectrum of a particular compound may not yield sufficient information regarding molecular fragmentations that allow positive identification of the presence of a BHP. There are a number of reasons for this, mainly due to the ionisation and trapping coefficient of the ion trap mass spectrometer or the presence of functional groups that enable a compound to retain a charge can lead to poor MS<sup>2</sup> fragmentations. In these cases, interpretation of the MS<sup>3</sup> spectrum can provide valuable information regarding the presence of a BHP.

### 5.4.1 NOVEL BHPs WITH A TERMINAL GROUP OF MASS 319 Da

Four compounds with  $[M+H]^+ = m/z$  1046, 1032, 988 and 974 have been identified during the analyses of BHP distribution of mat-forming microbial consortia (Figure 5.15; See also Chapter 3; Zhang *et al.*, 2007). These compounds contain a common chemical functionality with a mass of 301 Da (TG), observable as an ion at  $m/z$  302 in the MS<sup>2</sup> and MS<sup>3</sup> spectra. Ions corresponding to TGOH (i.e.  $[TGOH_2]^+ = m/z$  320) were not observed in the MS<sup>2</sup> spectra of this group of compounds. Loss of TGOH from  $[M+H]^+ = m/z$  1032 and 1046 produces ions in MS<sup>2</sup> and MS<sup>3</sup> spectra at  $m/z$  713 and 727, indicating the presence of non-methyl and methylated penta-functionalised components respectively. Differences observed in the retention times during HPLC separation indicate a BHP with a C-2 methylation (Figure 5.15). Likewise, loss of TGOH from  $[M+H]^+ = 974$  and 988 produces ions at  $m/z$  655 and 669, indicating the presence of a non-methylated and methylated tetra-functionalised BHP. Further evidence for the identification of novel BHPs is provided by the production of C<sub>31</sub> ββ bishomohopanol and C<sub>32</sub> ββ homohopanol during PA/NaBH<sub>4</sub> treatment of polyfunctionalised BHP precursors (Figure 5.16; Figure 5.17). 2-methylated homologues

are also observed in the  $m/z$  205 mass chromatogram. The sample shown is a microbial mat collected from OK, as this mat was shown to only contain novel BHPs with a TG of mass 301 Da and BHT, only these compounds could be the precursors to the observed homohopanols.

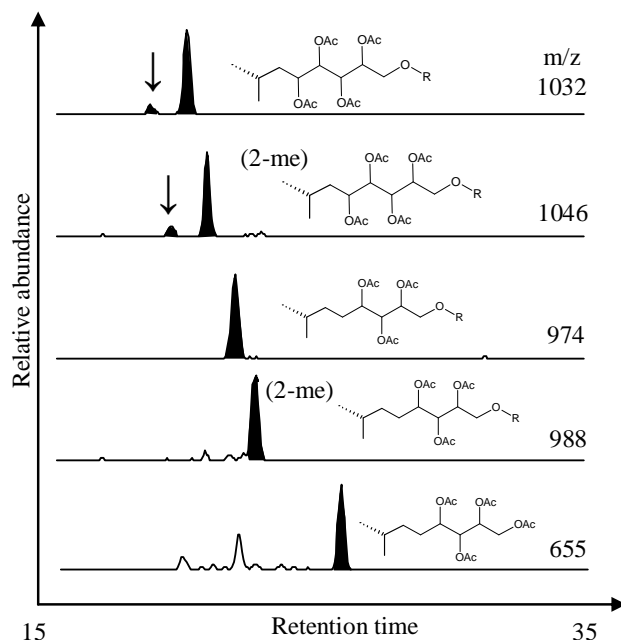


Figure 5.15 Partial mass chromatogram showing distribution of novel BHPs from mat-forming cyanobacteria. Arrows indicate early-eluting isomers of penta-functionalised compounds.

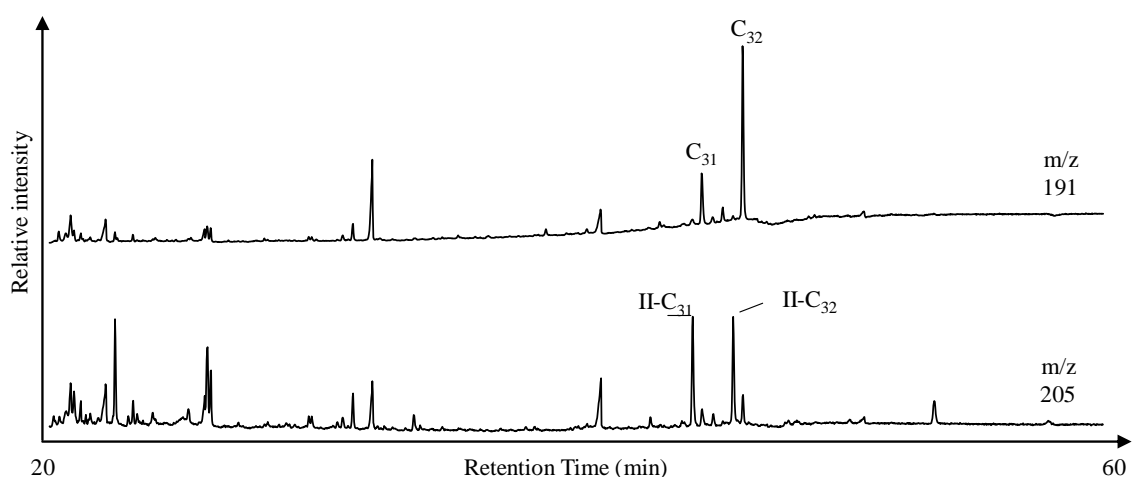


Figure 5.16 Products released via  $PA/NaBH_4$  cleavage of BHPs extracted from microbial mats.  $C_{31}$  refers to  $C_{31}$   $\beta\beta$  homohopanols,  $C_{32}$  refers to  $C_{32}$   $\beta\beta$  bishomohopanols. Prefix II refers to C-2 methylated homologues.

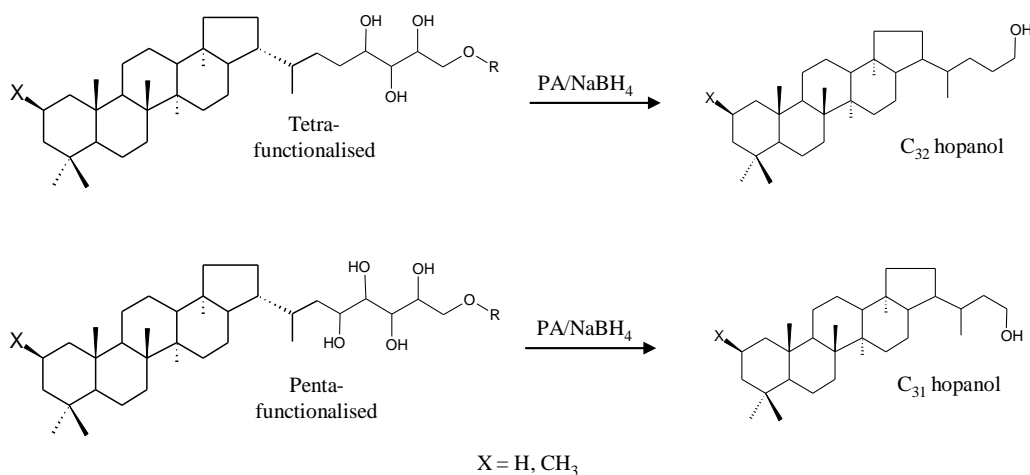


Figure 5.17 Schematic of cleavage of side-chain component of novel BHPs and resulting GC-MS amenable products

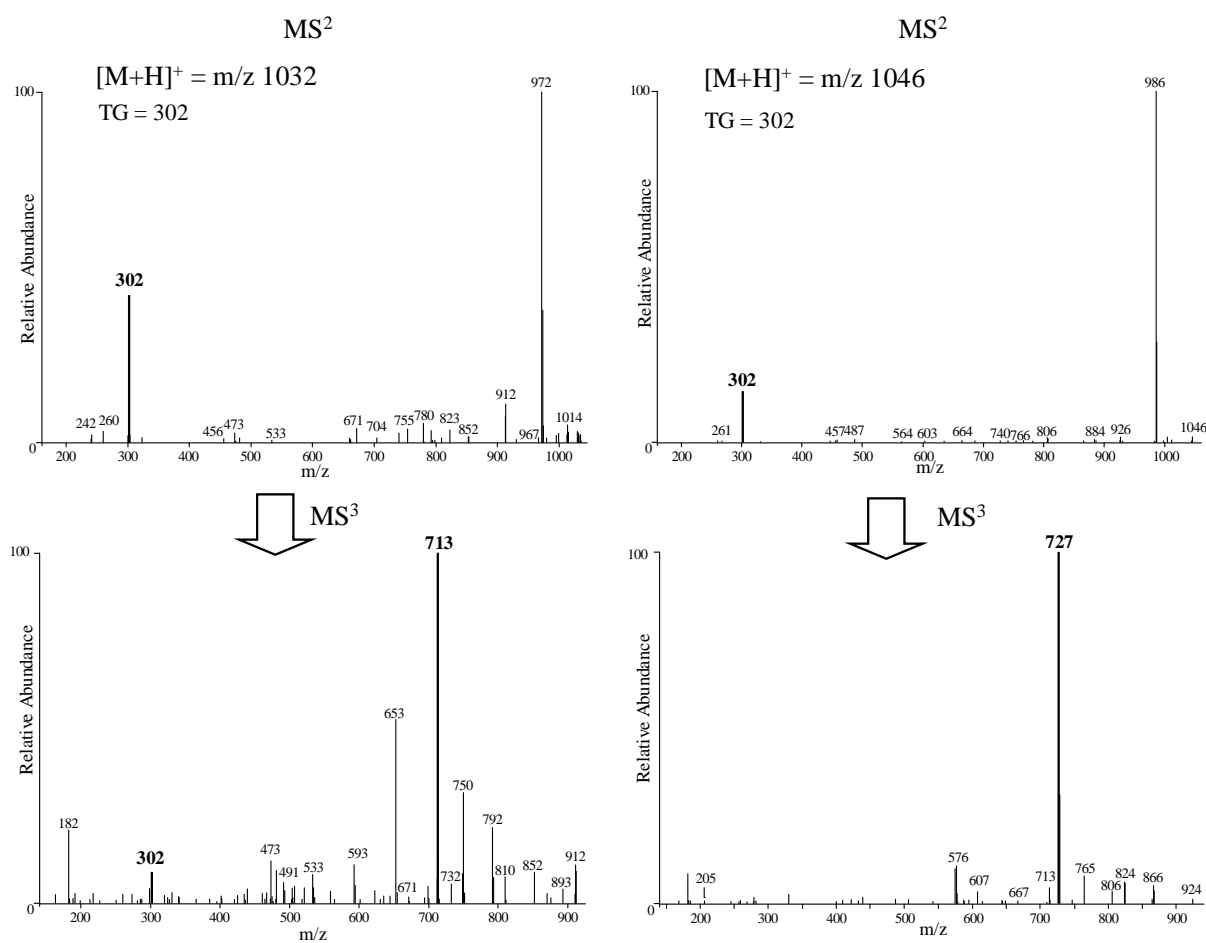


Figure 5.18 MS<sup>2</sup> and MS<sup>3</sup> spectra of novel BHPs identified in mat-forming cyanobacteria. Left: MS<sup>2</sup> (top) and MS<sup>3</sup> (bottom) of  $[M+H]^+ = m/z$  1032. Right: MS<sup>2</sup> (top) and MS<sup>3</sup> (bottom) of  $[M+H]^+ = m/z$  1046

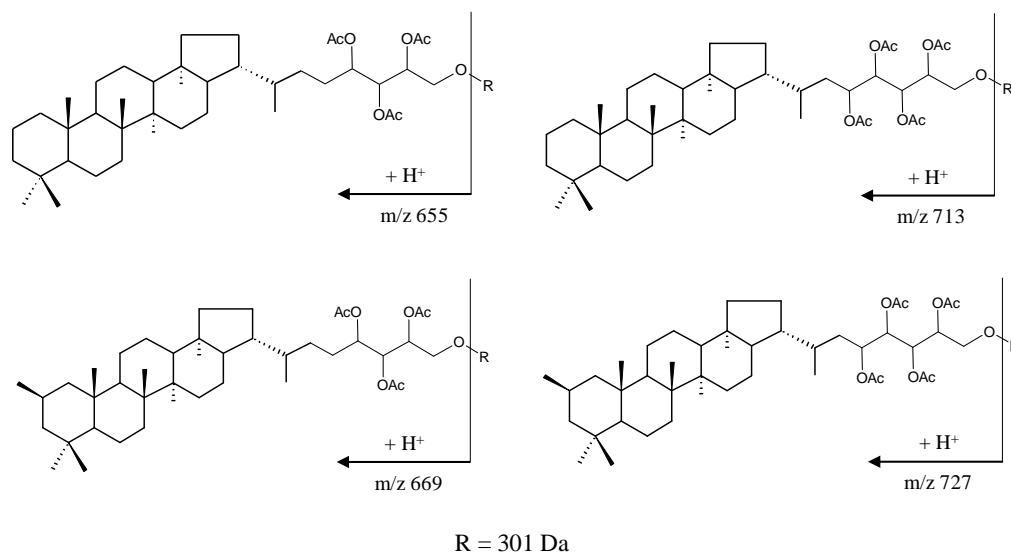


Figure 5.19 Structures of novel compounds identified in microbial mats from geothermal vents. R group = 301 Da, identified by peak at m/z 302. Letters refer to ordering of structures throughout text and can be found in Table 5.9

Table 5.4 Assignment of ions observed in APCI-MS<sup>n</sup> spectra of novel BHPs from mat-forming microbial consortia

Compound/ion	m/z 1032	<sup>a</sup> [M+H] <sup>+</sup> =		
		m/z 1046	m/z 974	m/z 988
[M+H] <sup>+</sup>	1032 <sup>b</sup>	1046 <sup>b</sup>	974 <sup>b</sup>	988 <sup>b</sup>
[M+H – AcOH] <sup>+</sup>	972	986	914	928
[M+H – 2AcOH] <sup>+</sup>	912	926	854	868
[M+H – 3AcOH] <sup>+</sup>	852	866 <sup>c</sup>	-	-
[M+H – 4AcOH] <sup>+</sup>	792	806	-	-
TG				
TG(OH)	302	302	302	302
[M+H – TG] <sup>+</sup>	713	727	655	669
[M+H – (TG + AcOH)] <sup>+</sup>	653 <sup>c</sup>	667 <sup>c</sup>	595	609
[M+H – (TG + 2AcOH)] <sup>+</sup>	593	607	535	549
[M+H – (TG + 3AcOH)] <sup>+</sup>	533	547	475	489
[M+H – (TG + 4AcOH)] <sup>+</sup>	473	487	-	-
[M+H – AB] <sup>+</sup>				
AB	840	840	782	782
	192	206	192	206

<sup>a</sup> Compounds reported in Zhang et al., 2007. <sup>b</sup> parent ion of MS<sup>2</sup> spectra. <sup>c</sup> expected ion not observed. AcOH = CH<sub>3</sub>COOH, TG = C<sub>35</sub> ether-linked terminal group ion, AB = products of ring C cleavage (192 Da),

## 5.4.2 NOVEL BHPs WITH A TERMINAL GROUP OF MASS 329 DA

A compound with peracetylated parent mass of  $[M+H]^+ = m/z$  984 was detected in samples RK2 and LR3N. It has been tentatively identified as a novel BHP based upon fragmentation pathways that are similar to that observed for BHT<sub>cyc</sub> or BHT<sub>gly</sub> (Talbot *et al.*, 2003b; Talbot *et al.*, 2007a). A compound with peracetylated mass of  $m/z$  984 has been previously noted from cultures of *Zymomonas mobilis* (Talbot *et al.*, 2003b). In this case, similarities were drawn with BHT<sub>cyc</sub> and the observed mass difference attributed to the presence of an unacetylated hydroxyl group on the terminal group (Talbot *et al.*, 2003b). However consideration of the mass difference between  $m/z$  984 and BHT<sub>cyc</sub> reveals that the two compounds differ by the absence of an unacetylated hydroxyl functionality, likely the C-5' hydroxyl group (Figure 5.20). The MS<sup>2</sup> of  $[M+H]^+ = m/z$  984 (Figure 5.20) shows multiple losses of CH<sub>3</sub>COOH from  $[M+H]^+$  i.e.,  $m/z$  924, 864, 804. The ion at  $m/z$  655 results from loss of the C-35 terminal group (TGOH = 329 Da) due to cleavage of the carbon-oxygen bond at C-35. This provides evidence indicating a tetra-functionalised component. The most abundant ion ( $m/z$  924) from the MS<sup>2</sup> spectrum provides the parent ion of the MS<sup>3</sup> spectra (Figure 5.20) where further fragmentation information provides more structural information. Multiple losses of CH<sub>3</sub>COOH from  $m/z$  655 are observable, i.e.,  $m/z$  595, 535, 475. The ion at  $m/z$  732 results on the MS<sup>2</sup> spectrum from loss of A and B rings via C-ring cleavage (192 Da).

From the information extracted from fragmentation pathways observed in the MS<sup>2</sup> and MS<sup>3</sup> spectra of  $m/z$  984 (Figure 5.20), it is clear there are structural similarities between  $m/z$  984 and BHT<sub>cyc</sub> (**9**). If these assumptions prove to be correct then the terminal group ion may be present in number of structural forms. Possible structures with fragmentations that enable tentative assignment are shown in Figure 5.21. BHT<sub>cyc</sub> (**9**) is also shown for comparison.

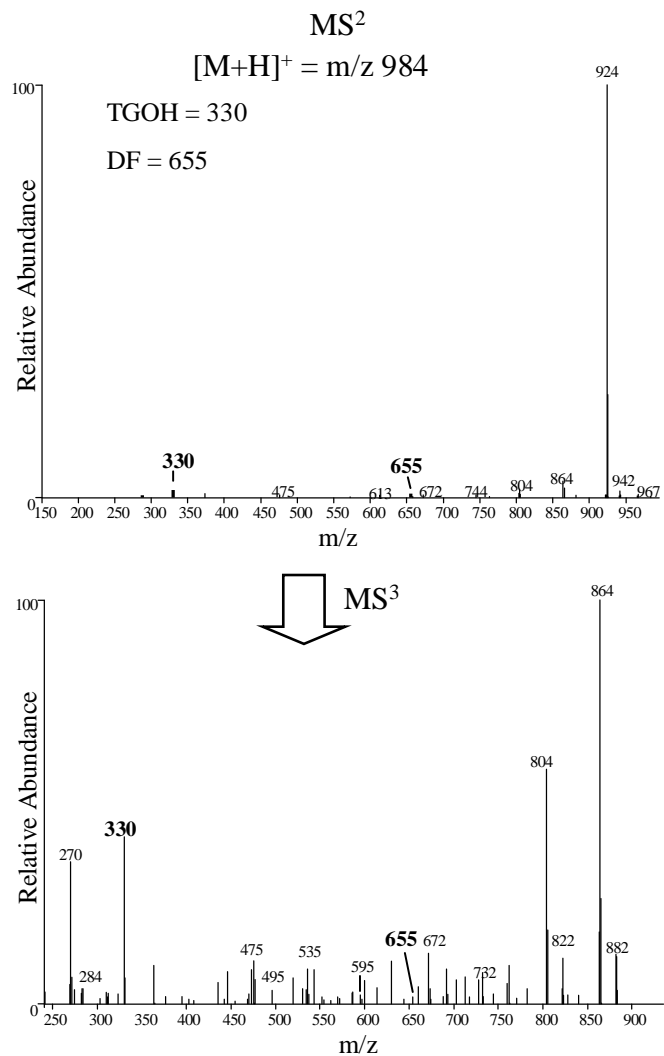


Figure 5.20 MS<sup>2</sup> and MS<sup>3</sup> Spectra of [M+H]<sup>+</sup> = m/z 984

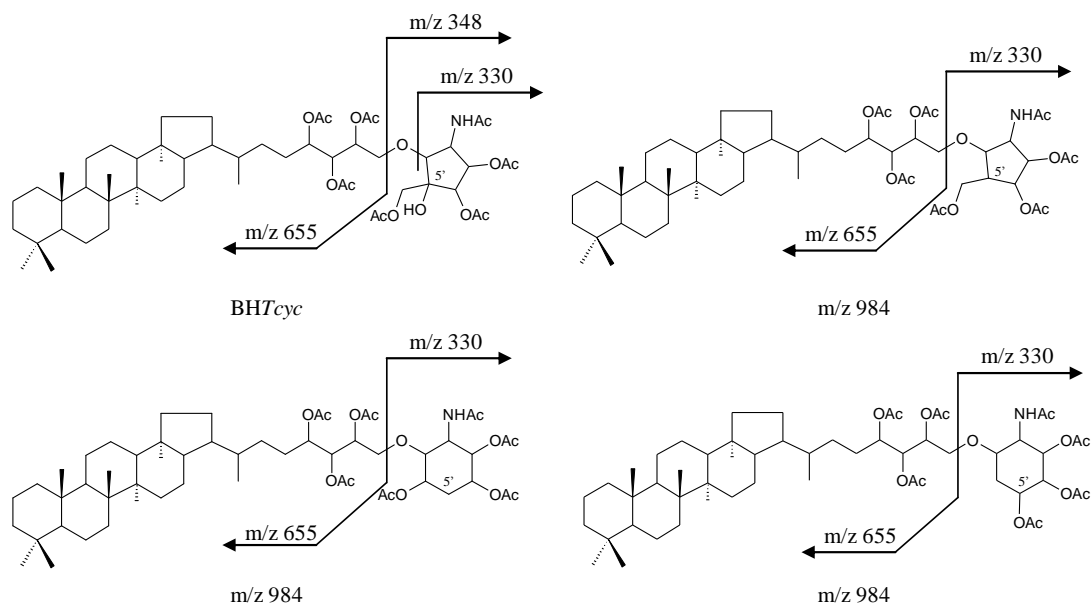


Figure 5.21 Possible structures and fragmentations that enable tentative structural assignment of novel BHP relating to  $m/z$  984. BHTcyc ( $m/z$  1002) shown for comparison.

#### 5.4.3 OTHER NOVEL BHPs

Compounds with  $[M+H]^+ = m/z$  1100 and 1114 have been identified in non-active sinters from LR. These compounds have been tentatively identified as BHPs, however, it is on the basis of unusual fragmentations. In this case, much of the characteristic structural information is contained within the  $MS^3$  spectrum. The  $MS^2$  appears to show a novel group of BHPs with unprecedented structural complexity. The compounds appear to contain an ‘anhydro-type’ side-chain component with a tethered glycolipid component. Assignment of ions can be found in Table 5.5. As an example fragmentations observed during APCI  $MS^n$  of  $m/z$  1100 are discussed. For instance, multiple losses of  $CH_3COOH$  from  $[M+H]^+$  are observable, i.e.  $m/z$  1040, 980 and 920. Multiple losses of  $CH_3COOH$  are observable from  $m/z = 940$ , i.e.  $m/z$  880 and 820 and are also observable from  $m/z = 958$ . The major ion present in the  $MS^2$  spectrum of  $[M+H]^+ = m/z$  1100 is  $m/z$  753 (DFR; Figure 5.23) which corresponds to neutral loss of 347 Da (TGOH) from  $[M+H]^+$ . The major ion present in the

$MS^2$  spectrum of  $[M+H]^+ = m/z$  1114 is  $m/z$  767 (DFR). This indicates loss of glycoside functionality, which is evidenced by the presence of ions at  $m/z$  348 ( $[TGOH_2]^+$ ) and 330 (TG) and suggests the presence of a cyclitol or glucosamine moiety. Consideration of this spectral data, i.e. the presence of ions at  $m/z$  611 (DF) and 348 suggest that this particular compound with  $[M+H]^+ = m/z$  1100 possesses an ‘anhydro-type’ side-chain conformation, an ether-linked glycoside functionality of  $m/z$  330 and an unknown functionality of  $m/z$  144 (R). Likewise,  $[M+H]^+ = m/z$  1114 possesses an ‘anhydro-type side-chain component, a glycoside, and an unknown component with  $m/z$  158 (R).

APCI- $MS^3$  spectrum was obtained via fragmentation of the most abundant ion from the  $MS^2$  spectrum, i.e.  $m/z$  753 (DFR). The major fragment ion in the APCI- $MS^3$  spectrum is  $m/z$  611 (DF). The spectrum is similar to that obtained during fragmentation of adenosylhopane (**2**) and other ‘Anhydro-type’ BHPs (**2**, **3**; Talbot *et al.*, 2007a). Loss of  $CH_3COOH$  from  $m/z$  611, i.e.  $m/z$  551 and 491 indicate a di-hydroxyl containing fragment. Further loss of 18 Da, i.e.  $m/z$  473 indicates the presence of an ether-oxygen functionality and provides further evidence for the presence of an anhydro-type BHP compound. These fragmentations could also indicate a compound similar to the ‘oxo-BHPs’ described above (Section 5.3.2), however, the retention times indicate a compound similar to AnhydroBHT.

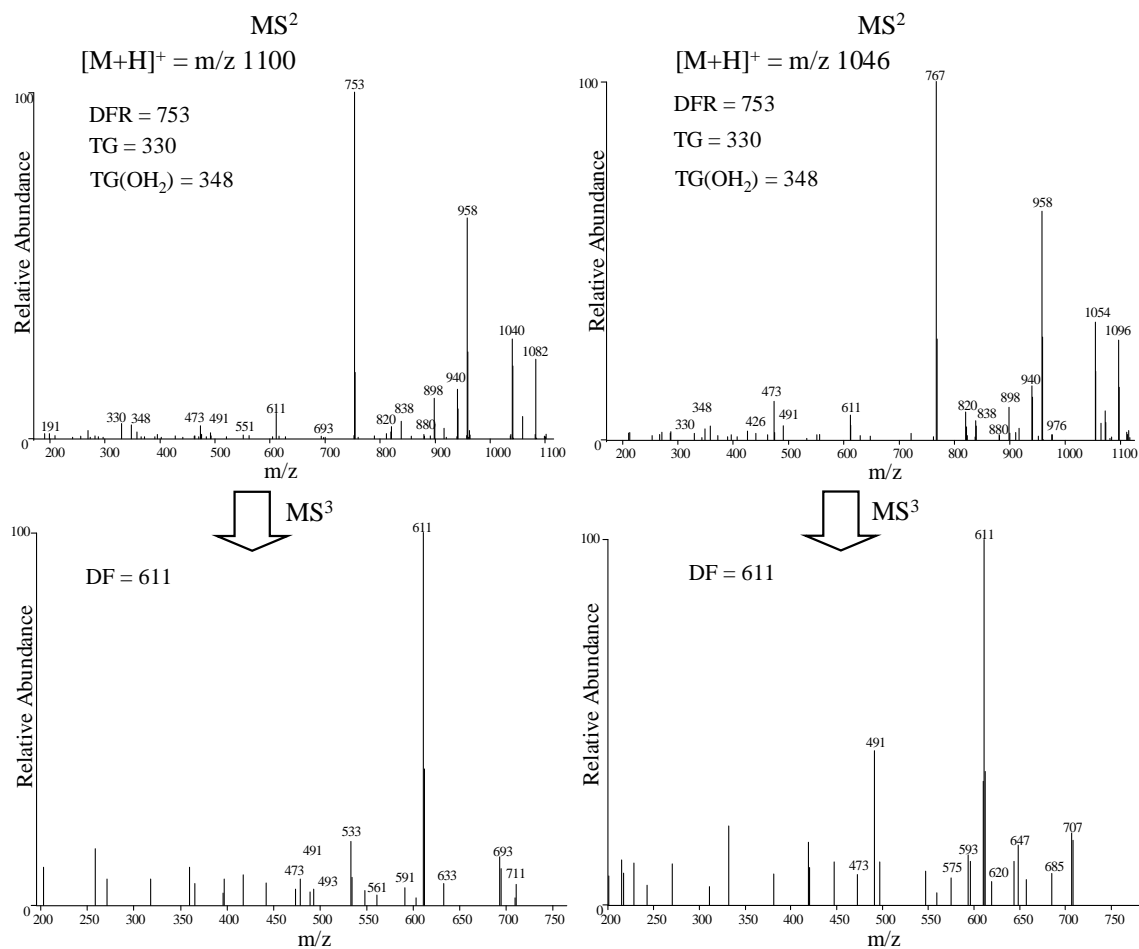


Figure 5.22 MS<sup>2</sup> and MS<sup>3</sup> spectra of novel BHPs with [M+H]<sup>+</sup> = m/z 1100 and m/z 1114. Left: MS<sup>2</sup> (top) and MS<sup>3</sup> (bottom) spectrum of m/z 1100. Right: MS<sup>2</sup> (top) and MS<sup>3</sup> (bottom) spectrum of m/z 1114

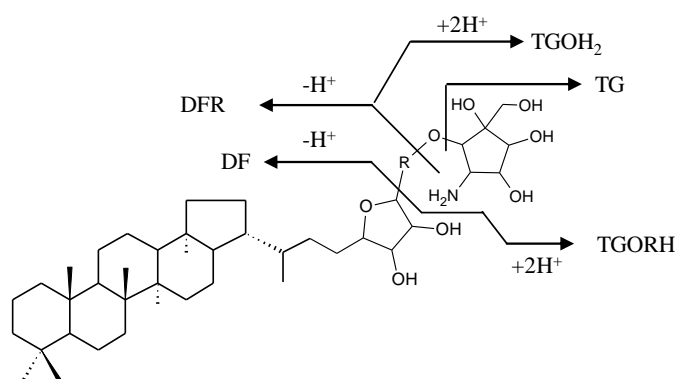


Figure 5.23 Putative structure showing main fragmentations observed during APCI-MS<sup>n</sup> analysis of [M+H]<sup>+</sup> = m/z 1100 and 1114. R = 144 and 158 for [M+H]<sup>+</sup> = m/z 1100 and 1114 respectively.

Table 5.5 Characteristic ions observed during APCI fragmentations of tentatively assigned novel BHPs.

Ion/Structure		
[M+H] <sup>+</sup>	1100 <sup>a</sup>	1114 <sup>a</sup>
[M+H - 18] <sup>+</sup>	1082	1096
[M+H - AcOH] <sup>+</sup>	1040	1054
[M+H - 2AcOH] <sup>+</sup>	980	994
[M+H - 3AcOH] <sup>+</sup>	920	934
TG	330	330
TGOH	348	348
[M+H - TGOH] <sup>+</sup>	753 <sup>b</sup>	767 <sup>b</sup>
R	144	158
[M+H - (R + TGOH)] <sup>+</sup>	611 <sup>c</sup>	611 <sup>c</sup>
[M+H - AcOH] <sup>+</sup>	551 <sup>c</sup>	551 <sup>c, d</sup>
[M+H - 2AcOH] <sup>+</sup>	491 <sup>c</sup>	491 <sup>c</sup>
[M+H - (2AcOH + 18)] <sup>+</sup>	473 <sup>c</sup>	473 <sup>c</sup>
AB	192 <sup>c</sup>	192 <sup>c</sup>
[M+H - (AB + R + TGOH)] <sup>+</sup>	561 <sup>c</sup>	575 <sup>c</sup>

<sup>a</sup> parent ion of MS<sup>2</sup> spectrum. <sup>b</sup> parent ion of MS<sup>3</sup> spectrum. <sup>c</sup> ions observed in MS<sup>3</sup> spectrum. <sup>d</sup> expected ion not observed. TG = C<sub>35</sub> ether-linked Terminal Group ion. AB = A + B rings produced during C-ring cleavage. R = 144 for m/z 1100 and 158 for m/z 1114. AcOH = CH<sub>3</sub>COOH. Fragmentations shown in Figure 5.23

## Chapter 5

Table 5.6 Abundance of tentatively-assigned BHPs observed in the study of floc, active and non-active sinters from TVZ and ETGF.

Sample <sup>a</sup>	[M+H] <sup>+</sup> = m/z																		
	1144	958	1016	611 <sup>b</sup>	669 <sup>b</sup>	960	1018	1146	1204	1198	1256	1032	1046	974	988	984	1100	1114	
CPf	- <sup>c</sup>	-	-	-	-	-	-	-	-	-	-	-	-	-	-	-	-	-	-
CP1	-	0.1	-	-	-	-	-	-	-	-	-	-	-	-	-	-	-	-	-
CP3	-	tr <sup>d</sup>	-	0.06	tr	-	-	-	-	-	-	-	-	-	-	-	-	-	-
CP6	-	0.1	-	-	-	0.09	-	-	-	-	-	-	-	-	-	-	-	-	-
CP7	-	0.1	-	0.15	-	-	-	-	-	-	-	-	-	-	-	-	-	-	-
CP8	-	0.53	0.02	0.26	0.03	-	0.02	-	-	-	-	-	-	-	-	-	-	-	-
CP11	tr	0.22	0.06	0.15	0.06	-	-	-	-	-	-	-	-	-	-	-	tr	tr	-
CP5	-	2.97	-	10.63	-	-	17.74	-	-	-	-	-	-	-	-	-	-	-	-
LR2A	-	0.03	-	0.1	-	-	-	-	-	-	-	-	-	-	-	-	-	-	-
LR2AS	-	0.04	-	-	-	-	-	-	-	-	-	-	-	-	-	-	-	-	-
LR3A	0.16	0.1	-	0.06	-	-	tr	-	-	-	-	-	-	-	-	-	-	-	-
LR3N	-	0.6	0.02	0.98	-	-	-	-	-	-	-	-	-	-	-	0.27	-	-	-
LR4N	-	0.18	-	-	-	-	0.14	-	-	-	-	-	-	-	-	-	-	-	-
LR5R	-	0.17	-	-	-	0.81	0.06	-	-	-	-	-	-	-	-	-	0.01	0.01	-
LR6R	-	0.25	-	0.01	-	-	-	-	-	-	-	-	-	-	-	-	-	-	-
OK1A-T	-	-	-	-	-	-	-	-	-	-	-	-	-	-	-	-	-	-	-
OK1A-M	-	-	-	-	-	-	-	-	-	-	0.01	-	-	-	-	-	-	-	-
OK1A-B	-	-	-	-	-	-	-	-	-	-	-	-	-	-	-	-	-	-	-
OK3A	-	0.34	-	-	-	-	0.34	-	-	-	-	-	-	-	-	-	-	-	-
OK4N	-	-	-	-	-	-	-	0.14	0.27	-	-	-	-	-	-	-	-	-	-
OK5N	-	-	-	-	-	-	-	-	-	-	-	-	-	-	-	-	-	-	-
OK6N	-	-	-	-	-	-	-	-	-	-	-	-	-	-	-	-	-	-	-
RK2N	0.6	2.64	0.07	1.05	-	-	-	-	-	-	-	-	-	-	-	0.73	-	-	-
RK3N	-	1.26	-	0.9	0.12	-	-	-	-	-	-	-	-	-	-	-	-	-	-
OP2A	-	-	-	-	-	-	-	-	-	-	-	-	-	-	-	-	-	-	-
OP7A	-	-	-	-	-	-	-	-	-	-	-	-	2.2	-	-	-	-	-	-
OP4N	-	-	-	-	-	-	-	-	-	-	-	-	-	-	-	-	-	-	-
OP5N	-	-	-	-	-	-	-	-	-	-	-	-	-	-	-	-	-	-	-
OP6N	-	-	-	-	-	-	-	-	-	-	-	-	-	-	-	-	-	-	-
ET1A	-	-	-	-	-	-	-	-	-	-	-	-	-	-	-	-	-	-	-
ET25A	-	-	-	-	-	-	-	-	-	-	-	0.01	-	-	-	-	-	-	-
ET26A	-	-	-	-	-	-	-	-	-	-	-	-	-	-	-	-	-	-	-

<sup>a</sup>Samples: CP = Champagne Pool, LR = Loop Road, OK = Orakei Korako, RK = Rotokawa, OP = Opaheke Pool, ET = El Tatio. <sup>b</sup> [M+H - AcOH]<sup>+</sup>. <sup>c</sup> - indicates not detected. <sup>d</sup> tr indicates trace amounts detected. Abundances are given as  $\mu\text{g}\cdot\text{g}^{-1}$  dry material. Structures presented in order of appearance through Chapter 5.

Novel BHPs

Table 5.7 Abundance of tentatively-assigned BHPs observed in the study of microbial mats from geothermal regions in TVZ, Nevada and California

Sample <sup>a</sup>	[M+H] <sup>+</sup> = m/z																				
	1144	958	1016	611 <sup>b</sup>	669 <sup>b</sup>	960	1018	1074	1132	1190	1146	1204	1198	1256	1032	1046	974	988	984	1100	1114
GBS03	- <sup>c</sup>	-	-	-	-	-	-	-	-	-	-	-	-	-	-	-	-	-	-	-	-
GBS08	-	-	-	-	-	-	-	-	-	-	-	-	-	-	0.3 <sup>e</sup>	0.47 <sup>e</sup>	-	-	-	-	-
GBS12	-	-	-	-	-	-	-	-	-	-	-	-	-	-	3.61 <sup>e</sup>	3.41 <sup>e</sup>	-	-	-	-	-
GBS18	-	-	-	-	-	-	-	-	-	-	-	-	-	-	0.41 <sup>e</sup>	0.61 <sup>e</sup>	-	-	-	-	-
GBS19	-	-	-	-	-	-	-	-	-	-	-	-	-	-	-	-	-	-	-	-	-
SV2ConSo <sup>d</sup>	-	-	-	-	-	-	-	-	-	-	-	-	-	-	-	-	-	-	-	-	-
SV2Con1	-	-	-	-	-	-	-	-	-	-	-	-	-	-	0.18 <sup>e</sup>	0.16 <sup>e</sup>	-	-	-	-	-
SV2Con2	-	-	-	-	-	-	-	-	-	-	-	-	-	-	-	-	-	-	-	-	-
SV2Con3	-	-	-	-	-	-	-	-	-	-	-	-	-	-	0.03 <sup>e</sup>	0.01 <sup>e</sup>	-	-	-	-	-
SV2Con4	-	-	-	-	-	-	-	-	-	-	-	-	-	-	-	-	-	-	-	-	-
SV2Con5	-	-	-	-	-	-	-	-	-	-	-	-	-	-	0.36 <sup>e</sup>	0.81 <sup>e</sup>	-	-	-	-	-
SV2Con6	-	-	-	-	-	-	-	-	-	-	-	-	-	-	-	-	-	-	-	-	-
RHC-So <sup>d</sup>	-	-	-	-	-	-	-	-	-	-	-	-	-	-	-	-	-	-	-	-	-
RHC04	-	-	-	-	-	-	-	-	-	-	-	-	-	-	-	-	-	-	-	-	-
RHC05	-	-	-	-	-	-	-	-	-	-	-	-	tr <sup>f</sup>	tr <sup>f</sup>	-	-	-	-	-	-	-
RHC06	-	-	-	-	-	-	-	-	-	-	-	-	-	-	-	-	-	-	-	-	-
RHC07	-	-	-	-	-	-	-	-	-	-	-	-	-	-	-	-	-	-	-	-	-
PV <sup>g</sup>	-	-	-	-	-	-	-	-	-	-	-	-	-	-	-	-	-	-	-	-	-
EV1 <sup>g</sup>	-	-	-	-	-	-	-	-	-	-	-	-	-	-	-	-	-	-	-	-	-
EV47	-	-	-	-	-	-	-	-	-	-	-	-	-	-	-	-	-	-	-	-	-
OK	-	-	-	-	-	-	-	-	-	-	-	-	-	-	0.21 <sup>e</sup>	1.52 <sup>e</sup>	0.21	1.39	-	-	-

<sup>a</sup>Samples: GBS = Great Boiling Spring, SV = Surprise Valley, RHC = Ricks' Hot Creek, PV = Paradise Valley, EV = Eagleville, OK = Orakei Korako. <sup>b</sup> [M+H - AcOH]<sup>+</sup>.

<sup>c</sup> - indicates not detected. <sup>d</sup> So = Source. <sup>e</sup> combined abundances of two isomers. <sup>f</sup> tr indicates trace amounts present (<0.005 µg.g<sup>-1</sup> dry material). <sup>g</sup> used in Zhang et al.,

2007. Abundances are given as µg.g<sup>-1</sup> dry material. Structures presented in order of appearance through Chapter 5.

## 5.5 DISCUSSION

Recently the work of Talbot and co-workers (e.g. 2001; 2003a; 2005; 2007a, b and references therein) and in particular the application of high performance liquid chromatography-mass spectrometric (HPLC-MS) methodology to the analysis of BHP distributions in environmental matrices and bacterial cultures has added new impetus to the application and usefulness of BHPs and hopanoids as markers for bacterial populations in sedimentary environments. The major success of this work is that this method allows separation of heterogeneous mixtures of highly polar, non-volatile compounds. Classically, analyses of the distribution of BHPs, hopanoids, hopanes and hopanoic acids in cultures and environmental matrices relied on a reductive cleavage of vicinal hydroxyl groups; a derivitisation which resulted in a corresponding mono-functionalised homohopanol, however, this method also removes all structural variety from the side-chain. The relationship between the structural complexity of a BHP molecule and its biological function is not well understood; however, the number of functional groups contained within the molecule can be indicative of certain groups of organisms and is therefore a useful tool when assessing bacterial populations occurring in environmental matrices. Atmospheric Pressure Chemical Ionisation High Performance Liquid Chromatography Multistage Mass Spectrometry (APCI HPLC-MS<sup>n</sup>) analysis of derivitised per-acetylated BHP compounds allows deduction of characteristic fragmentation pathways (e.g. Talbot *et al.*, 2003a, b; Talbot *et al.*, 2007a, b). This enables subtle structural nuances to be distinguished that contribute further to more accurate, and rapid, method of characterising lipid assemblages in bacterial cultures and sedimentary depositions.

However, the utility of this class of compound relies upon a better understanding of the extent of BHP-producing organisms and the pathways of biosynthesis within these organisms.

BHPs in the majority are produced by mainly aerobic bacteria. Yet somewhat paradoxically BHP biosynthesis occurs independently of molecular oxygen. Several reports, dating back to 1985 (Schmidt *et al.*, 1986) demonstrate BHP-biosynthesis in bacterial cultures grown under anaerobic conditions. Until recently BHP-biosynthesis was unconfirmed in strictly anaerobic bacterial species (Sinninghe Damsté *et al.*, 2004; Hartner *et al.*, 2005; Blumenberg *et al.*, 2006), however, along with the presence of strongly  $\delta^{13}\text{C}$  depleted hopanoids in the black sea (e.g. Thiel *et al.*, 2003) has shown that this traditional view needs re-evaluation.

It would be unreasonable to suggest that a complete survey of BHP-producing bacteria in all environmental conditions would be possible so new methods of screening (Krisnamurthy and Ross, 1996) and new methods for culturing bacteria (e.g. Head *et al.*, 2000; Gray and Head, 2000) are required. Comparative surveying of genomic databases for particular genes involved with BHP-biosynthesis have shown that a great number of bacteria contain the necessary machinery to synthesise the hopane hydrocarbon moiety (Fischer and Pearson, 2007). Although estimates of the true extent of the distribution of BHP biosynthesis either via surveying taxonomic groups or observing the distribution of gene sequences encoding for squalene cyclases throughout bacteria seem to be rather variable (Rohmer *et al.*, 1984; Pearson *et al.*, 2007), and it may be worthwhile to consider that the presence of squalene cyclase is still not *defacto* evidence for the presence of BHP-biosynthesis.

Further investigations are required to determine the origin and nature of ribose-derived side-chain in order to fully appreciate the structural variety observed in BHP biosynthesis. Undeniably, analysis of 'intact' BHPs has improved the utility of hopanoids and BHPs as biomarkers but it has also opened up questions as to the extent of the lipid repertoire of this class of compounds as each novel BHP-lipid is indicative of a novel biochemical pathway that potentially may have uses that reach further than geochemical interpretations (e.g. Nagumo *et al.*, 1991; Moreau *et al.*, 1997). As investigations concerning the gene sequences that encode

for enzymatic activity intrinsic to BHP biosynthesis are further investigated and the full extent of the diversity and nature of structural complexity contained within a BHP-lipid are undertaken it may be necessary to re-address the issue that BHPs are the evolutionary precursor to sterols (Volkman, 2005; Summons *et al.*, 2006, Fischer and Pearson, 2007). Similarities between the mechanisms of formation and steric dimensions of hopane and sterane hydrocarbons suggest that the primary function of the two may be similar, i.e. molecular architecture within the lipid membrane. However, it would appear counter-intuitive that the apparent plethora of structural variety contained within C-5 side chain of a BHP molecule is accidental and suggests that BHP molecules may serve currently undetermined secondary applications (e.g. Bolanos *et al.*, 2004).

#### 5.5.1 IDENTIFICATION OF NOVEL BACTERIOHOPANEPOLYOLS IN

##### ENVIRONMENTAL MATRICES AND BACTERIAL CULTURES

Traditionally identification of novel BHP compounds required mass cultivation of a known BHP-producing bacterial species in order to isolate a suitable amount of lipid for structural characterisation via  $^1\text{H}$  or  $^{13}\text{C}$  NMR analysis (e.g. Langworthy *et al.*, 1976; Rohmer *et al.*, 1984; Neunlist and Rohmer, 1985a, b, c; Zundel and Rohmer, 1985a, b; Neunlist *et al.*, 1988; Bisseret and Rohmer, 1989; Flesch and Rohmer, 1989; Herrmann *et al.*, 1996a; Seeman *et al.*, 1999; Rosa-Putra *et al.*, 2001). The compounds reported in this section of the thesis remain tentatively-assigned as novel BHPs and are based upon characteristic fragmentations (e.g. Talbot *et al.*, 2003a, b; Talbot *et al.*, 2007a, b) that are based upon the structural identification made by the authors above. Potential novel BHPs can be identified by the presence of fragments that are diagnostic for a BHP containing a particular degree of functionalisation (DF; Table 5.10). Many of the compounds reported here contain this fragment along with a further chemical functionality. This additional functionality can be identified by subtracting the neutral fragment loss of DF from the parent mass of the  $\text{MS}^n$

spectra. This can be positively identified by the presence of an ion at the corresponding  $m/z$  value in the mass spectrum. Other expected fragmentations relating to loss  $\text{CH}_3\text{COOH}$  or loss of ring-C cleavage products (AB) provide further evidence of the presence of a peracetylated BHP compound (e.g. Talbot *et al.*, 2003a, b; Talbot *et al.*, 2007a, b).

Table 5.8 Diagnostic ions of tetra-, penta- and hexa-functionalised BHPs

Ion ( $m/z$ )	Degree of functionalisation contained within BHP-side chain component
655	Tetra-functionalised BHP
669	Tetra-functionalised BHP + A-ring methylation
713	Penta-functionalised BHP
727	Penta-functionalised BHP + A-ring methylation
771	Hexa-functionalised BHP
785	Hexa-functionalised BHP + A-ring methylation
611	'Anhydro-type'
671	'Anhydro-type' + hydroxyl group located at C-31
653	Tetra-functionalised BHP + mono-unsaturated C-ring
651	Tetra-functionalised BHP + di-unsaturated C-ring
711	Penta-functionalised BHP + mono-unsaturated C-ring
709	Penta-functionalised BHP + di-unsaturated C-ring

### 5.5.2 NOVEL BACTERIOHOPANEPOLYOLS

The detection of novel BHP compounds may indicate the presence of a novel-BHP producing bacterial species, previously known BHP-producing bacteria which produce a different assemblage of compounds under these environmental settings or a novel diagenetic pathway. The tentative structural determination of several novel BHP compounds is possible because they form a more functionalised counterpart of a previously assigned BHP structure. Although structural characterisations remain tentative, this report represents the first

observation of these compounds. As more environmental situations and bacteria cultures are analysed these compounds are likely to form part of a more elaborate lipid inventory than is currently understood.

#### 5.5.2.1 GUANIDINE-SUBSTITUTED BACTERIOHOPANEPENTOL CYCLITOL ETHER

Tetra-functionalised, Guanidine-substituted BHT<sub>cyc</sub> was originally detected in *Methylobacterium organophilum* (Renoux and Rohmer, 1985) and subsequently detected in pink-pigmented facultative methanotrophs (Knani *et al.*, 1994; Section 1.8). Therefore it would be intuitive to suggest that this compound would derive from bacteria possessing methylotrophic metabolic capabilities. The presence of a novel penta-functionalised homologue of (24) may be a strategy to maintain membrane integrity under the environmental conditions of geothermal vents.

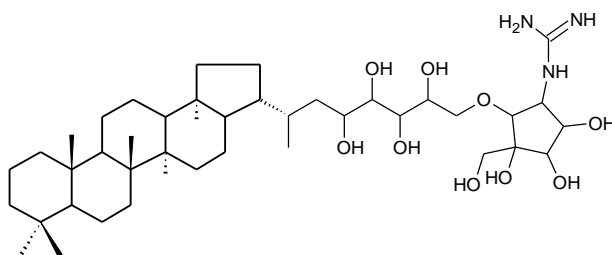


Figure 5.24 Tentative structural assignment of guanidine-substituted BHP<sub>cyc</sub>

## 5.5.2.2 OXO BACTERIOHOPANEPOLYOLS

Four novel BHP structures have been detected throughout analyses of TVZ sinters and have been tentatively assigned as *oxo-BHP<sub>cyc</sub>*, *oxo-BHT<sub>cyc</sub>*, *oxo-BH<sub>tetrol</sub>*, and *oxo-BH<sub>triol</sub>* (Figure 5.26). Structurally similar *oxo-BHT<sub>gly</sub>* (**24**) was first detected in *Zymomonas mobilis* (Flesch and Rohmer, 1989; Figure 5.27) when grown under micro-aerophilic conditions. The assignment of these compounds remains tentative and is based upon structural determination made by Flesch and Rohmer (1989) and Talbot *et al.* (2007a). As mentioned in Section 3.3.1.2, these compounds likely derive from currently unidentified, thermophilic bacteria colonising micro-aerated portions of the pool. *Oxo-BH<sub>triol</sub>* and *oxo-BH<sub>tetrol</sub>* may derive from loss of composite group from more functionalised *oxo-BHT<sub>cyc</sub>* and *oxo-BHP<sub>cyc</sub>*.

The biosynthesis of more functionalised BHP compounds must be a mechanism by which BHP-producing bacteria colonising the vent and locality maintain the integrity of the cell membrane. Whether this additional functionality is a response to temperature or pH remains to be determined, however, indicates a novel biochemical pathway.

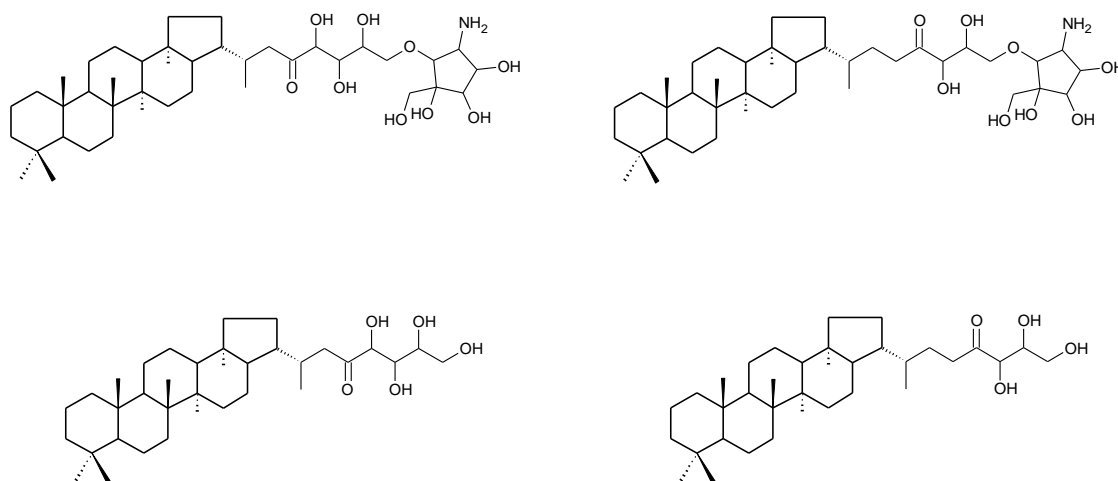


Figure 5.25 *Oxo-BHPs*. Tentative structural characterisation of structures detected in CP sinters

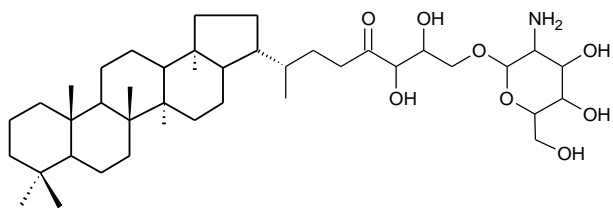


Figure 5.26 oxo bacteriohopanetetrol glucosamine (24). Flesch and Rohmer, 1989.

### 5.5.2.3 NOVEL COMPOSITE-BHPs

It has been possible to provide partial structural identification to a number of novel composite BHPs that contain a currently-unidentified chemical moiety. It has been shown that production of composite BHPs, such as BHT<sub>cyc</sub> and BHP<sub>cyc</sub>, increases when incubation temperature increases or pH decreases. It is therefore plausible to suggest that bacteria produce these compounds to counteract the environmental conditions that prevail at the sample locations investigated during this study. However, the variety of the structures described suggests that compounds either derive from unknown BHP-producing bacteria or form part of a secondary metabolic purpose other than simply membrane re-enforcement.

Previously identified high molecular weight BHPs (i.e. BHPs with  $[M+H]^+ > m/z$  1200) are known to contain fatty acid residues which are bonded to C-35 ether-linked composite functionalities (i.e. Talbot *et al.*, 2007a). However without further spectroscopic characterisation it is impossible to gain further structural information. The occurrence of this compound at two high temperature vents is discussed in Chapter 3, Section 3.4.5

Table 5.9 Tentatively-assigned novel BHPs as identified during APCI MS<sup>n</sup> analysis

[M+H] <sup>+</sup> =	Side-chain conformation (DF)	TG	TGOH	[TGOH <sub>2</sub> ] <sup>+</sup>
960	Tetra	287 (m/z 288)	305	306
1018	Penta	287 (m/z 288)	305	306
1146	Penta	415 (m/z 416)	433	434
1204	Hexa	415 (m/z 416)	433	434
1198	Tetra	525 (m/z 526)	543	544
1256	Penta	525 (m/z 526)	543	544
1032	Penta	-	301	302
1046	Penta	-	301	302
974	Tetra	-	301	302
988	Tetra	-	301	302
1100	Anhydro-type	329 (m/z 330)	347	348
1144	Anhydro-type	329 (m/z 330)	347	348

## 5.6 CONCLUSIONS

HPLC/MS methodologies have been very successful in extending the inventory of biomarkers leading to more accurate investigations of the biogeochemistry of modern ecosystems (Hopmans, *et al.*, 2000; Talbot *et al.*, 2003a; b; Sturt *et al.*, 2004; Weijers *et al.*, 2006; Van Mooy *et al.*, 2006). Throughout the study of the distribution of BHPs deriving from bacteria colonising terrestrial vents and surrounding vicinity has shown that there remains a significant number of BHP structures that further extends the observations of structural variants of BHPs in bacteria. As the bacterial populations of environments that have previously received little or no attention with respect to BHP distributions are studied, it is highly likely that the current inventory of BHP compounds will be extended further. As this library of compounds increases, more accurate reconstructions and improvement in the utility of BHPs as biomarkers in recent environments will be possible. However, it is necessary to note that the ever expanding repertoire of BHP lipids provides evidence that the cellular

function of BHPs is more complex than to only provide rigidity and BHPs likely serve as compounds with secondary purposes.

During this study, eighteen compounds have been identified as novel BHPs. This includes compounds that contain characteristic mass spectral fragmentations and have been found to occur in more than one sample or appear to form part of a homologous series. The mass spectra of a number of other potential candidates are reported in the Appendix. Furthermore, BHPs were found to be widespread throughout the sample suite of sinters and microbial mats. Novel oxo-BHP signatures detected in sinters from the TVZ are thought to derive from bacteria inhabiting the air-water interface, whilst novel BHP-signatures from mat-forming consortia are assumed to derive from ‘*Synechococcus*-like’ cyanobacteria (See Chapter 3, Section 3.4.4) for further discussion.

The work in this study imparts itself directly at the intersection of extremophilic microbial biochemistry and geochemistry, whilst providing a record and reference point for future projects concerned with the geochemical investigations of modern bacterial communities.

## 6 INVESTIGATING BHP DIAGENESIS IN SILICA SINTERS

### 6.1 INTRODUCTION

In order to complement previous chapters concerning the distribution of polyfunctionalised BHPs that derive from bacteria colonising various geothermal locations from around the world a survey of degraded and non-extended hopanoids, geohopanoids, has been carried out. Geohopanoids are the molecular fossils of BHPs and are abundant in sedimentary and bituminous matter dating back to the Archean (Eigenbrode *et al.*, 2008). The composition of distributions of geohopanoids is determined by precursor biota and any post-depositional diagenetic processes. Investigation of modes of diagenesis affecting hopanoid distributions provides evidence that enables this class of compound to be used as recognisable molecular fossils (Farrimond *et al.*, 2000, 2004). A variety of post-depositional diagenetic processes dictates that a number of products are possible from one precursor molecule (e.g. Simoneit, 1996; See Chapter 1, Section 1.8 for further discussion).

The application of geohopanoids as biomarkers for paleo-environments relies upon a reliable assessment of their origin and diagenetic fate across a range of depositional environments. The processes involved in the initial steps of degradation of BHPs are not well understood as contrasting reports exist detailing rapid diagenesis and incorporation into macromolecular aggregates (Farrimond *et al.*, 2003) and also long-term preservation of BHPs in sedimentary material. For instance, a number of BHPs have been detected in sediments of the Congo fan dating back to 1.2 Mya before present (Cooke *et al.*, 2008a; Handley *et al.*, 2009) and BHtetrol (**1**) has been detected in sediments upto 50 Mya (Mega annum; van Dongen *et al.*, 2006). However, the side-chain remains a labile molecular component and has been shown to be readily degraded upon deposition (Sinninghe Damsté *et al.*, 1995; Rodier *et al.*, 1999; Schaeffer *et al.*, 2008). AnhydroBHT (**2**) has been detected in sediments dating back to the Jurassic

(Bednarczyk *et al.*, 2005). The presence of contradicting reports arises because a large variety of BHP compounds, many of which remain uncharacterised (See Chapter 5 for examples), are likely produced by a huge inventory of contributing organisms.

The complex reactions that affect BHP preservation remain largely unresolved (e.g. Brocks and Summons, 2004) and dictate that investigations concerning the initial stages of BHP diagenesis in a range of sedimentary environments are important in interpreting BHP and geohopanol distributions in ancient settings.

Previous studies concerning the diagenesis of BHPs in lake and marine sediments has shown that oxidative processes result in sequential degradation of chemical functionality within the side-chain moiety (Farrimond *et al.*, 2000; Watson, 2002).

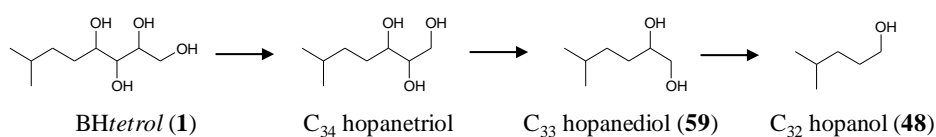


Figure 6.1 Formation of C<sub>32</sub> ββ hopanol (48) from BHtetrol(1) via sequential degradation of side-chain component (Watson, 2002)

However, it has been suggested the oxidation of alcohols to carboxylic acids and subsequent decarboxylation is the primary mechanism of side-chain degradation (Sinninghe Damsté *et al.*, 1995; Brocks and Summons, 2004).

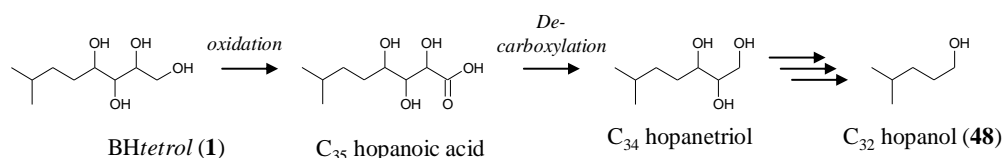


Figure 6.2 Formation of C<sub>32</sub> ββ hopanol(48) from BHtetrol (1) via oxidation and decarboxylation of terminal alcohol group (e.g. Sinninghe Damsté *et al.*, 1995)

AnhydroBHT (**2**) is an important component of geohopanoid distributions (e.g. Bednarczyk *et al.*, 2005; Talbot *et al.*, 2005). AnhydroBHT (**2**) has been shown to be formed via cyclisation of tetra-functionalised side-chain (Schaeffer *et al.*, 2008; Figure 6.3). Alternatively, loss of adenine moiety from adenosylhopane (**6**) is another potential source (Bednarczyk *et al.*, 2005; Cooke *et al.*, 2008b; Figure 6.4). However, adenosylhopane (**6**) is only found in BHP distributions of soils (e.g., Cooke *et al.*, 2008a) or environments with a large input from terrestrial run-off (e.g. Talbot and Farrimond, 2007; Cooke *et al.*, 2008b) and is not thought to be a major source of sedimentary anhydroBHT (**2**).

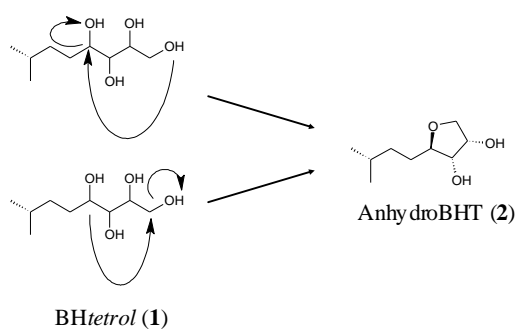


Figure 6.3 Formation of AnhydroBHT (**2**) via intramolecular cyclisation of BHtetrol (**1**) (Schaeffer *et al.*, 2008).

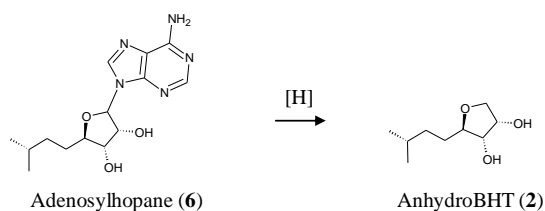


Figure 6.4 Hypothetical formation of AnhydroBHT (**2**) from Adenosylhopane (**6**).

Previous reports of geohopanoids preserved in silica sinters from geothermal environments are relatively scarce (Pancost *et al.*, 2005, 2006; Talbot *et al.*, 2005; Kaur, 2009). These initial investigations showed that geohopanoids are sufficiently well preserved that interpretations and reconstructions of bacterial populations over time and changing

environmental condition are possible. However, no investigations of BHP-degradation pathways were reported. AnhydroBHT (2) was shown to be present in sinters from CP and RK (Talbot *et al.*, 2005), and hopanoic acids have been shown to be present in the range of samples used within this study (Kaur, 2009). Assessment of geohopanoic acid distributions from ‘extreme’ environmental conditions allows constraints to be developed concerning the origin and distribution of geohopanoic acids that are used in paleo-environmental reconstructions.

## 6.2 AIMS

The work in this chapter aims to describe the distribution of the intermediate products of BHP diagenesis including free hopanols, free hopanediols and triols, anhydroBHPs, hopanals and hopanoic acids that are formed during the diagenesis of BHPs preserved in silica sinters of TVZ and ETGF. The general objective of this research is to gain insight into the initial stages of degradation of BHPs preserved in a silica sinter. Diagenetic end members such as hopanes, diahopanes and nor-hopanes or hopanoic-acid compounds that become incorporated in macromolecular aggregates are not the focus of this study.

- Observe any common diagenetic pathways that occur in this particular depositional setting and expand current understanding of the effect of environmental situation in determining observed geohopanoic acid distributions
- Interpret the extent to what geohopanoic acid distributions reflect biohopanoic acid input
- Examine distributions of geohopanoic acids preserved in active and non-active silica sinters, extrapolate and assess the possibility of using geohopanoic acids as biomarkers for ancient geothermal populations

### 6.3 RESULTS

The geohopanooid distributions preserved in siliceous sinter samples collected from a number of geothermal locations are described below. The loss of chemical functionality during early-stages of diagenetic transformation means geohopanooids are no longer suitable for analysis using LC-MS<sup>n</sup>. Using Gas Chromatography Mass Spectrometry (GC-MS), geohopanooids i.e. free hopanols and other degraded counterparts (See 1.8) are analysed as peracetylated compounds. Hopanoic acids are analysed as methyl esters (Chapter 2, Section 2.3.2.2). A summary of compounds identified by GC-MS is given in Table 6.1.

A typical *m/z* 191 chromatogram geohopanooid distribution obtained via GC-MS analysis of the acetylated fraction is shown in Figure 6.5 (actual sample LR3N). As mentioned above the purpose of this study is to investigate free hopanols (structures **46**, **47**, **48**), hopanediols and hopanetriols (**49** – **53**) and anhydroBHPs (**2** and **3**). Biohopanooids, BH*tetrol*, BH*pentol*, diploptene, Hop-21-ene and diplopterol (**1**, **13**, **4**, **4'**, **5**) are also observed during GC-MS analysis of the acetylated fraction. Where present, the abundances of biohopanooids have been reported but are not the focus of this chapter. In the example shown in Figure 6.5 an isomeric form of BH*tetrol* is also observable (indicated as **1\***). Where appropriate other mass chromatograms will be shown i.e. where distributions have been found to contain unusual or novel geohopanooids. Differences in retention times of hopanooids during analysis are caused by trimming of the GC-column during analysis. All structures contain the biological conformation 17 $\beta$ (H), 21 $\beta$ (H) unless stated.

## BHP Diagenesis

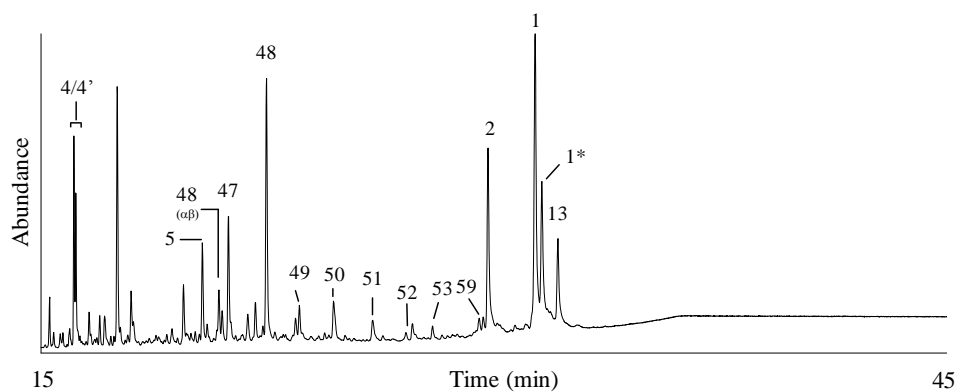


Figure 6.5  $m/z$  191 Chromatogram of acetylated fraction showing typical distribution of hopanoids.

Hopanoic acids (**55**, **56**, **57**) are analysed as methyl esters (Chapter 2, Section 2.3.2.2) and a typical distribution is given in Figure 6.6.

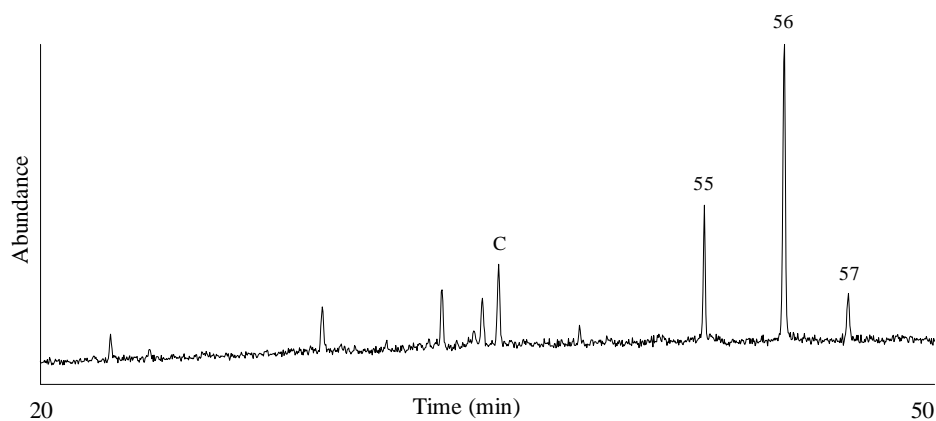


Figure 6.6  $m/z$  191 chromatogram (20 – 50 min) showing distribution of hopanoic acids. 'C' is an unknown contamination.

Table 6.1 Structures, abbreviations and peak numbers of geohopanoids used throughout the text

Peak Number <sup>a</sup>	Structure	Abbreviation
1	32,33,34,35 Bacteriohopanetetrol <sup>b</sup>	BHtetrol
2	32,35 Anhydrobacteriohopanetetrol <sup>b</sup>	AnhydroBHT
4	Diploptene <sup>b</sup>	Diploptene
4'	Hop-(17)21-ene <sup>b</sup>	Hop-21-ene
13	31,32,33,34,35 Bacteriohopanepentol <sup>b</sup>	BHpentol
46	C <sub>30</sub> 17β(H), 21β(H) hopanol	C <sub>30</sub> ββ hopanol
47	C <sub>31</sub> 17β(H), 21β(H) homohopanol	C <sub>31</sub> ββ hopanol
48	C <sub>32</sub> 17β(H), 21β(H) bishomohopanol	C <sub>32</sub> ββ hopanol
49	C <sub>31</sub> 17β(H), 21β(H) hopane 30,31 diol	C <sub>31</sub> ββ hopanediol
50	C <sub>32</sub> 17β(H), 21β(H) hopane 31,32 diol	C <sub>32</sub> ββ hopanediol
51	C <sub>33</sub> 17β(H), 21β(H) hopane 32,33 diol	C <sub>33</sub> ββ hopanediol
52	C <sub>34</sub> 17β(H), 21β(H) hopane 33,34 diol	C <sub>34</sub> ββ hopanediol
53	C <sub>33</sub> 17β(H), 21β(H) hopane 31,32,33 triol	C <sub>33</sub> ββ hopanetriol
54	C <sub>30</sub> 17β(H), 21β(H) hopanoic acid	C <sub>30</sub> ββ hopanoic acid
55	C <sub>31</sub> 17β(H), 21β(H) homohopanoic acid	C <sub>31</sub> ββ hopanoic acid
56	C <sub>32</sub> 17β(H), 21β(H) bishomohopanoic acid	C <sub>32</sub> ββ hopanoic acid
57	C <sub>33</sub> 17β(H), 21β(H) trishomohopanol	C <sub>33</sub> ββ hopanol
58	C <sub>33</sub> 17β(H), 21β(H) hopene 31,32,33 triol	C <sub>32</sub> ββ hopenetriol
59	C <sub>32</sub> 17β(H), 21β(H) hopanone	C <sub>32</sub> ββ hopanone
60	C <sub>33</sub> 17β(H), 21β(H) hopanone	C <sub>33</sub> ββ hopanone
61	C <sub>32</sub> 17β(H), 21β(H) hopane 30, 32 diol	C <sub>30, 32</sub> hopanediol

<sup>a</sup> Peak numbers refer to structures in the order that they appear throughout the text and in chromatograms provided in Figures 6.1, 6.2 and 6.3. Structure numbers of geohopanoids refer to the 17β,21β(H) conformation unless stated.

<sup>b</sup> Bacteriohopanepolyols and biohopanoids amenable to GC-MS analysis of peracetylated fractions are included for completeness.

BHP Diagenesis

Table 6.2 Abundances ( $\mu\text{g}\cdot\text{g}^{-1}$  dry sinter) of selected geohopanooids identified in active sinters of TVZ and ETGF

Geohopanooid	Struc. <sup>b</sup>	Active Sinter Sample <sup>a</sup>													
		CPf	CP1A	OK1-TA	OK1-MA	OK1-BA	OK3A	LR2A	LR2AS	LR3A	OP2A	OP7A	ET1A	ET25A	ET26A
AnhydroBHT	<b>2</b>	0.07	0.12	tr <sup>c</sup>	tr	tr	0.6	0.03	0.08	0.08	- <sup>d</sup>	0.02	0.04	-	-
C <sub>33</sub> ββ hopanol	<b>57</b>	-	-	0.06	0.03	0.01		-	-	-	-	-	-	-	-
C <sub>32</sub> ββ hopanol	<b>48</b>	-	0.16	-	tr	tr	0.2	-	0.11	0.03	-	0.01	0.01	-	-
C <sub>31</sub> ββ hopanol	<b>47</b>	-	0.6	0.01	0.01	tr	2.0	0.16	1.2	0.4	-	tr	0.16	-	0.01
C <sub>30</sub> ββ hopanol	<b>46</b>	-	-	0.02	0.01	tr	-	0.05	0.42	-	-	-	-	-	-
C <sub>34</sub> ββ hopanediol	<b>52</b>	-	0.01	-	-	-	-	-	-	-	-	-	-	-	-
C <sub>33</sub> ββ hopanediol	<b>51</b>	-	0.06	-	-	-	0.1	-	-	-	-	-	-	-	-
C <sub>32</sub> ββ hopanediol	<b>50</b>	-	0.05	-	-	-	0.12	-	-	-	-	-	-	-	tr
C <sub>31</sub> ββ hopanediol	<b>49</b>	-	0.04	tr	-	-	0.12	-	-	-	-	-	0.02	-	tr
C <sub>32</sub> ββ hopanone	<b>60</b>	-	-	-	-	-	-	-	-	-	-	-	-	-	-
C <sub>33</sub> ββ hopanone	<b>61</b>	-	-	-	-	-	-	-	-	-	-	-	-	-	-
C <sub>33</sub> ββ hopanoic acid	<b>54</b>	nd <sup>e</sup>	tr	0.06	0.63	0.26	0.76	0.15	nd	0.02	-	-	4.4	4.0	-
C <sub>32</sub> ββ hopanoic acid	<b>55</b>	nd	tr	0.64	0.75	0.17	4.0	1.7	nd	0.18	-	-	1.4	0.5	-
C <sub>31</sub> ββ hopanoic acid	<b>56</b>	nd	-	0.22	-	-	0.06	0.1	nd	0.09	-	-	-	-	-
Total geohopanooid <sup>f</sup>		0.07	0.31	1.0	1.4	0.44	8.0	2.2	1.8	0.8	0	0.03	6.0	4.5	0.01

<sup>a</sup>samples: CP = Champagne Pool, OK = Orakei Korako, LR = Loop Road, OP = Opaheke Pool, ET = El tatio. <sup>b</sup>Structures. <sup>c</sup>tr = Trace amounts

detected (<0.005  $\mu\text{g}\cdot\text{g}^{-1}$  dry sinter). <sup>d</sup>- Not detected. <sup>e</sup>nd = not determined. <sup>f</sup>total geohopanooid = total abundance of selected geohopanooids.

## Chapter 6

Table 6.3 Abundances ( $\mu\text{g.g}^{-1}$  dry sinter) of selected geohopanooids identified in non-active sinters of TVZ

Geohopanooid	Struc <sup>b</sup>	Inactive sinter sample <sup>a</sup>															
		CP3N	CP7N	CP8N	CP11N	OK4N	OK5N	OK6N	LR3N	LR4N	LR5R	LR6R	OP4N	OP5N	OP6N	RK2N	RK3N
AnhydroBHT	<b>2</b>	1.8	0.12	0.94	1.9	0.1	- <sup>c</sup>	tr <sup>d</sup>	tr	0.15	tr	0.04	0.01	0.53	2.1	1.1	1.8
C <sub>33</sub> $\beta\beta$ hopanol	<b>57</b>	-	-	-	-	-	-	-	-	-	-	-	-	-	-	-	-
C <sub>32</sub> $\beta\beta$ hopanol	<b>48</b>	0.19	0.14	0.07	0.93	-	tr	-	tr	0.04	0.01	tr	0.01	1.3	0.84	0.11	0.12
C <sub>31</sub> $\beta\beta$ hopanol	<b>47</b>	3.5	0.6	0.59	6.4	0.02	0.03	0.01	0.05	0.7	0.02	tr	0.03	3.9	3.7	0.1	0.46
C <sub>30</sub> $\beta\beta$ hopanol	<b>46</b>	0.98	-	0.44	2.2	-	tr	-	-	0.11	tr	-	-	0.39	-	0.38	0.22
C <sub>33</sub> $\beta\beta$ hopanetriol	<b>59</b>	-	-	-	-	-	-	-	-	-	tr	-	-	-	-	0.16	0.77
C <sub>34</sub> $\beta\beta$ hopanediol	<b>52</b>	0.08	0.03	-	-	-	-	-	-	-	-	-	-	-	-	-	-
C <sub>33</sub> $\beta\beta$ hopanediol	<b>51</b>	0.06	0.04	0.03	-	-	-	-	tr	-	tr	-	-	0.45	0.23	-	0.11
C <sub>32</sub> $\beta\beta$ hopanediol	<b>50</b>	0.12	0.06	0.09	0.4	0.01	-	-	0.01	tr	-	-	-	-	-	-	0.1
C <sub>31</sub> $\beta\beta$ hopanediol	<b>49</b>	0.14	0.11	0.07	0.57	0.01	-	-	0.02	tr	-	-	-	-	-	-	-
C <sub>32</sub> $\beta\beta$ hopanone	<b>60</b>	-	-	-	-	-	-	-	-	-	-	-	0.01	-	-	0.31	-
C <sub>33</sub> $\beta\beta$ hopanone	<b>61</b>	-	-	-	-	-	-	-	-	-	-	-	-	0.09	0.59	0.05	-
C <sub>34</sub> $\beta\beta$ hopanone	<b>62</b>	-	-	-	-	-	-	-	-	-	-	-	-	0.08	0.08	-	-
C <sub>33</sub> $\beta\beta$ hopanoic acid	<b>54</b>	0.56	nd <sup>e</sup>	0.06	0.13	0.98	-	-	-	0.09	0.2	0.11	12.4	10.0	8.4	0.92	0.34
C <sub>32</sub> $\beta\beta$ hopanoic acid	<b>55</b>	3.2	nd	0.45	0.70	5.4	0.12	0.22	0.29	0.45	0.7	0.39	113	10.6	48	1.5	1.9
C <sub>31</sub> $\beta\beta$ hopanoic acid	<b>56</b>	1.5	nd	0.19	0.27	1.7	0.02	0.08	0.27	0.22	0.07	0.08	30.1	0.4	10.7	1.2	0.9
Total geohopanooid <sup>f</sup>		12.13	1.1	2.9	13.5	8.2	0.17	0.31	0.64	1.8	1.0	0.63	156	6.8	6.9	4.6	6.7

<sup>a</sup>Samples: CP = Champagne Pool, OK = Orakei Korako, LR = Loop Road, OP = Opaheke Pool, RK = Rotokawa. <sup>b</sup>Structures. <sup>c</sup>not detected <sup>d</sup>tr = Trace amounts ( $<0.005 \mu\text{g.g}^{-1}$  dry sinter). <sup>e</sup>nd = not determined. <sup>f</sup>total geohopanooid = total abundance of selected geohopanooids.

### 6.3.1 GC-MS ANALYSIS OF HOPANOID DISTRIBUTIONS FROM ACTIVE FACIES OF CHAMPAGNE POOL

#### 6.3.1.1 CPF

GC-MS analysis of the acetylated fraction of sample CPf (Figure 6.6) showed the presence of the biohopanoids, BH*tetrol*, BH*pentol*, diploptene and Hop-(17)21-ene (**1**, **13**, **4**, **4'**). Hop-(17)21-ene (**4'**) was found to be the least abundant biohopanoid and BH*tetrol* (**1**) was the most abundant biohopanoid, with concentrations ranging from 0.04 to 0.65  $\mu\text{g}\cdot\text{g}^{-1}$  dry sinter (Table 6.2). AnhydroBHT (**2**) was the only geohopanoid detected and was present in a concentration of 0.07  $\mu\text{g}\cdot\text{g}^{-1}$  dry sinter. No homohopanols (**48**, **47**, **46**) were observed and analysis of hopanoic acids (**52**, **51**, **50**) was not possible due to the small amount of material collected.

#### 6.3.1.2 CP1A

The acetylated fraction of sample CP1A contained the biohopanoids, BH*tetrol*, BH*pentol*, diploptene and hop-(17)21-ene (**1**, **13**, **4**, **4'**). Diploptene was the least abundant biohopanoid and BH*tetrol* was the most abundant biohopanoid, concentrations range from 0.14 to 0.88  $\mu\text{g}\cdot\text{g}^{-1}$  dry sinter (Table 6.2). The geohopanoids included a series C<sub>31</sub> – C<sub>34</sub> 17 $\beta$ (H),21 $\beta$ (H) hopanediols (Table 6.2), C<sub>31</sub> hopanol and C<sub>32</sub> hopanol. A high abundance of C<sub>31</sub> hopanol relative to C<sub>32</sub> hopanol is observed with abundances ranging from 0.16 to 0.6  $\mu\text{g}\cdot\text{g}^{-1}$  (Table 6.2).

17 $\beta$ (H),21 $\beta$ (H) bishomohopanoic acid (C<sub>32</sub>) and 17 $\beta$ (H),21 $\beta$ (H) homohopanoic acid (C<sub>31</sub>; analysed as methyl esters) were detected in trace amounts in sample CP1 (Table 6.2).

### 6.3.2 GC-MS ANALYSIS OF HOPANOID DISTRIBUTIONS FROM NON-ACTIVE FACIES OF CHAMPAGNE POOL

#### 6.3.2.1 CP3N

Analysis of the acetylated fraction showed the presence of biohopanoids and geohopanoids. The biohopanoids include *BHtetrol*, *BHpentol*, diploptene and hop-(17)21-ene (**1**, **13**, **4**, **4'**). Hop-(17)21-ene was the least abundant biohopanoid and *BHtetrol* the most abundant with concentrations ranging from 0.65 to 2.98  $\mu\text{g}\cdot\text{g}^{-1}$  dry sinter (Table 6.3). The distribution of geohopanoids consisted of anhydroBHT,  $\text{C}_{32}$   $\beta\beta$  hopanol,  $\text{C}_{31}$   $\beta\beta$  hopanol and  $\text{C}_{30}$   $\beta\beta$  hopanol (**2**, **48**, **47**, **46**). A series of  $\text{C}_{31}$  –  $\text{C}_{34}$   $\beta\beta$  hopanediols were also identified (**50**, **51**, **52**, **53**).  $\text{C}_{34}$   $\beta\beta$  hopanediol (**53**) was found to be the least abundant hopanoid and  $\text{C}_{31}$   $\beta\beta$  hopanol (**48**) was the most abundant with abundances ranging from 0.08 to 3.8 ( $\mu\text{g}\cdot\text{g}^{-1}$  dry sinter; Table 6.3).

$\text{C}_{33}$   $\beta\beta$  hopanoic acid,  $\text{C}_{32}$   $\beta\beta$  hopanoic acid and  $\text{C}_{31}$   $\beta\beta$  hopanoic acid were detected during analysis of the methylated fraction (**56**, **55**, **54**).  $\text{C}_{33}$   $\beta\beta$  hopanoic acid (**56**) was the least abundant and  $\text{C}_{32}$   $\beta\beta$  hopanoic acid (**54**) the most abundant hopanoic acid detected with abundances ranging from 0.56 to 3.2  $\mu\text{g}\cdot\text{g}^{-1}$  dry sinter (Table 6.3).

#### 6.3.2.2 CP6N

The acetylated fraction of sample CP6 showed the presence of biohopanoids and geohopanoids. The distribution of biohopanoids consisted of *BHpentol*, *BHtetrol*, diploptene and hop-21-ene (**1**, **13**, **4**, **4'**). The distribution of geohopanoids detected in CP6 consisted of anhydroBHT,  $\text{C}_{32}$   $\beta\beta$  hopanol,  $\text{C}_{31}$   $\beta\beta$  hopanol,  $\text{C}_{31}$   $\alpha\beta$  hopanol,  $\text{C}_{30}$   $\beta\beta$  hopanol,  $\text{C}_{32}$   $\beta\beta$  hopanediol and  $\text{C}_{31}$   $\beta\beta$  hopanediol (**2**, **48**, **47**,  $\alpha\beta$ -**47**, **46**, **50**, **49**).  $\text{C}_{33}$   $\beta\beta$  hopanediol (**51**) was detected in trace amounts. Amounts range from 0.01 to 0.19  $\mu\text{g}\cdot\text{g}^{-1}$  dry sinter.  $\text{C}_{31}$   $\beta\beta$  hopanol

(**47**) was the most abundant geohopanoic acid detected representing 57% of the total geohopanoic acids identified in this sample.

C<sub>33</sub> ββ hopanoic acid, C<sub>32</sub> ββ hopanoic acid and C<sub>31</sub> ββ hopanoic acid (**56**, **55**, **54**) were detected during GC-MS analysis of the methyl ester fraction. C<sub>32</sub> ββ hopanoic acid (**55**) was the most abundant and C<sub>33</sub> ββ hopanoic acid (**56**) was the least abundant hopanoic acid detected, with abundances ranging from 0.07 to 0.35 μg.g<sup>-1</sup> dry sinter (Table 6.3).

#### 6.3.2.3 CP7N

The acetylated fraction showed the presence of biohopanoic acids and geohopanoic acids. Biohopanoic acids consisted of BH*pentol*, BH*tetrol*, diploptene and hop-21-ene (**1**, **13**, **4**, **4**). The geohopanoic acids consisted of anhydroBHT, C<sub>32</sub> ββ hopanol, C<sub>31</sub> ββ hopanol, C<sub>30</sub> ββ hopanol (**2**, **48**, **47**, **46**). C<sub>32</sub> hopanol (**48**) was the least abundant hopanol and C<sub>31</sub> ββ hopanol (**48**) the most abundant hopanol with abundances ranging from 0.14 to 0.6 μg.g<sup>-1</sup> dry sinter. A series of C<sub>31</sub> – C<sub>34</sub> ββ hopanediols (**49**, **50**, **51**, **52**) were also identified with abundances ranging from 0.03 to 0.11 μg.g<sup>-1</sup> dry sinter (Table 6.3).

#### 6.3.2.4 CP8N

The acetylated fraction showed the presence of the biohopanoic acids, BH*tetrol*, BH*pentol*, diploptene and hop-(17)21-ene (**1**, **13**, **4**, **4'**). Diploptene (**4**) was the least abundant biohopanoic acid and BH*tetrol* (**1**) was the most abundant biohopanoic acid, concentrations range from 0.14 to 0.88 μg.g<sup>-1</sup> dry sinter (Table 6.3). The distribution of geohopanoic acids identified in sample CP8N consisted of anhydroBHT, C<sub>32</sub> ββ hopanol, C<sub>31</sub> ββ hopanol, C<sub>30</sub> ββ hopanol (**2**, **48**, **47**, **46**). AnhydroBHT (**2**) was the most abundant hopanoic acid detected in this sample (0.94 μg.g<sup>-1</sup> dry sinter; Table 6.3). Abundances of free hopanols detected in this sample were 0.07, 0.59 and 0.44 μg.g<sup>-1</sup> dry sinter for C<sub>32</sub>, C<sub>31</sub> and C<sub>30</sub> ββ hopanols respectively (Table 6.3). A

series of C<sub>31</sub> – C<sub>33</sub> ββ hopanediols were also identified (**52**, **51**, **50**, **49**), with abundances ranging from 0.03 to 0.09 μg.g<sup>-1</sup> dry sinter (Table 6.3).

C<sub>33</sub> ββ hopanoic acid, C<sub>32</sub> ββ hopanoic acid and C<sub>31</sub> ββ hopanoic acid (**56**, **55**, **54**) were detected during GC-MS analysis of the methyl ester fraction. C<sub>32</sub> ββ hopanoic acid (**56**) was the most abundant and C<sub>33</sub> ββ hopanoic acid (**56**) the least abundant hopanoic acid detected, with abundances ranging from 0.06 to 0.45 μg.g<sup>-1</sup> dry sinter (Table 6.3).

#### 6.3.2.5 CP11N

The acetylated fraction showed the presence of the biohopanoids, BH*tetrol*, BH*pentol*, diploptene and hop-(17)21-ene (**1**, **13**, **4**, **4'**; Table 6.3). Diploptene was found to be the least abundant biohopanoid and BH*tetrol* the most abundant biohopanoid, concentrations range from 0.14 to 0.88 μg.g<sup>-1</sup> dry sinter (Table 6.3). The distribution of geohopanoids identified in sample CP11N consisted of anhydroBHT, C<sub>32</sub> ββ hopanol, C<sub>31</sub> ββ hopanol, C<sub>31</sub> αβ hopanol, C<sub>30</sub> ββ hopanol and C<sub>30</sub> αβ hopanol (**2**, **48**, **47**, αβ-**48**, **47**, **ab-47**). C<sub>31</sub> ββ hopanol (**47**) was the most abundant hopanol detected (6.42 μg.g<sup>-1</sup> dry sinter; Table 6.3). C<sub>32</sub> and C<sub>31</sub> ββ hopanediols (**50**, **49**) were also identified and were present in abundances 0.14 to 0.57 μg.g<sup>-1</sup> dry sinter respectively.

C<sub>33</sub> ββ hopanoic acid, C<sub>32</sub> ββ hopanoic acid and C<sub>31</sub> ββ hopanoic acid (**56**, **55**, **54**) were detected during analysis of the methyl ester fraction. C<sub>33</sub> ββ hopanoic acid (**56**) was the least abundant and C<sub>32</sub> ββ hopanoic acid (**55**) the most abundant hopanoic acid detected, with abundances ranging from 0.13 to 0.7 μg.g<sup>-1</sup> dry sinter (Table 6.3).

#### 6.3.2.6 CP5N

The acetylated fraction showed the presence of the biohopanoids, BH*tetrol*, BH*pentol*, diploptene and hop-(17)21-ene (**1**, **13**, **4**, **4'**). Diploptene was found to be the least abundant

biohopanoid and *BHtetrol* was the most abundant biohopanoid with concentrations ranging from 0.14 to 0.88  $\mu\text{g}\cdot\text{g}^{-1}$  dry sinter (Table 6.3). The geohopanoids include anhydroBHT,  $\text{C}_{32}$   $\beta\beta$  hopanol,  $\text{C}_{31}$   $\beta\beta$  hopanol and  $\text{C}_{30}$   $\beta\beta$  hopanol (**2**, **48**, **47**, **46**).  $\text{C}_{31}$   $\beta\beta$  hopanol (**47**) was the most abundant hopanol detected (7.0  $\mu\text{g}\cdot\text{g}^{-1}$  dry sinter). A series of  $\text{C}_{31}$  –  $\text{C}_{33}$  hopanediols (**49**, **50**, **51**) were also identified with abundances ranging from 0.5 to 1.19  $\mu\text{g}\cdot\text{g}^{-1}$  dry sinter (Table 6.3).

$\text{C}_{33}$   $\beta\beta$  hopanoic acid,  $\text{C}_{32}$   $\beta\beta$  hopanoic acid and  $\text{C}_{31}$   $\beta\beta$  hopanoic acid (**56**, **55**, **54**) were detected during analysis of the methyl ester fraction.  $\text{C}_{32}$   $\beta\beta$  hopanoic acid (**55**) was the most abundant and  $\text{C}_{33}$   $\beta\beta$  hopanoic acid (**56**) was the least abundant hopanoic acid detected, with abundances ranging from 1.95 to 11.46  $\mu\text{g}\cdot\text{g}^{-1}$  dry sinter (Table 6.3).

### 6.3.3 GC-MS ANALYSIS OF ACTIVE SINTERS FROM ORAKEI KORAKO

#### 6.3.3.1 FRED AND MAGGIE'S POOL: VENT

Analysis of the acetylated fraction of the upper layer of the active sinter from FMP (sample OK1-TA; Figure 6.7) showed the presence of the biohopanoids *BHpentol*, 2me-*BHpentol*, *BHtetrol*, 2me-*BHtetrol*, diploptene and hop-21-ene (**13**, **II-13**, **1**, **II-1**, **5**, **4**, **4'**; Table 6.2). The geohopanoids included a series of  $\text{C}_{30}$  to  $\text{C}_{33}$   $\beta\beta$  hopanols (**46**, **47**, **48**, **57**).  $\text{C}_{33}$  hopanol was present in  $\beta\beta$ ,  $\beta\alpha$  and  $\alpha\beta$  stereoisomers (**57**,  $\alpha\beta$ -**57**,  $\beta\alpha$ -**57**). AnhydroBHT (**2**) and  $\text{C}_{31}$   $\beta\beta$  hopanediol (**49**) was present in trace amounts. The most abundant geohopanoid detected in analysis of the acetylated fraction of OK1-TA was  $\text{C}_{33}$   $\beta\beta$  hopanol (**58**; 0.06  $\mu\text{g}\cdot\text{g}^{-1}$  dry sinter; Table 6.2). This compound appears to be an early eluting isomer of  $\text{C}_{33}$   $\beta\beta$  hopanol (see Figure 6.8 for GC-MS spectrum) with a retention time similar to of  $\text{C}_{32}$   $\beta\beta$  hopanol (**49**), identification is based upon comparison with previously published spectra (e.g. Philp, 1983).

$C_{33}$   $\beta\beta$  hopanoic acid,  $C_{32}$   $\beta\beta$  hopanoic acid,  $C_{32}$   $\beta\alpha$  hopanoic acid and  $C_{31}$   $\beta\beta$  hopanoic acid (**56**, **55**,  $\beta\alpha$ -**55**., **54**; Table 6.2) were identified during analysis of hopanoic acids. 2-me  $C_{32}$   $\beta\beta$  hopanoic acid, 2-me  $C_{32}$   $\beta\alpha$  hopanoic and 2-me  $C_{31}$   $\beta\beta$  hopanoic acid was also identified (**II-56**, **II- $\beta\alpha$ -55**, **II-54**).  $C_{32}$   $\beta\beta$  hopanoic acid (**55**) was the most abundant compound detected and 2-me  $C_{32}$   $\beta\alpha$  hopanoic acid (**II- $\beta\alpha$ -57**) was the least abundant compound identified with concentrations ranging from 0.02 – 0.64  $\mu\text{g}\cdot\text{g}^{-1}$  dry sinter. The overall abundance of hopanoic acids in sample OK1-TA was 1.39  $\mu\text{g}\cdot\text{g}^{-1}$  dry sinter.

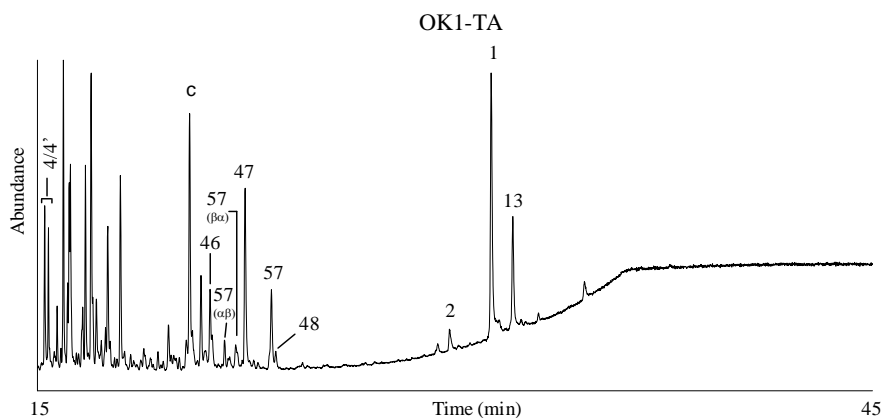


Figure 6.7 Partial  $m/z$  191 mass chromatogram (15 – 45 min) showing distribution of geohopanooids identified in acetylated fraction of sample OK1-TA

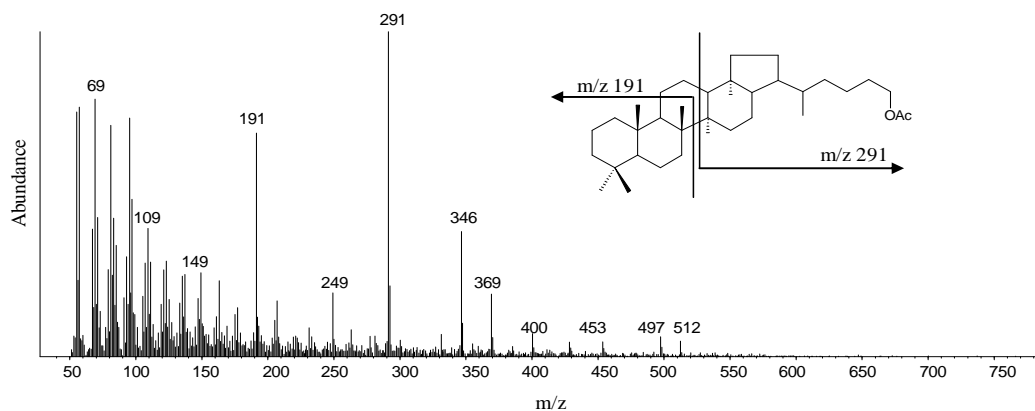


Figure 6.8 GC-MS spectra of early eluting isomer of acetylated  $C_{33}$   $\beta\beta$  hopanol (**57**)

The acetylated fraction of the middle layer (Sample OK1-MA) of the active sinter from FMP (Table 6.2) showed the presence of the biohopanoids *BHpentol*, *BHtetrol*, diploptene and hop-21-ene (**13**, **1**, **4**, **4'**). The geohopanoids included a series of C<sub>30</sub> to C<sub>33</sub> ββ hopanols (**46**, **47**, **48**, **57**). C<sub>33</sub> hopanol was present in ββ, βα and αβ stereoisomers (**57**, βα-**57**, αβ-**57**) and C<sub>30</sub> hopanol was present in ββ and αβ isomers (**46**, αβ-**46**). C<sub>32</sub> ββ hopanol (**47**) was present in trace amounts and C<sub>33</sub> ββ hopanol (**57**) was the most abundant geohopanoid identified (0.03 μg.g<sup>-1</sup> dry sinter; Table 6.2).

C<sub>33</sub> ββ hopanoic acid and C<sub>32</sub> ββ hopanoic acid (**56**, **55**) were detected during analysis of hopanoic acids. Abundances were 0.63 and 0.75 μg.g<sup>-1</sup> dry sinter respectively (Table 6.2). Overall abundances of hopanoids in this sample were 1.38 μg.g<sup>-1</sup> dry sinter.

The acetylated fraction of the bottom layer of the active sinter from FMP (sample OK1-BA; Table 6.2) showed the presence of the biohopanoids, *BHpentol*, *BHtetrol*, diplopterol, and hop-21-ene (**13**, **1**, **4**, **4'**). The distribution of geohopanoids consisted of a series of C<sub>30</sub> to C<sub>33</sub> ββ hopanols (**46**, **47**, **48**, **57**). C<sub>33</sub> hopanol (**57**) was the most abundant hopanol identified (0.01 μg.g<sup>-1</sup> dry sinter) and C<sub>32</sub>, C<sub>31</sub> and C<sub>30</sub> ββ hopanol (**48**, **47**, **46**) were present in trace amounts (i.e. mass < 0.01 μg.g<sup>-1</sup> dry sinter). Overall abundance of hopanoids in this sample was 0.16 μg.g<sup>-1</sup> dry sinter.

C<sub>33</sub> ββ hopanoic acid, 2-me C<sub>31</sub> ββ hopanoic acid, C<sub>30</sub> ββ hopanoic acid and 2-me C<sub>30</sub> ββ hopanoic acid (**56**, **II-56**, **55**, **II-55**; Table 6.2) were detected during analysis of hopanoic acids. C<sub>33</sub> ββ hopanoic (**56**) was the most abundant hopanoic acid identified and 2-me C<sub>32</sub> hopanoic acid (**II-55**) was the least abundant hopanoic acids identified with concentrations ranging from 0.02 – 0.26 μg.g<sup>-1</sup> dry sinter. Overall abundances on this sample were 0.47 μg.g<sup>-1</sup> dry sinter (Table 6.2).

### 6.3.3.2 FRED AND MAGGIE'S POOL: OUTFLOW CHANNEL

The acetylated fraction of sample OK3A showed the presence of biohopanoids and geohopanoids. The biohopanoids included BH*pentol*, BH*tetrol*, diploptene and Hop-21-ene (**13**, **1**, **5**, **4**, **4'**). BH*tetrol* (**1**) was the most abundant biohopanoid detected during this analysis ( $17.0 \mu\text{g}\cdot\text{g}^{-1}$  dry sinter; Table 6.2). Isomeric versions of BH*tetrol* and anhydroBHT were also detected. The distribution of geohopanoids consisted of anhydroBHT,  $\beta\beta$  C<sub>33</sub> hopanol,  $\beta\beta$  C<sub>32</sub> hopanol, C<sub>31</sub>  $\beta\beta$  hopanol, C<sub>31</sub>  $\alpha\beta$  hopanol, C<sub>30</sub>  $\beta\beta$  hopanol and C<sub>31</sub>  $\beta\beta$  hopanediol, C<sub>32</sub>  $\beta\beta$  hopanediol and C<sub>33</sub>  $\beta\beta$  hopanediol (**2**, **57**, **48**, **47**,  $\alpha\beta$ -**47**, **46**, **49**, **50**, **51**). C<sub>31</sub>  $\beta\beta$  hopanol (**47**) was the most abundant geohopanoid ( $1.99 \mu\text{g}\cdot\text{g}^{-1}$  dry sinter). C<sub>31</sub>  $\alpha\beta$  hopanol ( $\alpha\beta$ -**47**) was also detected albeit in small amounts ( $0.01 \mu\text{g}\cdot\text{g}^{-1}$  dry sinter). C<sub>32</sub> hopenetriol (**58**) was also tentatively identified and was present in a concentration of  $0.13 \mu\text{g}\cdot\text{g}^{-1}$  dry sinter (Table 6.2).

Analysis of hopanoic acids showed the presence of C<sub>33</sub>  $\beta\beta$  hopanoic acid, C<sub>32</sub>  $\beta\beta$  hopanoic acid, C<sub>32</sub>  $\alpha\beta$  hopanoic acid and C<sub>31</sub>  $\beta\beta$  hopanoic acid (**56**, **55**,  $\alpha\beta$ -**55**, **54**; Table 6.2). C<sub>32</sub>  $\beta\beta$  hopanoic acid (**56**) was the most abundant hopanoic acid detected and C<sub>31</sub>  $\alpha\beta$  hopanoic acid ( $\alpha\beta$ -**55**) was the least abundant hopanoic acid detected, with concentrations ranging from  $0.47$  to  $36.09 \mu\text{g}\cdot\text{g}^{-1}$  dry sinter (Table 6.2).

### 6.3.4 GC-MS ANALYSIS OF NON-ACTIVE SINTERS OF ORAKEI KORAKO

#### 6.3.4.1 OK4N

The acetylated fraction of OK4N showed the presence of biohopanoids and geohopanoids. The biohopanoids included BH*pentol*, 2-me BH*pentol*, BH*tetrol*, 2-me BH*tetrol*, diploptene and hop-21-ene (**13**, **II-13**, **1**, **II-1**, **4**, **4'**) 2-me BH*pentol* (**II-13**) was present in trace amounts and BH*tetrol* (**1**) was the most abundant biohopanoid detected ( $0.28$

$\mu\text{g.g}^{-1}$  dry sinter; Table 6.3). The geohopanoids included anhydroBHT,  $\text{C}_{31}$   $\beta\beta$  hopanol,  $\text{C}_{32}$   $\beta\beta$  hopanediol and  $\text{C}_{33}$   $\beta\beta$  hopanediol (**2**, **47**, **50**, **51**). Abundances of geohopanoids were low, with abundances ranging from  $0.01 \mu\text{g.g}^{-1}$  dry sinter for  $\text{C}_{32}$   $\beta\beta$  hopanediol and  $\text{C}_{33}$   $\beta\beta$  hopanediol, to  $0.1 \mu\text{g.g}^{-1}$  dry sinter for anhydroBHT (**2**; Table 6.3).

$\text{C}_{33}$   $\beta\beta$  hopanoic acid,  $\text{C}_{32}$   $\beta\beta$  hopanoic acid and  $\text{C}_{32}$   $\beta\alpha$  hopanoic acid (**56**, **55**, **54**) were identified during analysis of hopanoic acids.  $\text{C}_{33}$   $\beta\beta$  hopanoic acid (**56**) was the least abundant and  $\text{C}_{32}$   $\beta\beta$  hopanoic acid (**55**) was the most abundant with concentrations ranging from 0.98 to  $5.43 \mu\text{g.g}^{-1}$  dry sinter (Table 6.3).

#### 6.3.4.2 OK5N

The acetylated fraction of OK5N showed the presence of biohopanoids and geohopanoids. In this particular sample the diversity of hopanoid compounds was particularly low. The biohopanoids included *BHpentol*, *BHtetrol* and *2me-BHtetrol* (**13**, **1**, **II-1**). Abundances were  $0.02$ ,  $0.04$  and  $0.01 \mu\text{g.g}^{-1}$  dry sinter respectively (Table 6.3). Analysis of the distribution of geohopanoids showed the presence of anhydroBHT and  $\text{C}_{31}$   $\beta\beta$  hopanol (**2**, **47**). anhydroBHT (**2**) was present in trace amounts and the abundance of  $\text{C}_{31}$   $\beta\beta$  hopanol (**48**) was  $0.01 \mu\text{g.g}^{-1}$  dry sinter (Table 6.3).

Analysis of hopanoic acids showed the presence of  $\text{C}_{32}$   $\beta\beta$  hopanoic acid and  $\text{C}_{31}$   $\beta\beta$  hopanoic acid (**48**, **47**) which were present in concentrations of  $0.12$  and  $0.02 \mu\text{g.g}^{-1}$  dry sinter respectively (Table 6.3).

#### 6.3.4.3 OK6N

The acetylated fraction of OK6N showed the presence of biohopanoids and geohopanoids. The distribution of biohopanoids consisted of *BHpentol*, *2-me BHpentol*, *BHtetrol*, *2-me BHtetrol*, *diplopterol*, *diploptene* and *Hop-21-ene* (**13**, **II-13**, **1**, **II-1**, **5**, **4**, **4'**).

2-me BH*tetrol* (**II-1**) was present in trace amount BH*tetrol* (**1**) was the most abundant biohopanoid detected ( $0.04 \mu\text{g}\cdot\text{g}^{-1}$  dry sinter; Table 6.3). Diplopterol (**5**) was also detected in significantly large amounts (compared to other hopanoid detected in this sample) in a concentration of  $0.03 \mu\text{g}\cdot\text{g}^{-1}$  dry sinter. The distribution of geohopanooids consisted of anhydroBHT, C<sub>33</sub> ββ hopanol and C<sub>31</sub> ββ hopanol, (**2, 57, 47**). All geohopanooids were present in a concentration of  $0.01 \mu\text{g}\cdot\text{g}^{-1}$  dry sinter or less (Table 6.2).

It was not possible to analyse hopanoic acids, presumably due to the low concentration of hopanooids in this sample and loss of organic material during the clean-up procedure required to render the hopanoid distributions amenable to GC-MS.

### 6.3.5 GC-MS ANALYSIS OF ACTIVE SINTERS FROM LOOP ROAD

#### 6.3.5.1 LR2AS

Analysis of the acetylated fraction of sample LR2AS showed the presence of biohopanooids and geohopanooids. The biohopanooids included BH*pentol*, BH*tetrol* and diploptene (**13, 2, 4**). Diploptene was the least abundant biohopanoid and BH*tetrol* was the most abundant biohopanoid with abundances ranging from  $0.08$  to  $0.24 \mu\text{g}\cdot\text{g}^{-1}$  dry sinter. The geohopanooids included anhydroBHT, C<sub>32</sub> ββ hopanol, C<sub>31</sub> ββ hopanol, and C<sub>30</sub> ββ hopanol (**2, 48, 47, 46**). AnhydroBHT (**2**) was the least abundant geohopanoid and was present in a concentration of  $0.08 \mu\text{g}\cdot\text{g}^{-1}$  dry material and C<sub>31</sub> ββ hopanol (**47**) was the most abundant geohopanoid ( $1.18 \mu\text{g}\cdot\text{g}^{-1}$  dry sinter; Table 6.2). Due to the small amount of material available it was not possible to carry out PA/NaBH<sub>4</sub> cleavage or analysis of the distribution of hopanoic acids.

## 6.3.5.2 LR2A

The acetylated fraction of sample LR2A was found to contain biohopanoids and geohopanoids. The distribution of biohopanoids consisted of BH*pentol*, BH*tetrol*, diplopterol and diploptene (**13**, **2**, **5**, **4**), abundances were 0.09, 0.08 and 0.03  $\mu\text{g}\cdot\text{g}^{-1}$  dry sinter respectively (Table 6.2). The distribution of geohopanoids showed the presence of anhydroBHT, C<sub>31</sub>  $\beta\beta$  hopanol and C<sub>30</sub>  $\beta\beta$  hopanol (**2**, **46**, **45**). C<sub>31</sub>  $\beta\beta$  hopanol (**46**) was the most abundant geohopanoid detected during this analysis (0.16  $\mu\text{g}\cdot\text{g}^{-1}$  dry sinter; Table 6.2).

Analysis of hopanoic acids shows the presence of C<sub>33</sub>, C<sub>32</sub> and C<sub>31</sub>  $\beta\beta$  hopanoic acid (**56**, **55**, **54**). C<sub>30</sub>  $\beta\beta$  hopanoic acid (**54**) was the least abundant compound and C<sub>31</sub>  $\beta\beta$  hopanoic acid (**55**) is the most abundant hopanoic acid with concentrations ranging from 0.1 to 1.71  $\mu\text{g}\cdot\text{g}^{-1}$  dry sinter (Table 6.2). The abundance of C<sub>32</sub>  $\beta\beta$  hopanoic acid (**56**) was 0.15  $\mu\text{g}\cdot\text{g}^{-1}$  dry sinter (Table 6.2).

## 6.3.5.3 LR3A

The acetylated fraction of LR3A was found to contain biohopanoids and geohopanoids. The biohopanoids included BH*pentol*, BH*tetrol* and diplopterol, diploptene and hop-21-ene (**13**, **2**, **5**, **4**, **4'**). Abundances were 0.17, 0.22 and 0.07  $\mu\text{g}\cdot\text{g}^{-1}$  dry sinter respectively (Table 6.2). The geohopanoids included anhydroBHT, C<sub>32</sub>  $\beta\beta$  hopanol C<sub>31</sub>  $\beta\beta$  hopanol and C<sub>30</sub>  $\beta\beta$  hopanol (**2**, **47**, **46**). Abundances are 0.08, 0.03, 0.4  $\mu\text{g}\cdot\text{g}^{-1}$  dry sinter respectively (Table 6.2).

Analysis of hopanoic acids showed the presence of C<sub>32</sub>  $\beta\beta$  hopanoic acid, C<sub>32</sub>  $\beta\beta$  hopanoic acid and C<sub>31</sub>  $\beta\beta$  hopanoic acid (**56**, **55**, **54**). Concentrations were 0.02, 0.18 and 0.09  $\mu\text{g}\cdot\text{g}^{-1}$  dry sinter respectively (Table 6.2).

### 6.3.6 GC-MS ANALYSIS OF NON-ACTIVE SINTER FACIES OF LOOP ROAD

#### 6.3.6.1 LR3N

Analysis of the acetylated fraction of sample LR3N (Figure 6.9) showed the presence of a complex distribution of biohopanoids and geohopanoids. The biohopanoids included BH*pentol*, BH*tetrol*, diplopterol, diploptene and hop-21-ene (**13**, **1**, **5**, **4**, **4'**). BH*pentol* (**13**) was the least abundant and BH*tetrol* (**1**) was the most abundant biohopanoid detected, with concentrations ranging from 0.02 to 1.53  $\mu\text{g}\cdot\text{g}^{-1}$  dry sinter (Table 6.3). An isomer of BH*tetrol* (**1**) was also identified. The geohopanoids included anhydroBHT, C<sub>34</sub>  $\beta\beta$  hopanediol, C<sub>33</sub>  $\beta\beta$  hopanediol, C<sub>32</sub>  $\beta\beta$  hopanediol, C<sub>31</sub>  $\beta\beta$  hopanediol, C<sub>32</sub>  $\beta\beta$  hopanol, C<sub>31</sub>  $\beta\beta$  hopanol, C<sub>31</sub>  $\beta\alpha$  hopanol, C<sub>31</sub>  $\alpha\beta$  hopanol and C<sub>30</sub>  $\beta\beta$  hopanol (**2**, **52**, **51**, **50**, **49**, **48**, **47**,  $\beta\alpha$ -**47**,  $\alpha\beta$ -**47**, **46**). AnhydroBHT (**2**) was present in trace amounts and the most abundant was C<sub>31</sub>  $\beta\beta$  hopanol (**47**; 0.84  $\mu\text{g}\cdot\text{g}^{-1}$  dry sinter; Table 6.3).

C<sub>32</sub>  $\beta\beta$  hopanoic acid and C<sub>31</sub> $\beta\beta$  hopanoic acids (**56**, **55**) were identified during analysis of hopanoic acids, abundances were 0.29 and 0.26  $\mu\text{g}\cdot\text{g}^{-1}$  dry sinter respectively (Table 6.3).

#### 6.3.6.2 LR4N

The acetylated fraction of sample LR4N showed the presence of biohopanoids and geohopanoids. The biohopanoids included BH*pentol*, BH*tetrol*, diploptene and hop-21-ene (**13**, **1**, **4**, **4'**). Diploptene (**4**) was detected in trace amounts and BH*tetrol* (**1**) was the most abundant biohopanoid detected, abundances of biohopanoids ranging from <0.01 to 0.67  $\mu\text{g}\cdot\text{g}^{-1}$  dry sinter (Table 6.3). The geohopanoids included anhydroBHT, C<sub>32</sub>  $\beta\beta$  hopanediol, C<sub>32</sub>  $\beta\beta$  hopanol and C<sub>31</sub>  $\beta\beta$  hopanol (**2**, **50**, **48**, **47**). C<sub>32</sub>  $\beta\beta$  hopanediol (**50**) was present in trace

amounts and C<sub>31</sub> ββ hopanol (**47**) was the most abundant geohopanoid and was present in a concentration of 0.7 μg.g<sup>-1</sup> dry sinter (Table 6.3).

C<sub>33</sub> ββ hopanoic acid, C<sub>32</sub> ββ hopanoic and C<sub>31</sub> ββ hopanoic (**56, 55, 54**) were identified during analysis of hopanoic acids, abundances were 0.09, 0.45 and 0.22 μg.g<sup>-1</sup> dry sinter respectively (Table 6.3).

#### 6.3.6.3 LR5R

The acetylated fraction of LR5R showed the presence of biohopanoids and geohopanoids. The biohopanoids included BH*pentol*, BH*tetrol*, diplopterol, diploptene and hop-21-ene (**13, 1, 5, 4, 4'**). BH*pentol* (**13**) was present in trace amounts and diploptene (**4**) was the most abundant biohopanoid detected during this analysis and was present in a concentration of 0.03 μg.g<sup>-1</sup> dry sinter (Table 6.3). The geohopanoids included anhydroBHT, C<sub>33</sub> ββ hopanediol, C<sub>32</sub> ββ hopanediol, C<sub>31</sub> ββ hopanediol, C<sub>32</sub> ββ hopanol and C<sub>31</sub> ββ hopanol (**2, 51, 50, 49, 48, 47**). AnhydroBHT (**2**) and C<sub>33</sub> ββ hopanediol (**51**) were present in trace amounts and C<sub>31</sub> ββ hopanol (**47**) was the most abundant geohopanoid and was present in a concentration of 0.02 μg.g<sup>-1</sup> dry sinter (Table 6.3).

Analysis of hopanoic acids showed the presence of C<sub>33</sub> ββ hopanoic acid, C<sub>32</sub> ββ hopanoic and C<sub>31</sub> ββ hopanoic (**56, 55, 54**), abundances were 0.2, 0.7 and 0.07 μg.g<sup>-1</sup> dry sinter respectively (Table 6.3).

#### 6.3.6.4 LR6R

The acetylated fraction of LR6R showed the presence of biohopanoids and geohopanoids. The biohopanoids included BH*pentol*, BH*tetrol*, diplopterol, diploptene and hop-21-ene (**13, 1, 5, 4, 4'**). Of the biohopanoids, hop-21-ene (**4'**) was the least abundant biohopanoid and BH*tetrol* (**1**) was the most abundant biohopanoid with concentrations

ranging from 0.01 to 2.31  $\mu\text{g}\cdot\text{g}^{-1}$  dry sinter (Table 6.3). Geohopanoids were present in very low abundances.  $\text{C}_{32}$   $\beta\beta$  hopanol and  $\text{C}_{31}$   $\beta\beta$  hopanol were identified (**48**, **47**) and were present in trace amounts. AnhydroBHT (**2**) was present in concentrations of 0.04  $\mu\text{g}\cdot\text{g}^{-1}$  dry sinter (Table 6.3).

$\text{C}_{33}$   $\beta\beta$  hopanoic acid,  $\text{C}_{32}$   $\beta\beta$  hopanoic acid and  $\text{C}_{31}$   $\beta\beta$  hopanoic acid (**56**, **55**, **54**) were identified during analysis of hopanoic acids.  $\text{C}_{32}$   $\beta\beta$  hopanoic acid was the most abundant and  $\text{C}_{31}$   $\beta\beta$  hopanoic acid the least abundant, with concentrations ranging from 0.08 to 0.39  $\mu\text{g}\cdot\text{g}^{-1}$  dry sinter (Table 6.3).

### 6.3.7 GC-MS ANALYSIS OF ACTIVE SINTER FACIES OF OPAHEKE POOL

#### 6.3.7.1 OP2A

The acetylated fraction of sample OP2A showed the presence of biohopanoids in low concentrations. The distribution consists of *BHpentol*, *BHtetrol* and diploptene (**13**, **1**, **4**). Diploptene (**4**) was present in trace amounts and *BHpentol* and *BHtetrol* are present in 0.16 and 0.13  $\mu\text{g}\cdot\text{g}^{-1}$  dry sinter respectively (Table 6.2).

#### 6.3.7.2 OP7A

Analysis of the acetylated fraction of OP7A showed a more complex distribution than sample OP2A. The distribution consists of the biohopanoids, *BHtetrol*, *BHpentol*, diploptene and hop-21-ene (**1**, **13**, **4**, **4'**). Of which *BHtetrol* (**1**) is the most abundant and is present in a concentration of 0.07  $\mu\text{g}\cdot\text{g}^{-1}$  dry sinter (Table 6.2). The remaining biohopanoids were present in amounts of 0.01  $\mu\text{g}\cdot\text{g}^{-1}$  dry sinter or less. Also present are the geohopanoids anhydroBHT,  $\text{C}_{32}$   $\beta\beta$  hopanol and  $\text{C}_{31}$   $\beta\beta$  hopanol (**2**, **49**, **48**). AnhydroBHT (**2**) were present in a

concentration of 0.02  $\mu\text{g}\cdot\text{g}^{-1}$  dry sinter and the remaining geohopanoids were present in 0.01  $\mu\text{g}\cdot\text{g}^{-1}$  dry sinter or less (Table 6.2).

### 6.3.8 GC-MS ANALYSIS OF NON-ACTIVE SINTER FACIES OF OPAHEKE POOL

#### 6.3.8.1 OP4N

Analysis of the acetylated fraction of sample OP4N (Figure 6.9) showed the presence of biohopanoids and geohopanoids. The distribution of biohopanoids consisted of BH*pentol*, BH*tetrol*, diploptene and hop-21-ene (**13**, **1**, **4**, **4'**). Abundances were 0.03, 0.03, 0.02 and 0.01  $\mu\text{g}\cdot\text{g}^{-1}$  dry sinter. The distribution of geohopanoids identified in this sample consisted of C<sub>32</sub>  $\beta\beta$  hopanol, C<sub>31</sub>  $\beta\beta$  hopanol and C<sub>31</sub>  $\alpha\beta$  hopanol (**48**, **47**,  $\alpha\beta$ -**47**). C<sub>32</sub>  $\beta\beta$  hopanol (**48**) was present in trace amounts and C<sub>31</sub>  $\beta\beta$  hopanol (**47**) was the most abundant free homohopanol detected and was present in concentrations of 0.03  $\mu\text{g}\cdot\text{g}^{-1}$  dry sinter. A tentatively assigned C<sub>32</sub> hopanone (**60**) was identified and was present in a concentration of 0.01  $\mu\text{g}\cdot\text{g}^{-1}$  dry sinter (Table 6.3).

Analysis of hopanoic acids showed the presence of C<sub>33</sub>  $\beta\beta$  hopanoic acid, C<sub>32</sub>  $\beta\beta$  hopanoic acid and C<sub>31</sub>  $\beta\beta$  hopanoic acid. C<sub>33</sub>  $\beta\beta$  hopanoic acid was the least abundant and C<sub>32</sub>  $\beta\beta$  hopanoic acid the most abundant hopanoic acid identified with concentrations ranging from 12.4 to 112.6  $\mu\text{g}\cdot\text{g}^{-1}$  dry sinter.

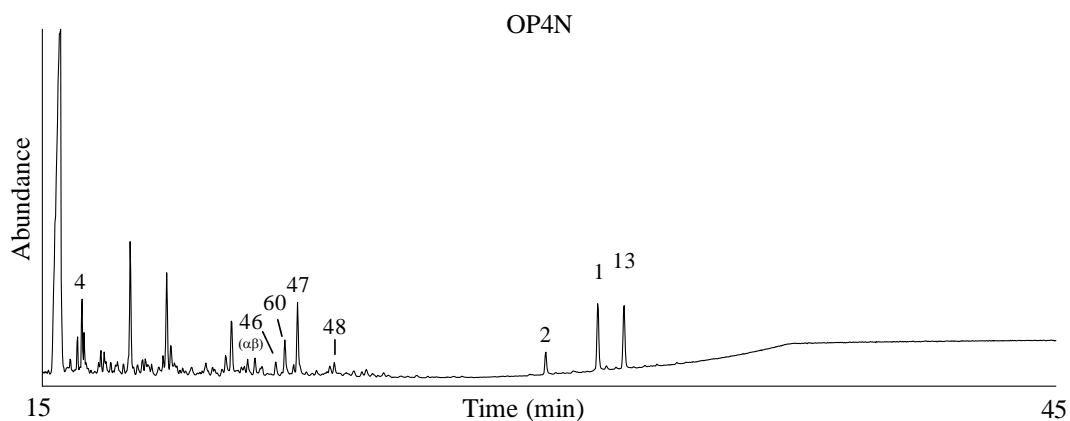


Figure 6.9 Partial  $m/z$  191 mass chromatogram (15 – 45 min) showing geohopanooids identified in sample OP4N

#### 6.3.8.2 OP5N

The acetylated fraction of sample OP5N showed a complex assemblage of hopanooids that consists of distributions of biohopanooids and geohopanooids. The biohopanooids present are BH*pentol*, BH*tetrol*, diploptene and hop-21-ene (**13**, **1**, **4**, **4'**). BH*pentol* (**13**) was present in the lowest abundance and BH*tetrol* (**1**) was the most abundant biohopanooid detected, with concentrations ranging from 0.47 to 2.07  $\mu\text{g}\cdot\text{g}^{-1}$  dry sinter. The geohopanooids consisted of C<sub>31</sub>  $\beta\beta$  hopanol (**48**) which was significantly more abundant than other geohopanooids, and was present in an abundance of 3.93  $\mu\text{g}\cdot\text{g}^{-1}$  dry sinter. The remaining distribution of geohopanooids consists of anhydroBHT, C<sub>32</sub>  $\beta\beta$  hopanol, C<sub>31</sub>  $\alpha\beta$  hopanol, C<sub>30</sub>  $\beta\beta$  hopanol and a series of C<sub>31</sub> – C<sub>33</sub>  $\beta\beta$  hopanediols (**2**, **48**,  $\alpha\beta$ -**47**, **46**, **51**, **50**, **49**). C<sub>32</sub> hopanone and C<sub>33</sub> hopanone (**60**, **61**) have been tentatively identified and were present in concentrations of 0.09 and 0.08  $\mu\text{g}\cdot\text{g}^{-1}$  dry sinter respectively (Table 6.3).

Analysis of hopanoic acids showed the presence of C<sub>33</sub>  $\beta\beta$  hopanoic acid, C<sub>32</sub>  $\beta\beta$  hopanoic acid and C<sub>31</sub>  $\beta\beta$  hopanoic acid. C<sub>33</sub>  $\beta\beta$  hopanoic acid was the least abundant and C<sub>32</sub>

$\beta\beta$  hopanoic acid was the most abundant hopanoic acid identified with abundances ranging from 8.4 to 48  $\mu\text{g}\cdot\text{g}^{-1}$  dry sinter.

#### 6.3.8.3 OP6N

The acetylated fraction of sample OP6N showed a complex assemblage of hopanoids that consists of biohopanoids and geohopanoids. The biohopanoids present are BH*pentol*, BH*tetrol*, diploptene and hop-21-ene (**13**, **1**, **4**, **4'**). BH*pentol* (**13**) was present in the lowest abundance and diploptene (**4**) was the most abundant biohopanoid detected, with concentrations ranging from 0.09 to 2.36  $\mu\text{g}\cdot\text{g}^{-1}$  dry sinter. As observed in sample OP5N, the geohopanoids identified in this sample comprise a diverse and complex distribution. AnhydroBHT and C<sub>31</sub>  $\beta\beta$  hopanol (**2**, **47**) were significantly more abundant than other geohopanoids, and were present in abundances of 2.05 and 3.67  $\mu\text{g}\cdot\text{g}^{-1}$  dry sinter respectively. The remaining geohopanoid distribution consists of C<sub>33</sub>  $\beta\beta$  hopanediol, C<sub>32</sub>  $\beta\beta$  hopanol, C<sub>31</sub>  $\alpha\beta$  hopanol and C<sub>30</sub>  $\beta\beta$  hopanol (**53**, **48**,  $\alpha\beta$ -**47**, **46**). Abundances range from 0.08  $\mu\text{g}\cdot\text{g}^{-1}$  dry sinter for C<sub>33</sub>  $\beta\beta$  hopanediol (**52**) to 0.84  $\mu\text{g}\cdot\text{g}^{-1}$  dry sinter for C<sub>32</sub>  $\beta\beta$  hopanol (**48**). C<sub>32</sub>  $\beta\beta$  hopanone and C<sub>33</sub>  $\beta\beta$  hopanone (**62**, **61**) were also tentatively identified and were present in concentrations of 0.59 and 0.08  $\mu\text{g}\cdot\text{g}^{-1}$  dry sinter respectively (Table 6.3).

C<sub>33</sub>  $\beta\beta$  hopanoic acid, C<sub>32</sub>  $\beta\beta$  hopanoic acid and C<sub>31</sub>  $\beta\beta$  hopanoic acid were identified during analysis of hopanoic acids. C<sub>31</sub>  $\beta\beta$  hopanoic acid was the least abundant and C<sub>32</sub>  $\beta\beta$  hopanoic acid was the most abundant hopanoic acid identified, with abundances ranging from 0.4 to 10.6  $\mu\text{g}\cdot\text{g}^{-1}$  dry sinter.

### 6.3.9 GC-MS ANALYSIS OF NON-ACTIVE SINTERS FROM ROTOKAWA

#### 6.3.9.1 RK2N

The acetylated fraction of a non-active sinter sample (RK2N; Table 6.3; Figure 6.10) contained biohopanoids and geohopanoids. The biohopanoids consisted of BH*pentol*, BH*tetrol*, diploptene and hop-21-ene (**13**, **1**, **4**, **4'**). A compound with an identical GC-MS spectra but slightly later retention time than is commonly observed for BH*tetrol* was observed. Diploptene was the least abundant biohopanoid and BH*tetrol* was the most abundant biohopanoid detected with concentrations ranging from 0.26 to 1.11  $\mu\text{g}\cdot\text{g}^{-1}$  dry sinter. The geohopanoids included anhydroBHT, C<sub>32</sub>  $\beta\beta$  hopanetriol, C<sub>32</sub>  $\beta\beta$  hopanol, C<sub>31</sub>  $\beta\beta$  hopanol, C<sub>33</sub>  $\beta\beta$  hopanone (Figure 6.12; Table 6.3), C<sub>32</sub>  $\beta\beta$  hopanone (Figure 6.11; Table 6.3) and C<sub>30</sub>  $\beta\beta$  hopanol (**2**, **58**, **48**, **47**, **60**, **61**, **46**). C<sub>32</sub>  $\beta\beta$  hopanone (**59**) was the least abundant geohopanoid identified and anhydroBHT (**2**) was the most abundant geohopanoid detected with concentrations ranging from 0.05 to 1.09  $\mu\text{g}\cdot\text{g}^{-1}$  dry sinter (Table 6.3).

Analysis of hopanoic acids showed the presence of C<sub>33</sub>  $\beta\beta$  hopanoic, C<sub>32</sub>  $\beta\beta$  hopanoic acid and C<sub>31</sub>  $\beta\beta$  hopanoic acid (**56**, **55**, **54**). C<sub>31</sub>  $\beta\beta$  hopanoic acid (**55**) was the dominant hopanoic acid identified and was present in an abundance of 1.46  $\mu\text{g}\cdot\text{g}^{-1}$  dry sinter. C<sub>32</sub>  $\beta\beta$  hopanoic acid (**57**) was the next most abundant hopanoic acid identified during this analysis and was present in 1.11  $\mu\text{g}\cdot\text{g}^{-1}$  dry sinter (Table 6.3). C<sub>33</sub>  $\beta\beta$  hopanoic acid (**56**) was the least abundant hopanoic acid and was present in an abundance of 0.92  $\mu\text{g}\cdot\text{g}^{-1}$  dry sinter.

## BHP Diagenesis

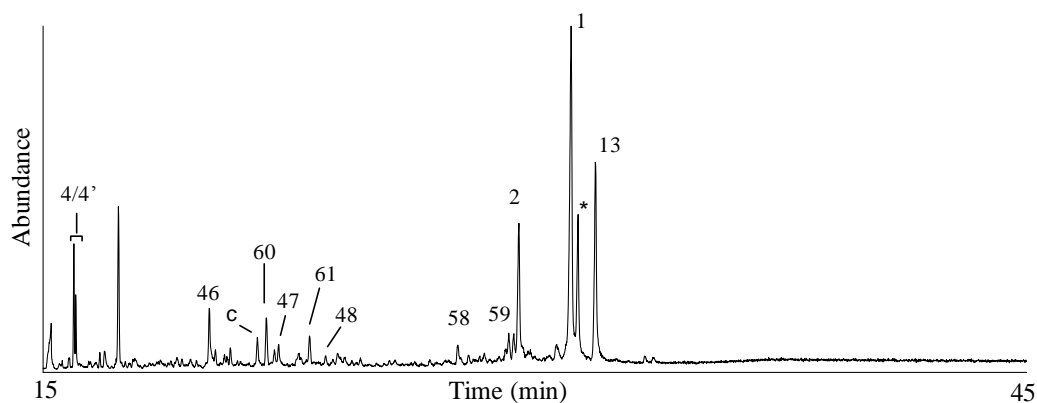


Figure 6.10 Partial  $m/z$  191 mass chromatogram (15 – 45 min) showing geohopanoids identified in sample RK2N. \* indicates a stereoisomer of BHtetrol (**1**)

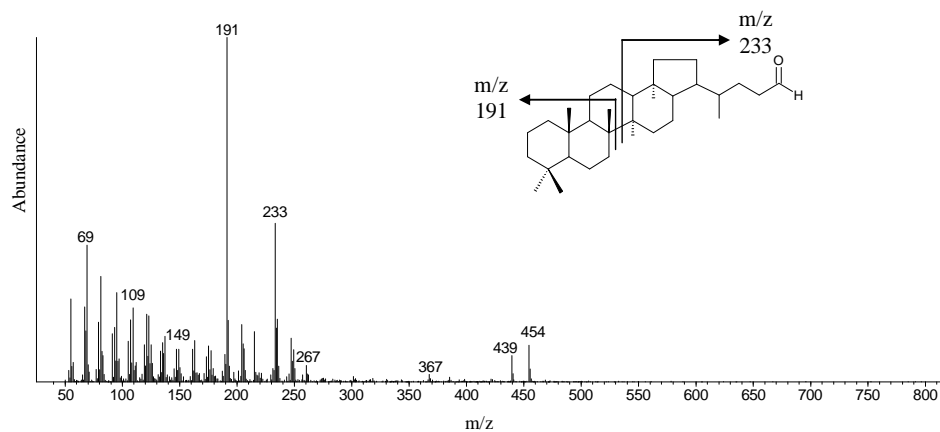


Figure 6.11  $C_{32}$   $\beta$  hopanone (**60**). Tentative structural assignment based upon relative retention time and comparison of fragment ions with previously published structures (Watson, 2002)

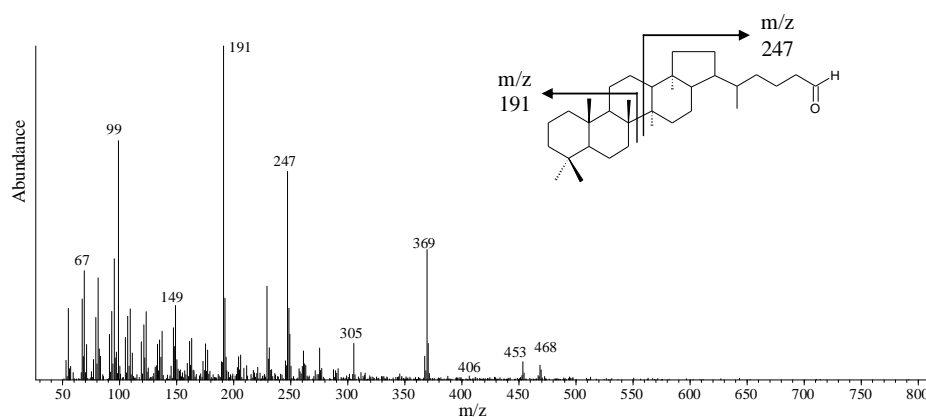


Figure 6.12  $C_{33}$   $\beta$  hopanone (**61**). Tentative structural assignment based upon relative retention time and comparison of fragment ions with previously published structures (Watson, 2002)

## 6.3.9.2 RK3N

The acetylated fraction of the non-active sinter RK3N showed the presence of biohopanoids and geohopanoids. The biohopanoids included BH*pentol*, BH*tetrol*, diploptene and hop-21-ene (**13**, **1**, **4**, **4'**). The least abundant biohopanoid identified was diploptene (**4**) and BH*tetrol* (**1**) was found to be the most abundant biohopanoid detected, with abundances ranging from 0.3 to 2.6  $\mu\text{g}\cdot\text{g}^{-1}$  dry sinter. Aminotriol (**22**) was also tentatively identified and was present in a concentration of 0.77  $\mu\text{g}\cdot\text{g}^{-1}$  dry sinter. The geohopanoids included anhydroBHT, C<sub>32</sub>  $\beta\beta$  hopanetriol, C<sub>33</sub>  $\beta\beta$  hopanediol, C<sub>32</sub>  $\beta\beta$  hopanediol, C<sub>32</sub>  $\beta\beta$  hopanol, C<sub>31</sub>  $\beta\beta$  hopanol and C<sub>30</sub>  $\beta\beta$  hopanol (**2**, **58**, **51**, **50**, **48**, **47**, **46**). C<sub>32</sub>  $\beta\beta$  hopanediol (**50**) was the least abundant geohopanoid and anhydroBHT (**2**) was the most abundant geohopanoid identified with abundances ranging from 0.1 to 1.81  $\mu\text{g}\cdot\text{g}^{-1}$  dry sinter (Table 6.3).

C<sub>33</sub>  $\beta\beta$  hopanoic acid, C<sub>32</sub>  $\beta\beta$  hopanoic acid and C<sub>31</sub>  $\beta\beta$  hopanoic acid (**56**, **55**, **54**) were identified during the analysis of hopanoic acids. C<sub>32</sub>  $\beta\beta$  hopanoic (**55**) was the most abundant compound identified and abundances were 0.34, 1.88 and 0.9  $\mu\text{g}\cdot\text{g}^{-1}$  dry sinter for C<sub>33</sub>, C<sub>32</sub> and C<sub>31</sub>  $\beta\beta$  hopanoic acid respectively (Table 6.3).

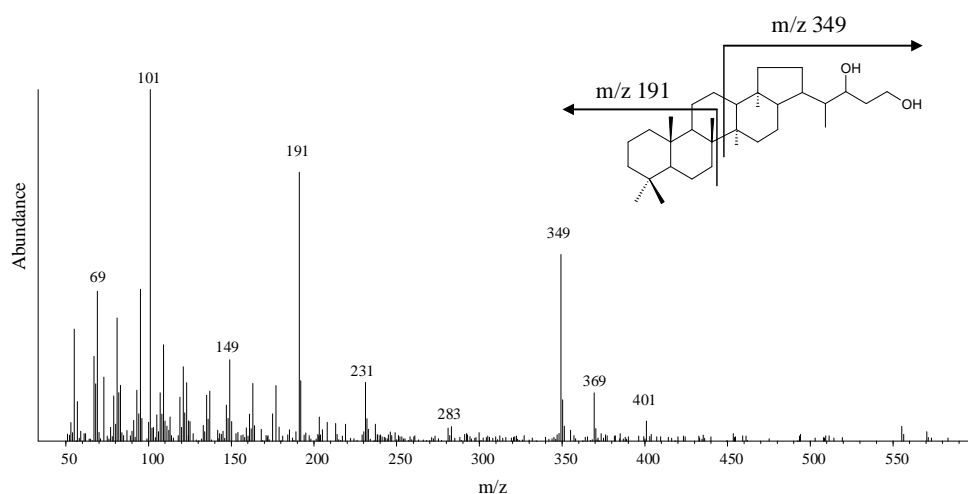


Figure 6.13 C<sub>32</sub>  $\beta\beta$  hopane-30,32-diol (**62**). GC-MS spectra of tentatively assigned hopanoid in sample RK3N. Structure identified by comparison with Watson (2002) and Allen (2006).

## 6.3.10 EL-TATIO GEYSER FIELD, CHILE

## 6.3.10.1 ET1A

Analysis of the acetylated fraction of sample ET1A (Figure 6.15) showed the presence of biohopanoids and geohopanoids. The distribution of biohopanoids consisted of BH*tetrol* and diplopterol (**1**, **5**). Both compounds were present in an abundance of  $0.08 \mu\text{g}\cdot\text{g}^{-1}$  dry sinter. The distribution of geohopanoids consisted of anhydroBHT, C<sub>32</sub>  $\beta\beta$  hopanol, C<sub>31</sub>  $\beta\beta$  hopanol and C<sub>31</sub>  $\beta\beta$  hopanediol (**2**, **48**, **47**, **49**). The least abundant geohopanoid was C<sub>32</sub>  $\beta\beta$  hopanol (**48**) and the most abundant geohopanoid identified was C<sub>31</sub>  $\beta\beta$  hopanol (**47**). Abundances ranged from  $0.01$  to  $0.16 \mu\text{g}\cdot\text{g}^{-1}$  dry sinter (Table 6.2).

Analysis of hopanoic acids showed the presence of C<sub>33</sub>  $\beta\beta$  hopanoic acid and C<sub>32</sub>  $\beta\beta$  hopanoic acid (**56**, **55**) which were present in a concentration of  $4.41$  and  $1.39 \mu\text{g}\cdot\text{g}^{-1}$  dry sinter (Table 6.2).

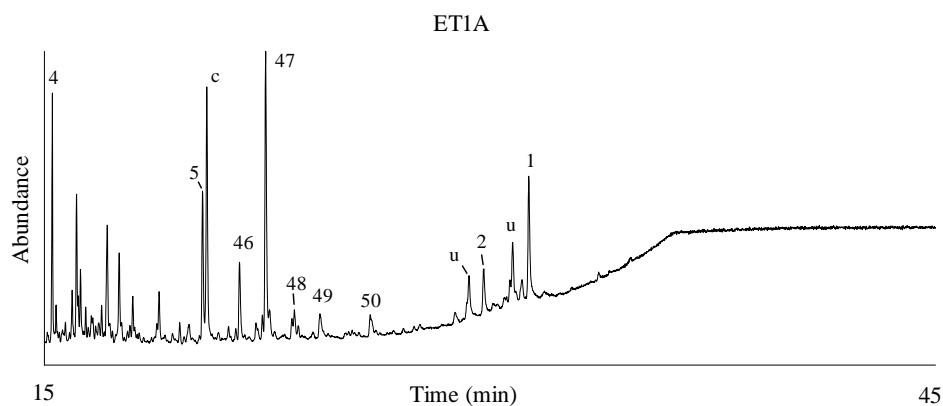


Figure 6.14 Partial  $m/z$  191 mass chromatogram (15 – 45 min) showing geohopanoids identified in sample ET1A. U indicates undetermined hopanoid

## 6.3.10.2 ET25A

The acetylated fraction of sample ET25A showed the presence of BH*tetrol* only. No geohopanoids were identifiable during this analysis. BH*tetrol* was present in an abundance of  $0.1 \mu\text{g}\cdot\text{g}^{-1}$  dry sinter (Table 6.2).

Analysis of hopanoic acids showed the presence of C<sub>33</sub> ββ hopanoic acid and C<sub>32</sub> ββ hopanoic acid (**57**, **56**). Abundances were 3.96 and  $0.5 \mu\text{g}\cdot\text{g}^{-1}$  dry sinter respectively (Table 6.2).

## 6.3.10.3 ET26A

The acetylated fraction of sample ET26A showed the presence of biohopanoids and geohopanoids, albeit in small amounts. The biohopanoids BH*tetrol* and BH*pentol* (**1**, **13**) were present in trace amounts as were the geohopanoids C<sub>31</sub> ββ hopanediol and C<sub>32</sub> ββ hopanediol (**49**, **50**). C<sub>32</sub> ββ hopanol (**48**) was also identified and was present in an abundance of  $0.01 \mu\text{g}\cdot\text{g}^{-1}$  dry sinter (Table 6.2).

Analysis of the methylated fraction showed an absence of hopanoic acids.

## 6.4 DISCUSSION

### 6.4.1 GEOHOPANOID COMPOSITION OF SILICA SINTERS

Geohopanoids have been identified in the majority of sinters analysed (Table 6.2 and 6.3). Geohopanoids were absent from sample OP2. The distributions observed consist of hopanols, hopanediols, hopanetriols, hopanoic acids, hopanones and anhydroBHT. Variation in geohopanoid distributions observed by comparing environmental conditions, depositional setting and differences observed between active and non-active sinters setting will now be discussed.

#### 6.4.1.1 HOPANOLS

The dominant hopanol detected in the majority of sinters was C<sub>31</sub> ββ hopanol. The exception to this is a predominance of C<sub>33</sub> ββ hopanols in sinters collected from FMP (Samples OK1-TA, OK1-MA and OK1-BA). These observations are in contrast with previous reports of distributions of geohopanoids in sediments and soils where C<sub>32</sub> ββ hopanol is the usually the most abundant hopanol detected. (Dastillung *et al.*, 1980; Rohmer *et al.*, 1980; Quirk *et al.*, 1984; Ries-Kautt and Albrecht, 1989; Innes *et al.*, 1997, 1998; Farrimond *et al.*, 2000; Blumenberg *et al.*, 2009). Hopanols were not identified in sample CPf, OP2A, ET25A or LR6R and were present in only small amounts (0.01 μg.g<sup>-1</sup> dry sinter or less) in samples OP7A, ET25A and OK6N.

The ratio of C<sub>31</sub> hopanol abundance relative to C<sub>32</sub> hopanol abundance (Tables 6.4 and 6.5) varies between 0.48 to 1. This ratio is compared to that of the precursor penta- and tetrafunctionalised BHPs (defined in equation 6.2; Table 6.4 and 6.5). Values range from 0 to 0.9 indicating a wide variation in the dominance of tetra- vs. pentafunctionalised BHPs throughout the sinters analysed but importantly showing no correlation to the ratios of terminal hopanols except in two of the active sinters (samples OK1-MA and LR2A) and one

non-active sinter RK2N (Figure 6.15). This indicates that a novel diagenetic process is affecting BHP distributions preserved in silica sinters.

### BHP Diagenesis

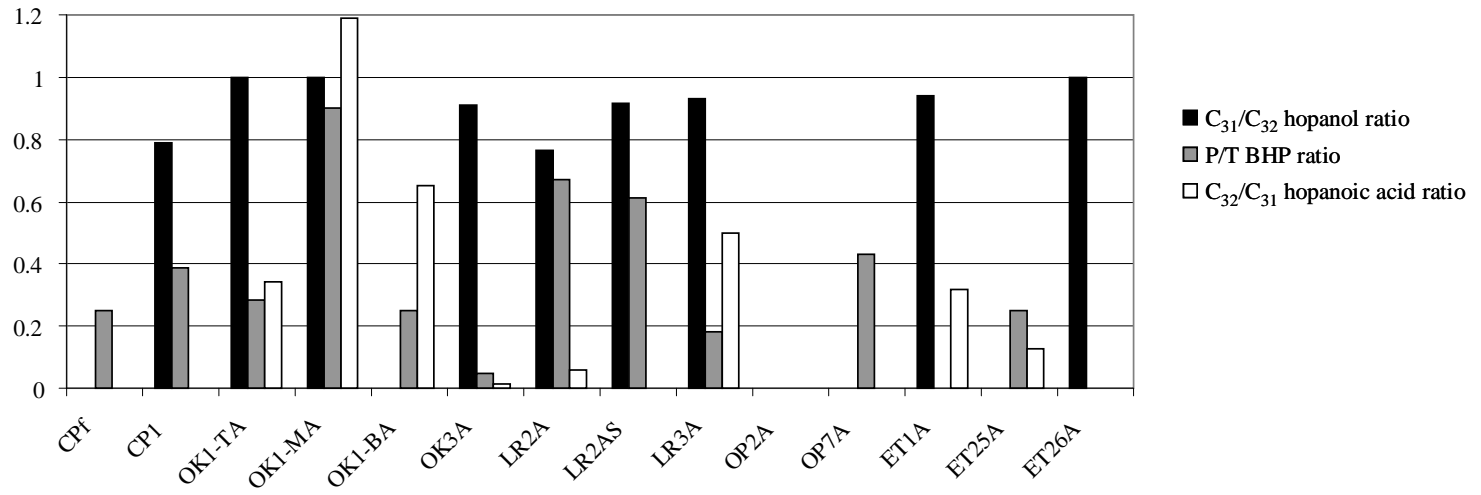


Figure 6.15 Ratios of geohopanooids and BHPs in active sinters

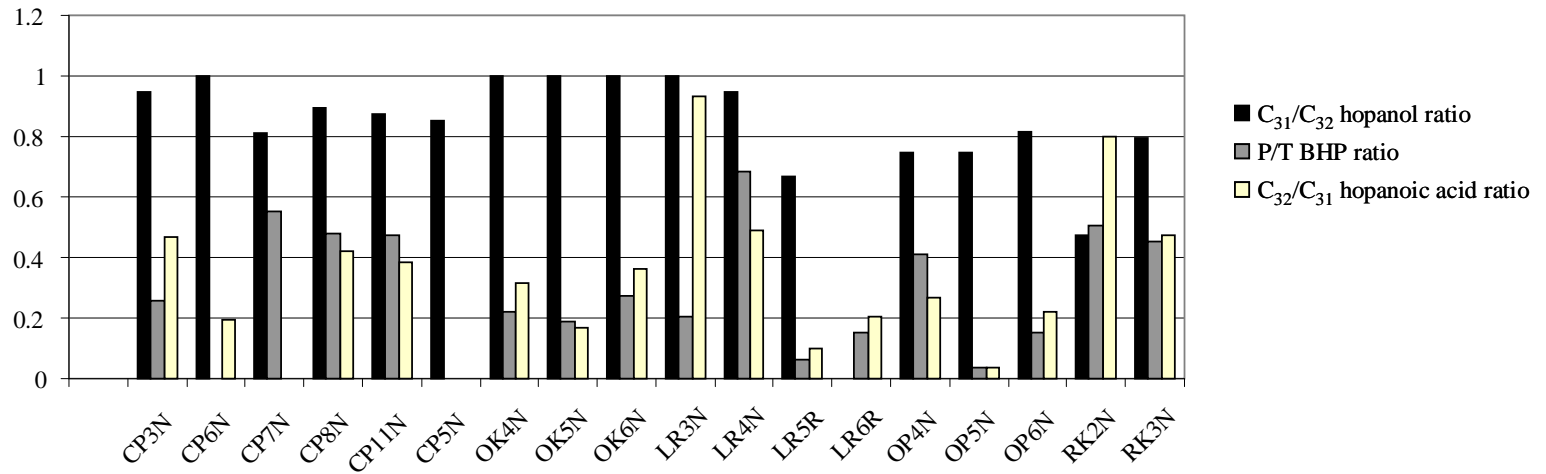


Figure 6.16 Ratios of geohopanooids and BHPs in non-active sinters

Previous studies have centred upon the distribution of hopanols in marine and lacustrine environments (e.g. Innes *et al.*, 1997; Rodier *et al.*, 1999; Watson, 2002; Blumenberg *et al.*, 2009). The relative distributions of C<sub>30</sub>, C<sub>31</sub> and C<sub>32</sub> ββ hopanol in different marine and lacustrine sediments is presented in Figure 6.17 (Watson, 2002). It is clear that the distributions of geohopanols observed in silica sinters are significantly different to those reported in previous studies. These investigations showed C<sub>32</sub> ββ hopanol to be the dominant hopanol present in sediments and the origin of this distribution was attributed to an increased input of tetra-functionalised BHP precursors compared to penta- or hexa-functionalised precursor BHPs. Marine sediments (Figure 6.17, top) show a predominance of C<sub>32</sub> hopanol which was assumed to derive from a predominance of tetrafunctionalised BHP precursor in marine bacteria. A predominance of C<sub>32</sub> hopanol has also been observed in lacustrine sediments however a contribution of C<sub>30</sub> hopanol is evident by the spread of data points towards the C<sub>30</sub> hopanol apex of the ternary figure (Figure 6.16, middle). This is thought to reflect an input from hexafunctionalised BHP-precursors deriving from methanotrophic organisms utilising methane produced by methanogenic archaea in the anoxic portions of the water column at the sites investigated (Watson, 2002).

The unprecedented observation of the predominance of C<sub>31</sub> hopanol (Figure 6.16, bottom) provides further evidence of the effect of environmental situation on distributions of terminal hopanols. This is further emphasised, and complicated, by the presence of C<sub>33</sub> homologues in sinters formed under the highest temperatures investigated at FMP (sample OK1-TA, OK1-MA and OK1-BA; water temperature 97.8°C at the time of sampling). C<sub>33</sub> homologues would be assumed to derive from a precursor BHP without a hydroxyl group at C<sub>32</sub> however, no precursors of this type are currently known.

## BHP Diagenesis

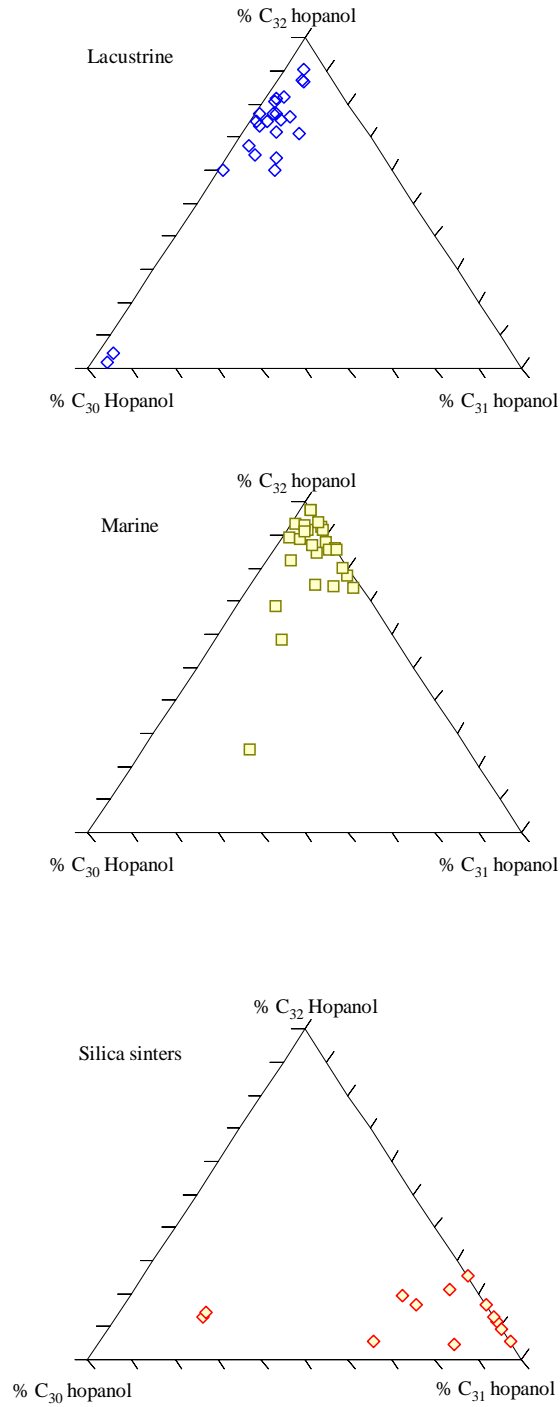


Figure 6.17 Relative distributions of terminal hopanols surveyed during this study. Distributions terminal hopanols are included for comparison of lacustrine (top) and marine sediments (middle; data adapted from Watson, 2002)

## 6.4.1.2 HOPANEDIOLS AND HOPANETRIOLS

Hopanediols and hopanetriols are thought to originate from degradation of polyfunctionalised side-chain components of BHPs (Watson, 2002). The presence of these compounds in silica sinters represents diagenetic intermediates. A series of C<sub>31</sub> ββ – C<sub>33</sub> ββ hopanediols has been identified in a number of samples (RK3, LR, OK3, ET1, OP5 and OP6) throughout this study and also in Chapter 3. Abundances roughly follow a trend of C<sub>31</sub> ββ > C<sub>32</sub> ββ > C<sub>33</sub> ββ hopanediol. C<sub>30, 32</sub> hopanediols have been tentatively identified in samples from RK and LR, a similar compound was detected in microbial mats (Boon *et al.*, 1981) and a derivative of BH*pentol*, possessing hydroxyl groups at C<sub>30,32,33,34,35</sub> (Iso-BH*pentol*; **14**) has been identified in cultures of *Nostoc* sp. (Bisseret *et al.*, 1985). However, Iso-BH*pentol* (**14**) was not observed during LC-MS<sup>n</sup> analysis.

## 6.4.1.3 HOPANOIC ACIDS

Hopanoic acids have been previously detected in a range of recent environmental settings including lacustrine and marine sediments (i.e. Rohmer *et al.*, 1980; Innes *et al.*, 1998; Watson, 2002), peats (Quirk *et al.*, 1984), mat-forming microbial consortia (Boon *et al.*, 1981; Zhang *et al.*, 2007) and also silica sinters (Talbot *et al.*, 2005; Kaur, 2009). Here they were detected in all samples analysed with the exception of ET26A, OP2A and OP7A and were only detected in trace amounts during the analysis of sample CP1A and low amounts of lipid extract from samples CPf and LR2AS meant that there was insufficient material available to prepare a methylated fraction. Hopanoic acids appear to be more abundant in non-active sinters than active sinters collected from the same location (Tables 6.4 and 6.5). With the exception of active and non-active sinters of CP and sample OP7A, hopanoic acids appear to more abundant than hopanols (Table 6.2 and Table 6.3) and the C<sub>32</sub> ββ homologue is the most abundant hopanoic acid identified in all samples except OK1-MA where C<sub>31</sub> hopanoic acid is dominant.

A ratio of C<sub>32</sub> hopanoic acid to C<sub>31</sub> hopanoic acid (Table 6.4 and Table 6.5) is used to compare distributions of hopanoic acids with input of penta- and tetrafunctionalised BHPs (P/T ratio; Table 6.4 and Table 6.5). Generally, in active sinters the correlations of ratios is poor with the exception of samples OK1-TA and OK3A (Figure 6.15). Comparison of C<sub>32</sub>/C<sub>31</sub> acid and P/T ratios in non-active sinters shows a good correlation and indicates that distributions of hopanoic acids in older sinters appear to mirror input of BHPs (Figure 6.16). The exceptions to this are samples CP3N, CP6N, CP7N and LR3N (Figure 6.16).

## Chapter 6

Table 6.4 Composition of distributions of geohopanoids and BHPs of active sinters

	Terminal hopanol composition				Hopanoic acid abundance				Composition of BHP distribution					Ratio		
	C <sub>30</sub> hopanol	C <sub>31</sub> hopanol	C <sub>32</sub> hopanol	C <sub>33</sub> hopanol	Anhydro	C <sub>31</sub>	C <sub>32</sub>	C <sub>33</sub>	Tetra	Penta	Hexa	Anhydro	Novel	C <sub>32</sub> /C <sub>31</sub>	C <sub>31</sub> /C <sub>32</sub>	P/T
CPF	-	-	-	-	0.07	-	-	-	5.08	1.7	-	-	-	0	nd	0.25
CP1	-	0.6	0.16	-	0.12	-	-	-	2.55	1.6	-	-	0.1	0	0.79	0.39
OK1-TA	0.02	0.01	-	0.06	-	0.22	0.64	0.06	0.15	0.06	-	0.01	-	0.34	1	0.29
OK1-MA	0.01	0.01	-	0.03	-	0.75	0.63	-	0.03	0.27	-	0.01	0.01	1.19	1	0.9
OK1-BA	-	-	-	0.01	-	0.17	0.26	-	0.12	0.04	-	-	-	0.65	nd	0.25
OK3A	-	2	0.2	-	0.6	0.06	4	0.76	492	25	-	1.2	0.68	0.02	0.91	0.05
LR2A	-	0.16	0.05	-	0.03	0.1	1.7	0.15	0.97	1.98	-	0.16	0.03	0.06	0.76	0.67
LR2AS	0.42	1.2	0.11	-	0.03	-	-	-	0.51	0.81	-	0.08	0.04	0	0.92	0.61
LR3A	-	0.4	0.03	-	0.08	0.09	0.18	0.02	1.9	0.42	-	0.19	0.07	0.5	0.93	0.18
OP2A	-	-	-	-	-	-	-	-	0.05	-	-	-	-	0	nd	0
OP7A	-	-	0.01	-	0.02	-	-	-	6.36	4.8	-	-	0.54	0	0	0.43
ET1A	-	0.16	0.01	-	0.04	1.4	4.4	-	0.27	-	-	-	-	0.32	0.94	0
ET25A	-	-	-	-	-	0.5	4	-	0.91	0.3	-	-	-	0.13	nd	0.25
ET26A	-	0.01	-	-	-	-	-	-	0.08	-	-	-	-	0	1	0

Key: <sup>a</sup>Terminal hopanol composition = Total  $\beta\beta+\beta\alpha+\alpha\beta$  of terminal hopanols identified in m/z 191 mass chromatogram. <sup>b</sup>Composition of BHP distribution = total abundance of tetra-, penta, hexafunctionalised components, also includes input of Anhydro-type BHPs and Novel BHPs identified in Chapter 5. <sup>c</sup>Ratio: C<sub>32</sub>/total acid =  $\sum C_{32}$  hopanoic acid / ( $\sum C_{31}$  hopanoic acid +  $\sum C_{32}$  hopanoic acid +  $\sum C_{33}$  hopanoic acid). C<sub>31</sub>/C<sub>32</sub> =  $\sum C_{31}$   $\beta\beta+\beta\alpha+\alpha\beta$  hopanol / ( $\sum C_{31}$   $\beta\beta+\beta\alpha+\alpha\beta$  hopanol +  $\sum C_{32}$   $\beta\beta+\beta\alpha+\alpha\beta$  hopanol). <sup>d</sup>ratio: P/T = [ $\sum$  pentafunctionalised BHPs / ( $\sum$  tetrafunctionalised BHPs +  $\sum$  pentafunctionalised BHPs)]. <sup>e</sup>sample: CP = Champagne Pool, OK = Orakei Korako, LR = Loop Road, OP = Opaheke Pool, ET = El-Tatio. <sup>f</sup>nd = not determined

## BHP Diagenesis

*Table 6.5 Composition of distributions of geohopanoids and BHPs of non-active sinters*

	Terminal hopanol composition				Hopanoic acid abundance				Composition of BHP distribution					Ratio		
	C <sub>30</sub> hopanol	C <sub>31</sub> hopanol	C <sub>32</sub> hopanol	C <sub>33</sub> hopanol	Anhydro	C <sub>31</sub> acid	C <sub>32</sub> acid	C <sub>33</sub> acid	Tetra	Penta	Hexa	Anhydro	Novel	C <sub>32</sub> /C <sub>31</sub>	C <sub>31</sub> /C <sub>32</sub>	P/T
CP3N	0.98	3.5	0.19	-	1.8	1.5	3.2	0.56	0.72	0.25	-	0.03	0.06	0.47	0.95	0.26
CP6N	0.02	0.05	-	-	0.02	0.07	0.36	0.23	-	-	-	-	-	0.19	1	
CP7N	-	0.6	0.14	-	0.12	nd	nd	nd	0.6	0.74	-	0.15	0.25	0	0.81	0.55
CP8N	0.44	0.59	0.07	-	0.94	0.19	0.45	0.06	4.88	4.5	-	0.7	0.86	0.42	0.89	0.48
CP11N	2.2	6.4	0.93	-	1.9	0.27	0.7	0.13	8.41	7.6	-	0.38	0.49	0.39	0.87	0.47
CP5N	3.44	7	1.21	-	1.12	nd	nd	nd	-	-	-	-	-	0	0.85	
OK4N	-	0.02	-	-	0.1	1.7	5.4	0.98	1.6	0.45	0.29	0.24	0.41	0.31	1	0.22
OK5N	-	0.03	-	-	-	0.02	0.12	-	0.93	0.22	0.05	-	-	0.17	1	0.19
OK6N	-	0.01	-	-	-	0.08	0.22	-	0.4	0.15	-	-	-	0.36	1	0.27
LR3N	-	0.05	-	-	-	0.27	0.29	-	3.84	1	-	1	1.87	0.93	1	0.21
LR4N	0.11	0.7	0.04	-	0.15	0.22	0.45	0.09	6.9	15	-	0.31	0.48	0.49	0.95	0.68
LR5R	-	0.02	0.01	-	-	0.07	0.7	0.2	24.79	1.6	-	2.3	1.04	0.1	0.67	0.06
LR6R	-	-	-	-	0.04	0.08	0.39	0.11	8.3	1.5	-	0.11	0.28	0.21	nd	0.15
OP4N	-	0.03	0.01	-	0.01	30.1	113	12.4	43	30	-	3.5	-	0.27	0.75	0.41
OP5N	0.39	3.9	1.3	-	0.53	0.4	10.6	10	18.64	0.76	0.2	0.47	-	0.04	0.75	0.04
OP6N	-	3.7	0.84	-	2.1	10.7	48	8.4	73.2	13.38	-	4.1	-	0.22	0.81	0.15
RK2N	0.38	0.1	0.11	-	1.1	1.2	1.5	0.92	15.61	16.1	-	1.86	4.56	0.8	0.48	0.51
RK3N	0.22	0.46	0.12	-	1.8	0.9	1.9	0.34	4.52	3.7	-	0.97	2.32	0.47	0.79	0.45

Key: <sup>a</sup>Terminal hopanol composition = Total ββ+βα+αβ of terminal hopanols identified in m/z 191 mass chromatogram.

<sup>b</sup>Composition of BHP distribution = total abundance of tetra-, penta, hexafunctionalised components, also includes input of Anhydro-type BHPs and novel BHPs identified in Chapter 5. <sup>c</sup>Ratio: C<sub>32</sub>/total acid =  $\sum C_{32}$  hopanoic acid / ( $\sum C_{31}$  hopanoic acid +  $\sum C_{32}$  hopanoic acid +  $\sum C_{33}$  hopanoic acid). C<sub>31</sub>/C<sub>32</sub> =  $\sum C_{31}$  ββ+βα+αβ hopanol / ( $\sum C_{31}$  ββ+βα+αβ hopanol +  $\sum C_{32}$  ββ+βα+αβ hopanol). <sup>c</sup>ratio: P/T = [ $\sum$  pentafunctionalised BHPs / ( $\sum$  tetrafunctionalised BHPs +  $\sum$  pentafunctionalised BHPs)]. <sup>d</sup>sample: CP = Champagne Pool, OK = Orakei Korako, LR = Loop Road, OP = Opaheke Pool, ET = El-Tatio. <sup>e</sup>nd = not determined

## 6.4.2 DISTRIBUTION OF INTERMEDIATE DIAGENETIC PRODUCT GROUPS IN SINTERS

### 6.4.2.1 CHAMPAGNE POOL

The sample of floc material (CPf) did not show the presence of free hopanols, hopanediols or hopanetriols and it was not possible to analyse for hopanoic acids due to the small amount of starting material. AnhydroBHT (2) was identified in this sample, indicating that diagenesis of BHPs produced by bacteria inhabiting the vent waters of CP is following a reductive mechanism (e.g. Schaffer *et al.*, 2008) and possibly that the highly reducing conditions of the pool are limiting degradation of organic matter (e.g. Simoneit, 1996).

Geohopanoids were detected in all silica sinter samples from CP (samples CP1A to CP5N; Table 6.2 and Table 6.3). They were less abundant in the actively-precipitating sinter (Sample CP1A) than in non-active silica sinters (samples CP3N, CP6N, CP7N, CP8N, CP11N and CP5N; Section 6.3.2; Table 6.2 and Table 6.3). Hopanols are the most abundant geohopanoids identified in sinters of CP (Figure 6.18), with C<sub>31</sub> ββ hopanol the abundant geohopanoid identified throughout (Table 6.2; Table 6.3).

Hopanediols are present as minor components of the geohopanoid distribution in samples CP1A, CP7N, CP8N and CP11N. AnhydroBHT is also present in significant amounts, contributing to between 5 and 30 % of the total geohopanoid composition (Figure 6.16).

With the exception of sample CP6N, hopanoic acids account for only small amounts of the total geohopanoid composition (Figure 6.18). This is consistent with the observation that BHP distributions in this particular sinter may be affected by input of organic matter from an allochthonous source (Chapter 3.4.1.1). Hopanoic acids are more abundant in non-active

sinters of CP and where present, C<sub>32</sub> ββ hopanoic acid was the most abundant geohopanoic acid present.

#### 6.4.2.2 ORAKEI KORAKO

The geohopanoic acid distributions of three separate depositional settings within the OK geothermal field were found to contain different products of BHP diagenesis. The three settings include active sinters from the edge of Fred and Maggie's Pool (FMP; Samples OK1-TA, OK1-MA and OK1-TA; Water temperature, 97.8°C at the time of sampling), a sinter collected from the outflow channel of FMP (Sample OK3A; water temperature, 63°C at the time of sampling) and three non-active sinters collected from the Golden Fleece sinter terrace (GFT; Samples OK4N, OK5N and OK6N). The dominant hopanol identified in sinters of FMP is a C<sub>33</sub> component (Table 6.2), however, in the sinter from the outflow channel, C<sub>31</sub> hopanol is the dominant compound. This indicates that the geohopanoic acid distributions of the FMP sinters are indigenous as a similar distribution could be expected to be recorded in a sinter that forms in the outflow channel of the vent source. Furthermore, C-2 methylated hopanoic acids were not detected during analysis of the sinter from the outflow channel (Samples OK3A) but were identified in the sinters of FMP (Samples OK1-TA, OK1-MA and OK1-BA).

Distributions of hopanols in non-active sinters collected from the sinter terrace at OK (Samples OK4N, OK5N and OK6N) showed that geohopanoic acids were present in low abundances (Table 6.3). C<sub>31</sub> ββ hopanol was the most abundant hopanol detected in each sample (Table 6.3).

Hopanoic acids were significantly more abundant than hopanols, hopanediols or triols or anhydroBHT (**2**; Table 6.3) in both active and non-active sinters of OK (Figure 6.17).

## 6.4.2.3 LOOP ROAD

Distributions of geohopanooids in sinters from LR vary significantly between samples. Hopanols are present in each sinter with the exception of sample LR6R. The most abundant hopanol identified in each sinter was C<sub>31</sub> ββ hopanol.

Hopanediols were present in non-active samples LR3N and LR4N (Table 6.3) but were absent from active sinters. C<sub>33</sub> ββ hopanetriol was identified in trace amounts only in Sample LR5R (Table 6.3).

Hopanoic acids comprised the major diagenetic products in active sample LR2A and non-active samples LR3N, LR5R and LR6R (Figure 6.18). However hopanoic acids account for only small fractions of the total abundance in active sample LR2AS and non-active samples LR3A and LR4N. LR is known to have been subject to various geological and hydrological changes over time and this may be reflected in the variable nature of the geohopanooid distributions observed in both active and non-active sinters. This suggests that the sinter collected from the current air-water interface may have been deposited in the past and is not a new deposition. This would explain the abundance of hopanoic acids in an active sinter (sample LR2A), as opposed to a predominance of hopanols as observed in other active sinters from LR (Samples LR2AS and LR3A) and CP (Sample CP1A). The pH of the vent fluids at LR (pH 5.6) are similar to that of CP (pH 5.5), it would be expected that the geohopanooid distributions of the active sinters would be similar, i.e. contain higher abundances of hopanols than hopanoic acids (Figure 6.16). However, the geohopanooid distribution of LR2A consists predominantly of hopanoic acids (Figure 6.17) which is difficult to explain. As sample LR2A was collected from the pool edge and was in contact with the vent fluids, it could also be expected to contain a high proportion of anhydroBHT (2) but this is not the case.

#### 6.4.2.4 ROTOKAWA

The geohopanoid assemblage observed in the non-active sinters of RK are more diverse than those observed at other sites and contains a larger contribution from hopanediols, hopanetriols and other geohopanoids such as C<sub>32</sub> and C<sub>33</sub> hopanone (Figure 6.20). Hopanols, hopanoic acids and anhydroBHT (**2**) were also present and in the most recently formed of the two samples, RK2N, C<sub>30</sub> ββ hopanol was found to be the most abundant free hopanol detected. In sample RK3N, C<sub>31</sub> ββ hopanol was the most abundant free hopanol detected.

Hopanetriols were present in both samples (RK2N and RK3N) and C<sub>32</sub> ββ hopanone and C<sub>33</sub> hopanone were identified in sample RK2N (Table 6.3).

Hopanoic acids are more abundant than other geohopanoids identified in samples and account for a significant amount of the total geohopanoid composition, however, they are less abundant than hopanoic acids identified in non-active sinters from other geothermal sites such as OK or OP. The pH at RK is lower than at other sites sampled (pH 2 at the time of sampling) therefore reduction of hopanoic acids to terminal hopanols, and other diagenetic products, may be affecting geohopanoid distributions.

#### 6.4.2.5 OPAHEKE POOL

Similar to the investigations of sinters from OK, sinters were analysed from three different depositional settings; An sinter from the pool edge (OP2A; water temperature 95°C at the time of sampling), an active sinter from the outflow channel (Sample OP7A; water temperature 68°C at the time of sampling) and three non-active sinters collected from the sinter flat (samples OP4N, OP5N and OP6N). Geohopanoid compositions appear to vary between active and non-active sinters, which is consistent with observations of geohopanoid distributions at OK. A similar observation was made during analysis of BHPs from this site (Chapter 3 and Chapter 4).

Hopanols were present in each sample with exception of OP2A and C<sub>31</sub> ββ hopanol was the most abundant hopanol identified in each sample.

Sample OP7A, from the outflow channel was found to contain a high proportion of anhydroBHT compared to C<sub>32</sub> ββ hopanol and C<sub>31</sub> ββ hopanol (**2**, **47**, **46**) but no hopanoic acids (Figure 6.19). Hopanediols and triols were not observed in sinters of OP (Table 6.2 and Table 6.3; Figure 6.19).

Hopanoic acids were absent from active sinters (OP2A and OP7A). Hopanoic acids were significantly more abundant than hopanols in non-active sinters of OP (Table 6.3; Figure 6.19).

#### 6.4.2.6 EL-TATIO

ββ C<sub>31</sub> hopanol was the most abundant hopanol detected in samples from ETGF (Samples ET1A and ET25A) but absent from ET26A. Sample ET1A showed the most diverse assemblage of compounds; C<sub>32</sub> ββ hopanol, C<sub>31</sub> ββ hopanol, C<sub>30</sub> ββ hopanol, C<sub>31</sub> ββ hopanediol were detected in this sample, albeit in low amounts. However, hopanoic acids consist of 96% of the total measured geohopanoic abundances (Figure 6.21). A similar distribution is observed in sample ET25A, however in this case, free hopanols were not present and the distribution of geohopanoic acids consists predominantly of hopanoic acids. In sample ET26A, only C<sub>31</sub> hopanol was detected (Figure 6.21).

Abundances of BHPs in ETGF sinters were also low and are thought to derive from mainly endolithic or cryptoendolithic cyanobacteria (e.g. Phoenix *et al.*, 2006). The abundances of hopanoids (BHPs and geohopanoic acids) detected in sinters from ETGF are similar to those observed from TVZ sites where water temperature is near to boiling point, i.e. OP (sample OP2A) and OK (samples OK1-TA, OK1-MA and OK1-BA). The high-altitude location of ETGF means local boiling point of water is around 86°C (Phoenix *et al.*, 2006).

The low diversity of bacteria at this site is thought to be a consequence of the particularly harsh conditions of the site, which include high quantities of UV radiation, boiling water temperatures and hyper-arid conditions (Piazena, 1996; Phoenix *et al.*, 2006).

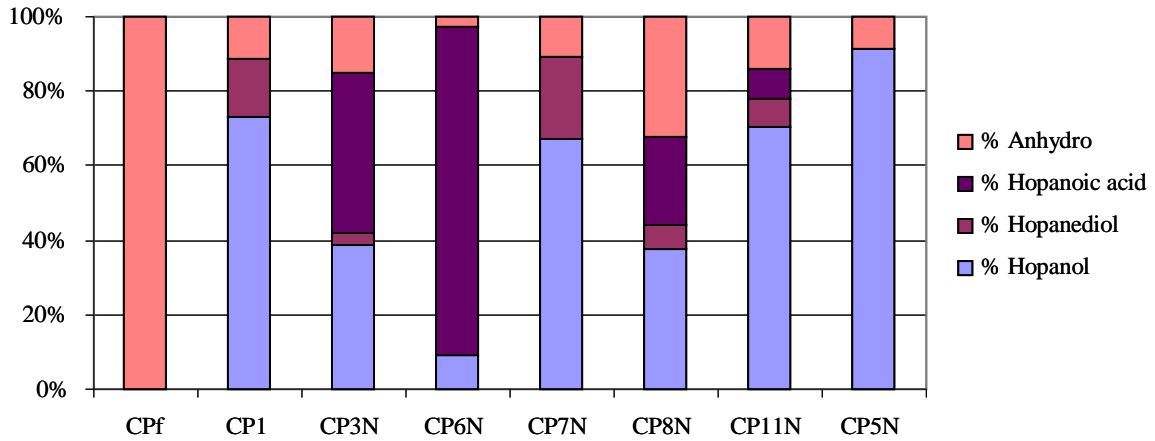


Figure 6.18 Composition of geohopanooid distributions observed in silica sinters from CP

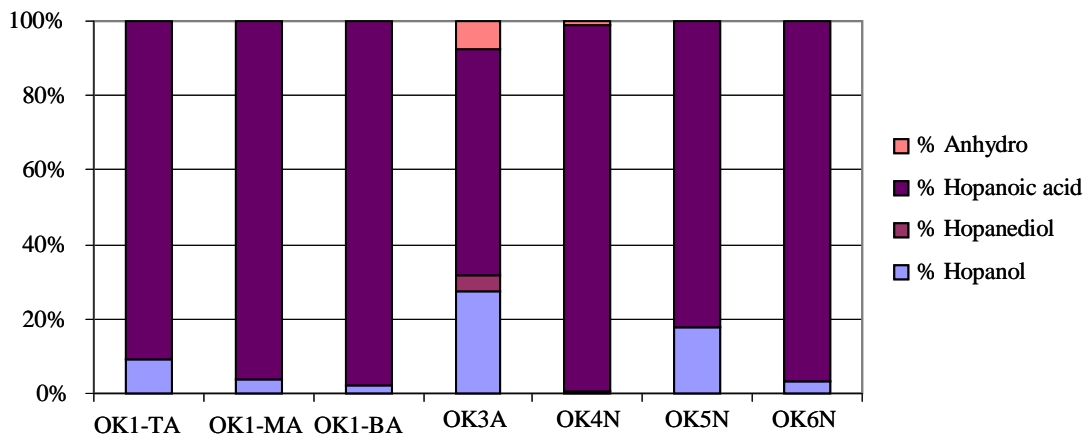


Figure 6.19 Composition of geohopanooid distributions observed in silica sinters from OK

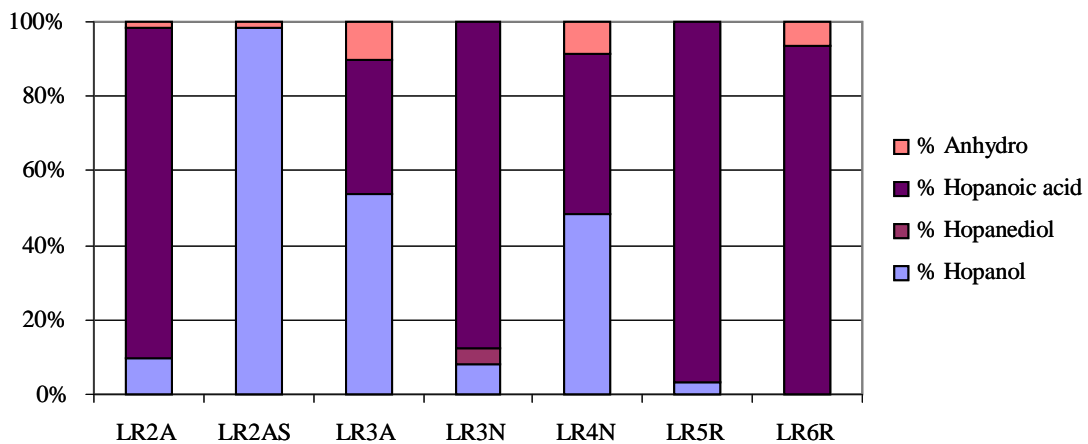


Figure 6.20 Composition of geohopanooid distributions observed in silica sinters from LR

BHP Diagenesis

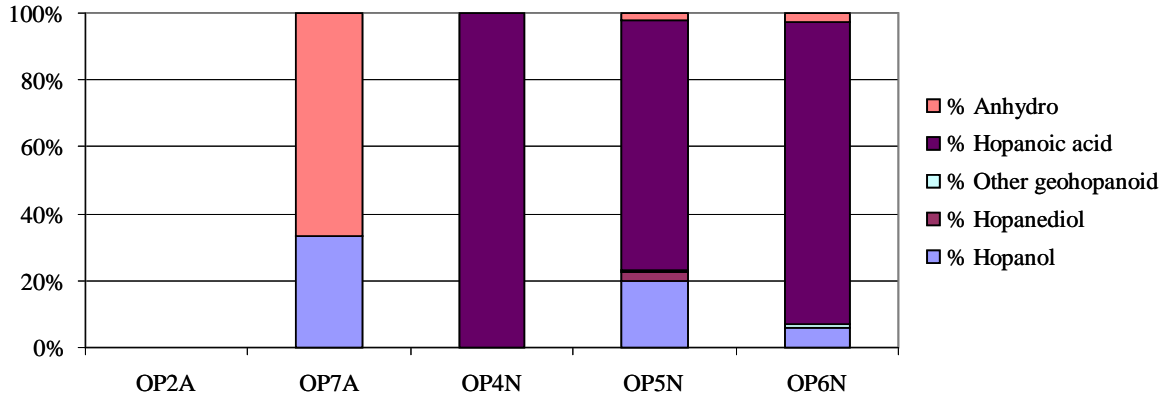


Figure 6.21 Composition of geohopanooid distributions observed in silica sinters from OP

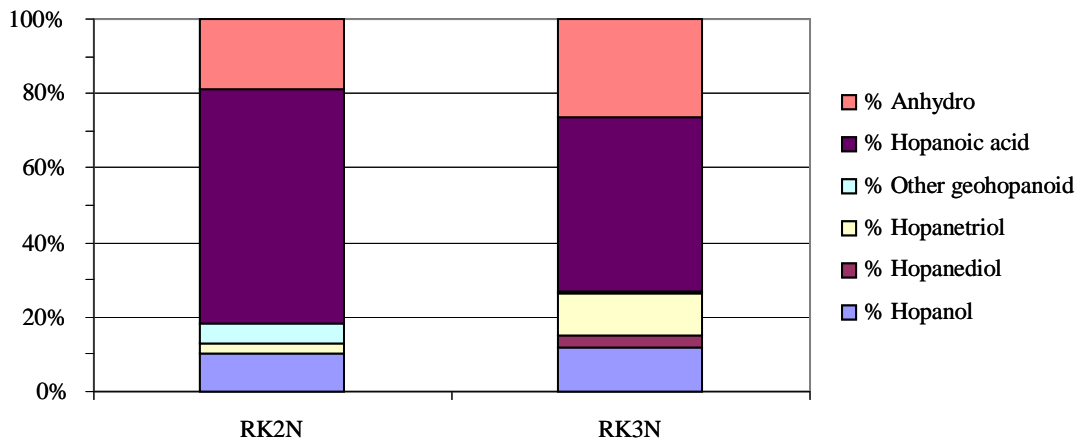


Figure 6.22 Composition of geohopanooid distributions observed in silica sinters from RK

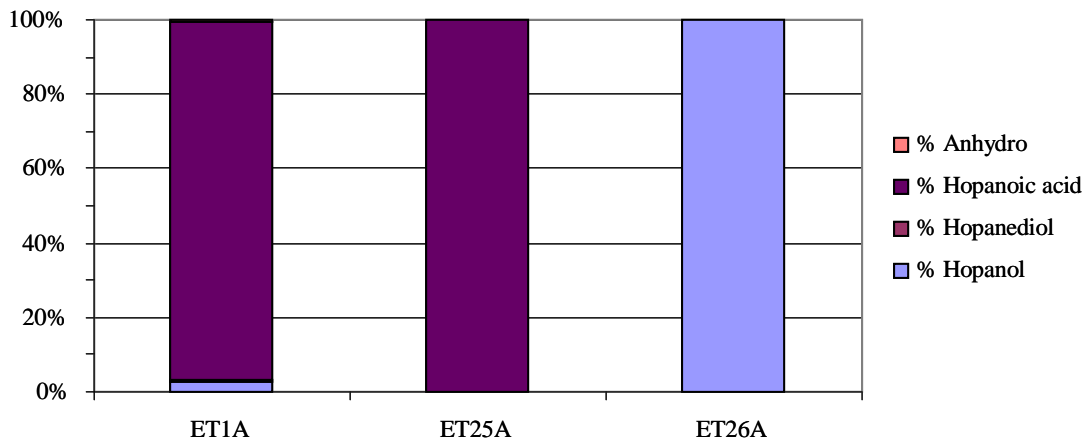


Figure 6.23 Composition of geohopanooid distributions observed in silica sinters from ETGF

### 6.4.3 GENERAL TRENDS AND SIMILARITIES

The presence of hopanols, hopanediols and hopanetriols suggests that diagenesis of BHPs in sinters may be proceeding via an oxidative diagenetic pathway, similar to that proposed by Watson (2002; Figure 6.1). This is consistent with the model of sinter formation (Mountain *et al.*, 2003), which is thought to proceed more readily at or above the air-water interface. As the pool waters are thought to be anoxic, the air-water interface can be considered analogous to an oxic-anoxic boundary. However, the presence of anhydroBHT, which is known to be produced via reductive pathways and was the only geohopanoic acid identified in sample CPF which forms in sub-aqueous settings, suggests that both oxidative and reductive mechanisms are affecting BHP distributions.

Hopanoic acids were detected throughout with the exception of sample OP2A, OP7A and ET26A and appear to be generally more abundant than 'geohopanoic acids'. Furthermore, hopanoic acids appear to be more abundant in sinters deposited under neutral, or near neutral conditions such as OK (pH 7.0 at the time of sampling) and OP (pH 7.2 at the time of sampling). Similarly distributions of geohopanoic acids are more diverse in acidic conditions. This indicates that hopanoic acids are more readily reduced to hopanols, and likely other unidentified components, under acidic conditions (e.g. site OK; Figure 6.17).

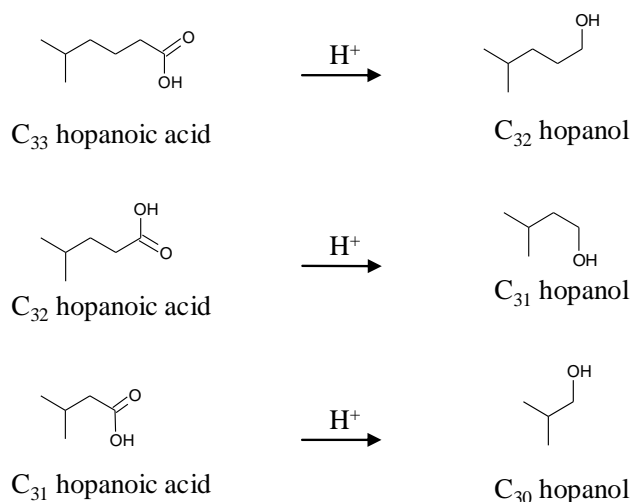


Figure 6.24 Reduction of hopanoic acids to terminal hopanols

#### 6.4.3.1 ACTIVE VERSUS NON-ACTIVE SINTERS

Geohopanoids have been detected in active and non-active sinters. Geohopanoids appear to be more abundant in non-active sinters than active sinters from the corresponding site (Table 6.2 and Table 6.3). As discussed above, non-active sinters are those that were deposited in the past and it is expected that they should contain a larger abundance of geohopanoids. Interestingly, hopanoic acids appear to form a larger percentage of the total geohopanoid composition in non-active sinters (Figure 6.16 to Figure 6.21), suggesting that hopanoic acids are more stable in sinter depositions.

Geohopanoids have been detected in the oldest sinters collected during this study (Samples CP11N, LR6R, OP6N, and RK3N). However, truly ancient sinters such as the Devonian Rhynie Cherts (Trewin, 1996) have previously been shown not to contain the presence of any recognisable molecular fossils (Summons *et al.*, 1996). Ancient hydrothermal siliceous deposits are known to exist throughout the geological record (for reviews on ancient hydrothermal deposits see Schopf, 1993; Walter, 1996; Knoll and Walter, 1996; Reysenbach and Cady, 2001), and where present one would expect highly degraded molecular fossils to

persist in low-maturity organic material or fluid inclusions. However, other factors such as the diagenesis of silica sinters from an amorphous to crystalline states will also affect the preservation of organic signatures preserved with the silica matrix (See Chapter 1, section 1.5; Cady and Farmer, 1996; Lynne and Campbell, 2004) in truly ancient silica-deposits.

#### 6.4.4 C<sub>31</sub> HOPANOL ANOMALY: ORIGIN AND SIGNIFICANCE

Throughout the investigation of geohopanol distributions in silica sinters, a high proportion of C<sub>31</sub> hopanol relative to C<sub>32</sub> or C<sub>30</sub> hopanol has been observed (Figure 6.16). This is in stark contrast to previous studies of meso-environmental settings where C<sub>32</sub> hopanol is usually the most abundant hopanol detected (Innes *et al.*, 1997; Watson and Farrimond, 2000; Farrimond *et al.*, 2000). It has been proposed that the predominance of C<sub>32</sub> hopanol components in lake and marine sediments (e.g. Watson and Farrimond, 2000; Farrimond *et al.*, 2000; Blumenberg *et al.*, 2009) derives from tetrafunctionalised BHP precursors. Therefore, it would be expected that penta-functionalised BHP should degrade to form C<sub>31</sub> hopanols. Pentafunctionalised BHPs are usually associated with cyanobacteria (Rohmer *et al.*, 1984; Zundel and Rohmer, 1985b; Zhao *et al.*, 1996; Talbot *et al.*, 2008a) and have also been found in methylotrophs, acetic acid bacteria and sulfate-reducing bacteria belonging to genus *Desulfovibrio sp.* (Neunlist and Rohmer, 1985a; Blumenberg *et al.*, 2006) and it is certainly plausible that organisms similar to these organisms may exist in terrestrial geothermal settings. A penta-functionalised homologue of guanidine-BHTcyc (**23**), a BHP originally detected in *Methylobacterium organophilum* was detected in sinters from CP, LR and RK (Samples CP11, LR3A and RK2N). Acetic acid bacteria are known to produce distinctive unsaturated BHPs (See section 1.8.4.3) and unsaturated aminotriol ( $\Delta$ -**22**) was detected in sample OP6N. Similarly aminotetrol, detected in *Desulfovibrio sp.* (Blumenberg *et al.*, 2006) was identified in sample OP5N. However, these compounds were present as only minor constituents of the total BHP distributions and the presence of these compounds cannot be

responsible for the predominance of C<sub>31</sub> hopanol. BHP-signatures of cyanobacteria have been detected in samples from OK, LR, OP, RK and ET (Chapter 3 and Chapter 4). However, it should be stressed that the input of pentafunctionalised BHPs is inconsistent with observations of C<sub>31</sub> hopanol. This may imply a number of possible outcomes;

- Undetermined diagenetic pathway that is controlled by environmental condition
- A significant proportion of penta-functionalised BHPs remain undetermined and undetectable via LC-MS<sup>n</sup> analysis
- Selective preservation of C<sub>31</sub> hopanoid compounds or selective degradation of C<sub>32</sub> compounds

The apparent mis-match between biological and geological hopanoid counterparts is further evidenced by the fact that hexafunctionalised BHPs were detected in only three samples i.e. OP5N, OK4N and OK6N (Chapter 4, Figures 4.7, 4.8 and 4.15), and in these samples hexa-functionalised BHPs constituted only minor components of the entire BHP assemblage. However, C<sub>30</sub> hopanol and C<sub>31</sub> hopanoic acid have been detected as minor compounds throughout this study in a variety of active and non-active sinters from CP, OK, LR, OP, RK and ET (Table 6.2 and Table 6.3). This is further evidence by a predominance of an apparent early eluting C<sub>33</sub> ββhopanol in sinters of the vent from FMP (Samples OK1-TA, OK1-MA and OK1-BA, Section 6.3.3, Figure 6.7 and Figure 6.8) as it is not easy to rationalise formation from known BHP precursors.

High C<sub>31</sub>/C<sub>32</sub> ratios have been associated with acidic/oxic conditions (Sinninghe Damsté *et al.*, 2005) and contrast strongly with investigations of hopanoid diagenesis from other settings (e.g. Innes, 1998; Farrimond *et al.*, 2000; Watson, 2002). The origin of the observation is unclear, however, does provide the basis with which to investigate ancient depositions where similar ratios are observed. To the best of our knowledge, the only report

of a predominance of C<sub>31</sub> hopanoid components is in organic matter associated with the Permo-Triassic boundary (Wang, 2007). An interesting parallel emerges in that the end-Permian is characterised by massive ecosystem collapse possibly triggered by acidification of the oxic portions of the oceans (Wignall and Twitchett, 1996) or by euxinic conditions (Grice *et al.*, 2005; Kump *et al.*, 2005). This provides a new and exciting proxy and highlights the importance of geochemical investigations of modern extreme environments in reconstructing periods of past environmental perturbation.

## 6.5 CONCLUSIONS

Distributions of geohopanoids, i.e. free hopanols, hopanes, hopenes, hopanoic acids that form during intermediate stages of diagenesis have been detected in silica sinters and associated depositional regimes from silica-depositing ecosystems from TVZ and ETGF. The purpose of this study was to analyse, where possible, these particular compounds to investigate and assess the preservation of bacterial hopanoids and any diagenetic processes that are occurring in this particular depositional setting. From this investigation it is possible to determine that oxidative diagenetic pathways similar to that reported from other recent sedimentary depositional environments are commonly occurring (e.g. Innes *et al.*, 1997; Farrimond *et al.*, 2000; Watson, 2002). However, one striking difference is clear: the end product of intermediate diagenesis appears to be different, with the majority of distributions displaying a predominance of C<sub>31</sub> hopanols rather than a C<sub>32</sub> component as mentioned in previous studies of hopanoid diagenesis in recent depositional regimes.

Hopanoic acids dominate distributions of geohopanoids in older, non-active sinters and C<sub>32</sub> ββ hopanoic acid is the most abundant compound in the majority of cases. Hopanoic acids are less prevalent in sinters deposited under acidic conditions which is thought to reflect

reduction of the acid functionality to a terminal hydroxyl group, observed as a predominance of hopanols in distributions of geohopanoids of CP and RK.

This investigation has shown that a unique diagenetic mechanism of BHP diagenesis controlled by environmental setting rather than solely by biological input to a particular facies appears to be prevalent in silica sinters. This unparalleled report shows no similarity to previously reported mechanisms of hopanoid diagenesis in modern and recent sediments and highlights the gap in knowledge concerning the initial stages of hopanoid degradation.

## 7 CONCLUSIONS AND FUTURE WORK

### 7.1 CONCLUSIONS

The general objective of this study has been to characterise distributions of bacteriohopanepolyols (BHPs) and hopanoids that become preserved in mineral depositions associated with silica-depositing terrestrial geothermal ecosystems. The distribution of BHPs preserved in silica sinters, organo-sedimentary accumulations and those that derive from mat-forming microbial consortia has been investigated with a view to understanding the bacterial diversity and abundance at vents in the Taupo Volcanic Zone, North Island, New Zealand (TVZ), the El-Tatio Geyser Field, Chile (ETGF) and geothermal locations of California and Nevada (USA). An investigation of the distributions of geohopanoids preserved in sinter material and associated depositions has been employed to investigate the early stages of diagenesis with a view to understanding the preservation of BHPs in silica sinters and to gain insight into the potential of using geohopanoids preserved in ancient geothermal deposits to reconstruct paleo-biological communities and paleo-environmental conditions by proxy.

The work in this thesis contributes to an expanding body of research concerning the origins and fate of BHPs and geohopanoids in a range of environmental settings. The ability to accurately use BHPs as biomarkers in a range of natural settings requires a thorough understanding of its distribution throughout a range of environmental situations. This is not solely to address the gap in knowledge concerning the possible biological sources and ultimate geological fate of the compounds but is also relevant to studies concerning the extent of BHP-producing bacteria throughout the modern world, and by inference the ancient world. BHPs are recognisable, quantifiable tools that indicate a rich, and diverse, bacterial assemblage at the vents studied. Furthermore, distributions of BHPs should provide complementary evidence to microbiological investigations of bacterial populations occurring in and around terrestrial

geothermal vents. A number of specific BHPs, such as those that are known to derive from fermentative bacteria, methylotrophic bacteria and cyanobacteria provide a basic grounding of bacterial populations in ecosystems that have received little or no attention with regard to microbiological populations occurring in-situ.

#### 7.1.1 DISTRIBUTION OF BHPs IN ACTIVE BIOFACIES

BHPs are present in active portions (Chapter 3) of the vents studied including sinters from the air-water interface, floc material precipitated under anoxic conditions and mat-forming microbial assemblages that occur in the discharge regions of geothermal vents. Clear differences have been observed between the BHP distribution observed from each biofacies.

##### 7.1.1.1 ACTIVELY-PRECIPIATING SILICA SINTERS

BHPs have been detected in silica sinters collected from the air-water interface of Champagne Pool (CP), Orakei Korako (OK), Loop Road (LR), Opaheke Pool (OP) and sinters of ETGF (Chapter 3). The suite of active sinters from OK can be divided into two categories, sinters from vent source (FMP; samples OK1-TA, OK1-MA and OK1-BA; water temp. 97.8°C at the time of sampling) and a sinter collected from the outflow channel (sample OK3A; water temp. 63°C at the time of sampling). Likewise, the active sinters of OP can be sub-divided into actively-precipitating sinters from pool edge (sample OP2A; water temp. 95°C at the time of sampling) and sinter collected from the outflow channel (sample OP7A; water temp. 68°C at the time of sampling).

Differences in the abundance and composition of BHP distributions is observable between different depositional settings at OK and OP sites, reflecting different bacterial communities between vent and outflow regions driven by different temperatures. Similar observations have been made by Kaur (2009) where lipid distributions at FMP and sinters collected from vent of OP contained a predominance of archaeal biomarkers and biomarkers of

*Aquificales*, which are not known to produce BHPs. Differences in BHP composition are also observable between sinters deposited under different pH conditions, for instance, active sinters from CP and LR (pH 5.5 and 5.6 respectively) display different BHP compositions when compared to those deposited under neutral or near-neutral conditions, such the sinters from FMP (OK), OP or ETGF. For instance, *BHT<sub>cyc</sub>* and *BHP<sub>cyc</sub>* (**9**, **10**) were the most abundant BHPs detected in active sinters of CP and LR. Composite BHPs have previously been shown to be produced in response to elevated temperature and decreasing pH (e.g. Poralla *et al.*, 1980). *BHP<sub>cyc</sub>*, *BHT<sub>cyc</sub>*, Aminotriol, and *BH<sub>tetrol</sub>* (**9**, **10**, **22**, **1**) were present in each sinter of CP and LR. However, these compounds are known to be produced by a variety of bacteria and it is not possible to assign them to any particular organism or groups of organisms.

The distributions of BHPs in actively-precipitating sinters also showed the presence of a number of tentatively-assigned novel BHPs. Oxo-*BHT<sub>cyc</sub>* (**27**) was identified in each sample from CP and LR, and was also present in the sample collected from the outflow channel of OK (Sample (OK3A)). It has been possible to structurally-assign this compound because the related structure, oxo-*BHT<sub>gly</sub>* (**24**) was previously identified in cultures of *Zymomonas mobilis* grown under micro-aerophilic conditions (Flesch and Rohmer, 1989). This represents the first observation of this compound in any natural setting and it is likely derived from bacteria colonising oxygen-depleted zones at the air-water interface at CP and LR. As oxo-*BHT<sub>cyc</sub>* was not present in sinters of OK, OP or ET, it is possible to further assume that this compound is produced by acidophilic bacteria. Novel Guanidine-*BHP<sub>cyc</sub>* (**30**) has also been identified and appears to be a penta-functionalised homologue to the previously reported Guanidine-*BHT<sub>cyc</sub>* (Renoux and Rohmer, 1985). The presence of Guanidine-*BHP<sub>cyc</sub>* may indicate the presence of methylotrophic bacteria at LR. Regardless of the source, novel BHPs indicate the presence of currently uncharacterised bacteria and novel biosynthetic pathways.

Where sinters are deposited at near neutral pH, distributions were found to contain abundant cyanobacterial BHP-signatures. Only sample OP2A which was collected from the pool edge of OP where water temperatures are 95°C was found not to contain any cyanobacterial signatures. The ‘pavlova’ sinter (sample OP7A) was found to contain 2-me BH*tetrol* (**1**) and 2 novel BHPs (**31**, **32**) which indicate the presence of a microbial mat, either in the outflow channel or incorporated into the sinter itself. The BHP distribution of FMP was dominated by the presence of cyanobacterial BHPs which is unexpected as the temperature of the vent was 98.7°C. Transfer of organic material from the mats surrounding the vent can be discounted by the fact that the BHP composition of cyanobacterial mats is very often dominated by the presence of up to six unique compounds (See section 7.1.1.3) which were not identified during analysis of the FMP samples. Furthermore, the BHP distribution of the outflow channel did not contain any specific cyanobacterial signatures. The origin of the cyanobacterial signatures remains elusive, and as stated in Chapter 3, one must pose the question:

‘Does the sinter itself provide refuge from the lethal water temperatures and facilitate cyanobacterial colonisation at high temperatures?’

Biosilification of cyanobacteria is known to allow colonisation of sinters at ETGF, a geothermal location that due its high altitude, low latitude location is exposed to levels of UV radiation usually lethal to cyanobacteria (Phoenix *et al.*, 2006). BHP distributions of sinter formations of El-Tatio (ETGF; Chapter 3) show that cyanobacterial signatures are abundant and show good correlation with previous studies concerning cyanobacterial colonisation at this site (e.g. Phoenix *et al.*, 2006). The study of BHPs in sinters from this high altitude geothermal location represents the first organic geochemical investigation of this site and provides evidence from a location that is geographically distinct to the TVZ of the utility of BHPs as biomarkers in terrestrial geothermal settings.

Silica sinters are known to be deposited more-readily at or above the air-water interface. Since the waters of the vents in question can be considered to be anoxic, or strongly dysoxic, then the air-water interface of the vents studied represent a boundary analogous to an oxic-anoxic boundary and the BHP distributions of silica sinters are likely recording bacteria inhabiting this oxic-anoxic transition zone (OATZ). Sub-aqueous depositions and accumulations, such as the floc material collected from Champagne Pool (sample CPf; Chapter 3, Section 3.3.1.1), provide a more suitable target with which to investigate bacterial populations colonising vent fluids (See section 7.1.1.2). By investigating the BHP distributions of a number of actively-precipitating sinters it appears that BHP distributions vary with environmental temperature and pH.

#### 7.1.1.2 SUB-AQUEOUS 'FLOC' MATERIAL

'Floc' material composed mainly of gold and silver bearing sulphide minerals (Jones *et al.*, 2001) readily precipitates from geothermal fluids at CP. It can be observed as an orange coating on the sub-aqueous sinter shelf.  $BHP_{cyc}$ ,  $BHT_{cyc}$ , aminotriol and  $BHtetrol$  (**9, 10, 22, 1**) were observed during analysis of this particular facies. Although the compounds are produced by a range of bacteria, the sub-aqueous formation of the floc material suggests that the observed BHP distributions derived from an anaerobic bacterial source. The same four compounds were also observed in an active sinter of CP and were also present in older, non-active sinters. This indicates that bacterial populations of the CP vent are being recorded in BHP distributions observed in sinter formations.

Previous investigations of the bacterial community at CP indicate a low-diversity assemblage (e.g. Hetzer *et al.*, 2007; Childs *et al.*, 2008) and as none of the bacteria reported in that study are known-BHP producers, the BHP distribution of the Floc material must derive from currently unidentified BHP-producing bacteria. Only a few reports exist of BHP-production in anaerobic bacteria (e.g. Sinninghe Damsté *et al.*, 2004; Hartner *et al.*, 2005; Blumenberg *et al.*,

2006; See Chapter 1, Section 1.8.4.4 for further references) and the detection of BHPs in material deposited under anoxic conditions at CP builds upon a number of reports challenging the traditional view of BHP-producing bacteria and their distribution in natural environments.

#### 7.1.1.3 MICROBIAL MATS

Microbial mats from the outflow regions of geothermal vents have also provided a rich source of information. Microbial mats have been sampled from OK (TVZ) and geothermal areas within Paradise Valley, Nevada (USA) and Egeville and Surprise Valley, California (USA). With the exception of the samples collected from the Rick's Hot Creek spring (RHC; Paradise Valley, USA), the BHP distribution of microbial mats are dominated by the presence of a suite of novel cyanobacterial signatures (**31, 32, 33, 34**). A full structural characterisation remains to be carried out and the exact source of this suite of compounds remains elusive however, *Synechococcus* sp. are known to be the dominant mat-building cyanobacteria at geothermal locations of the USA and New Zealand (Papke *et al.*, 2003; discussed below). Although the BHP distributions at the RHC site were different to others observed during the study of microbial mats, they were composed mainly of cyanobacterial signatures and may indicate different BHP-producing cyanobacteria at this site.

The inclusion of microbial mats to the sample suite is important as it has enabled two key observations to be made:

- 1) The BHP distributions of mat-forming microbial consortia are distinctively different to the distributions of BHPs preserved in silica sinters. Microbial mats are known to be abundant at terrestrial geothermal ecosystems around the world, and particularly large cyanobacterial mats are known to be present at Orakei Korako (OK, TVZ) and ETGF. It is therefore an important to provide evidence that distinguishes between BHP distributions of vent biota and those of the microbial mats that colonise the outflow regions of the vents in question.

- 2) The BHP distributions of microbial mats investigated in this study show that a novel groups of BHPs are widespread throughout mat-forming microbial consortia from geographically distinct geothermal locations. Samples from Orakei Korako (TVZ, New Zealand), Paradise Valley (Nevada, USA) and Eagleville and Surprise Valley (California, USA) have been found to be dominated by a suite of novel BHPs. The BHPs remain to be fully structurally characterised but were tentatively-assigned as BHPs on the basis of MS<sup>n</sup> fragmentations and via PA/NaBH<sub>4</sub> reduction of polyfunctionalised BHP precursors. It is thought that the novel BHPs derive from *Synechococcus* sp. which are known to be the dominant mat-building cyanobacteria in geothermal locations of North America and New Zealand (e.g. Papke *et al.*, 2003) and thermophilic species have previously been found to produce BHPs (Llopiz *et al.*, 1996). As a common BHP signature has been identified in two geographically distinct locations, it is possible that the biosynthetic pathways responsible for the formation of this group of BHPs evolved before the radiation of this organism and may have played a key role in the diversification and adaption to high temperature environments.

#### 7.1.2 BHP DISTRIBUTIONS OF NON-ACTIVE SINTERS

BHPs have been detected in each non-active sinter analysed (Chapter 4). The observed BHP compositions include a diverse range of known and novel structures. The presence of polyfunctionalised, complex BHP structures in older samples demonstrates that BHPs are a useful tool in investigating changing bacterial populations over time. BHP<sub>cyc</sub>, BHT<sub>cyc</sub>, aminotriol and BH<sub>tetrol</sub> appear to be detected throughout non-active sinters from various sites but, as mentioned above, it is not possible to assign these compounds to any particular bacterial source. Other BHP-signatures specific to particular groups of bacteria have been identified in some of the non-active sinters and demonstrate the potential of BHPs to record the presence and activity of bacteria in silica sinters. For instance, cyanobacterial signatures (e.g. **II-1**, **13**, **II-13**, **17**, **II-22**) have been detected in non-active samples collected from OK, LR and RK. BHP-

signatures of Type I and Type II methanotrophic bacteria were identified in a non-active sinter of OP (15, III-15, 21, III-21; sample OP5N). Guanidine-BHT<sub>cyc</sub> (23) which has only previously been identified in methylotrophic bacteria (Renoux and Rohmer, 1985; Knani *et al.*, 2001) has also been identified in sinters from CP, LR and RK and may indicate the presence of methylotrophic bacteria at these sites. The presence of novel compounds also strongly suggests the presence of currently unidentified BHP-producing bacteria throughout the sites investigated (See Section 7.1.1.4 for further discussion).

In general, BHP abundances were higher in non-active sinters than actively-precipitating sinters collected from the same sample site. This may indicate changing bacterial populations driven by changing environmental conditions such as temperature (e.g. Kaur *et al.*, 2008) or possibly post-depositional colonisation of sinters. The sequence of non-active sinters from CP were collected in a putative time sequence that includes the oldest sinter material that would have been deposited at the time of the formation of the pool, around 900 years before present. Kaur *et al.* (2008) show that the microbial population has changed over the course of the lifetime of CP and it was proposed that this change in microbial population was driven by higher temperatures in the past as a result of the hydrothermal eruption which formed the pool. The abundances of BHPs are higher in older sinters and a decrease in modern sinters and show good correlation to data presented by Kaur (2009). However, the argument is complicated somewhat when considering the physiological response of BHP-producing bacteria to increased temperatures. It has been demonstrated that BHP composition of bacteria is sensitive to changing environmental temperature (e.g. Poralla *et al.*, 1980; Joyeux *et al.*, 2004) and reports demonstrate that biosynthesis of composite-BHPs is particularly sensitive. As composite BHPs are the most abundant BHPs identified in CP sinters, do BHP distributions reflect a change in bacterial population? Alternatively, does the bacteria population remain static in which case are

BHPs recording a physiological response to changing conditions? Nevertheless, the BHP distributions still record changing environmental conditions.

Overall the BHP distributions of active and non-active sinters at CP contain BHPs that exhibit a low-specificity, i.e. the structures observed are known to be produced by a variety of bacterial groups. No cyanobacterial signatures were observed in CP sinters, however. The presence of novel BHPs indicates that the bacterial assemblage associated with the sinters at CP includes currently unidentified BHP-producing bacteria.

It was not possible to collect all non-active sinters in a similar fashion to those at CP. Primarily this is because of the unique nature of the sinter terrace at CP as at other sites, such as OK, the sinters can become part of a sinter terrace or sinter flat which comprises silica-deposited from many vents and sinter terraces at other sites may be unsafe to sample as the sinter can often form a thin crust over geothermal pools. However, it is clear that non-active sinters contain a more abundant and diverse assemblage of BHP components than active sinters. The exception to this observation are non-active sinters from Golden Fleece Terrace (GFT, OK; Samples OK4N, OK5N, and OK6N) where BHP abundance is low and appears to contain input from soil bacteria from the surrounding Waikato Forrest (Chapter 4, Section 4.4.1.2). A higher abundance and more complex BHP distribution may, as stated above, indicate changing environmental conditions over time. However, it may also indicate colonisation of sinters by bacteria after the sinter has become deposited. Due to the nature of sinter formation which results in 'radial contraction' (Kaur, 2009) of the pool surface, non-active sinters are no longer in contact with the pool waters therefore providing a niche for colonisation whereby exposure to the hot vent waters is reduced or minimised but the availability of gases, such as NH<sub>3</sub>, CH<sub>4</sub>, H<sub>2</sub>S, CO<sub>2</sub> and H<sub>2</sub>, emanating from the pool, or via diffusion through pore spaces in the sinter formation could provide a suitable metabolic substrate for growth. Sinter development can proceed long after the formation of the initial sinter (Rodgers *et al.*, 2004) as splashing of vent waters from turbid

vents, such as FMP or RK, or wave motion from large pools such as CP causes further silica deposition leading to textural development and laminations to occur (e.g. Mountain *et al.*, 2003). This mechanism could conceivably lead to the incorporation of new organic matter into non-active sinter formations. This indicates that BHPs recorded in silica sinters must be interpreted with great care as the distributions may contain input from both vent biota and bacteria that colonise the sinter after deposition has occurred.

It appears that BHPs provide a good basis with which to begin to investigate the presence of a particular organism or groups of organisms, but disentangling the complex relationship of changing populations, physiological response and overprint of post-depositional colonisation must to be considered when reconstructing changing bacterial communities.

### 7.1.3 DISTRIBUTIONS OF GEOHOPANOIDS IN SILICA SINTERS

An investigation of the distributions of geohopanoids was undertaken to gain insight into the initial stages of diagenesis of BHPs preserved in sinter material (Chapter 6). Geohopanoids form during diagenetic transformation of sedimentary BHPs. It became clear from the early stages of this investigation that a novel diagenetic pathway was affecting BHP preservation. Geohopanoids have been detected in all facies investigated, with the exception of samples OP2A, OP7A and ET26A.

As with the studies of BHP distributions of active biofacies (Chapter 3, section 7.1.1) and non-active sinters (Chapter 4, section 7.1.2), the distributions of geohopanoids present a number of unusual findings that contrast strongly with previous investigations concerning BHP and hopanoid diagenesis. With the exception of sinters of FMP (OK, samples OK1-TA, OK1-MA and OK1-BA), the analysis of geohopanoids show that C<sub>31</sub> ββ hopanol appears to be the major end-point of the intermediate stages of diagenesis of BHPs in silica sinters. Due to the presence of a hydroxyl group at C-31 of pentafunctionalised BHPs it would be expected that an increased

abundance of C<sub>31</sub> hopanol (**47**) would reflect an increased abundance of pentafunctionalised BHPs. However, in many cases the abundance of C<sub>31</sub> hopanol is inconsistent with the corresponding input of pentafunctionalised BHPs. This indicates that environmental conditions and not biological input is the key determining factor of the composition of geohopanooid distributions in silica sinters. Further evidence of this observation is provided by a predominance of C<sub>33</sub> ββ hopanol (**57**) in sinters of FMP. It is difficult to rationalise formation of this particular geohopanooid from any known BHP precursor. The observation that C<sub>33</sub> ββ hopanol dominates geohopanooid distributions of FMP rather than C<sub>31</sub> hopanol as observed at other sites is also unclear; however, one may suggest that temperature may be the defining factor as the water temperature at FMP is significantly higher than that observed at other sample locations where sinters were found to contain geohopanooids.

The geohopanooids investigated in this study were hopanols, hopanediols, hopanetriol, hopanoic acids and anhydroBHPs. The presence of hopanetriols, hopanediols and hopanols in sediments is thought to indicate sequential, oxidative degradation of BHP side-chain components (e.g. Watson and Farrimond, 2000; Watson, 2002). Likewise hopanoic acids are thought to form via oxidation of terminal alcohol groups and subsequent decarboxylation (Sinninghe Damsté *et al.*, 1995). Therefore the presence of these compounds in silica sinters dictates that BHP diagenesis is proceeding via oxidative degradation pathways, which is consistent with the model of sinter formation. However, anhydroBHT (**2**) which is known to be formed via reductive cyclisation of BHP side-chains has also been identified throughout the analysis and indicates that both oxidative and reductive pathways are affecting BHP preservation. AnhydroBHT (**2**) was the only geohopanooid identified in the floc material sampled from CP (sample CPf). This indicates that the reducing properties of the waters of geothermal vents are limiting the diagenesis of BHPs and that degradation of organic matter in sub-aqueous depositions likely follows a reductive mechanism.

The unprecedented observation of high abundances of C<sub>31</sub> hopanol (**47**) appears to be unique to the locations studied throughout this work.

#### 7.1.3.1 POTENTIAL OF HOPANOIDS AS BIOMARKERS FOR ANCIENT GEOTHERMAL SYSTEMS

The diagenesis of BHPs in silica-deposits has received limited attention in the past (e.g. Summons *et al.*, 1996; Pancost *et al.*, 2005, 2006; Talbot *et al.*, 2005; Kaur, 2009), previously only the presence of anhydroBHT (**2**) has been described by Talbot *et al.* (2005). The processes affecting BHP and hopanoid distributions in modern silica sinters are of direct relevance to the preservation of organic matter in ancient siliceous deposits, such as the Rhynie Cherts (e.g. Trewin, 1996). An unprecedented predominance of C<sub>31</sub> ββ hopanol (**47**) has been observed in the majority of sinters with the exception of active sinters from Fred and Maggie's Pool at the Orakei Korako Geothermal Field (OK, Samples OK1-TA, OK1-MA, OK1-BA; Chapter 6, Section 6.3.3.1), therefore it would be expected that where ancient geothermal deposits contain organic matter, that a predominance of C<sub>31</sub> components would be expected. Burhan *et al.* (2002) suggested that chemical functionality promotes loss of the terminal carbon, in which case, a predominance of C<sub>30</sub> hopane (**I**) would be expected. However, mineralogical changes to the silica matrix must also be considered when exploring the utility of hopanoids as biomarkers for ancient geothermal ecosystems. The physical changes that take place during sinter diagenesis result in formation of a more crystalline state of silica mineral which ultimately results in the formation of quartz crystals (Lynne and Campbell, 2004). This process likely displaces any organic matter from the mineral matrix and the search for organic remains in truly ancient siliceous deposits may be affected by such a process.

#### 7.1.4 THE IDENTIFICATION OF NOVEL BHPs

Novel BHPs are also widespread throughout non-active sinters analysed, leading to tentative-identification of eighteen novel BHPs (Chapter 5) of which it has been possible to attempt a structural characterisation on five structures. This includes 35-O- $\beta$  guanidine-substituted cyclitol Bacteriohopane-31,32,33,34,35-ol (Guanidine-BHP<sub>cyc</sub>; **30**) 35-O- $\beta$  cyclitol bacteriohopane-32 oxo-33,34,35-ol (oxo-BHT<sub>cyc</sub>; **27**), 35-O- $\beta$  cyclitol bacteriohopane-31 oxo-32,33,34,35-ol (oxo-BHP<sub>cyc</sub>; **36**), 32-oxo-bacteriohopane-33,34,35 triol (oxo-BH<sub>triol</sub>; **38**) and 31-oxo-bacteriohopane-32,33,34,35 tetrol (oxo-BH<sub>tetrol</sub>; **37**). It has been possible to assign thirteen other novel compounds as BHPs on the basis that they contain recognisable fragments during APCI-MS<sup>n</sup> analysis, however, the nature of the terminal group at C-35 remains to be elucidated. They have been reported on the basis that they have been detected at more than one setting and/or contain a chemical functionality which indicates they form part of a homologous series of BHPs. The spectra of a number of other potential BHP candidates are given in Appendix II. The quantity of possible compounds that display some structural similarities to known BHP compounds is remarkable and demonstrates that current understanding vastly underestimates the extent of BHP diversity and BHP-producing bacteria.

Although it has not been possible to complete a full structural characterisation of these compounds, this observation extends the inventory of BHP compounds and our understanding of the ecology of BHP-producing bacteria. Furthermore, each new BHP compound identified is representative of a novel biosynthetic pathway and as environments that have previously received little or no attention with respect to investigations of BHP-producing bacteria then it is likely that this inventory will be extended even further. This suggests that the true potential of BHPs as chemotaxonomic biomarkers has yet to be realised. However, this observation raises questions as to cellular function of BHPs as it seems illogical that so many structures would be produced to serve one purpose. As discussed in Chapter 1 and Chapter 5, the steric dimensions

and formation of the hopane hydrocarbon is similar to that of the sterane hydrocarbon, but an ever expanding inventory of known structures suggests that cellular function may more complex than just regulating membrane permeability. It has been suggested that the polyfunctionalised side-chains may provide ‘tethers’ for protein rafts (Summons *et al.*, 2006) and could be involved with cell signalling pathways (Bolanos *et al.*, 2004). Pearson *et al.* (2007) estimated that around 10% of bacteria in the open ocean produce BHPs, if this is the case then by what mechanism do the remaining 90% of bacteria use to regulate membrane fluidity?

As the structures reported here become fully characterised and biological precursors become known, our understanding of the origin of the BHP distributions observed during this study will improve and extend our knowledge of the ecology of BHP-producing bacteria and the biogeochemical processes occurring in and around terrestrial geothermal vents.

### 7.1.5 SUMMARY

Preservation of BHPs in silica sinters shows that molecular composition is retained upon deposition leading to the identification of complex and diverse BHP distributions. A number of specific signatures have been identified throughout this study that indicate the presence of cyanobacteria, Type I and Type II methanotrophic bacteria and methylotrophic bacteria at the vents investigated. This report expands our current understanding of the ecology of BHP-producing bacteria contributing to the sedimentary record.

The investigation of the distribution of BHPs over a number of depositional settings (Chapter 3) has enabled a number of exciting observations regarding the distribution of BHP-producing bacteria in a natural setting. These include the identification of BHPs in suspended sulphide minerals deposited under anoxic conditions, a suite of novel cyanobacterial signatures from mat-forming consortia that may have contributed to the evolution and radiation of thermophilic *Synechococcus* sp. The remarkable preservation of organic matter observed in sinters has enabled the identification of a number of novel compounds, this includes a suite of ketone-containing BHPs, dubbed 'oxo-BHPs' and a novel BHP that is thought to derive from aerobic methylotrophic bacteria.

The utility of BHPs as biomarkers in geothermal settings is improved by the observation that they remain intact in older, non-active sinter material collected from sinter terraces, rhizolith secretions and extinct geysers. Examination of BHPs in sinters deposited over spatial and temporal scales has demonstrated the potential of BHPs to record changing bacterial populations and vent geochemistry over the life-time of the pool. Furthermore, the unprecedented observation of an unusual diagenetic pathway affecting BHPs preserved in sinter deposits has highlighted significant short-comings in our understanding of the processes that occur during the initial stages of diagenesis of BHPs.

The investigation of the distribution of BHPs preserved in sinters of silica-depositing terrestrial geothermal ecosystems has proved to be fruitful and has elaborated upon current understanding of the ecology of BHP-producing bacteria and demonstrated the utility of BHPs as biomarkers for extremophilic bacterial communities and biogeochemical processes occurring in modern and recent environments. The results of this investigation have also questioned much of the current ideology concerning the extent of BHP-structural diversity and our understanding of the processes governing the preservation of BHPs.

The vents studied during this thesis are unique in terms of their physico-chemical parameters and the microbial life that thrives within. The observed BHP and hopanoid distributions reflect this and may provide deeper insight into the ecology, present and past, of the spring.

Clearly the results presented here show that further work is required to establish BHPs as biomarkers for bacteria in geothermal ecosystems. However, the potential of BHPs as biomarkers for extremophilic bacterial populations has been demonstrated and as future investigations are undertaken they will surely result in an array of unusual and exciting findings.

## 7.2 FUTURE WORK AND RECOMMENDATIONS

The research presented throughout has provided a number of ideas concerning the distribution of BHPs in bacteria and the ecology of BHP-producing bacteria. These findings could be further refined by inclusion of more samples from a particular site, more samples from different depositional settings within a given sample site and complimentary data from the surrounding areas of the vents. Some future directions that would enable more succinct future studies and allow elaboration on the results presented in this thesis are now discussed.

### 7.2.1 PARALLEL MICROBIOLOGICAL INVESTIGATIONS

Understanding the structural diversity, distribution and biochemistry of BHPs within microbial communities adapted to a range of extremophilic conditions (temperature, pH, salinity, oxygen content, UV radiation, pressure etc.) would be advantageous to this study and could provide the focus for future research. One might suggest that as we have proved that BHP-producing organism(s) exists at Champagne Pool, then efforts should be made to cultivate representatives of this community and their BHP compositions analysed. Samples from other locations have been analysed during this study however the geological history and the chemical and physical conditions of Champagne Pool are well characterised, this makes the location ideal for a biogeochemical study. The ideal scenario would involve large scale cultivation in order to obtain enough material that novel BHPs could be analysed by more rigorous analytical methods, such  $^1\text{H}$  and  $^{13}\text{C}$  NMR. Furthermore, investigations on how BHP production changes in response to changing culture conditions, for instance, how the BHP composition changes over a range of growth temperatures would provide interesting complimentary data to this study and allow a better understanding of the physiological response of BHP-producing bacteria to chemical and physical conditions of geothermal vents. The possibility exists that a cultivated organism may not produce BHPs in culture, in this case identification of genetic machinery involved with BHP

biosynthesis, such as the presence of squalene-hopene-cyclase (SHC) would provide evidence of the ability to produce BHPs. One may circumvent the issue of culturing a bacteria by applying a metagenomic approach to study SHC directly in the vent fluids or in sinters. However, parallel investigations of metagenomics and physiological response would provide the most information regarding how to interpret BHP distributions in geothermal environments. It appears that a combined approach of modern techniques in microbiology, microbial ecology and biogeochemistry is crucial in improving our understanding of thermophilic and hyperthermophilic microbial populations.

Future studies might also include analysis of intact polar lipid biomarkers (IPLs), which are becoming popular tools to assess microbial activity in a range of recent environmental settings (Sturt *et al.*, 2004). IPLs are degraded rapidly after cell death and are generally regarded to be robust biomarkers for *living* microbial communities. Furthermore, IPLs that are specific to organisms with a unique metabolic profile, such as IPL-ladderanes for bacteria capable of anaerobic oxidation of ammonia (Anammox; Jaeschke *et al.*, 2009), would provide further insight into the microbial community whilst shedding light on important biogeochemical processes occurring in-situ. Methanogenic archaea are also known to produce specific membrane lipids (Koga *et al.*, 1993; Schouten *et al.*, 2008). One topic of contention in this thesis is the apparent presence of cyanobacteria in the vent waters of Fred and Maggie's Pool (Chapter 3) at temperatures above that which photosynthetic organisms can no longer survive. IPLs specific to cyanobacteria, such as betaines and sulfoquinovosyl diacyl glycerols (SQDGs; e.g. van Mooy *et al.*, 2006, 2009) would help to clarify this issue.

Such investigations could be complimented by metagenomic approaches centred upon functional gene analysis with specific primers for processes that are known to occur in terrestrial vents such as dissimilatory sulfate reductase, methyl co-enzyme A reductase, methane monooxygenase or ammonia oxidase. This should provide a more in-depth investigation of

microbial populations coupled with an investigation of biogeochemical processes occurring in situ (e.g. Kuypers *et al.*, 2003; Biddle *et al.*, 2008). Metatranscriptomics represents a state-of-the-art technique that not only describes genetic diversity but also genetic expression in an environmental setting (Frias-Lopez *et al.*, 2008), thereby giving an more accurate picture of active microbial populations. The application of this technique is in its infancy but the prospect to apply this method to analysing the dynamics of modern geothermal ecosystems is very exciting. Within the framework of understanding BHP distributions in geothermal environments, and other environmental settings, this is a particularly interesting approach as there are wide ranging estimates of the distribution of BHPs within both BHP-producing organisms and the environment (e.g. Rohmer *et al.*, 1984; Pearson *et al.*, 2007). This will also provide basis of investigations into the evolution of BHP-producing organisms. Something further to consider is that if we begin to better understand what proportion of bacteria produce BHPs, then two questions require further attention in the future. Firstly, what lipids do the remaining bacteria synthesise to perform the same or similar function to BHPs? Secondly, BHP producing bacteria appear to be widely distributed throughout bacterial lineages. Does this dispersal represent the divergence of an ancient biosynthetic pathway or simply a bias in sampling? The recommendations outlined above provide a basis with which to better understand the physiology, environmental distribution and phylogenetic relationships of BHP producing bacteria in modern terrestrial geothermal settings.

### 7.2.2 BHP-SIGNATURES FROM MAT-FORMING CYANOBACTERIA

Papke *et al.* (2003) showed that *Synechococcus* sp. cyanobacteria were genetically distinct, falling into 3 distinct phylogenetic clades that appear to be dependant upon geographical location. It has also been shown that *Synechococcus* sp. cyanobacteria are not present in Icelandic hot-springs. Future investigations should include mats collected from Iceland, Japan and further samples collected from New Zealand should provide further insight into the

distribution of the novel suite of cyanobacterial BHPs potentially demonstrating the utility of BHPs in biogeography.

Structural elucidation of the six novel BHP (**31**, **32**, **33**, **34** plus two isomers) compounds reported from mat-forming cyanobacteria in this study and by Zhang *et al.* (2007) will be sought. Future sampling expeditions should include collecting a large amount of cyanobacterial mats to be extracted using the methods employed during this study. Structural identification by  $^1\text{H}$  and  $^{13}\text{C}$  NMR to elucidate the nature of the C-35 terminal group and the origin of stereo-isomers observed will follow isolation of these compounds via preparative liquid chromatography (prep-LC).

### 7.2.3 DIAGENESIS OF BHPs

Understanding the reactions and processes that take place during the intermediate stages of BHP deposition are of utmost importance when interpreting distributions of sedimentary BHPs and geohopanoids. This applies to every environmental setting and is not just confined to terrestrial geothermal locations. The work in chapter 6 of this thesis highlighted a novel diagenetic pathway affecting BHP preservation in sinter material. As more environmental situations are investigated and more BHP structures become known then the number of diagenetic transformation is sure to increase even further. Investigations concerning the diagenesis of BHPs are required to enhance reconstruction of paleo-environmental conditions and populations using hopanoids.

It is apparent that a great diversity of BHP structures exist (See Chapter 5) many of which remain to be fully characterised. They are produced by a wide-variety of bacteria, of which only a very small percentage of which have been cultured and identified. Furthermore, it appears that BHP-production is often vastly different when comparing bacteria in culture to those that exist in a natural setting. Many post-depositional mechanisms affect the distributions

of these compounds, therefore well preserved BHPs are a rare but useful commodity when interpreting bacteria in older and ancient sediments. Paradoxically it appears that side-chain functionality can dictate diagenetic processes. For instance, it has been suggested that hydroxyl groups are thought to promote oxidative loss of the carbon to which they are attached. Burhan *et al.* (2002) attribute a predominance of C<sub>30</sub> hopanes and C<sub>30</sub> nor hopanes to the presence of methanotrophs which are known to produce BHPs with a hydroxyl group at C<sub>30</sub>. A strong <sup>13</sup>C isotopic composition of C<sub>30</sub> hopane provides further evidence of this association. Likewise, bisnorhopanes and trisnorhopanes have been associated with sulphidic water columns, yet it is difficult to provide a mechanism for their production from any known BHP precursor.

Understanding early stage diagenetic reactions not only applies to intact BHPs but also to other ‘intact polar lipids’ such as bacterial phospho- and glycerol diethers which are used to investigate viable bacterial communities, particularly in the deep sub-surface (e.g. Zink *et al.*, 2003), and Archaeal Glycerol Dialkyl Glycerol Tetraethers (GDGTs) which are the central focus of paleo-temperature reconstructions (e.g. Weijers *et al.*, 2003).

The contribution of post-depositional alteration, heterotrophic grazing, incorporation into macro-molecular aggregates and over-printing by non-syngenetic organic matter must be playing a crucial role in the observed geohopanoid distributions of any given depositional setting.

#### 7.2.4 OTHER EXTREME ENVIRONMENTAL SETTINGS

Microbiota colonising ‘extreme’ environmental conditions are notoriously difficult to culture and characterise. Therefore lipid distributions, and in particular intact polar lipids such as BHPs, provide useful tools which with to investigate the ecology and biogeochemistry of the locations in question. Whether the organic geochemistry of environments that have received little or no attention in the past, such as high-temperature, black smoker vents from the Mid-Atlantic Ridge (MAR) or frozen Antarctic lakes, these are all likely to further yield fruitful and

surprising results which lead to an ever-increasing set of tools upon which to base reconstructions of past environmental settings.

As the topic of this research has been centred upon terrestrial geothermal settings, the next logical step would be to investigate their distribution in sub-marine hydrothermal vents. The conditions of MAR sites are vastly different to the terrestrial settings, however, the reducing nature of the environments should mean that molecular preservation is good. Off-axis or serpentinite-hosted systems such as the Lost City Hydrothermal Field (Kelley *et al.*, 2005) yield significantly lower temperature vents than hydrothermal fields located at spreading centres and are characterised by high quantities of methane and hydrogen, similar to terrestrial vents, and pose intriguing targets for future BHP and hopanoid-based research.

REFERENCES

A

Ageta, H., Shiojima, K., Arai, Y., 1987. Acid induced rearrangement of triterpenoid hydrocarbons belonging to the hopane and migrated hopane series. *Chemical and Pharmaceutical Bulletin* 35, 2705 – 2716.

Allen, M.A., 2006. An astrobiology-focussed analysis of microbial mat communities from Hamelin Pool, Shark Bay, Western Australia. PhD thesis. Sydney, Australia: University of New South Wales.

B

Baptiste, E., Boucher, Y., 2007. Lateral gene transfer challenges principles of microbial systematics. *Trends in Microbiology* 18, 200 – 207.

Bednarczyk, A., Carrillo-Hernandez, T., Schaeffer, P., Adam, P., Talbot, H.M. Farrimond, P., Riboulleau, A., Rohmer, M., Albrecht, P., 2005. 32,35-Anhydrobacteriohopanetetrol: An unusual bacteriohopanepolyol widespread in Recent and past environments. *Organic Geochemistry* 36, 673 – 677.

Bennett, B., Fustic, M., Farrimond, P., Huang, H., Larter, S.R., 2006. 25-Norhopanes: formation during biodegradation of petroleum in the subsurface. *Organic Geochemistry* 37, 787 – 797.

Benning, L., Phoenix, V.R., Mountain, B.W., 2005. Biosilification: the role of cyanobacteria in silica sinter deposition, p131 - 150. In G.M. Gadd, K.T. Semple, H.M Lappin-scott, 'Microorganisms and earth systems – advances in Geomicrobiology. Cambridge University Press.

## References

- Benz, R., Hallmann, D., Poralla, K., Eibl, H., 1983. Incorporation of hopanoids with phosphatidylcholines containing oleic and  $\omega$ -cyclohexyldodecanoic acid in bilayer membranes. *Chemistry and Physics of Lipids* 34, 7 – 24.
- Biddle, J.F., Fitz-Gibbon, S., Schuster, S.C., Brenchley, J.E., House, C., 2008. Metagenomic signatures of the Peru margin seafloor biosphere show a genetically distinct environment. *Proceedings of the National Academy of Sciences* 105, 10583 – 10588.
- Birgel, D., Thiel, V., Hinrichs, K.U., Elvert, M., Campbell, K.A., Reitner, J., Farmer, J.D., Peckmann, J., 2006. Lipid biomarker patterns of methane-seep microbialites from the Mesozoic convergent margin of California. *Organic Geochemistry* 37, 1289 - 1302.
- Birnbaum, S.J., Wireman, J.W., 1984. Bacterial sulfate reduction and pH: implications for early diagenesis. *Chemical Geology* 43, 143 – 149.
- Birnbaum, S.J., Wireman, J.W., Borowski, R., 1989. Silica precipitation by the anaerobic sulfate-reducing bacterium *Desulfovibrio desulfuricans*: effects upon cell morphology and implications for preservation. In *Origin, Evolution and Modern Aspects of Biomineralisation in Plants and Animals*. Plenum Press, New York, 507 – 516.
- Bisseret, P., Rohmer, M., 1989. Bacterial sterol surrogates. Determination of the absolute configuration of Bacteriohopanetetrol side chain by hemisynthesis of its diastereoisomers. *Journal of Organic Chemistry* 54, 2958 - 2964.
- Bisseret, P., Zundel, M., Rohmer, M., 1985. Prokaryotic triterpenoids 2. 2 $\beta$ -Methylhopanoids from *Methylobacterium organophilum* and *Nostoc muscorum*, a new series of prokaryotic triterpenoids. *European Journal of Biochemistry* 150, 29 - 34.

## References

- Bisseret, P., Seeman, M., Rohmer, M., 1994. Dimethyldioxirane oxidation of aminobacteriohopanetriol: obtention of a putative intermediate in bacterial hopanoid biosynthesis. *Tetrahedron Letters* 35, 2687 – 2690.
- Bisseret, P., Baron, A., Rodier, C., Neunlist, S., 1997. Geomimetic autooxidation of biohopanoids: a route to *Bis*-hopanoids, potential new sedimentary molecular fossils. *Tetrahedron letters* 38, 3905 – 3908.
- Bligh, E.G., 1978. Citation Classics 52, p 16.
- Bligh, E.G., Dyer, W.J., 1959. A rapid method of total lipid extraction and purification. *Canadian Journal of Biochemistry and Physiology* 37, 911 – 917.
- Blumenberg, M., Seifert, R., Rietner, J., Pape, T., Michaelis, W., 2004. Membrane lipids typify distinct anaerobic methanotrophic consortia. *Proceedings of the National Academy of Sciences* 101, 11111 – 11118.
- Blumenberg, M., Kruger, M., Nauhaus, K., Talbot, H. M., Oppermann, B. I., Seifert, R., Pape, T., Michaelis, W., 2006. Biosynthesis of hopanoids by sulfate-reducing bacteria (genus *Desulfovibrio*). *Environmental Microbiology* 8, 1220 – 1227.
- Blumenberg, M., Seifert, R., Michaelis, W., 2007. Aerobic Methanotrophy in the oxic-anoxic transition zone of the Black Sea water column. *Organic Geochemistry* 38, 84 – 91.
- Blumenberg, M., Seifert, R., Kasten, S., Bahlmann, E., Michaelis, W., 2009. Euphotic Zone bacterioplankton sources major sedimentary bacteriohopanepolyols in the Holocene Black Sea. *Geochimica et Cosmochimica Acta* 73, 750 – 766.
- Bock, G.R., Goode, J.A., 1996. Evolution of hydrothermal ecosystems on Earth (and Mars?). Ciba Foundation Symposium no. 202. Wiley, Chichester, United Kingdom.

## References

- Bolanos, L., Lukaszewski, K., Bonilla, I., Blevins, D., 2004. Why Boron? *Plant Physiology and Biochemistry* 42, 907 – 912.
- Boon, J.J., Hines, H., Burlingame, A.L., Klok, J., Rijpstra, W.I.C., de Leeuw, J.W., Edmunds, K.E., Eglinton, G.E., 1981. Organic geochemical studies of solar lake laminated cyanobacterial mats. *Advances in Organic Geochemistry*, 207 – 227.
- Bouloubassi, I., Aloisi, G., Pancost, R.D., Hopmans, E., Pierre, C., Sinninghe Damsté, J.S., 2006. Archaeal and bacterial lipids in authigenic carbonate crusts from eastern Mediterranean mud volcanoes. *Organic Geochemistry* 37, 484 – 500.
- Bradley, A.S., Marx, C. J., Summons, R.E., 2007. Assessing the role of sterol methyltransferase homologues in the methylhopanoid synthesis pathway of *Methylobacterium extorquens* AM-1. Conference abstract, The 23<sup>rd</sup> International Meeting on Organic Geochemistry. Torquay, U.K.
- Brasier, M.D., Green, O.R., Jephcoat, A.P., Kleppe, A.K., van Kranendonk, M.J., Lindsay, J.F., Steele, A., Grassineau, N.V., 2002. Questioning the evidence for Earth's earliest fossils. *Nature* 416, 76 - 81.
- Bravo, J.M., Perzi, M., Hartner, T., Kannenberg, E.L., Rohmer, M., 2001. Novel methylated triterpenoids of the gammacerane series from the nitrogen-fixing bacterium *Bradyrhizobium japonicum* USDA 110. *European Journal of Biochemistry* 268, 1323 – 1331.
- Bringer, S., Hartner, T., Poralla, K., Sahm, H., 1985. Influence of ethanol on the hopanoid content and the fatty acid pattern in batch and continuous cultures of *Zymomonas mobilis*. *Archives of Microbiology* 140, 312 – 316.

## References

- Brock, T.D., 1978. Thermophilic microorganisms and life at high temperatures. Springer-Verlag, New York.
- Brocks, J. J., Summons, R. E., 2004. Sedimentary hydrocarbons, biomarkers for early life. In: Treatise on geochemistry, vol 8, Biogeochemistry. Schlesinger WH (ed) Elsevier – Oxford Publishing, p 63 – 115.
- Brocks, J. J., Logan, G. A., Buick, R., Summons, R. E., 1999. Archean molecular fossils and the early rise of eukaryotes. *Science* 285, 1033 – 1036.
- Broda, E., 1977. Two kinds of lithotrophs ‘missing’ in nature. *Zeitschrift für Allgemeine Mikrobiologie* 17, 491 – 493.
- Burhan, R.Y.P., Trendel, J.M., Adam, P., Wehrung, P., Albrecht, P., Nissenbaum, A., 2002. A fossil bacterial ecosystem at methane seeps: Origin of organic matter from Be’eri sulphur deposit, Isreal. *Geochimica et Cosmochimica Acta* 66, 4085 – 4101.

## C

- Cady, S.L., Farmer, J.D., 1996. Fossilization processes in siliceous thermal springs: trends in preservation along thermal gradients, p 150 - 170. In G. R. Bock and J. A. Goode (ed.), Evolution of hydrothermal ecosystems on Earth (and Mars?). Ciba Foundation Symposium no. 202. Wiley, Chichester, United Kingdom.
- Capone, D.G., Kiene, R.P., 1988. Comparison of microbial dynamics in marine and freshwater sediments – contrasts in anaerobic carbon catabolism. *Limnology and Oceanography* 33, 725 – 749.
- Carr, M.H., 1996. Water on early Mars. In Bock, G.R. and Goode, J.A. (Eds) Evolution of hydrothermal ecosystems on Earth (and Mars?). Wiley, Chichester, 249 – 267.

## References

- Castenholz, R.W., 1969. Thermophilic blue-green algae and the thermal environment. *Bacteriology Reviews* 33, 476 – 504.
- Castenholz, R.W., 1979. Life in thermal habitats. *Science* 9, 538 – 539.
- Childs, A.M., Mountain, B.W., O'Toole, R., Stott, M.B., 2008. The correlation between the microbial community and physicochemical parameters of a hot spring: Champagne Pool, Waiotapu, New Zealand. *Geomicrobiology* 25, 441 - 453.
- Cockell, C.S., Stokes, M.D., 2005. Widespread colonization of polar hypoliths. *Nature* 431, 414.
- Cooke, M.P., Talbot, H.M., Wagner, T., 2008a. Tracking soil organic carbon transport to continental margin sediments using soil-specific hopanoid biomarkers: a case study from the Congo fan area. *Organic Geochemistry* 39, 958 - 971.
- Cooke, M.P., Talbot, H.M., Farrimond, P., 2008b. Bacterial populations recorded in bacteriohopanepolyol distributions in soils from Northern England. *Organic Geochemistry* 39, 1347 - 1350.
- Coolen M.J.L, Talbot H.M., Abbas, B.A., Ward, C., Schouten, Volkman, J.K., Sinninghe Damsté, J.S., 2008. Sources for sedimentary bacteriohopanepolyols as revealed by 16S rDNA stratigraphy. *Environmental Microbiology* 10, 1783 - 1803.
- Corbett, R.E., Young, H., 1966. Lichens and fungi. Part II. Isolation and structural elucidation of 7 $\beta$ -acetoxy-22-hydroxyhopane from *Sticta billardierii* del. *Journal Chemical Society C*, 1556 – 1563.
- Costantino, V., Fattoruso, E., Imperatore, C., Mangoni, A., 2001. A biosynthetically significant new bacteriohopanoid present in large amounts in the Caribbean sponge *Plakortis simplex*. *Tetrahedron* 57, 4045 – 4048.

## References

Cvejic, J.H., Bodrossy, L., Kovacs, K.L., Rohmer, M., 2000a. Bacterial triterpenoids of the hopane series from methanotrophic bacteria *Methylocaldum* spp.: phylogenetic implications and first evidence for an unsaturated aminobacteriohopanepolyol. *FEMS Microbiology Letters* 182, 361 – 365.

Cvejic, J.H., Rosa Putra, S., El-Beltagy, A., Hattori, R., Hattori, T., Rohmer, M., 2000b. Bacterial triterpenoids of the hopane series as biomarkers for the chemotaxonomy of *Burholderia*, *Psuedomonas* and *Ralstonia* spp. *FEMS Microbiology Letters* 183, 295 – 299.

## D

Dastillung, M., Albrecht, P., Ourisson, G., 1980. Aliphatic and polycyclic alcohols in sediments: hydroxylated derivatives of hopane and of 3-methyl hopane. *Journal of Chemical Research* 168 – 169.

Dobson, G., Ward, D.M., Robinson, N., Eglinton, G., 1988. Biogeochemistry of hot spring environments - extractable lipids of a cyanobacterial mat. *Chemical Geology* 68, 155 - 179.

Duvold, T., Rohmer, M., 1999. Synthesis of ribosylhopane, the putative biosynthetic precursor of bacterial triterpenoids of the hopane series. *Tetrahedron* 55, 9847 – 9858.

## E

Eigenbrode, J. L., Freeman, K. H., Summons, R. E., 2008. Methylhopane biomarker hydrocarbons in Hammersley Province sediments provide evidence for neoarchaeal aerobiosis. *Earth and Planetary Science Letters* 273, 323 - 331.

## References

- Eijk, G.W., Roeijmans, H.J., Seykens, D., 1986. Hopanoids from the entomogenous fungus *Aschersonia aleyrodis*. *Tetrahedron Letters* 27, 2533 – 2534.
- Ellis, G., Bizzoco, R.L.W., Maezato, Y., Baggett, J.N., Kelley, S.T., 2005. Microscopic examination of acidic hot springs of Waiotapu, North Island, New Zealand. *New Zealand Journal of Marine and Freshwater Research* 39, 1001 - 1012.
- Elvert, M., Niemann, H., 2008. Occurrence of an unusual steroid and hopanoids derived from aerobic methanotrophs at a marine mud volcano. *Organic Geochemistry* 39, 167 - 177.
- Elvert, M., Whiticar, M.J., Suess, M., 2001. Diploptene in varied sediments of Saanich Inlet: indicator of increasing bacterial activity under anaerobic conditions during the Holocene. *Marine Geology* 174, 371 – 383.

## F

- Farrimond P., Fox P. A., Innes H. E., Miskin I. P., and Head I. M., 1998. Bacterial sources of hopanoids in recent sediments: Improving our understanding of ancient hopane biomarkers. *Ancient Biomolecules* 2, 147 – 166.
- Farrimond. P., Head. I. M., Innes. H. I., 2000. Environmental influence on the biohopanoids composition of recent sediments. *Geochimica et Cosmochimica Acta* 64, 2985 - 2992.
- Farrimond P., Love G.D., Bishop A.N., Innes H., Watson D.F., Snape C.E., 2003. Evidence for the rapid incorporation of hopanoids into kerogen. *Geochimica et Cosmochimica Acta* 67, 1383 - 1394.
- Farrimond, P., Talbot, H.M., Watson, D.F., Schulz, L.K., Wilhelms, A., 2004. Methylhopanoids: Molecular indicators of ancient bacteria and a petroleum correlation tool. *Geochimica et Cosmochimica Acta* 68, 3873 - 3882.

## References

- Fernandez-Turiel J.L., Garcia-Valles, M., Gimeno-Torrente, D., Saavedra-Alonso, J., Martinez-Manent, S., 2005. The hot spring and geyser sinters of El Tatio, northern Chile. *Sedimentary Geology* 180, 125 – 147.
- Ferris, F. G., Fyfe, W.S., Beveridge, T.J., 1987. Manganese oxide deposition in a hot-spring microbial mat. *Geomicrobiology* 5, 33 – 42.
- Ferris, F.G., Fyfe, W.S., Beveridge, T.J., 1988. Metallic ion binding by *Bacillus subtilis*: implications for the fossilisation of microorganisms. *Geology* 16, 149 – 152.
- Fischer, W. W., Pearson, A., 2007. Hypotheses for the origin and early evolution of triterpenoid cyclases. *Geobiology* 5, 19 – 34.
- Fischer, W. W., Summons, R. E., Pearson, A., 2005. Targeted genomic detection of biosynthetic pathways: anaerobic production of biomarkers by a common sedimentary microbe. *Geobiology* 3, 33 – 40.
- Flesch, G., Rohmer, M., 1988. Prokaryotic hopanoids: the biosynthesis of the bacteriohopane skeleton. Formation of isoprenic units from two distinct acetate pool and a novel type of carbon/carbon linkage between a triterpene and D-ribose. *European Journal of Biochemistry* 175, 405 – 411.
- Flesch, G., Rohmer, M., 1989. Prokaryotic triterpenoids. A novel hopanoid from the ethanol producing bacterium *Zymomonas mobilis*. *Biochemical Journal* 262, 673 – 675.
- Ford Doolittle, W., Baptiste, E., 2007. Pattern pluralism and the tree of life hypothesis. *Proceedings of the National Academy of Sciences* 104, 2043 – 2049.
- Forster, H.J., Biemann, K., Haigh, W.G., Tattrie, N.H., Colvin, J.R., 1973. The structure of novel C<sub>35</sub> pentacyclic terpenes from *Acetobacter xylinum*. *Biochemical Journal* 135, 133 – 143.

## References

- Fouke, B.W., Bonheyo, G.T., Sanzenbacher, B., Frias-Lopez, J., 2003. Partitioning of Bacterial communities between travertine depositional facies at Mammoth hot springs, Yellowstone National Park, USA. *Canadian Journal of Earth Sciences* 40, 1531 – 1548.
- Fox, P.A., Carter, J., Farrimond, P., 1998. Analysis of bacteriohopanepolyols in sediment and bacterial extracts by high performance liquid chromatography/atmospheric pressure chemical ionisation mass spectrometry. *Rapid Communications in Mass Spectrometry* 12, 609 – 612.
- Frias-Lopez, J., Shi, Y., Tyson, G.W., Coleman, M.L., Schuster, S.C., Chisolm, S.W., Delong, E.F., 2008. Microbial community gene expression in ocean surface waters. *Proceedings of the National Academy of Sciences* 11, 3805 – 3810.

## G

- Geptner, A.R., Ivanovskaya, T.A., Pokrovskaya, E.V., 2005. Hydrothermal fossilization of microorganisms at the Earth's surface in Iceland. *Lithology and Mineral Resources* 40, 505 – 520.
- Gibson, R.A., Talbot, H.M., Kaur, G., Pancost, R.D., Mountain, B., 2008. Bacteriohopanepolyol signatures of cyanobacterial and methanotrophic bacterial populations recorded in a geothermal vent sinter. *Organic Geochemistry* 39, 1020 - 1023
- Gray, N.D., Head, I.M., 2000. Linking genetic identity and function in genetic communities of uncultured bacteria. *Environmental Microbiology* 3, 481 – 492.
- Grice, K., Cao, C.Q., Love, G.D., Bottcher, M.E., Twitchett, R.J., Grosjean, E., Summons, R.E., Turgeon, S.C., Dunning, W., Jin, Y.G., 2005. Photic zone euxinia during the Permian–Triassic superanoxic event. *Science* 307, 706 – 709.

## References

### H

- Hakemian, A. S., Rosenzweig, A. C., 2007. The biochemistry of methane oxidation. *Annual Reviews in Biochemistry* 76, 223 – 41.
- Handley, L., Talbot, H.M., Cooke, M.P., Wagner, T., 2009. Cyclical methane emission/oxidation from the Congo Deep Sea Fan and associated biotic and climatic changes over the last 1 million years. Conference abstract, 23<sup>rd</sup> International Meeting on Organic Geochemistry, Bremen, Germany.
- Hanson, R.S., Hanson, T.E., 1996. Methanotrophic bacteria. *Microbiological Reviews*, 439-471.
- Hartner, T., Straub, K. L., Kannenburg, E. K., 2005. Occurrence of hopanoid lipids in anaerobic *Geobacter* species. *FEMS Microbiology Letters* 243, 59 – 64.
- Head, I.M., Gray, N.D., Babenzien, H.D., Glockner, F.O., 2000. Uncultured giant sulphur bacteria of the genus *Achromatium*. *FEMS Microbial Ecology* 3, 171 – 180.
- Hermans, M.A.F., Neuss, B., Sahm.H., 1991. Content and composition of hopanoids in *Zymomonas mobilis* under various growth conditions. *Journal of Bacteriology*, 5595 – 5595.
- Herrmann, D., Bisseret, P., Connan, J., Rohmer, M., 1996a. A non-extractable triterpenoid of the hopane series in *Acetobacter xylinum*. *FEMS Microbiology Letters* 135, 323 – 326.
- Herrmann, D., Bisseret, P., Connan, J., Rohmer, M., 1996b. Relative configurations of carbapseudopentose moieties of the hopanoids of the bacterium *Zymomonas mobilis* and the cyanobacterium *Anacystis montana*. *Tetrahedron Letters* 37, 1791 – 1794.
- Hetzer, A., 2009. Sequestration of metal and metalloid ions by thermophilic bacteria. Ph.D. Thesis, University of Waikato, New Zealand.

## References

- Hetzer, A., Morgan, H.W., McDonald, I.R., Daughney, C.J., 2007. Microbial life in Champagne Pool, a geothermal spring in Waiotapu, New Zealand. *Extremophiles* 11, 605 – 614.
- Hetzer, A., Macdonald, I.R., Morgan, H.W., 2008. *Venenivibrio stagnispumantis* gen. nov., sp nov., a thermophilic hydrogen-oxidising bacterium isolated from Champagne Pool, Waiotapu, New Zealand. *International Journal of Systematics and Evolutionary Microbiology* 58, 398 – 403.
- Hinrichs, K.U., Hayes, J.M., Sylva, S.P., Brewer, P.G., DeLong, E.F., 1999. Methane consuming archaeobacteria in marine sediments. *Nature* 398, 802 - 804.
- Hirner, A.V., Feldmann, J., Krupp, E., Grumping, R., Goguel, R., Cullen, W.R., 1998. Metal(loid) organic compounds in geothermal gases and waters. *Organic Geochemistry* 29, 1765 – 1778.
- Hopmans, E.C., Schouten, S., Pancost, R.D., van der Meer, M.T.J., Sinninghe Damsté, J.S. 2000. Analysis of intact tetraether lipids in archaeal cell material and sediments by high performance liquid chromatography/atmospheric pressure chemical ionization mass spectrometry. *Rapid Communications in Mass Spectrometry* 14, 585 - 589.
- Huber, R., Wilharm, T., Huber, D., Trincone, A., Burggraf, S., König, H., Rachel, R., Rockinger, I., Fricke, H., Stetter, K.O., 1992. *Aquifex pyrophilus* gen. nov. sp. nov. represents a novel group of marine hyperthermophilic hydrogen-oxidizing bacteria. *Systematic and Applied Microbiology* 15, 340 - 351.
- Huber, R., Rossnagel, P., Woese, C.R., Rachel, R., Langworthy, T.A., and Stetter, K.O., 1996. Formation of ammonium from nitrate during chemolithoautotrophic growth of the extremely thermophilic bacterium *Ammonifex degensii* gen. nov. sp. nov. *Systematic and Applied Microbiology* 19, 40 – 49.

## References

### I

- Inagaki, F., Motomura, Y., Ogata, S., 2003. Microbial silica deposition in geothermal hot waters. *Applied Microbiology and Biotechnology* 60, 605 – 611.
- Innes, H.E., 1998. Hopanoid distributions and diagenesis in recent sediments. PhD thesis, University of Newcastle-upon-Tyne, U.K.
- Innes, H.E., Bishop, A.N., Head, I.M., Farrimond, P., 1997. Preservation and diagenesis of hopanoids in recent lacustrine sediments of Priest Pot, England. *Organic Geochemistry* 26, 565 – 576.
- Innes, H.E., Bishop, A.N., Fox, P.A., Head, I.M., Farrimond, P., 1998. Early diagenesis of bacteriohopanoids in Recent sediments of Lake Pollen, Norway. *Organic Geochemistry* 29, 1285 - 1295.

### J

- Jaeschke, A., Op den Camp, H.J.M., Harhangi, H., Klimiuk, A., Hopmans, E.C., Jetten, M.S.M, Schouten, S., Sinninghe Damsté, J.S., 2009. 16S rRNA and lipid biomarker evidence for anaerobic ammonium-oxidizing bacteria (anammox) in California and Nevada hot springs. *FEMS Microbial Ecology* 67, 343 – 350.
- Jahnke, L.L., Summons, R.E., Hope, J.M., Des Marais, D.J., 1999. Carbon isotopic fractionation from methanotrophic bacteria II: The effects of physiology and environmental parameters on the biosynthesis and isotopic signatures of biomarkers. *Geochimica et Cosmochimica Acta* 63, 79 – 93.
- Jahnke, L.L., Eder, W., Huber, R., Hope, J.M., Hinrichs, K-U., Hayes, J., des Marais, D.J., Cady, S.L., Summons, R.E., 2001. Signature lipids and stable carbon isotope analyses of

## References

- Octopus Spring hyperthermophilic communities compared with those of *Aquificales* representatives. *Applied and Environmental Microbiology*, 5179 - 5189.
- Jahnke, L.L., Embaye T., Hope, J., Turk, K.A., van Zuilen, M., des Marais, D.J., Farmer, J.D., Summons, R.E., 2004. Lipid biomarker and carbon isotopic signatures for stromatolite-forming, microbial mat communities and *Phormidium* cultures from Yellowstone National Park. *Geobiology* 2, 31 - 47.
- Jakosky, B.M., Haberla, R.M., Arvidson, R.E., 2005. The changing picture of volatiles and climate on Mars. *Science* 310, 1439 – 1440.
- Jones, B., Renaut, R.W., 1996. Influence of thermophilic bacteria on calcite and silica precipitation in hot springs with water temperatures above 90°C: Evidence from Kenya and New Zealand. *Canadian Journal of Earth Sciences* 33, 72 – 83.
- Jones, B., Renaut, R.W., 2007. Selective mineralization of microbes in Fe-rich precipitates (jarosite, hydrous ferric oxides) from acid hot springs in the Waiotapu geothermal area, North Island, New Zealand. *Sedimentary Geology* 194, 77 – 98.
- Jones, B., Renaut, R.W., Rosen, M.R., Klyen, L., 1998. Primary siliceous rhizoliths from Loop Road hot-springs, North Island, New Zealand. *Journal of Sedimentary Research* 68, 115 – 123.
- Jones, B., Renaut, R.W., Rosen, M.R., 2001. Biogenicity of gold- and silver-bearing siliceous sinters forming in hot (75°C) anaerobic spring-waters of Champagne Pool, Waiotapu, North Island, New Zealand. *Journal of the Geological Society* 158, 895 – 911.
- Joyeux, C., Fouchard, S., Llopiz, P., Neunlist, S., 2004. Influence of the temperature and growth phase on the hopanoids and fatty acids content of *Frateuria aurantia* (DMSZ 6220). *FEMS Microbiology Ecology* 47, 371 – 379.

## References

### K

- Kannenburg, E. L., Poralla, K., 1999. Hopanoid biosynthesis and function in bacteria. *Naturwissenschaften* 86, 168 – 176.
- Kannenbergl, E.L., Poralla, K., Blume, A., 1980. A hopanoid from the thermo-acidphilic *Bacillus acidocaldarius* condenses membranes. *Naturwissenschaften* 67, 458 – 459.
- Kannenbergl, E.L., Perzl, M., Härtner, T., 1995. The occurrence of hopanoid lipids in *Bradyrhizobium* bacteria. *FEMS Microbiology Letters* 127, 255 - 262.
- Kannenbergl, E.L., Perzl, M., Müller, P., Härtner, T., Poralla, K., 1996. Hopanoid lipids in *Bradyrhizobium* and other plant-associated bacteria and cloning of the *Bradyrhizobium japonicum* squalene-hopene cyclase gene. *Plant and Soil* 186, 107 – 112.
- Kappler, A., Pasquero, C., Konhauser, K.O., Newman, D.K., 2005. Deposition of banded iron formations by anoxygenic phototrophic Fe(II)-oxidising bacteria. *Geology* 33, 865 – 888.
- Kates, M., 1975. Techniques of lipidology. In: Work, T.S., Work, E., (Eds). Laboratory techniques in biochemistry and molecular biology. Elsevier, p269 – 610.
- Kaur, G., 2009. Microbial membrane lipids in geothermal environments. Ph.D. Thesis, University of Bristol, U.K.
- Kaur, G., Mountain, B.W., Pancost, R.D., 2008. Microbial membrane lipids in active and inactive sinters from Champagne Pool, New Zealand: Elucidating past geothermal chemistry and microbiology. *Organic Geochemistry* 39, 1024 - 1028.
- Kelley, D.S., Karsson, J.A., Blackman, D.K., Fruh-Green, G.L., Butterfield, D.A., Lilley, M.D., Olson, E.J., Schrenk, M.O., Roe, K.K, Lebon, G.T, Rimizzigno, P., 2001. An off-axis hydrothermal vent field near the mid-Atlantic ridge at 30 degrees N. *Nature* 412, 145 – 149.

## References

- Kelley, D.S., Karson, J.A., Fruh-Green, G.L., Yoerger, D.R., Shank, T.M., Butterfield, D.A., Hayes, J.M., Schrenk, M.O., Olson, E.J., Proskurowski, G., Jakuba, M., Bradley, A., Larson, B., Ludwig, G., Glickson, D., Buckman, K., Bradley, A.S., Brazelton, W.J., Roe, K., Elend, M.J., Delacour, A., Bernasconi, S.M., Dilley, M.D., Baross, J.A., Summons, R.E., Sylva, S.P., 2005. A serpentinite hosted ecosystem: the Lost City Hydrothermal Field. *Science* 307, 1428 – 1434.
- Knani, M., Corpe, W.A., Rohmer, M., 1994. Bacterial hopanoids from pink-pigmented facultative methylotrophs (PPFMs) and from green plant surfaces. *Microbiology* 140, 2755 – 2759.
- Knoll, A.H., 1985. Exceptional preservation of photosynthetic organisms in silicified carbonates and silicified peats. *Royal Philosophical Transactions of London* 311, 11 - 122.
- Knoll, A.H., Walter, M. R., 1996. The limits of palaeontological information: finding the gold among the dross, p198 – 209. In G. R. Bock and J. A. Goode (ed.), *Evolution of hydrothermal ecosystems on Earth (and Mars?)*. Ciba Foundation Symposium no. 202. Wiley, Chichester, United Kingdom.
- Koga, Y., Nishihara, M., Morii, H., Akagawa-Matsushita, M., 1993. Ether polar lipids of methanogenic bacteria: Structures, comparative aspects and biosynthesis. *Microbiological Reviews* 57, 164 – 182.
- Konhauser, K.O., Phoenix, V.R., Bottrell, S.H., Adams, D.G., Head, I.M., 2001. Microbial-silica interactions in Icelandic hot spring sinter: possible analogues for some Precambrian siliceous stromatolites. *Sedimentology* 48, 415 – 433.

## References

- Krisnamurthy, T., Ross, P., 1996. Rapid identification of bacteria by matrix assisted laser desorption/ionisation mass spectrometric analysis of whole cells. *Rapid Communications in Mass Spectrometry* 10, 1992 – 1996.
- Krupp, R., Seward, T.M., 1990. Transport and deposition of metals in the Rotokawa geothermal system, New Zealand. *Mineralium Deposita* 25, 73 - 81.
- Kump, L.R., Pavlov, A., Arthur, M.A., 2005. Massive release of hydrogen sulphide to the surface ocean and atmosphere during intervals of anoxia. *Geology* 33, 750 – 766.
- Kuypers, M.M.M., Jorgenson, B.B., 2008. The future of single-cell microbiology. *Environmental Microbiology* 9, 1 – 11.
- Kuypers, M.M.M., Sliemers, A.O., Lavik, G., Schmid, M., Jorgensen, B.B., Kuenen, G.J., Sinninghe Damsté, J.S., Strous, M., Jetten, M.S.M., 2003. Anaerobic ammonium oxidation by anammox bacteria in the Black Sea. *Nature* 422, 608 – 611.

## L

- Lalonde, S.V., Konhauser, K.O., Reysenbach, A-L., Grant-Ferris, F., 2005. The experimental silification of *Aquificales* and their role in hot-spring sinter formation. *Geobiology* 3, 41 – 52.
- Lalonde, S.V., Smith, D.S., Owttrim, G.W., Konhauser, K.O., 2008a. Acid-Base properties of cyanobacterial surfaces I: Influences on growth phase and nitrogen metabolism on cell surface reactivity. *Geochimica et Cosmochimica Acta* 72, 1257 – 1268.
- Lalonde, S.V., Smith, D.S., Owttrim, G.W., Konhauser, K.O., 2008b. Acid-Base properties of cyanobacterial surfaces II: Silica as a chemical stressor influencing cell surface reactivity. *Geochimica et Cosmochimica Acta* 72, 1269 – 1280.

## References

- Lange, M.B., Rujan, T., Martin, W., Croteau, R., 2000. Isoprenoid biosynthesis: the evolution of two ancient and distinct pathways across genomes. *Proceedings of the National Academy of Sciences* 97, 13172 – 13177.
- Langworthy, T.A., Mayberry, W.R., Smith, P.F., 1976. A sulfonolipid and novel glucosamidyl glycolipids from the extreme thermoacidophile *Bacillus acidocaldarius*. *Biochimica et Biophysica Acta* 431, 550 – 569.
- Llopiz, P., Neunlist, S., Rohmer, M., 1992. Prokaryotic triterpenoids: *O*- $\alpha$ -D-glucuronopyranosyl bacteriohopanetetrol, a novel hopanoid from the bacterium *Rhodospirillum rubrum*. *Biochemistry Journal* 287, 159 – 161.
- Llopiz, P., Jurgens, U. J., Rohmer, M., 1996. Prokaryotic triterpenoids: Bacteriohopanetetrol glycuronosides from the thermophilic cyanobacterium *Synechococcus* PCC 6907. *FEMS Microbiology Letters* 140, 199 – 202.
- Lutnaes, B.F., Bruun, T.K., Osen, H., 2004. (22S)-6-O-Acetyl-21 $\beta$ H-hopane-3 $\beta$ , 6 $\beta$ , 22,29-tetrol from oakmoss (*Evernia prunastri*). *Natural Products Research* 18, 379 – 385.
- Lynne, B.Y., Campbell, K.A., 2003. Diagenetic transformation (opal-A to quartz) of low- and mid-temperature microbial textures in siliceous hot-spring deposits, Taupo Volcanic Zone, New Zealand. *Canadian Journal of Earth Sciences* 40, 1439 – 1442.
- Lynne, B.Y., Campbell, K.A., 2004. Morphological and mineralogic transition from opal-A to opal-CT in low temperature siliceous sinter diagenesis, Taupo Volcanic Zone, North Island, New Zealand. *Journal of Sedimentary Research* 74, 561 – 579.

## M

- Miller, S.R., Castenholz, R.W., 2000. Evolution of thermotolerance in hot spring cyanobacteria of the genus *Synechococcus*. *Applied and Environmental Microbiology* 66, 4222 – 4229.

## References

- Miller, S.R., Strong, A.L., Jones, K.L., Ungerer, M.C., 2009. Barcoded pyrosequencing reveals shared bacterial community properties along two alkaline hot spring temperature gradients in Yellowstone National Park. *Applied and Environmental Microbiology* 75, 4565 – 4572.
- Moldowan J.M., McCaffrey M.A., 1995. A novel hydrocarbon degradation pathway revealed by hopane demethylation in a petroleum reservoir. *Geochimica et Cosmochimica Acta* 59, 1891 - 1894.
- Moreau, R. A., Powell, M.J., Osman, S.F., Whitaker, B.D., Fett, W.F., Roth, L., O'Brien, D.J., 1995. Analysis of intact hopanoids and other lipids from the bacterium *Zymomonas mobilis* by high-performance liquid chromatography. *Analytical Chemistry* 224, 293 – 301.
- Moreau, R. A., Agnew, J., Hicks, K. B., Powell, M.J., 1997. Modulation of lipoxygenase activity by bacterial hopanoids. *Journal of Natural Products* 60, 397 – 398.
- Mountain, B.W., Benning, L.G., Boerema, J.A., 2003. Experimental studies on New Zealand hot spring sinters: rates of growth and textural development. *Canadian Journal of Earth Sciences* 40, 1642 – 1667.
- Mycke, B., Narjes, F., Michaelis, W., 1987. Bacteriohopanetetrol from chemical degradation of an oil shale. *Nature* 326, 179 – 181.

## N

- Nagumo, A., Takanashi, K., Hojo, H., Suzuk., Y., 1991. Cytotoxicity of bacteriohopan-32-ol against mouse leukaemia L1210 and P388 cells in vitro. *Toxicology Letters* 3, 309 – 313.

## References

- Neunlist, S., Rohmer, M., 1985a. The hopanoids of '*Methylosinus trichosporium*': Aminobacteriohopanetriol and aminobacteriohopanetetrol. *Journal of General Microbiology* 131, 1363 – 1367.
- Neunlist, S. Rohmer, M. 1985b. A novel hopanoid, 30-(5'-adenosyl)hopane, from the purple non-sulphur bacterium *Rhodopseudomonas acidophila*, with possible DNA interactions. *Biochemical Journal* 228, 769 – 771.
- Neunlist, S., Rohmer, M., 1985c. Novel hopanoids from the methylotrophic bacteria *Methylococcus capsulatus* and *Methylomonas methanica*. *Biochemical Journal* 231, 635 – 639.
- Neunlist, S., Holst, O., Rohmer, M., 1985. Prokaryotic triterpenoids. The hopanoids of the purple non-sulphur bacterium *Rhodomicrobium vannielii*: an aminotriol and its aminoacyl derivatives, *N*-tryptophanyl and *N*-ornithinyl aminotriol. *European Journal of Biochemistry* 147, 561 – 568.
- Neunlist, S., Bissere, P., Rohmer, M., 1988. The hopanoids of the purple non-sulfur bacteria *Rhodopsuedomonas palustris* and *Rhodopsuedomonas acidophila* and the absolute configuration of bacteriohopanetetrol. *European Journal of Biochemistry* 171, 245 – 252.
- Nisbet, E.G., Sleep, N.H., 2001. The habitat and nature of early life. *Nature* 409, 1083 – 1091.

## O

- Oehler, J.H., Schopf, J.W., 1971. Artificial microfossils: experimental studies of permineralisation of blue-green algae in silica. *Science* 174, 1229 – 1231.

## References

- Orcutt, B., Boetius, A., Elvert, M., Samarkin, V., Joye, S.B., 2005. Molecular biogeochemistry of sulphate reduction, methanogenesis and the anaerobic oxidation of methane at Gulf of Mexico cold seeps. *Geochimica et Cosmochimica Acta* 69, 4267 – 4281.
- Ourisson, G., 1987. Bigger and better hopanoids. *Nature* 326, 126 – 127.
- Ourisson, G., Albrecht, P., 1992. Geohopanoids 2: The most abundant natural product on Earth? *Accounts of Chemical Research* 25, 398 – 402.
- Ourisson, G., Rohmer, M., 1992. Hopanoids 2: Biohopanoids: A novel class of bacterial lipids. *Accounts of Chemical Research* 25, 403 – 408.
- Ourisson, G., Rohmer, M., Poralla, K., 1987. Prokaryotic hopanoids and other polyterpenoid sterol surrogates. *Annual Reviews in Microbiology* 41, 301 – 333.

## P

- Pancost, R.D., Sinninghe Damsté, J.S., De Lint, S., Van der Maarel, M.J.E.C, Gottschal, J.C., and the Medinaut shipboard party, 2000. Biomarker evidence for widespread anaerobic methane oxidation in Mediterranean sediments by a consortium of methanogenic archaea and bacteria. *Applied and Environmental Microbiology* 66, 1126 – 1132.
- Pancost, R.D., Hopmans, E.C., Sinninghe Damsté and The MEDINAUT shipboard scientific party, 2001. Archaeal lipids in Mediterranean Cold Seeps: Molecular proxies for anaerobic methane oxidation. *Geochimica et Cosmochimica Acta* 65, 1611 - 1627.
- Pancost, R.D., Pressley, S., Coleman, J.M., Benning, L.G., Mountain, B.W., 2005. Lipid biomolecules in silica sinters: indicators of microbial diversity. *Environmental Microbiology* 7, 66 - 77.

## References

- Pancost, R.D., Pressley, S., Coleman, J.M., Talbot, H.M., Kelly, S.P., Farrimond, P., Schouten, S., Benning, L., Mountain, B.W., 2006. Composition and implications of diverse lipids in New Zealand geothermal sinters. *Geobiology* 4, 71 - 92.
- Papke, R.T., Ramsing, N.B., Bateson, M.M., Ward, D.M., 2003. Geographical isolation in hot spring cyanobacteria. *Environmental Microbiology* 5, 650 – 659.
- Pearson, A., Budin, M., Brocks, J.J., 2003. Phylogenetic and biochemical evidence for sterol synthesis in the bacterium *Gemmata obscuriglobus*. *Proceedings of the National Academy of Sciences* 100, 15352 – 15357.
- Pearson, A., Huang, Z., Ingalls, A.E., Romanek, C.S., Wigal, J., Freeman, K.H., Smittenberg, R.H., Zhang, C.L., 2004. Non-marine crenarchaeol in Nevada hot springs. *Applied and Environmental Microbiology* 70, 5229 – 5237.
- Pearson, A., Flood Page, S.R., Jorgenson, T.L., Fischer, W.W., Higgins, M.B., 2007. Novel hopanoid cyclases from the environment. *Environmental Microbiology* 9, 2175 – 2188.
- Pentecost, A., 1996. High temperature ecosystems and chemical interactions with their environment. p99 – 111. In G. R. Bock and J. A. Goode (ed.), *Evolution of hydrothermal ecosystems on Earth (and Mars?)*. Ciba Foundation Symposium no. 202. Wiley, Chichester, United Kingdom.
- Pentecost, A., 2005. The microbial ecology of some Italian hot-spring travertines. *Microbiology* 81, 45 – 58.
- Peters K. E., Moldowan J. M., 1993. *The Biomarker Guide. Interpreting molecular fossils in petroleum and ancient sediments*. Prentice Hall.
- Peters, K.E., Walters, C.C., Moldowan, J.M., 2005. *The biomarker guide. Volume 2*. Cambridge University Press.

## References

- Phoenix, V.R., Konhauser, K.O., 2008. Benefits of bacterial biomineralisation. *Geobiology* 6, 303 – 308.
- Phoenix, V.R., Adams, D.G., Konhauser, K.O., 2000. Cyanobacterial viability during hydrothermal biomineralisation. *Chemical Geology* 169, 329 – 338.
- Phoenix, V.R., Renaut, R.W., Jones, B., Ferris, F.G., 2005. Bacterial S-layer preservation and rare arsenic-antimony-sulphide bioimmobilization in siliceous sediments from Champagne Pool hot spring, Waiotapu, New Zealand. *Journal of the Geological Society*, 162, 323 – 331.
- Phoenix, V.R., Bennett, P.C., Engel, A.S., Tyler, S.W., Ferris, F.G., 2006. Chilean high-altitude hot spring sinters: a model system for UV screening mechanisms by early Precambrian cyanobacteria. *Geobiology* 4, 15 – 28.
- Philp, R.P., 1985. Fossil Fuel Biomarkers. Elsevier, The Netherlands.
- Piazena, H., 1996. The effect of altitude upon the solar UV-B and UV-A irradiance in the tropical Chilean Andes. *Solar Energy* 57, 133 – 140.
- Pieseler, B., Rohmer, M., 1991. Prokaryotic triterpenoids. (22*R*, 32*R*)-34,35-dinorbacteriohopane-32,33-diols from *Acetobacter aceti* ssp. *xylinum*: New bacteriohopane derivatives with shortened side-chain. *Journal of the Chemical Society: Perkin Transactions* 1, 2449 - 2453.
- Pope., J.G., McConchie, D.M., Clark, M.D., Brown, K.L., 2004. Diurnal variations in the chemistry of geothermal fluids of Champagne Pool, Waiotapu, New Zealand. *Chemical Geology* 253 – 272.

## References

Poralla, K., Kannenberg, E., Blume, A., 1980. A glycolipid containing hopane isolated from the acidophilic thermophilic *Bacillus acidocaldarius*, has a cholesterol-like function in membranes. *FEBS Letters* 113, 107 – 110.

Poralla, K., Hartner, T., Kannenberg, E., 1984. Effect of temperature and pH on the hopanoid content of *Bacillus acidocaldarius*. *FEMS Microbiology Letters* 23, 253 – 256.

Poralla, K., Muth, G., Hartner, T., 2000. Hopanoids are formed during transition from substrate to aerial hyphae in *Streptomyces coelicolor* A3(2). *FEMS Microbiology Letters* 189, 93 – 95.

## Q

Quirk, M.M., Wardroper, A.M.K., Wheatley, R.E., Maxwell, J.R., 1984. Extended hopanoids in peat environments. *Chemical Geology* 42, 25 – 43.

## R

Rashby, S.E., Sessions, A.L., Summons, R.E., Newman, D.K., 2007. Biosynthesis of 2-methylbacteriohopanepolyols by an anoxygenic phototroph. *Proceedings of the National Academy of Sciences* 104, 15099 – 15104.

Rasmussen, B., Fletcher, I.R., Brocks, J.J., Kilburn, M.R., 2008. Reassessing the first appearance of eukaryotes and cyanobacteria. *Nature* 455, 1101 – 1104.

Renaut, R.W., Jones, B., Tiercelin, J.J., 1998. Rapid in situ silicification of microbes at Loburu hot-springs, Lake Bogoria, Kenya Rift Valley. *Sedimentology* 45, 1083 – 1103.

Renoux, J.M., Rohmer, M., 1985. Prokaryotic triterpenoids. New bacteriohopanetetrol cyclitol ethers from the methylotrophic bacterium *Methylobacterium organophilum*. *European Journal of Biochemistry* 151, 405 – 410.

## References

- Reysenbach, A-L., Cady, S.L., 2001. Microbiology of ancient and modern hydrothermal systems. *Trends in Microbiology* 9, 79 – 86.
- Reysenbach, A-L., Wickham, G.S., Pace, N.R., 1994. Phylogenetic analysis of the hyperthermophilic pink filament community in Octopus Spring, Yellowstone National Park. *Applied and Environmental Microbiology* 60, 2113 – 2119.
- Ries-Kautt, M., Albrecht, P. 1989. Hopane-derived triterpenoids in soils. *Chemical Geology* 76, 143 – 151.
- Robinson, N., Eglinton, G., 1990. Lipid chemistry of Icelandic hot-spring microbial mats. *Organic Geochemistry* 15, 291 – 298.
- Rodgers, K.A., Browne, P.R.L., Buddle, T.F., Cook, K.L., Greatrex, R.A., Hampton, W.A., Herdianita, N.R., Holland, G.R., Lynne, B.Y., Martin, R., Newton, Z., Pastars, D., Sannazarro, K.L., and Teece, C.I.A. 2004. Silica phases in sinters and residues from geothermal fields of New Zealand. *Earth Science Reviews* 66, 1 – 61.
- Rodier, C., Llopiz, P., Nuenlist, S., 1999. C<sub>32</sub> and C<sub>34</sub> hopanoids in Recent sediments of European Lakes: novel intermediates in the early diagenesis of biohopanoids. *Organic Geochemistry* 30, 713 – 716.
- Rohmer, M., 1993. The biosynthesis of triterpenoids of the hopane series in the Eubacteria: A mine of new enzyme reactions. *Pure and Applied Chemistry* 65, 1293 – 1298.
- Rohmer, M., 1999. A mevalonate-independent route to isopentenyl diphosphate. In: *Comprehensive Natural Product Chemistry*. Pergamon, Vol.2, p 45 – 68.
- Rohmer, M., 2007. Diversity in isoprene unit biosynthesis: The Methylerythritol phosphate pathway in bacteria and plastids. *Pure and Applied Chemistry* 79, 739 – 751.

## References

- Rohmer, M., Ourisson, G., 1986. Unsaturated bacteriohopanepolyols from *Acetobacter xylinum* spp. aecti. *Journal of Chemical Research* 3037 – 3059.
- Rohmer, M., Dastillung, M., Ourisson, G., 1980. Hopanoids of from C<sub>30</sub> to C<sub>35</sub> in recent mud. *Naturwissenschaften* 67, 456 – 458.
- Rohmer, M., Bouvier-Nave, P., Ourisson, G., 1984. Distribution of hopanoid triterpenes in Prokaryotes. *Journal of General Microbiology* 130, 1137 – 1150.
- Rohmer, M., Knani, M., Simonin, P., Sutter, B., Sahm, H., 1993. Isoprenoid biosynthesis in bacteria: a novel pathway for the early steps leading to isopentenyl disphosphate. *Biochemistry Journal* 295, 517 – 524.
- Rosa-Putra, S., Nalin, R., Domenach, A-M., Rohmer, M., 2001. Novel hopanoids from *Frankia* spp. and related soil bacteria. Squalene cyclization and significance of geological biomarkers revisited. *European Journal of Biochemistry* 268, 4300 - 4306.
- Rossel, P.E., Lipp, J.S., Fredricks, H.F., Arnds, J., Boetius, A., Elvert, M., Hinrichs, K.U., 2008 Intact polar lipids of anaerobic methanotrophic archaea and associated bacteria. *Organic Geochemistry* 398, 992 - 999.
- Rusch, A., Walpersdorf, E., deBeer, D., Currieri, S., Amend, J.P., 2005. Microbial communities near the oxic/anoxic interface in the hydrothermal system of Vulcano Island, Italy. *Chemical Geology* 224, 169 – 182.

## S

- Saenz, J.P., 2010. Hopanoid enrichment in a detergent resistant membrane fraction of *Crocospaera watsonii*: implications for bacterial lipid raft formation. *Organic Geochemistry* 41, 853 – 856.

## References

- Schaeffer, P., Adam, P., Phillippe, E., Trendel, J.M., Schmid, J-C., Behrens, A., Connan, J., Albrecht, P., 2006. The wide-diversity of hopanoid sulfides evidenced by the structural identification of several novel hopanoid series. *Organic Geochemistry* 37, 1590 – 1616.
- Schaeffer, P., Schmitt, G., Adam, P., Rohmer, M., 2008. Acid-catalysed formation of 32,35-anhydrobacteriohopanetetrol from bacteriohopanetetrol. *Organic Geochemistry* 39, 1479 – 1482.
- Schmidt, A., Bringer-Meyer, S., Poralla, K., Sahm, H., 1986. Effect of alcohols and temperature on the hopanoid content of *Zymomonas mobilis*. *Applied Microbiology and Biotechnology* 25, 32 – 36.
- Schopf, W.J., 1993. Microfossils of the early Archean Apex chert – new evidence of the antiquity of life. *Science* 260, 640 - 646.
- Schouten, S., Baas, M., Hopmans, E.C., Reysenbach, A-L., Sinninghe Damsté, J.S., 2008. Tetraether membrane lipids of *Candidatus "Acidolipifundum boonei"*, a cultivated obligate thermoacidophile euryarchaeote from deep-sea hydrothermal vents. *Extremophiles* 12, 119 – 124.
- Schwartzman, D.W., Lineweave, C.H., 2004. The hyperthermophilic origin of life revisited. *Biochemical Society Transactions* 32, 168 – 171.
- Seeman, M., Bisseret, P., Tritz, J-P., Hooper, A.B., Rohmer, M., 1999. Novel bacterial triterpenoids of the hopane series from *Nitrosomonas europaea* and their significance for the formation of the C<sub>35</sub> bacteriohopane skeleton. *Tetrahedron Letters* 40, 1681 - 1684.
- Shatz, M., Yosief, T., Kashman, Y., 2000. Bacteriohopanehexol, a new triterpene from the marine sponge *Petrosia* species. *Journal of Natural Products* 63, 1554 – 1556.

## References

- Shiea, J., Brassell, S.C., Ward, D.M., 1991. Comparative analysis of extractable lipids in hot spring microbial mats and their component photosynthetic bacteria. *Organic Geochemistry* 17, 309 – 319.
- Simoneit, B.R.T., 1996. Molecular indicators (biomarkers) of past life. *The Anatomical Record* 268, 186 – 195.
- Simonin P., Jürgens J., Rohmer, M., 1992 35-O- $\beta$ -6-Amino-6-deoxyglucopyranosyl bacteriohopanetetrol, a novel triterpenoid of the hopane series from the cyanobacterium *Synechocystis* sp. PCC 6714. *Tetrahedron Letters* 33, 3629 - 3632
- Simonin, P., Tindall, B., Rohmer, M., 1994. Structure elucidation and biosynthesis of 31-methylhopanoids from *Acetobacter europaeus*. *European Journal of Biochemistry* 225, 765 - 771.
- Simonin P., Jürgens J., Rohmer, M., 1996. Bacterial triterpenoids of the hopane series from the prochlorophyte *Prochlorothrix hollandica* and their intracellular localization. *European Journal of Biochemistry* 241, 865 - 871.
- Sinninghe Damsté, J.S., van Duin, A.C.T., Hollander, D., Kohnen, M.E.L., de Leeuw, J.W., 1995. Early diagenesis of bacteriohopanepolyol derivatives: Formation of fossil homohopanoids. *Geochimica et Cosmochimica Acta* 59, 5141 – 5147.
- Sinninghe Damsté, J.S., Rijpstra, W. I C., Schouten, S., Fuerst, J A., Jetten, M. S. M., Strous, M., 2004. The occurrence of hopanoids in Planctomycetes: implications for the sedimentary biomarker record. *Organic Geochemistry* 35, 561 – 566.
- Sinninghe Damsté, J.S., Raghoebarsing, A.A., Smolders, A.J.P., Schmid, M.C., Rijpstra, W.I.C., Wolters-Arts, M., Derksen, J., Jettem, M.S.M, Schouten, S., Lamers, L.P.M., Roelofs, J.G.M., Op den Camp, H.J.M., Strous, M., 2005. The methane cycle in peat bogs

## References

- revisited: methanotrophic symbionts provide carbon for photosynthesis. Conference abstract, The 22<sup>st</sup> International Meeting on Organic Geochemistry. Seville, Spain.
- Skirnsidottir, S., Hreggriðsson, G.O., Hjørleifsdóttir, S., Marteinson, V.T., Petursdóttir, S.K., Holst, O., Kristiansson, J.K., 2000. Influence of sulphide and temperature on species composition and community structure of hot-spring microbial mats. *Applied and Environmental Microbiology* 66, 2835 – 2841.
- Squyers, S.W., Grotzinger, J.P., Arvidson, R.E., Bell III, J.F., Calvin, W., Christensen, P.R., Clark, B.C., Crisp, J.A., Farrard, W.H., Herkenhoff, K.E., Johnson, J.R., Klingelhofer, G., Knoll, A.H., McLennan, S.M., McSween Jr, H.Y., Morris, R.V., Rice Jr, J.W., Rieder, R., Soderblom, L.A. 2004. In situ evidence for an ancient aqueous environment at Meridani Planum, Mars. *Science* 306, 1709 – 1714.
- Squyers, S.W., Arvidson, R.E., Ruff, S., Gellert, R., Morris, R.V., Ming, D.W., Crumpler, L., Farmer, J.D., Des Marais, D.J., Yen, A., McLennan, S.M., Calvin, W., Bell III, J.F., Clark, B.C., Wang, A., McCoy, T.J., Schmidt, M.E., de Souza Jr, P.A., 2008. Detection of silica-rich deposits on Mars. *Science* 320, 1063 – 1067.
- Stetter, K.O., 1996 Hyperthermophiles in the history of life, p1 - 18. In G. R. Bock and J. A. Goode (ed.), *Evolution of hydrothermal ecosystems on Earth (and Mars?)*. Ciba Foundation Symposium no. 202. Wiley, Chichester, United Kingdom.
- Stroeve, P., Pettit, C.D., Vasques, V., Kim, I., Berry, A. M., 1998. Surface active behaviour of hopanoid lipids: bacteriohopanetetrol and phenylacetate monoester bacteriohopanetetrol. *Langmuir* 14, 4261 – 4265.
- Sturt, H., Summons, R.E., Smith, K., Elvert, M., Hinrichs, K-U., 2004. Intact polar membrane lipids in prokaryotes and sediments deciphered by high-performance liquid

## References

- chromatography/electrospray ionization multistage mass spectrometry – new biomarkers for biogeochemistry and microbial ecology. *Rapid Communications in Mass Spectrometry* 18, 617 - 628.
- Summons, R.E., Jahnke, L.L., 1993. Hopanes and Hopanes of methylated in Ring-A: Correlation of the hopanoids from extant methylotrophic bacteria with their fossil analogues. p182 – 200. In: Biological markers in sediments and petroleum. Moldowan, Albrecht and Philp (ed.).
- Summons, R.E., Jahnke, L.L., Hope, J., Logan, G., 1999. 2-methylhopanoids as biomarkers for oxygenic photosynthesis. *Nature* 400, 554 – 557.
- Summons, R. E., L. L. Jahnke, and B. R. T. Simoneit. 1996. Lipid biomarkers for bacterial ecosystems: studies of cultured organisms, hydrothermal environments and ancient sediments, p. 174-194. In G. R. Bock and J. A. Goode (ed.), Evolution of hydrothermal ecosystems on Earth (and Mars?). Ciba Foundation Symposium no. 202. Wiley, Chichester, United Kingdom.
- Summons, R.E., Bradley, A., Jahnke, L.L., Waldbauer, J., 2006. Steroids, triterpenoids and molecular oxygen. *Philosophical Transactions of the Royal Society B* 361, 951 – 968.
- Sunthirasingham, C., Simpson, M.J., 2006. Investigation of bacterial hopanoid inputs to soils from Western Canada. *Applied Geochemistry* 21, 964 - 976.
- ## T
- Talbot, H.M., Farrimond, P., 2007. Bacterial populations recorded in diverse sedimentary biohopanoids distributions. *Organic Geochemistry* 38, 1212 – 1225.
- Talbot, H.M., Watson, D.F., Murrell, J.C, Carter, J. F., Farrimond, P., 2001. Analysis of intact bacteriohopanepolyols from methanotrophic bacteria by reversed-phase high-

## References

- performance liquid chromatography-atmospheric pressure chemical ionisation mass spectrometry. *Journal of Chromatography A* 921, 175 – 185.
- Talbot, H.M., Squier, A.H., Keely, B.J., Farrimond, P., 2003a. Atmospheric pressure chemical ionisation reversed-phase liquid chromatography/ion trap mass spectrometry of intact bacteriohopanepolyols. *Rapid Communications in Mass Spectrometry* 17, 728 – 737.
- Talbot, H.M., Summons R.E., Jahnke, L.L., Farrimond, P., 2003b. Characteristic fragmentation of bacteriohopanepolyols during atmospheric pressure chemical ionisation liquid chromatography/ion trap mass spectrometry. *Rapid Communications in Mass Spectrometry* 17, 2788 – 2796.
- Talbot, H.M., Watson, D.F., Pearson, E.J., Farrimond, P., 2003c. Diverse hopanoid compositions of non-marine sediments. *Organic Geochemistry* 34, 1353 - 1371.
- Talbot, H.M., Farrimond, P., Schaeffer, P., Pancost, R.D., 2005. Bacteriohopanepolyols in hydrothermal vent biogenic silicates. *Organic Geochemistry* 36, 663 – 672.
- Talbot, H.M., Rohmer, M., Farrimond, P., 2007a. Rapid structural elucidation of composite bacterial hopanoids by atmospheric pressure chemical ionisation liquid chromatography/ion trap mass spectrometry. *Rapid Communications in Mass Spectrometry* 21, 880 – 892.
- Talbot, H.M., Rohmer, M., Farrimond, P., 2007b. Structural characterisation of unsaturated bacterial hopanoids by atmospheric pressure chemical ionisation liquid chromatography/ion trap mass spectrometry. *Rapid Communications in Mass Spectrometry* 21, 1613 – 1622.

## References

- Talbot, H.M., Summons, R.E., Jahnke, L.L., Cockell, C.S., Rohmer, M., Farrimond, P., 2008a. Cyanobacterial bacteriohopanepolyol signatures from cultures and natural environmental settings. *Organic Geochemistry* 39, 232 – 263.
- Talbot, H.M., Coolen, M.J.L., Sinninghe Damsté, J.S., 2008b. Identification of an unusual 17 $\alpha$ , 21 $\beta$ (H) bacteriohopanetetrol in Holocene sediments from Ace Lake (Antarctica). *Organic Geochemistry* 39, 1029 - 1032.
- Thiel, V., Blumenberg, M., Pape, T., Seifert, R., Michaelis, W., 2003. The unexpected occurrence of hopanoids at gas seeps in the Black Sea. *Organic Geochemistry* 34, 81 – 87.
- Toporski, J.K.W., Steele, A., Westall, F., Thomas-Keprta, K.L., McKay, D.S., 2002. The simulated silification of bacteria – New clues to the modes and timing of bacterial preservation and implications for the search for extraterrestrial microfossils, *Astrobiology* 2, 1 – 26.
- Trewin, N.H., 1996. The Rhynie cherts: an early Devonian ecosystem preserved by hydrothermal activity, p 131 - 149. In G. R. Bock and J. A. Goode (ed.), *Evolution of hydrothermal ecosystems on Earth (and Mars?)*. Ciba Foundation Symposium no. 202. Wiley, Chichester, United Kingdom.
- Tritz, P.J., Hermann, D., Bissert, P., Rohmer, M., 1999. Abiotic and biological transformation: towards the formation of molecular fossils of the hopane series. *Organic Geochemistry* 30, 499 – 514.

## U

## References

### V

- van der Meer, M.T.J., Schouten, S., van Dongen, B.E., Rijpstra, W.I.C., Fuchs, G., Sinninghe Damsté, J.S., de Leeuw, J. W., Ward, D.M., 2001. Biosynthetic controls on the  $^{13}\text{C}$ -contents of organic components in the photoautotrophic bacterium *Chloroflexus aurantiacus*. *Journal of Biological Chemistry* 276, 10971 - 10976.
- van der Meer, M.T.J., Lammerts, L., Skirnisdottir, S., Sinninghe Damsté, J.S., Schouten, S., 2008. Distribution and isotopic composition of bacterial lipids in microbial mats from a sulphidic Icelandic hot spring. *Organic Geochemistry* 39, 1015 – 1019.
- van Dongen, B.E., Talbot, H.M., Schouten, S., Pearson, P. N., Pancost, R.D., 2006. Well preserved Palaeogene and Cretaceous biomarkers from the Kilwa area, Tanzania. *Organic Geochemistry* 37, 539 – 557.
- van Mooy, B.A.S, Rocap, G., Fredericks, H.F., Evans, C.T., Devol, A.H., 2006. Sulfolipids dramatically decrease phosphorous demand by picocyanobacteria in oligotrophic marine environments. *Proceedings of the National Academy of Sciences* 103, 8607 – 8612.
- van Mooy, B.A.S, Fredericks, H.F., Pedler, B.E., Dyhrman, S.T., Karl, D.M., Koblizek, M., Lomas, M.W., Mincer, T., Moore, L.R., Moutin, T., Rappe, M.S., Webb, E.A., 2009. Phytoplankton in the ocean substitute lipids in response to phosphorus scarcity. *Nature* 485, 69 – 72.
- Volkman, J. K., 2005. Sterols and other triterpenoids: source specificity and evolution of biosynthetic pathways. *Organic Geochemistry* 36, 139 – 159.

## References

### W

- Walter, M. R., 1996. Ancient hydrothermal ecosystems on Earth: a new palaeobiological Frontier, p112 – 127. In G. R. Bock and J. A. Goode (ed.), Evolution of hydrothermal ecosystems on Earth (and Mars?). Ciba Foundation Symposium no. 202. Wiley, Chichester, United Kingdom.
- Wang, C., 2007. Anomalous hopane distributions at the Permian-Triassic boundary, Meishan, China – Evidence for the end-Permian marine ecosystem. *Organic Geochemistry* 38, 52 – 66.
- Ward, D.M., Brassell, S.C., Eglinton, G., 1985. Archaeobacterial lipids in hot-spring microbial mats. *Nature* 318, 656 – 659.
- Ward, D.M., Ferris, M.J., Nold, S.C., Bateson, M.M., 1998. A natural view of microbial biodiversity within hot spring cyanobacterial mat communities. *Microbiology and Molecular Biology Reviews* 62, 1353 - 1370.
- Watson, D. F., 2002. Environmental distribution and sedimentary fate of hopanoid biological marker compounds. PhD Thesis, University of Newcastle.
- Watson, D.F., Farrimond, P., 2000. Novel polyfunctionalised geohopanooids in a recent lacustrine sediment (Priest Pot, UK). *Organic Geochemistry* 31, 1247 - 1252
- Weijers, J.W., Schouten, S., Hopmans, E.C., Geenevasen, J.A., David, O.R., Coleman, J.M., Pancost, R.D., Sinninghe Damsté, J.S., 2006. Membrane lipids of mesophilic anaerobic bacteria thriving in peats have typical archaeal traits. *Environmental Microbiology* 8, 648 - 657.

## References

Westall, F., 1997. The influence of cell wall composition on the fossilisation of bacteria and the implications for the search for early life forms. In *Astronomical and biochemical origins and the search for life in the universe*. Cosmovici, Bologna, 491 – 504.

Wignall, P.B., Twitchett, R.J., 1996. Oceanic anoxia and the end Permian mass extinction. *Science* 272, 1155 – 1158.

## X

Xu, Y., Cooke, M.P., Talbot, H.M., Simpson, M.E., 2009. Bacteriohopanepolyol signatures of bacterial populations in western canadian soils. *Organic Geochemistry* 40, 79 - 86.

## Y

Yee, N., Phoenix, V.R., Konhauser, K.O., Benning, L., Ferris, F.G., 2003. The effect of cyanobacteria on silica precipitation at neutral pH: implications for bacterial silicification in geothermal hot springs. *Chemical Geology* 199, 83 - 90.

## Z

Zeng, Y.B., Ward, D.M., Brassell, S.C., Eglinton, G., 1992. Biogeochemistry of hot-spring environments. 3. Apolar and polar lipids in the biologically-active layers of a cyanobacterial mat. *Chemical Geology* 95, 347 – 360.

Zhang, C.L., Fouke, B.W., Bonheyo, G.T., Peacock, A.D., White, D.C., Huang, Y., Romanek, C.S., 2004. Lipid biomarkers and carbon-isotopes of modern travertine deposits (Yellowstone National Park, USA): Implications for biogeochemical dynamics in hot-spring systems. *Geochimica et Cosmochimica Acta* 68, 3157 - 3169.

Zhang, C.L., Huang, Z., Li, Y.-L., Romanek, C.S., Mills, G., Gibson, R.A., Talbot, H.M., Wiegel, J., Noaks, J., Culp, R., White, D.C., 2007. Lipid biomarkers, carbon isotopes,

## References

- and phylogenetic characterization of bacteria in California and Nevada Hot Springs. *Geomicrobiology* 24, 519 - 534.
- Zhao, N., Berova, N., Nakanishi, K., Rohmer, M., Mougénou, P., Jurgens, U.J., 1996. Structures of two bacteriohopanoids with acyclic pentol side-chains from the cyanobacterium *Nostoc* PCC 6720. *Tetrahedron* 52, 2777 – 2788.
- Zink, K.G., Wilkes, H., Disko, U., Elvert, M., Horsfield, B., 2003. Intact phospholipids - microbial “life markers” in marine deep subsurface sediments. *Organic Geochemistry* 34, 755 - 769.
- Zundel, M., Rohmer, M., 1985a. Hopanoids of the methylotrophic bacteria *Methylococcus capsulatus* and *Methylomonas* sp. as possible precursors of C<sub>29</sub> and C<sub>30</sub> hopanoid chemical fossils. *FEMS Microbiology Letters* 28, 61 – 64.
- Zundel, M., Rohmer, M., 1985b. Prokaryotic triterpenoids 3. The biosynthesis of 2 $\beta$ -methylhopanoids and 3 $\beta$ -methylhopanoids of *Methylobacterium organophilum* and *Acetobacter pasteurianus* spp.. *European Journal of Biochemistry* 150, 35 – 39.

## APPENDIX

### MS<sup>2</sup> AND MS<sup>3</sup> SPECTRA OF POSSIBLE NOVEL BHP COMPOUNDS

This section of the thesis is used to present mass spectral data that is thought to correspond to unidentified BHPs. The compounds presented were not commented upon during the analysis of samples because it was not possible to carry out further structural identification and they were observed only once during the analysis of intact BHPs.

A short summary of key fragments is presented for each potential BHP compound. As more BHP structures become known it is hoped that the mass spectra shown here will be used to for comparison and should allow further refinement of the conclusions given in the thesis.

Figure A1: *MS<sup>2</sup> and MS<sup>3</sup> spectra of possible novel BHP compounds with  $[M+H]^+ = m/z 731$*

The presence of ions with m/z 611 and 671 indicates an anhydro-type BHP. Both ions indicate loss of AcOH from  $[M+H]^+ = m/z 731$ , this may indicate an anhydro-type BHP with four alcohols. This could be formed during intra-molecular cyclisation of hexafunctionalised BHPs (e.g Schaeffer et al., 2008). Loss of 18 from  $[M+H]^+ = m/z 731$  produces an ion of m/z 713 which provides the parent ion for the MS<sup>3</sup> spectrum. Two losses of AcOH from  $[M+H - H_2O]^+ = m/z 713$  are observed at m/z 653 and 473.

Figure A2: *MS<sup>2</sup> and MS<sup>3</sup> spectra of possible novel BHP compounds with  $[M+H]^+ = m/z 847$*

The presence of an ion with m/z 611 indicates an anhydro-type BHP compound. The presence of an ion with m/z 671 indicates a penta-functionalised anhydroBHP with an extra functionality of mass 177. The presence of an ion an m/z 159 (158.8) likely represents the terminal group (TG; See Chapter 5, Figures 5.7 and 5.8 for explanation) functionality and

## Appendix

suggests that this extra-functionality is ether-linked to the pentafunctionalised anhydro side chain component. The presence of an ion at  $m/z$  191 results from cleavage of A+B rings from the hydrocarbon component and provides further evidence of the presence of a BHP.

Figure A3:  $MS^2$  and  $MS^3$  spectra of possible novel BHP compounds with  $[M+H]^+ = m/z$  916

The presence of an ion with  $m/z$  611 indicates a BHP with an ‘anhydro’ type side chain configuration and containing an extra functionality which has a mass of 304 Da. Two losses of AcOH from  $m/z$  611 are observable at  $m/z$  551 and 491 which provide further evidence for the presence of an anhydroBHP. Multiple losses of AcOH are observed from  $[M+H]^+ = m/z$  916 are observed in the  $MS^2$  spectrum, i.e.  $m/z$  856 and 796. No ion is observed with  $m/z$  305 that would indicate the presence of an extra functionality of mass 304 Da, however, an ion with  $m/z$  287 is present and likely forms from loss of  $H_2O$  from the Terminal group (TG). This indicates that TG is linked via an ether bond to C-35 and that the ether oxygen is retained upon the BHP side chain during fragmentation producing an ion with  $m/z$  287.

Figure A4:  $MS^2$  and  $MS^3$  spectra of possible novel BHP compounds with  $[M+H]^+ = m/z$  918

The presence of ion with  $m/z$  655 indicates a tetrafunctionalised BHP with C-35 (TGOH) linked head group of mass 263 Da, which is observed as an ion ( $[TGOH_2]^+$ ) with  $m/z$  264 (263.6). Multiple loss of AcOH from  $m/z$  655 can be observed, i.e.  $m/z$  595, 535 and 476. The ion with  $m/z$  476 is likely an isotopically heavy fragment with  $m/z$  475. Multiple losses of AcOH are observable from  $[M+H]^+ = m/z$  918, i.e.  $m/z$  858 and 738. Which indicates that C-35 linked moiety contains at least three alcohol groups. Loss of 18, i.e.  $H_2O$  which indicates a free hydroxyl group, from  $[M+H]^+ = m/z$  918 gives the parent ion of the  $MS^3$  spectra. In the  $MS^3$  spectra, multiple losses of AcOH from  $[M+H]^+ = m/z$  900 are observable, i.e.  $m/z$  840 and 780.

## Appendix

Figure A5:  $MS^2$  and  $MS^3$  spectra of possible novel BHP compounds with  $[M+H]^+ = m/z 1040$

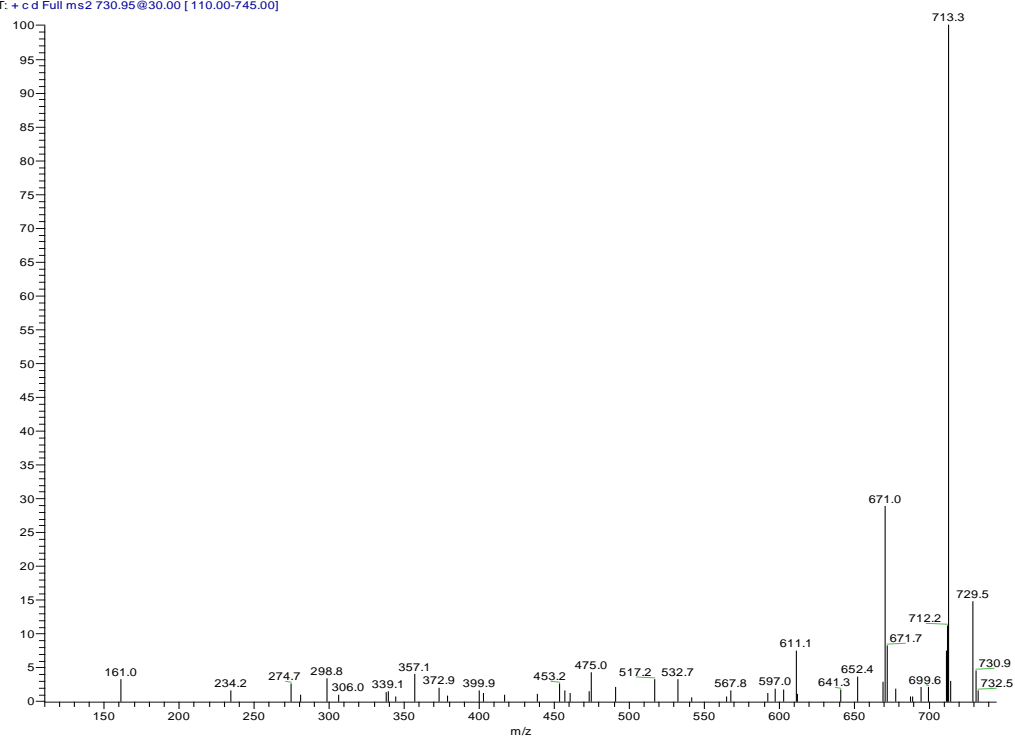
The presence of ions with  $m/z$  611, 551 and 491 indicate the presence of an anhydroBHP. An ion with  $m/z$  753 was also observed in two novel BHP compounds with  $[M+H]^+ = m/z$  1100 and 1114 which were detected from the Loop Road hot-springs (Section 5.4.3). The loss of a fragment with weight 142 Da from  $m/z$  753 to give an ion with  $m/z$  611 and also observed in other unidentified BHPs (Section 5.4.3; Section 8.3) suggests that this particular compound may belong to a homologous series of currently unidentified BHPs. Ion with  $m/z$  611, 551 and 491 were also observed as characteristic fragments in *oxoBHT<sub>cyc</sub>* and *oxoBH<sub>triol</sub>* (Chapter 5, Section 5.3.2), however, the late retention time of  $[M+H]^+ = m/z$  1040 suggests that this compound does not belong to the oxo-BHPs.

Figure A6:  $MS^2$  and  $MS^3$  spectra of possible novel BHP compounds with  $[M+H]^+ = m/z 1100$

A number of ions present in the  $MS^2$  spectra are also observed in the  $MS^2$  spectra of *oxo-BHT<sub>cyc</sub>* (Section 5.4.3) i.e.  $m/z$  958, 898, 611, 348 and 330. The differences in the observed mass of  $[M+H]^+ = m/z$  1100 and *oxo-BHT<sub>cyc</sub>* ( $[M+H]^+ = m/z$  958) is attributed to the presence of an extra-functionality on the C-35 ether-linked terminal group. The extra functionality has a mass of 142 Da.

# Appendix

RG2362 LR5-1 Loop Road #917 RT: 20.66 AV: 1 NL: 1.08E5  
T: + c d Full ms2 730.95@30.00 [ 110.00-745.00]



RG2362 LR5-1 Loop Road #918 RT: 20.68 AV: 1 NL: 2.84E3  
T: + c d Full ms3 730.95@30.00 713.26@30.00 [ 185.00-725.00]

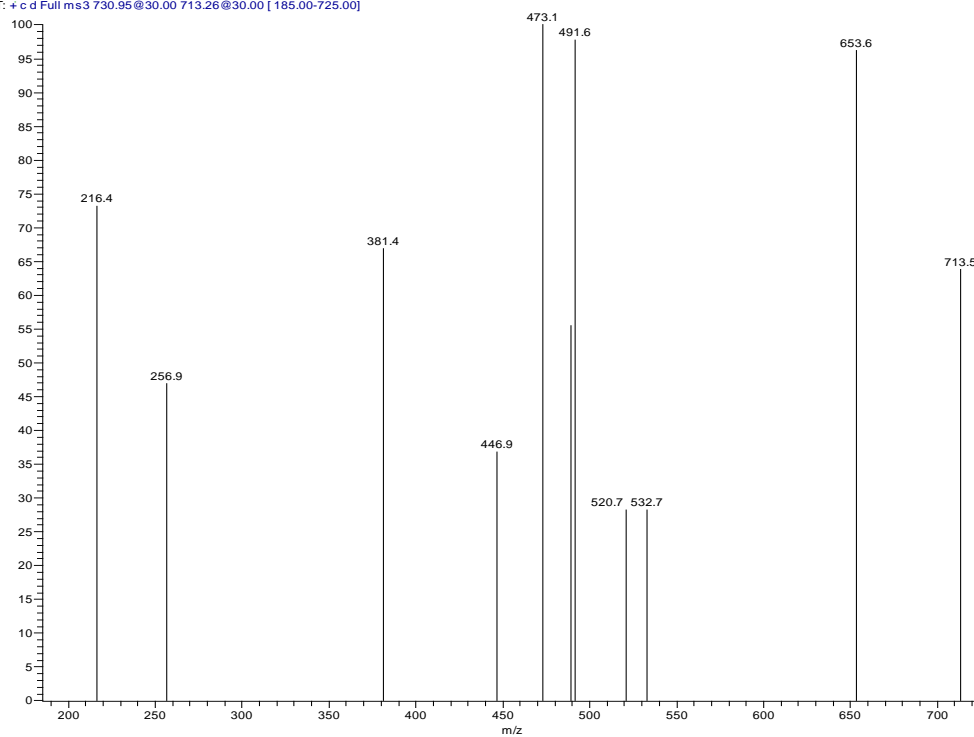
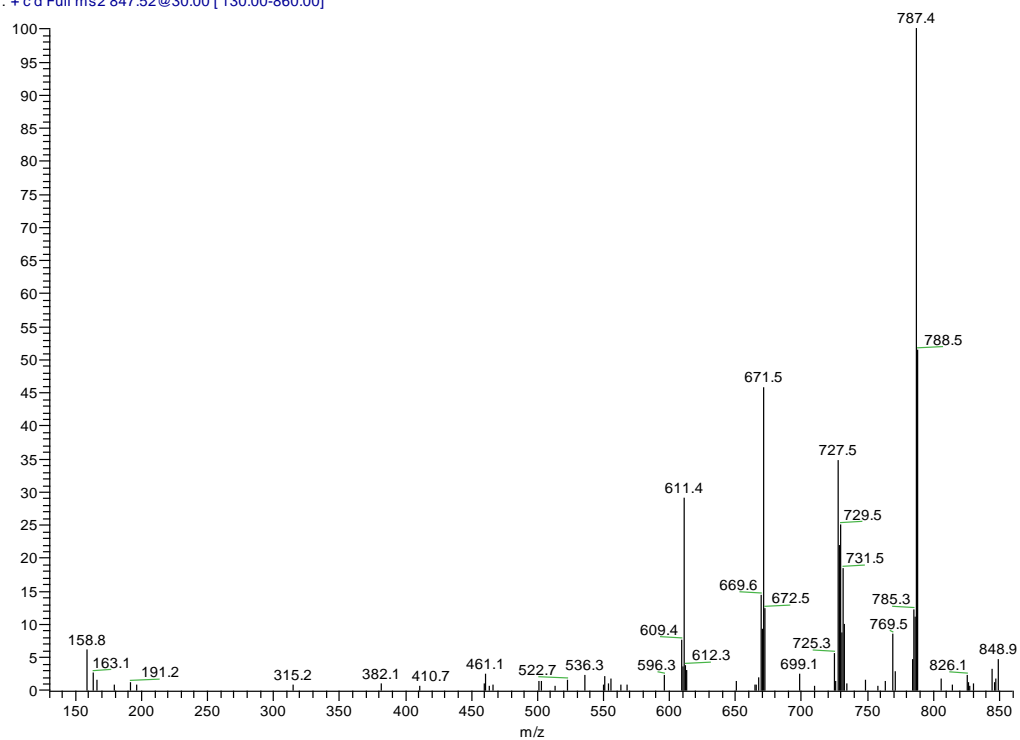


Figure A1  $MS^2$  and  $MS^3$  spectra of possible novel BHP compounds with  $[M+H]^+ = m/z 731$ .

## Appendix

RG2055 RGCP11-EF BandD Rep #1290 RT: 29.66 AV: 1 NL: 1 7<sup>2</sup>F5  
T: + c d Full ms2 847.52@30.00 [130.00-860.00]



RG2055 RGCP11-EF BandD Rep #1291 RT: 29.69 AV: 1 NL: 3 14F4  
T: + c d Full ms3 847.52@30.00 787.45@30.00 [205.00-800.00]

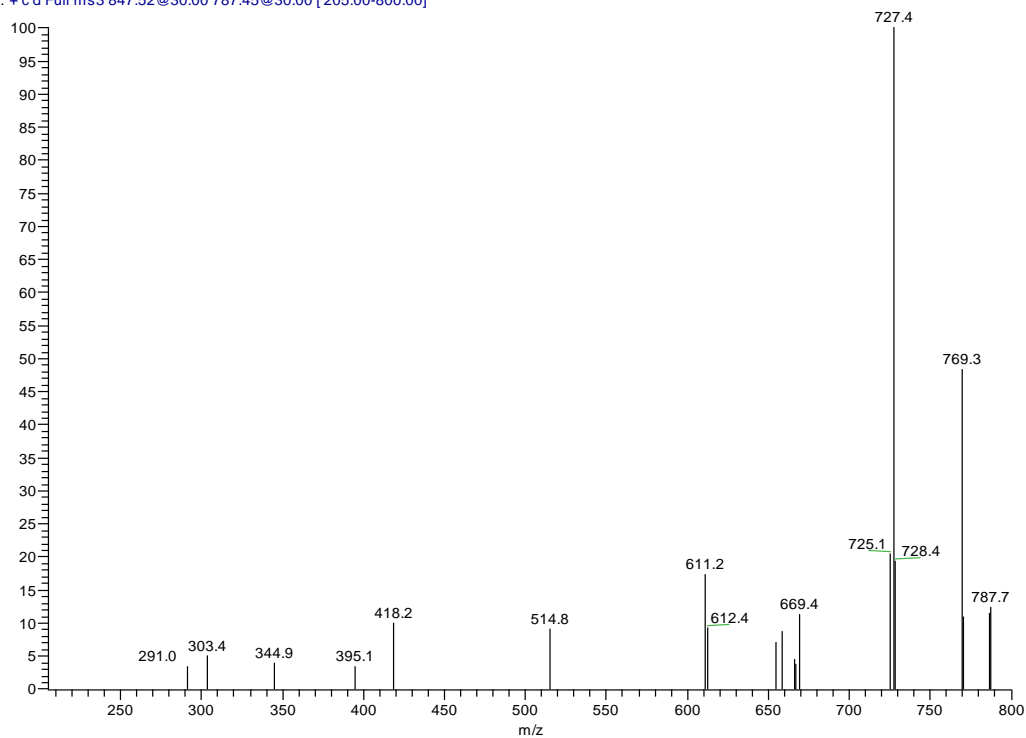
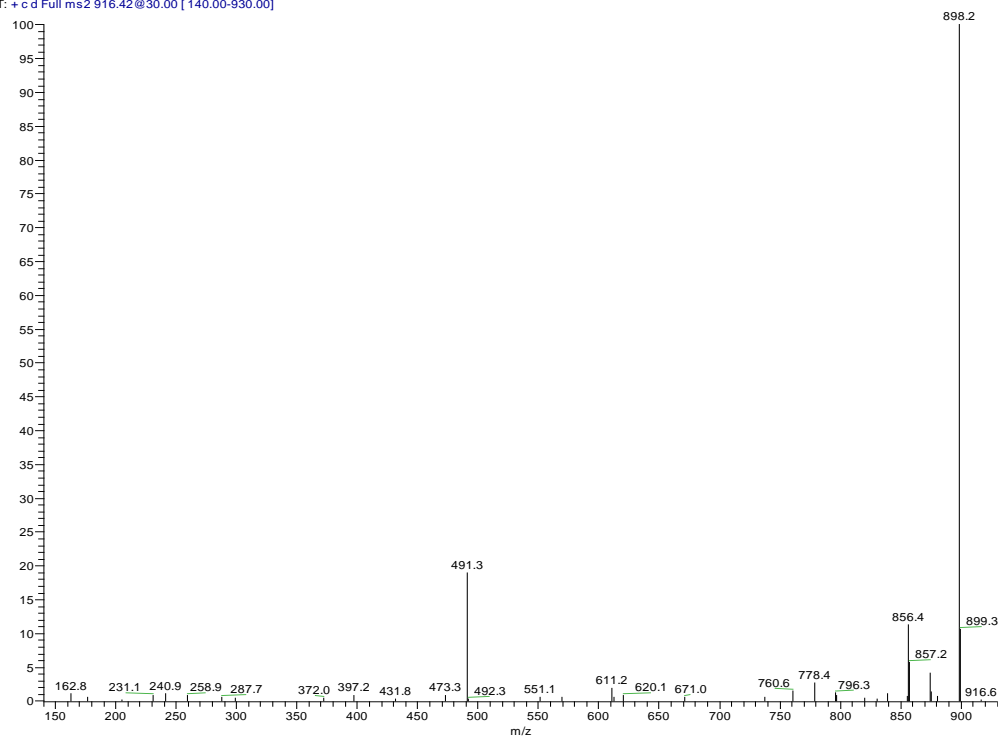


Figure A2 MS<sup>2</sup> and MS<sup>3</sup> spectra of possible novel BHP compounds with  $[M+H]^+ = m/z$  848.

# Appendix

RG2372 CP5-2 Champagne Pool Rep #718 RT: 17.28 AV: 1 NL: 3.33E5  
T: + c d Full ms2 916.42@30.00 [140.00-930.00]



RG2372 CP5-2 Champagne Pool Rep #719 RT: 17.31 AV: 1 NL: 5.41E4  
T: + c d Full ms3 916.42@30.00 898.17@30.00 [235.00-910.00]

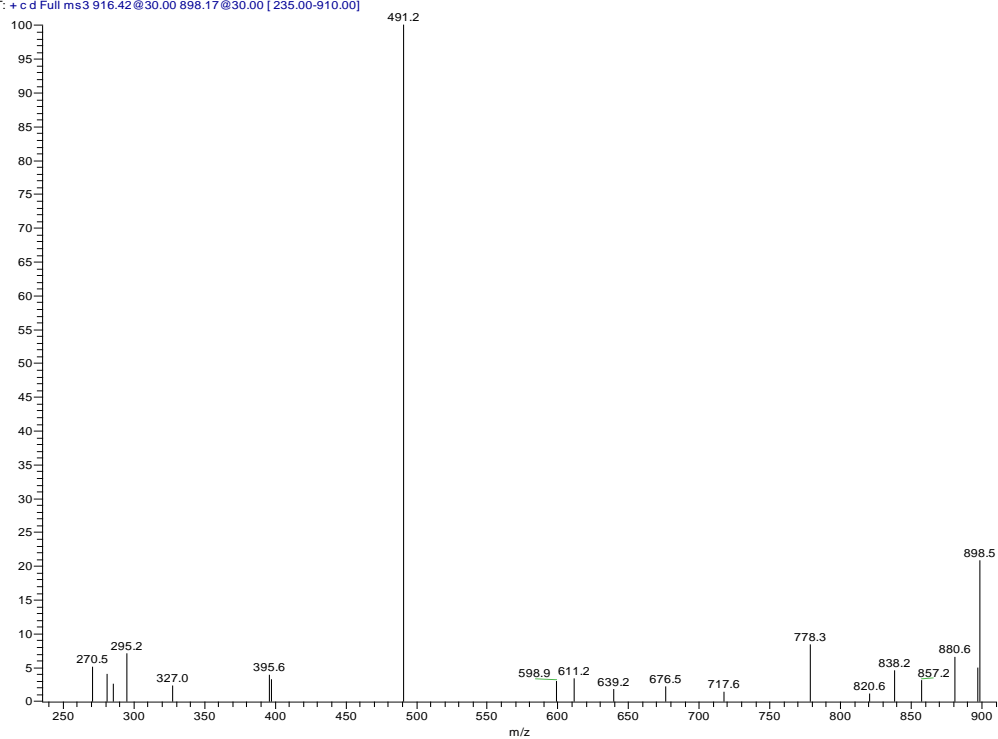
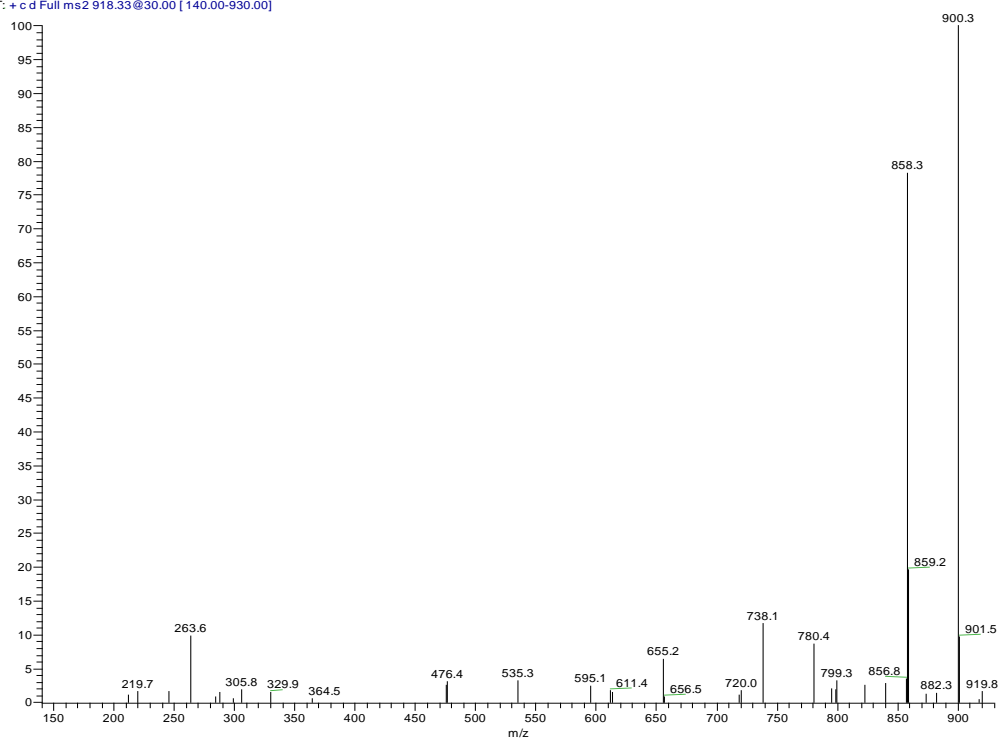


Figure A3  $MS^2$  and  $MS^3$  spectra of possible novel BHP compounds with  $[M+H]^+ = m/z$  916.

# Appendix

RG2372 CP5-2 Champagne Pool Rep #861 RT: 20.68 AV: 1 NL: 1.36E5  
T: + c d Full ms2 918.33@30.00 [140.00-930.00]



RG2372 CP5-2 Champagne Pool Rep #862 RT: 20.70 AV: 1 NL: 1.44E4  
T: + c d Full ms3 918.33@30.00 900.32@30.00 [235.00-915.00]

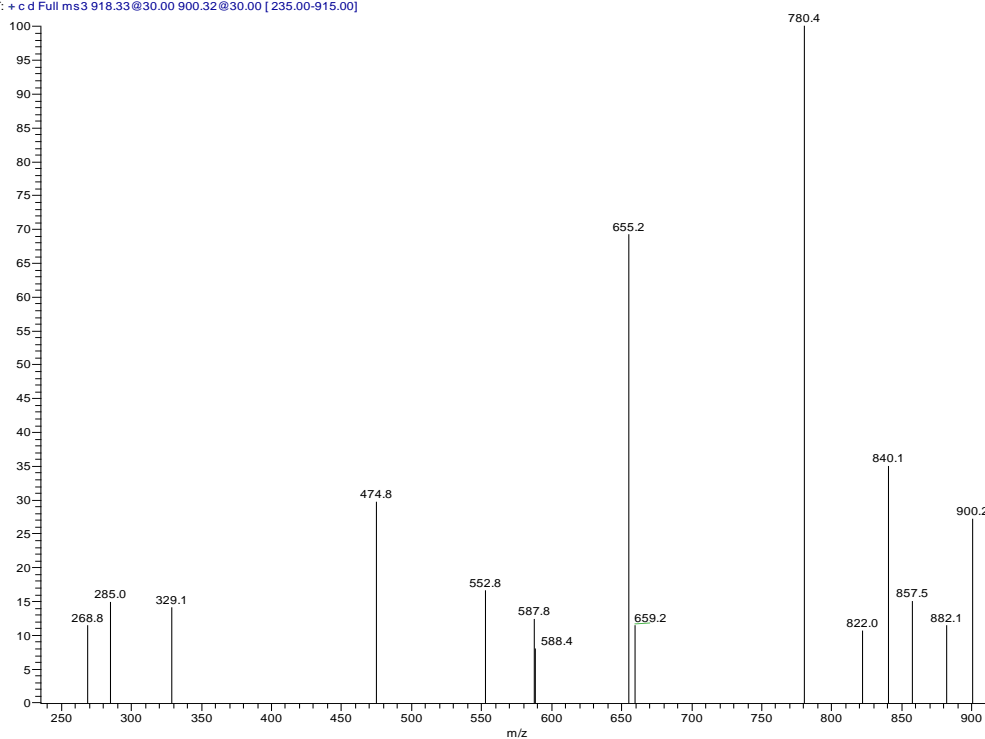


Figure A4 MS<sup>2</sup> and MS<sup>3</sup> spectra of possible novel BHP compounds with  $[M+H]^+ = m/z 918$ .

# Appendix

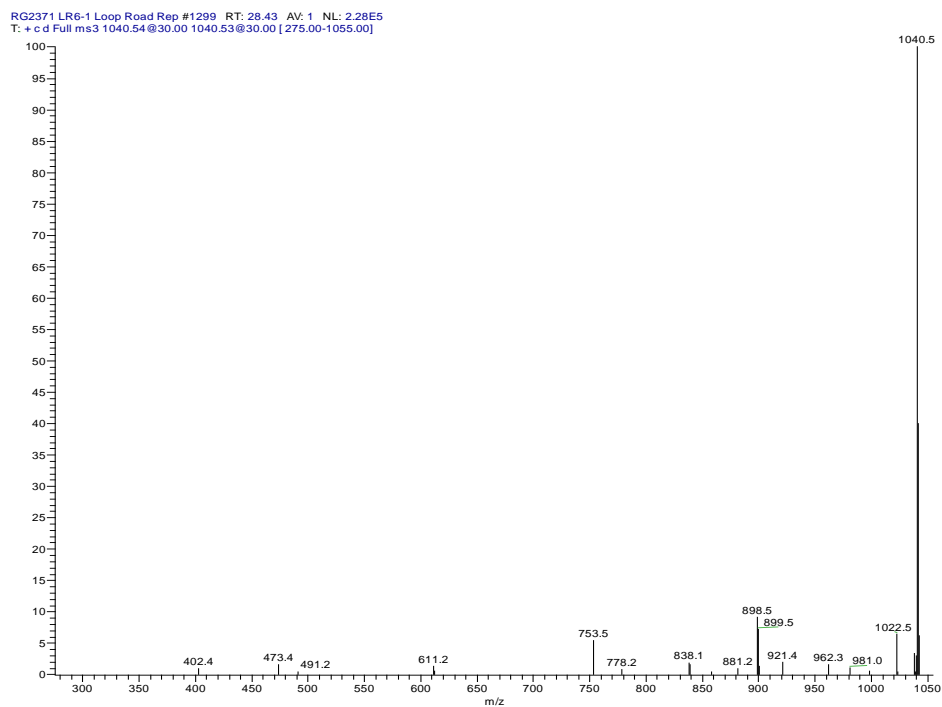
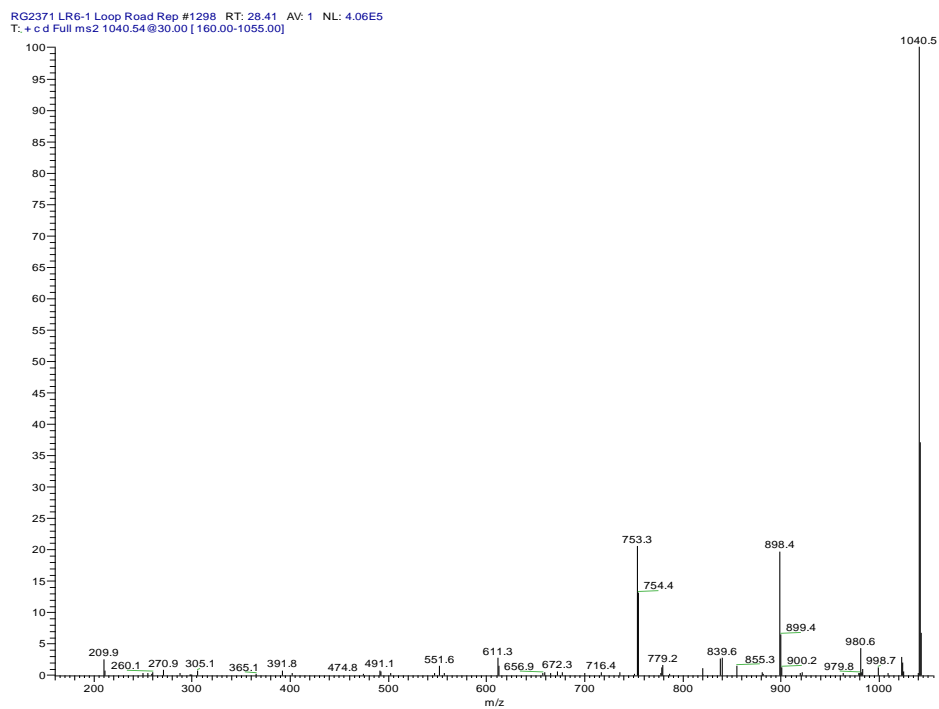
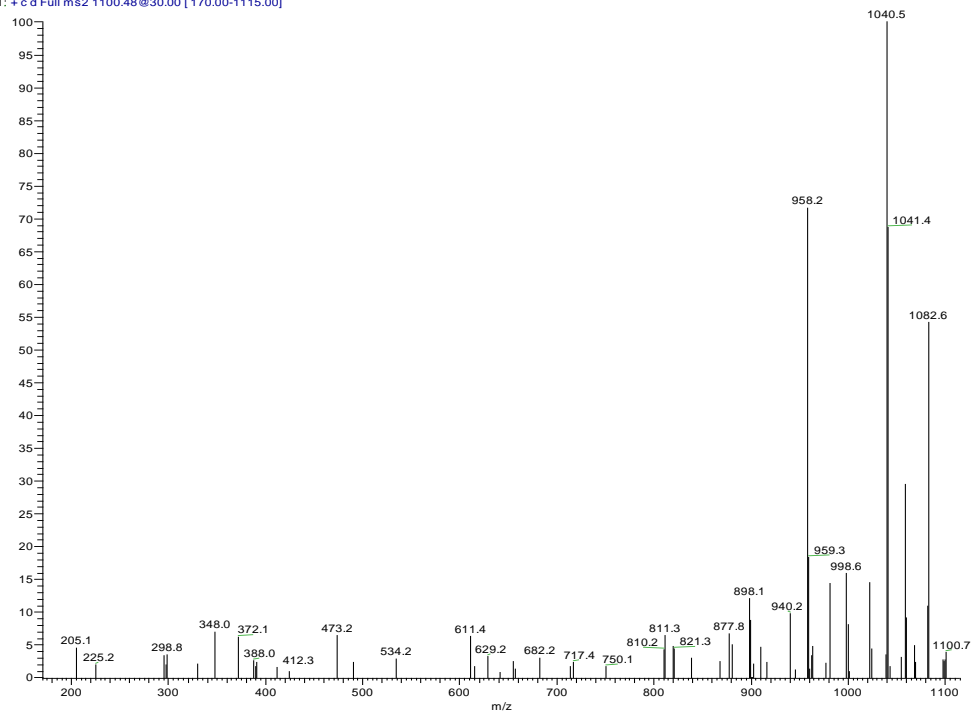


Figure A5  $MS^2$  and  $MS^3$  spectra of possible novel BHP compounds with  $[M+H]^+ = m/z$  1040.

# Appendix

RG2371 LR6-1 Loop Road Rep #1208 RT: 26.39 AV: 1 NL: 6.59E4  
T: + c d Full ms2 1100.48@30.00 [170.00-1115.00]



RG2371 LR6-1 Loop Road Rep #1209 RT: 26.42 AV: 1 NL: 1.26E4  
T: + c d Full ms3 1100.48@30.00 1040.46@30.00 [275.00-1055.00]

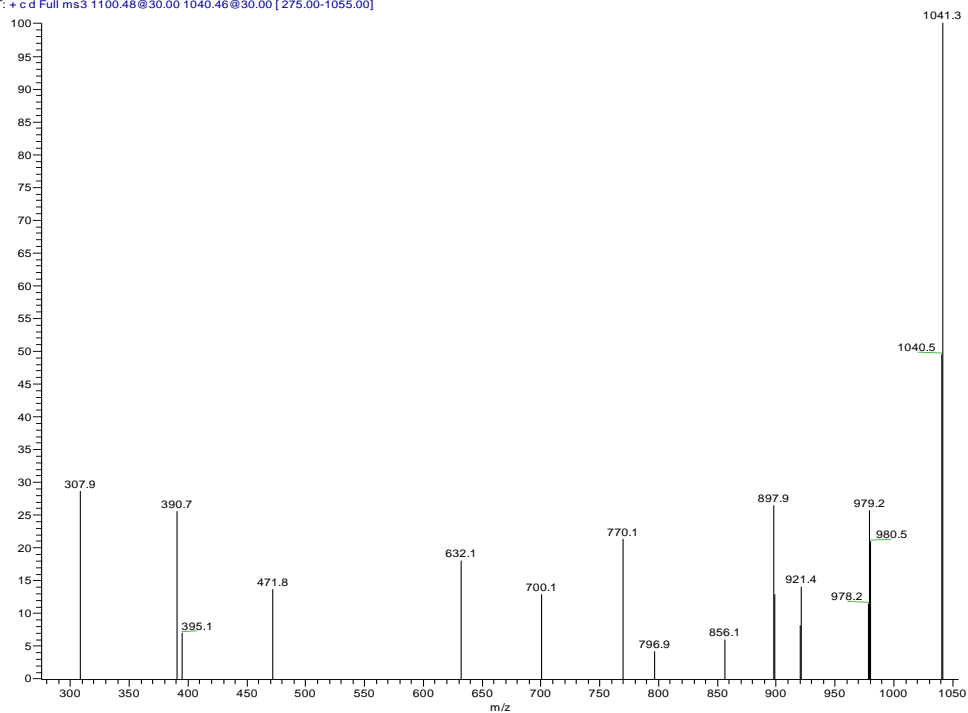


Figure A6 MS<sup>2</sup> and MS<sup>3</sup> spectra of possible novel BHP compounds with  $[M+H]^+ = m/z 1100$ .